IN SITU CAPPING OF CONTAMINATED SEDIMENTS: SPATIAL AND TEMPORAL CHARACTERIZATION OF BIOGEOCHEMICAL AND CONTAMINANT BIOTRANSFOMATION PROCESSES

A Dissertation
Presented to
The Academic Faculty

By

David W. Himmelheber

In Partial Fulfillment
Of the Requirements for the Degree
Doctor of Philosophy in Environmental Engineering in the
School of Civil and Environmental Engineering

Georgia Institute of Technology

April 2008

IN SITU CAPPING OF CONTAMINATED SEDIMENTS: SPATIAL AND TEMPORAL CHARACTERIZATION OF BIOGEOCHEMICAL AND CONTAMINANT BIOTRANSFOMATION PROCESSES

Approved by:

Dr. Joseph B. Hughes, Advisor
School of Civil and Environmental Engineering
School of Materials Science and Engineering
Georgia Institute of Technology

Dr. Kurt D. Pennell, Advisor
School of Civil and Environmental Engineering
Georgia Institute of Technology
Center for Neurodegenerative Disease, Department of Neurology
Emory University School of Medicine

Dr. Frank E. Löffler
School of Civil and Environmental Engineering
School of Biology
Georgia Institute of Technology

Dr. Danny D. Reible
Department of Civil, Architectural and Environmental Engineering
University of Texas at Austin

Dr. Jim C. Spain
School of Civil and Environmental Engineering
Georgia Institute of Technology

Dr. Terry W. Sturm
School of Civil and Environmental Engineering
Georgia Institute of Technology

Dr. Martial Taillefert
School of Earth and Atmospheric Sciences
Georgia Institute of Technology

Date Approved: 11/20/2007

Nothing ever comes to one, that is worth having, except as a result of hard work.

- Booker T. Washington

Just Do It.

- Nike

To Denise,

You have been right beside throughout this experience,
now let’s move on to our next adventures.

ACKNOWLEDGEMENTS

This has been a formidable test of determination and hard work that I still feel lucky to be given the opportunity to pursue. I've been surrounded at Georgia Tech by many friendly, sharp, and interesting people – I will remember the personal connections long after I've forgotten the technical content of this document.

Denise has provided continuous emotional support and always reminded me to maintain proper perspective and keep a positive attitude. Her interest in my work has provided motivation, and her help in grading papers and performing lab tasks made the mundane fun. Weekends at work were much better when she would accompany me, just so we could be together. I know I could not have done this without her love and support. I would also like to thank my family, who have all been wonderful role models. I look forward to being a more-available brother, son, and husband.

I would like to thank my primary research advisor, Joe Hughes, for his advice and support. He's provided guidance as well as freedom to allow me to grow as a student, researcher, and professional. He's shown enthusiasm for my work and believed in me, even when I lost those feelings. I don't remember ever wishing I had another advisor, and I've enjoyed developing healthy relationships both professionally and personally.

I would like to thank my co-advisor Kurt Pennell for allowing me to work with him upon arrival at Georgia Tech, and for staying connected with my research after changing projects. It would have been easy for him to become uninvolved, but he remained loyal and I've tried to do the same for him. Kurt has been a trusted source of objective advice and always had my best-interests in mind. I am also deeply grateful to

Martial Taillefert, who allowed me to enter his lab, use his resources, take his time, and pick his mind without (genuine) complaints. Much of this thesis, in terms of technical-lab work, data interpretation, and manuscript preparation, literally would not have been possible without his assistance. Thank you for the opportunity to work with you and your group. The same can be said for Frank Löffler, who has also allowed me to work in his lab and with his research group. I've always felt welcome working with you and have learned to appreciate and even enjoy microbiology. I would also like to thank Danny Reible, Jim Spain, and Terry Sturm for serving on my committee. I have a great deal of respect for each of you and appreciate your time to help improve my work.

Special recognition should be given to members of the Hughes, Pennell, Löffler, and Taillefert research groups for their help. Specifically, Rebecca Daprato provided much training and insight regarding microbial techniques, Ben Amos and Eric Suchomel supplied much laboratory advice, Deidre Meiggs took time to train me about microelectrodes, Sara Thomas allowed me to use her custom primers and taught me microbiology whenever I asked, and John Fortner has been an ever-ready source of advice and a good friend. There are too many other meaningful contributions from students, in terms of technical support and friendship, to mention here individually but each has made my time at Georgia Tech more enjoyable. I would also like to acknowledge help from Dr. Zhu, Andrea Bé, Antionette Keith, and Therese Rehkopf.

Funding for this research was provided by the Hazardous Substance Research Center – South and Southwest. Fellowship support was also provided by Georgia Tech. Horne Engineering obtained and shipped sediment samples from the Anacostia River, with the assistance of Danny Reible.

TABLE OF CONTENTS

LIST OF TABLES

LIST OF FIGURES

NOMENCLATURE

Acronyms

ACS	American Chemical Society
ATCC	American Type Culture Collection
BTEX	benzene, toluene, ethylbenzene, xylenes
bp	base pairs
CCA	canonical correspondence analysis
cis-DCE	*cis*-dichloroethene
CSOs	combined sewer overflows
CSWV	cathodic square wave voltammetry
CWI	cap-water interface
DBL	diffusive boundary layer
DCE	dichloroethene
DCEs	dichloroethenes
DIRB	dissimilatory iron-reducing bacteria
DGGE	denaturing gradient gel electrophoresis
DGT	diffusive gradient in thin film
DOC	dissolved organic carbon
dsr	dissimilatory sulfite reductase
dsrA	dissimilatory sulfite reductase, alpha subunit
ED	electron donor
ESTCP	Environmental Security Technology Certification Program
FID	flame ionization detector
GC	gas chromatography
HOCs	hydrophobic organic contaminants
HSRC-SSW	Hazardous Substance Research Center – South and Southwest
LSV	linear sweep voltammetry
mcr	methyl coenzyme-M reductase
mcrA	methyl coenzyme-M reductase, alpha subunit
MNA	monitored natural attenuation
NAPL	non-aqueous phase liquid
OW	Owls mixed dechlorinating consortium
PAHs	polycyclic aromatic hydrocarbons
PAT	phylogenetic assignment tool
PCBs	polychlorinated biphenyls
PCE	tetrachloroethene
PCR	polymerase chain reaction
PLFA	phospholipid fatty acid analysis
POC	particulate organic carbon
qPCR	quantitative real-time polymerase chain reaction
RCRA	Resource Conservation and Recovery Act
RDases	reductive dehalogenase
Rfu	relative fluorescence unit

SERDP	Strategic Environmental Research and Development Program
SRPs	sulfate-reducing prokaryotes
SVOCs	semi-volatile organic compounds
SWI	sediment-water interface
TCE	trichloroethene
TEAPs	terminal electron accepting processes
T-RFLP	terminal-restriction fragment length polymorphism
USDOD	United States Department of Defense
USEPA	United States Environmental Protection Agency
USGS	United States Geological Survey
VC	vinyl chloride
VOCs	volatile organic compounds

Symbols

$C_{w,0}$	initial aqueous phase concentration ($mg \cdot L^{-1}$)
$C_{w,eq}$	aqueous phase equilibrium concentration ($mg \cdot L^{-1}$)
$C_{w,t}$	aqueous phase concentration ($mg \cdot L^{-1}$) at time *t* (hr)
D_m	dispersion coefficients ($cm^2 \cdot d^{-1}$)
E_h	redox potential (mV)
E_{var}	Smith and Wilson evenness value
f_{oc}	fraction organic carbon (g oc·g solid^{-1})
H	Shannon's diversity index
k	adsorption rate coefficient (hr^{-1})
K_D	linear distribution coefficient ($mL \cdot g$ solid^{-1})
K_{oc}	organic carbon partitioning coefficient ($mL \cdot g\,oc^{-1}$)
S	species richness
ΣH_2S	$H_2S + HS^- + S^{2-} + S^0 + S_x^{2-}$

SUMMARY

Contaminated aquatic sediments pose health risks to fish, wildlife, and humans and can limit recreational and economic uses of surface waters. Technical and cost effective *in situ* approaches for sediment management and remediation have been identified as a research need. Subaqueous *in situ* capping is a promising remedial approach; however, little is known regarding its impact on underlying sedimentary processes and the feasibility of bioaugmented caps at sites subject to contaminated groundwater seepage. This work specifically addresses (1) the impact of capping on biogeochemical processes at the sediment-water interface, (2) the ability and degree to which indigenous sediment microorganisms colonize an overlying cap, (3) the effect of advective flow direction on redox conditions within a cap, (4) natural contaminant bioattenuation processes within capped sediment, and (5) limitations toward a functional bioreactive *in situ* cap.

Laboratory-scale experiments with capped sediment columns demonstrated that emplacement of a sand-based *in situ* cap induced an upward, vertical shift of terminal electron accepting processes into the overlying cap while simultaneously conserving redox stratification. Upflow conditions simulating a groundwater seep compressed anaerobic processes towards the cap-water interface. Microorganisms indigenous to the underlying sediment colonized cap material and spatial population differences generally reflected redox stratification. Downflow of oxic surface water through the cap, simulating tidally-induced recharge, created fully oxic conditions within the cap, demonstrating that flow direction strongly contributes to redox conditions. Experiments

simulating capped sediment subject to contaminated groundwater seepage revealed a reduction of natural bioattenuation processes with time, stemming from the elimination of labile organic matter deposition to the sediment and a subsequent lack of electron donor. Thus, parent contaminants within groundwater seeps will be subject to minimal biotransformations within the sediment before entering a reducing cap. A bioreactive cap, inoculated with microorganisms capable of reductive dehalogenation, was established to reductively dechlorinate tetrachloroethene present in the groundwater; however electron donor amendments to sediment effluent were required to achieve complete dechlorination of tetrachloroethene to non-toxic ethene. Results from this work improve understanding of biogeochemical and bioattenuation processes within capped aquatic sediments and should aid in the development of active capping technologies.

CHAPTER 1.
INTRODUCTION

Contaminated aquatic sediments are a widespread environmental concern in the United States, and remediation of these sites has proven to be a significant challenge. Contaminants present in sediments are toxic to macrofauna and aquatic life and continued exposure can cause detrimental health effects. Biomagnification of contaminants through the food web creates health risks for predatory fish, wildlife, and humans who consume aquatic organisms. Elevated contaminant concentrations in sediments can also limit recreational and economic uses of surface waters. Many point- and non-point sources of sediment contamination exist, but the prevalence of sediment contamination has repeatedly been correlated with urban, industrialized settings. Land development and urbanization present the potential for continued sources of contamination to sediments, demonstrated by increasing trends of some contaminant concentrations in urban sediments.

Compounding the problem of sediment contamination is the lack of remedial options available for treatment. One remedial method is monitored natural attenuation (MNA), which relies on intrinsic processes to decrease contaminant concentrations in the aqueous phase but generally does not provide significant reductions in contaminant exposure. Contaminated sediment removal (e.g., dredging) has been the conventional method of active sediment remediation and can provide rapid reductions in contaminant concentrations in localized regions. Concerns related to residual contamination and sediment resuspension represent significant deterrents to dredging. Another remedial option is *in situ* capping, which is now being utilized at many sites. Capping involves

placing a layer of clean fill material (typically sand) at the sediment-water interface to physically isolate contaminated sediments and prevent contact with benthic macrofauna and overlying water. Capping immediately reduces contaminant exposures, but uncertainties regarding long-term integrity and future contaminant breakthrough of the cap present limitations. The risk of contaminant breakthrough can be diminished if natural attenuation processes continue to occur below or in the cap, but little is known about how capping impacts natural processes in the underlying sediment or what processes in the cap will effect contaminant fate and transport.

To alleviate risks associated with contaminant breakthrough, active caps are being developed and are designed to reduce contaminant concentrations within the cap through sorptive and reactive processes. Biologically-active caps employing microbially-mediated contaminant transformations have not yet been investigated and may provide a cost-effective, long-term remedial option. However, knowledge regarding contaminant discharge into caps and biogeochemical conditions within caps and capped sediment are required for development of the biologically-active caps.

The overarching objective of the research presented and discussed herein was to characterize biogeochemical and biotransformation processes within sand-based *in situ* caps for the development of a biologically-active cap. This document begins with a literature review (Chapter 2) intended to provide background information on sediment contamination and remediation. Subsections within the literature review discuss the scope of aquatic sediment contamination, common sediment contaminants, salient contaminant transport pathways, and sediment remediation techniques. Particular attention is devoted to *in situ* capping and the state of its development and application,

addressing current research directions, and identifying knowledge gaps. Information is also provided regarding the measurement of redox stratification using advanced analytical techniques, with emphasis placed on the coupling of geochemical and microbiological tools to fully characterize biogeochemical processes.

Chapters 3 through 7 describe the results of laboratory experiments designed to address the following specific research objectives:

1. Characterize the spatial and temporal distribution of biogeochemical processes in aquatic sediments and monitor the alteration of these processes after emplacement of an *in situ* cap under stagnant and upflow conditions. (Chapter 3).
2. Assess the ability and degree to which microorganisms indigenous to sediments colonize an overlying sand cap. (Chapter 4).
3. Determine the contribution of advective flow direction to redox conditions within a sand-based cap. (Chapter 5).
4. Investigate temporal trends in natural bioattenuation processes within a capped sediment. (Chapter 6).
5. Identify limitations of microbial activity within a biologically-active cap and determine if amendments are required to sustain contaminant biotransformation. (Chapter 7).

Conclusions reached from each research chapter are provided in a bullet-point format in Chapter 8. A summary paragraph compiles results and conclusions from each specific objective and discusses their contribution to the overall objective of characterizing biogeochemical and biotransformation processes within sand-based *in situ*

caps. The engineering significance of these findings is presented in Chapter 9. Recommendations for future research are offered in Chapter 10 and include discussions of research needs in the areas of biogeochemical characterization and continued biologically-active cap development.

CHAPTER 2.
LITERATURE REVIEW

2.1. Introduction

The United States Environmental Protection Agency (USEPA) defines aquatic sediments as contaminated when they contain chemical substances in excess of appropriate geochemical, toxicological, or sediment quality criteria, or are otherwise considered to pose a threat to human health or the environment (*1*). It has recently been estimated that approximately 10 percent of aquatic sediments underlying United States (U.S.) surface waters are sufficiently contaminated to pose potential risks to fish and to humans and wildlife that eat fish (*1*). This represents about 1.2 billion yards^3 of contaminated surface sediments, where many bottom-dwelling organisms live and where exchange processes between the sediment and overlying surface water can occur. In addition, approximately 300 million yards^3 of sediments are dredged from navigational waterways annually to maintain commerce, with 5 to 10 percent of that material sufficiently contaminated to require special handling and disposal (*1*). Thus, the scope of the sediment contamination problem in the U. S. is substantial. The spatial distribution of contaminated sediment sites appear to be focused in urban, industrialized locations. The United States Geological Survey (USGS) reported almost half of their sediment screening sites in urban settings contain contaminant concentrations which, they deemed, could cause adverse biological effects (*2*). Lopes and Furlong (*3*) examined over 500 sites in 20 river basins within the U.S. and concluded, in part, that urbanization had a profound, detrimental effect on sediment quality. Additionally, Van Metre and Mahler (*4*) analyzed

38 lakes in the U.S. and reported strong associations between the detection of organic sediment contaminants and urban environments.

The large extent of contaminated sediments, especially in populated areas, creates the need to protect the health of benthic and aquatic organisms as well as wildlife and humans. Contaminated sediments can create uninhabitable areas for benthic organisms, and documented adverse ecological effects from sediment contaminants include fin rot, increased tumor frequency, and reproductive toxicity in fish as well as decreased biodiversity in aquatic ecosystems (*1*). Sediment contaminants can also bioaccumulate in fish, birds, and mammals to levels that threaten neurological, developmental, and reproductive health (*5*). In order to reduce human pollutant exposures, the USEPA issues advisories against consuming fish from contaminated environments. In 2006, the USEPA issued 3,852 fish consumption advisories or bans because of risks stemming from pollutants such as polychlorinated biphenyls (PCBs), polycyclic aromatic hydrocarbons (PAHs), mercury, dioxins, and chlordane transferring into the food chain (*6*). These advisories represent 38% of the nation's total lake acreage, and 26% of the nation's total river miles. Moreover, a total of 22 states and the District of Columbia reported that 100% of their lake acres and river miles were under advisory for one or more contaminants (*6*). The USEPA fish advisories are intended to limit contaminant exposures associated with fish consumption, but they also limit recreational and economic usage of surface waters. Therefore, financial benefits or losses present an additional motivating factor for the remediation of contaminated aquatic sediments.

Impediments to sediment remediation include not only the sheer scope of contamination but also technical challenges and escalating costs associated with cleanup.

The amount of contaminated material present at a typical Superfund sediment site can extend from hundred of thousand to millions of cubic yards, creating multiple engineering challenges for cleanup (*7*). Sediment remediation methods are not as mature as groundwater techniques, and the development of *in situ* remediation techniques has recently been identified as a priority research need (*8*). *In situ* treatment techniques for groundwater contamination are generally more cost-effective compared to traditional methods (*9, 10*) and potentially shorten total treatment time. Translating such advantages to contaminated sediment sites is important considering that complete remediation of U.S. Naval sites alone, comprising approximately 200 identified sites, is estimated to cost over $1 billion (*8*). As of September 2005, remedies had been selected at more than 150 Superfund sediment sites, including eleven requiring sediment cleanup costs exceeding $50 million (*11*). The development of technically feasible and cost-effective *in situ* remediation approaches is therefore recognized as a high-priority research need for contaminated sediment management.

2.2. Contaminants in Aquatic Sediments

Sediments underlying surface waters can play dual roles of sink and source in regards to contaminant fate and transport. Contaminants are introduced into the sedimentary environment from a variety of sources, including: municipal sewage treatment plants; combined sewer overflows (CSOs); storm water discharges from municipal and industrial facilities; direct industrial discharges of process waste; runoff and leachate from hazardous and solid waste sites, agricultural operations, mining operations, and industrial manufacturing and storage sites; atmospheric deposition; and

contaminated groundwater discharges to surface water (*12*). Once introduced into aquatic sediments, hydrophobic organic contaminants (HOCs) are subject to long-term retention within the sediment via sorption to organic matter (*13*). Metals are also stored in the sediment and are typically bound to iron and manganese oxyhydroxides in the oxic layer (*14*) and to iron/sulfide precipitates in anaerobic regions (see further discussions in subsection 2.3.3). Sediments can also serve as contaminant sources, however, if pollutant concentrations within the sediment and porewaters exceed those in the overlying water, or if benthic organisms come in direct contact with pollutants.

Common sediment contaminants include PCBs, PAHs, pesticides, nutrients, and metals. Metals of concern typically found in aquatic sediments include copper, zinc, lead, cadmium, chromium, nickel, iron, manganese, and mercury (*12*). A list of contaminants detected at select United States Department of Defense (DOD) contaminated sediment sites is provided in Table 2.1 and illustrates that metals and HOCs are most commonly found at these sites (*15*). A survey of Naval sites exclusively (*16*) showed a slightly different contaminant distribution compared with other DOD data, as the most common contaminants reported were metals (76%), PCBs (72%), other hydrocarbons (72%), pesticides (55%), and fuels (45%). Temporal analysis of sediment HOCs using sediment cores to evaluate water-quality histories has revealed contaminant-specific trends. Downward temporal trends in PCB and dichloro-diphenyl-trichloroethane (DDT) sediment contamination have been reported in a variety of environmental settings (*4, 17, 18*) following regulatory control of these compounds. The rates of these decreases are slow and concentrations are still relatively high, suggesting these compounds persist and remain bioavailable for extended periods.

Table 2.1. Frequency of contaminant sub-group at DOD contaminated sediment sites with data. [a]

Contaminant Sub-Group	Number of DOD Sites Reporting Contaminants	Percentage of Sites Reporting Contaminants
Metals	913	81.0
Miscellaneous Inorganic Elements and Compounds	449	39.8
PAHs	445	39.5
Pesticides	369	32.7
Non-halogenated VOCs	263	23.3
Non-halogenated SVOCs	424	21.5
Halogenated VOCs	211	18.7
PCBs	165	14.6
BTEX	151	13.4
Phenols	84	7.5
Halogenated SVOCs	58	5.2
Explosives and Propellants	38	3.3
Other Organics (Coal Tar, Creosote)	4	0.4
Radioactive Materials	3	0.3
Other	2	0.2
No Group Determined	1	0.1

[a] Reproduced from USEPA, *Cleaning Up the Nation's Waste Sites: Markets and Technology Trends, Appendix C: Department of Defense Sites.* 2004, U.S. EPA Office of Solid Waste and Emergency Response. EPA 542-R-04-015.

A trend of increasing PAH contamination with time was reported by Van Metre and Mahler (*4*), who sampled 38 different lakes in the United States. A positive correlation between temporally increasing PAH concentrations and urbanization was found and the authors argue continued urbanization and development could lead to continued increases in sediment PAH contamination (*4*).

The discharge of contaminated groundwater plumes into aquatic sediments serves as an additional source of contamination and can often bring pollutants not traditionally found in aquatic sediments. Groundwater seepage into surface waters is common (*19*) and groundwater contaminants can be transported from upgradient source zones of residual or non-aqueous phase liquid (NAPL) (*10*) contamination. It is estimated that 75% of Superfund and Resource Conservation and Recovery Act (RCRA) sites are located within one half-mile of surface water bodies, with half of the Superfund sites reporting interaction between contaminated groundwater and surface water (*20*). Contaminants present in groundwater seeps threaten water quality and present dangers to the benthic community as well as to fish and humans. The chlorinated solvents tetrachloroethene (PCE) and trichloroethene (TCE) are common groundwater contaminants (*21*) whose plumes can extend considerable distances from their source to potentially discharge into surface water bodies (*22-27*) and are classified as either suspected or known carcinogens (*28*).

2.3. Contaminant Fate and Transport Processes within Sediments

Multiple fate and transport processes occur within aquatic sediment environments which can mobilize contaminants into porewaters and overlying surface waters and

become bioavailable. Generally, fine-grained sediments accumulate contaminants via sorption and immobilization and can serve as a contaminant reservoir to reduce toxic exposures to aquatic organisms. Changes in sediment biogeochemistry, however, can result in contaminant desorption or transformation to more bioavailable or toxic chemical forms. Contaminant mobility within sediments is often controlled by site-specific environmental variables (e.g., advective flow, redox conditions, organic matter content, etc.) in addition to molecular diffusion. The participation of contaminants in a particular pathway is dependent on chemical speciation of the contaminant and its associated physicochemical properties. Figure 2.1 presents a diagram of multiple contaminant mobilization pathways. Reible et al. (*29*) and Eggleton and Thomas (*30*) each provide reviews of contaminant fate and transport processes within aquatic sediments, and discussion here will be limited to only a few dominant processes relevant for the treatment of contaminants with an *in situ* cap at locations subject to advective transport.

2.3.1. Advective Transport

Advective transport can be a dominant process for porewater solute transport within the porewaters, provided flow rates are high enough. Documented groundwater seepage rates in aquatic sediments typically range between 0.0026 to 720 $cm \cdot day^{-1}$ (*31*); however, even a low advective flux can significantly alter contaminant behavior. Cornett (*32*) used a tritium tracer to observe groundwater flows through lake sediment and reported a significant influence of advective transport on porewater tracer profiles even at flow rates of less than 2.74×10^{-5} $cm \cdot day^{-1}$. Advective transport within sediments also leads to greater degree of contaminant dispersion in porewaters due to shear induced by velocity gradients (*33*).

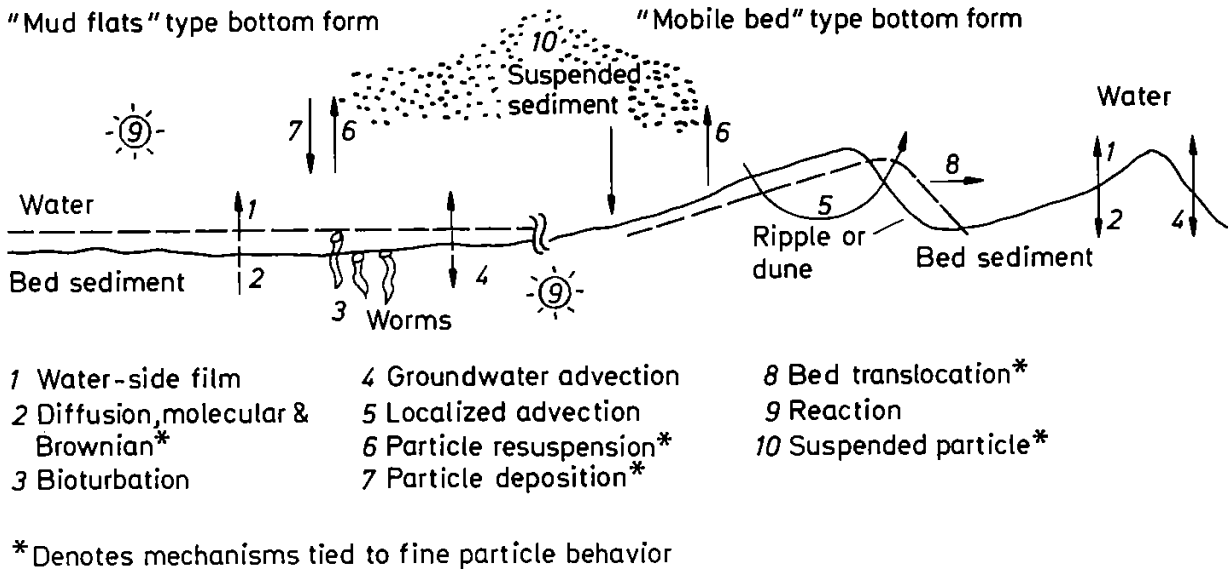

Figure 2.1. Contaminant transport processes between sediment and water under diffusive, "mud flats" conditions and advective, "mobile bed" conditions. Reproduced from (*29*).

Advective flow in stream sediments can also originate from cross-flow and hyporheic flow near the sediment-water interface (SWI) (*19*). Hyporheic flow paths, defined as flow patterns that begin in the surface waters, enter subsurface porewaters, then return to the surface waters, provide interactions between overlying water and biogeochemcially active sediment (*34*). Enhanced microbial rates of nitrification (*35*), uptake of dissolved organic carbon (*36*), and manganese oxidation (*37*) have all been documented in the hyporheic zone. Increased microbial activity impacts biotransformations and redox stratification within the sediment, in turn impacting contaminant fate and transport (see discussions below). Advective flows within contaminated sediments also result in the movement of sediment particles and possibly contaminant release (*38*). Many studies have investigated the role of colloid- and particle-facilitated transport of contaminants in sediments (see references (*39, 40*) as examples); however, sediment transport is not quantified in studies described herein and any effects of advective flow on contaminant fate and transport focuses solely on porewater solute transport. Likewise, effects of hyporheic and cross-flows are also not examined here, but included in Future Research Recommendations (Chapter 10).

2.3.2. Bioturbation

The sediment-water interface in biologically-active sediments is often continuously mixed by the activities of benthic macroinvertebrates such as clams and worms (see illustration of transport mechanism 3 in Figure 2.1). These activities include burrowing, ingestion/defecation, tube-building, and bio-deposition and are collectively referred to as bioturbation. The height of the bioturbation zone is typically 6-10 cm deep, but can extend significantly deeper (*29*). Burrows and tubes constructed by

macroinvertebrates provide more stable physical environments compared to surrounding bulk sediments, and also increase the effective surface area across which solutes can diffuse into or out of the sediments (*41*). As a result of their activity, bioturbating organisms create vertical and horizontal channels to enhance solute transport and exchange with overlying water (*33, 42-44*). Van Rees et al. (*45*) packed multiple columns with natural sediments, varying from a sandy sediment to peat, and found that the presence of benthic organisms increased apparent solute dispersion coefficients (D_m) by factors ranging from 1.6 to 15. Work et al. (*33*) performed experiments in a laboratory flume simulating bed sediments and reported that bioturbators initially reduced tracer concentrations by 5 to 40% in the upper sediment before advection and bioturbation reduced concentrations to insignificant levels, underscoring the mixing effects of bioturbators. They also found that bioturbation increases vertical concentration gradients, increasing vertical diffusion rates and impacting contaminant transport in deeper sediment layers despite the restriction of organisms to the SWI. Reible et al. (*46*) calculated that pyrene flux from their natural, bioturbated sediment would be 370 times greater than flux from a non-bioturbated sediment (*46*).

Another impact of bioturbation is the introduction of oxygen and other solutes into anoxic sediments when burrows and tubes are irrigated with surface waters (*43, 47*). Potentially inhibitory compounds can simultaneously be removed during this process (*48*). Additionally, burrow structures contain potential electron donors and acceptors which can support microbial activity and biomass at levels that are elevated relative to surrounding bulk sediments (*42, 49, 50*). Thus, bioturbation can enhance porewater transport and cause indirect changes in biogeochemical conditions and microbial activity.

2.3.3. Sorption/Immobilization

The sequestration of contaminants onto solid-phase particles within aquatic sediments is an important attenuation mechanism which removes toxic chemical species from the bioavailable aqueous phase. Allen (*51*) reviewed how metal toxicity to aquatic organisms is proportional to the concentration of free metal ions, emphasizing the significance of sorption/immobilization processes. Metal contaminants exhibit different affinities for each solid-phase sequestering fraction within sediments (Table 2.2). In oxic sediments regions, metal sequestration is generally dominated by Fe and Mn oxides and organic matter; whereas dominant sequestration processes in anoxic sediment regions are the formation of metal sulfides and partitioning onto organic matter (*14*). The sequestration of metals by microbial activity is also possible and has been reviewed in the literature (*52*). One example is the reduction of the mobile radionuclide U(VI) to immobile U(IV) by *Geobacter* (*53*), *Anaeromyxobacter* (*54*), and *Shewanella* (*55*) species. Examination of metal mobility is discussed in Future Research Recommendations (Chapter 10), however completed studies described herein do not analyze for metal contaminants, so discussion here will focus on HOC sorption.

The process of HOC sorption to soil and sediment solid materials has been intensively studied during the past twenty years and a detailed understanding has emerged. The predominant sorbent for HOCs in aquatic sediments is organic matter (*13*), which includes detritus, lignin, and humic substances (*56*). Kile et al. (*57*) demonstrated a positive relationship between HOC soil-water distribution coefficients for soils and sediments and organic matter content. The generally accepted mechanism of HOC sorption to organic matter is that neutral HOCs partition into natural organic matter to

Table 2.2. Contaminant sequestering agents found in aquatic sediments. [a]

Contaminant	Sequestering Agent in Sediment	Reference
Cu^{2+}	Sulfide	(*58*)
	Organic matter	(*58, 59*)
	Residual [b]	(*60-62*)
Pb^{2+}	Mn oxides	(*58, 60, 63*)
	Sulfides	(*64*)
Cd^{2+}	Fe/Mn oxides	(*63, 65, 66*)
	Organic matter	(*61*)
	Exchangeable cations/carbonates	(*58*)
	Sulfides	(*64*)
Zn^{2+}	Sulfides	(*61*)
Cr^{2+}	Fe/Mn oxides	(*58, 67*)
Ni	Residual	(*58*)
	Iron Sulfides	(*64*)
	Organic matter	(*64*)
PCBs	Mineral solids/organic matter	(*68*)
PAHs	Organic carbon	(*13, 69*)
Organotins	Organic matter	(*70*)
Methyl-mercury	Dissolved organic carbon	(*70, 71*)

[a] reproduced from Eggleton, J. and Thomas, K. V, 2004 (*30*).

[b] defined as the fraction of metals found in sediments but not bound to carbonates, iron-manganese oxides, metal-exchangeable sites, organic matter, and sulfides.

escape the polar environment of aqueous solutions (*72*). The ability of organic carbon to indefinitely sequester HOCs has stimulated the idea of organic sorbent addition to sediments to reduce contaminant bioavailability (*73-75*) (see discussion in subsection 2.4.3.2), and recent research has focused on the contribution of "black" carbon on the sorption of HOCs (see reference (*76*) as an example). The sorption of aqueous phase organic chemicals can be modeled using multiple approaches depending on sorbent/sorbate characteristics and resulting isotherm data. A Langmuir isotherm is utilized for systems exhibiting limited sorption capacities (*77*), but is rarely applicable to HOC sorption to organic matter. More suitable models of HOC sorption are the linear and Freundlich isotherms. The linear model assumes ideal partitioning behavior with a linear distribution coefficient (K_D) describing aqueous- and sorbed-phase concentrations. When HOC sorption into organic matter is the presumed dominant process, values of K_D can be calculated from the product of the soil fraction of organic carbon (f_{oc}) and the organic carbon partitioning coefficient (K_{oc}) (*77*). An experimental value of sedimentary fraction organic carbon content can therefore be calculated from linear isotherm data and known K_{oc} values. More complex discussions and mathematical descriptions of K_D are provided elsewhere (*72*). Substantial time periods may be required to reach equilibrium conditions, however (*78*), and slow sorption kinetics within sediments can lead to non-ideal behavior and requires more sophisticated process modeling. One- and two-site physicochemical nonequilibrium models incorporate rate-limited conditions between the contaminants and sorbents (*79*), demonstrated to be more representative of natural systems than assumed equilibrium conditions (*77, 80*). Causes for nonequilibrium sorption have been discussed and reviewed extensively (*78, 81*) and include retarded

intraparticle diffusion, intraorganic matter diffusion, and slow chemical kinetics. Physical nonequilibrium conditions, common within natural sediments, arise from macro- and pore-scale heterogeneities in hydrology causing some porewater to become immobile (*77*). The presence of physical nonequilibrium affects sorption as well as solute transport and is detected by unsymmetrical breakthrough curves of solutes (i.e., tracers) through porous media (*77*). From tracer tests, the amount of immobile porewaters can be calculated (*79*). As noted above, sediments can act as both a contaminant sink and source, and desorption represents a long-term HOC source (*82-85*) and a route of contaminant exposure to benthic organisms (*86-89*), despite slow desorption rates (*90, 91*) and observed hysteresis (*92-94*).

2.3.4. Transformations

Multiple contaminant transformation pathways exist within aquatic sediments and contribute to contaminant attenuation. Traditional sediment contaminants, as well as those introduced from groundwater plumes, can be transformed both abiotically and microbially within sediment beds with some pathways leading to non-toxic end products. Contaminant transformations will be defined here as a change in chemical composition of the contaminant in order to make a distinction from trace metals changing redox state (e.g., U(VI) to U(IV)).

2.3.4.1. Abiotic Transformations. Contaminant transformations at mineral surfaces occur within sediments and often are tied to specific redox conditions. The reducing nature of sediment beds leads to contaminant reduction, especially under iron-reducing conditions. The reduction of nitroaromatic contaminants by iron minerals has been demonstrated and subsequently studied extensively (*95-99*). Heijman et al. (*100*) proposed a cycling of

nitroaromatic reduction coupled to oxidation of surface-bound Fe(II) to Fe(III), followed by microbial reduction back to ferrous iron during heterotrophic organic matter oxidation (Figure 2.2). Williams et al. (*97*) used advanced spectroscopic techniques to confirm nitrobenzene reduction by Fe(II) adsorbed at the surface of various Fe(III)-containing minerals. These mechanisms are especially important for aquatic sediments, which are subject to transient redox fluctuations and reoxidation of reduced iron. The rates of chloronitrobenzene and hexachloroethane reduction by mineral-bound Fe(II) have been experimentally-derived for a suite of different iron minerals, including siderite ($FeCO_3$), nontronite (ferruginous smectite SWa-1), hematite (α-Fe_2O_3), lepidocrocite (γ-FeOOH), goethite (α-FeOOH), magnetite (Fe_3O_4), sulfate green rust ($Fe^{II}_4Fe^{III}_2(OH)_{12}SO_4 \cdot 4H_2O$), pyrite ($FeS_2$), and mackinawite (FeS) (*95*). The reduction of chlorinated organics has also been documented by zero-valent metals such as zinc (*101*) and iron (*102*).

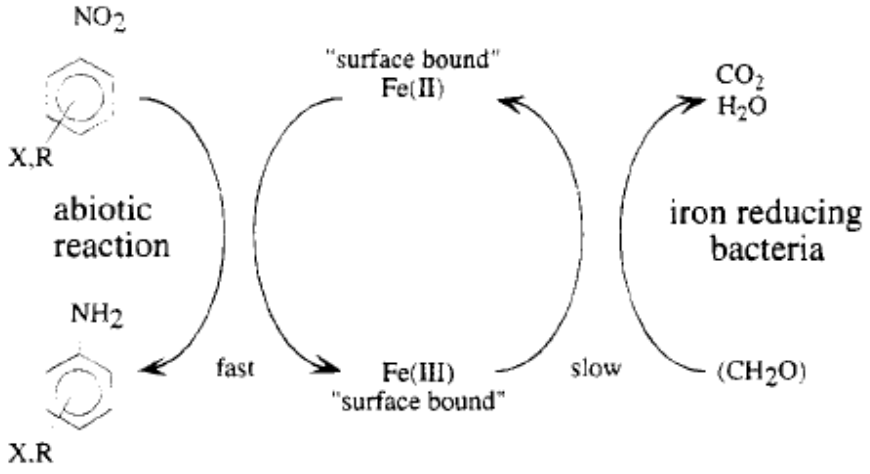

Figure 2.2. Proposed scheme of nitroaryl reduction and iron cycling coupled to heterotrophic organic matter oxidation. Reproduced from (*100*).

Cumulatively,these reductions demonstrate how numerous iron minerals, found both in oxic (goethite) and anoxic (pyrite) environments, can abiotically mediate dehalogenation and nitroaryl reduction, two important and environmentally-relevant mechanisms of contaminant transformations. Mercury methylation has been observed during sulfate reduction (*103*), which is a detrimental transformation due to the toxicity of methyl-mercury. PCBs and PAHs, two classes of HOCs which are traditional sediment contaminants, are observed to be generally recalcitrant to abiotic reactions.

2.3.4.2. Microbially-Mediated Transformations. Aquatic sediments tend to have active and diverse microbial communities due to their ample sources of organic matter, carbon, and electron donor. Significant positive relationships have been determined between sediment organic matter and bacterial abundance (*104*), production (*105*), respiration (*106*), and community composition (*107*). However, bacterial abundance and activity generally decrease with sediment depth due to the prevalence of more recalcitrant carbon sources below the surface (*108*). For example, terrestrial detritus and phytoplankton detritus settling at the SWI degrade at different rates; terrestrial detritus has a higher lignin content, is more recalcitrant, and thus has a greater chance of becoming buried and oxidized through anaerobic processes (*56*).

The high levels of bacterial abundance and activity in the aerobic layer promote oxidative contaminant biotransformations in this region. Hydrophobic organic contaminant classes vulnerable to aerobic biotransformation, and documented within sediments, include petroleum hydrocarbons, PAHs, certain PCBs, and certain chloroethenes. Aromatic petroleum hydrocarbons, collectively referred to as BTEX (benzene, toluene, ethylbenzene, and xylenes) are subject to aromatic ring cleavage via

monoxygenase or dioxygenase enzymatic attack to produce carbon dioxide (*109*). PAHs are not degraded as quickly as monoaromatic species but are still susceptible to ring fission via dioxygenase attack (*109*), carried out by multiple microbial populations (*110*). Certain PCB congeners are degraded aerobically (*111, 112*) following initial, anaerobic biotransformations, which increase their aerobic biodegradability and metabolism. The anaerobic, reductive dechlorination of PCBs has been reviewed (*113*) and recent evidence links PCB dechlorination with bacteria belonging the *Dehalococcoides* group (*114*). *Dehalococcoides* are also capable of complete reductive dechlorination of chlorinated solvents (e.g., PCE and TCE), which may be introduced into the sedimentary environment via contaminated groundwater plumes. PCE is sequentially dechlorinated by multiple bacterial strains under anaerobic conditions to TCE and dichloroethenes (DCEs), but only *Dehalococcoides* reduce DCEs to vinyl chloride (VC), and finally nontoxic ethene (*115-119*) (Figure 2.3). During this process, dissolved-phase chloroethenes serve as electron acceptors for *Dehalococcoides* while the source of electrons is hydrogen (*120, 121*), supplied from the oxidation of organic substrates by fermenting microbial communities (*122, 123*). In addition to PCBs and chloroethenes, *Dehalococcoides* organisms have been reported to dehalogenate chlorobenzenes (*124*), dioxins (*125*), chlorophenols (*126*), and polybrominated diphenyl ethers (*127*). *Dehalococcoides* and multiple other dechlorinating organisms capable of only partial dechlorination (i.e., dechlorination ceases at DCEs) have been detected in enrichments originating from river sediments (*128-130*). Daprato (*131*) provided a thorough review and description of several known organisms capable of chloroethene reductive dechlorination. In the aerobic sediment region, methanotrophic bacteria producing

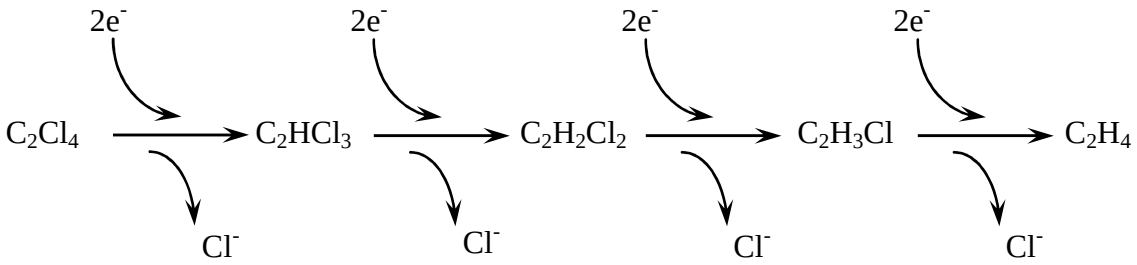

Figure 2.3. Pathway of reductive PCE dechlorination by *Dehalococcoides* strains.

monoxygenase enzymes can cometabolically degrade DCEs and VC (*132*, *133*) and represent an alternative detoxification pathway for chlorinated ethenes.

2.4. Sediment Remediation Methods

Remedial options for sediment reclamation are limited when compared to groundwater aquifer remediation, and consist of only monitored natural attenuation, sediment removal, and *in situ* capping. The choice of approach(es) is dependent on the contaminants and concentrations present, as well as site-specific variables (e.g., groundwater seepage, microbial activity, burial rate). Descriptions of each sediment remediation method are provided here, with emphasis placed on *in situ* capping.

2.4.1. Monitored Natural Attenuation

Monitored natural attenuation, also referred to as monitored natural recovery, relies on intrinsic sedimentary processes to gradually decrease contaminant concentrations with time. The most common natural attenuation processes occurring in sediments, listed from most to least effective, are (*7*): (1) abiotic or biotic contaminant transformation to less toxic forms; (2) sorption or binding to reduce contaminant mobility

and bioavailability; (3) sedimentation and burial of contaminants; and (4) dispersion to reduce contaminant concentrations. The transformation and sorption of contaminants, as discussed in Section 2.3, is dependent on site-specific characteristics such as mineralogy, microbial activity, and organic matter concentration. Sedimentation rates are also site specific and can lead to natural capping and the burial of contaminants. However, source control is necessary to prevent further contamination by freshly deposited particles (*7*). Dispersion includes molecular diffusion, mechanical dispersion under advection conditions, bioturbation, and dilution with overlying water to reduce aqueous phase concentrations. The applicability of monitored natural attenuation (MNA) at a site is predicated upon the presence and efficacy of these intrinsic processes.

Multiple lines of evidence are required to demonstrate MNA success (*7*), including decreased contaminant levels in higher trophic-level biota, overlying surface water, and surface sediments. Primary advantages of MNA include its relatively low economic costs and nondisruptive nature to the sedimentary environment. Limitations of MNA include the risk of continued contaminant exposure until the natural processes eventually reduce the exposure. Site-specific variables, such as sediment/contaminant movement induced by advection and flooding, insufficient burial rates, lack of source control, and slow contaminant transformation rates can reduce MNA effectiveness (*7*). Because of complex contamination and site characteristics, MNA has become the default remedial approach at many sites. Contaminant burial and microbial transformation have been documented at sites where MNA was selected (*134, 135*). Technical guidance documents provide more information regarding the applicability and effectiveness of monitored natural attenuation (*136*).

2.4.2. Contaminated Sediment Removal

Sediment removal has been the traditional approach for sediment remediation and is preferred over MNA because it can result in rapid contaminant mass removal from local environments. Sediment removal, either by dredging or excavation, ideally removes all contaminated surface sediments without leaving residual contamination at the SWI, while also minimizing sediment resuspension and subsequent contaminant release (*136*). Dredging is the removal of submerged material, while excavation refers to the removal of contaminated sediment after water has been diverted or drained. Sediment removal is the most common remedial technique applied for by the Superfund program at sediment sites, with sediment removal selected as a cleanup method at more than 100 Superfund sites (*136*). Detailed descriptions of sediment removal are provided elsewhere (*136*), with only brief discussions provided here.

The primary advantage of sediment removal is that it minimizes uncertainty regarding future contaminant exposure, provided that adequate clean-up levels are met. Other advantages of sediment removal are faster time scales needed to achieve remedial goals (relative to MNA and *in situ* capping) and greater flexibility for water body use following treatment (*136*). Potential limitations with the method include increased cost and complexity associated with mobilization of equipment and implementation of the technique compared to other options. It is also difficult to estimate residual contamination following dredging/excavation. The potential for resuspension of sediment particles during dredging operations presents another route of contaminant exposure and transport (*136-141*) and can be a significant deterrent. Both dredging and excavation also necessitate transportation of contaminated sediment to a location for ex-

situ treatment and/or disposal. Finally, sediment removal causes a temporary destruction of the aquatic community and habitat within the remediation area. Reible et al. (*142*) examined long term risks associated with sediment dredging for the Fox River, WI and provide additional discussion on beneficial and detrimental effects of dredging. The potential for residual contamination, sediment resuspension and subsequent contaminant release, and the necessity to treat removed sediment ex situ, has also contributed to a need for more advanced technologies.

2.4.3. *In Situ* Capping

In situ capping is the subaqueous placement of clean fill material at the SWI in attempt to prevent contact of sediment contaminants with overlying surface waters and benthic macrofauna. Depending on the contaminants and sediment environment, a cap is designed to reduce risk through (*136*): (1) physical isolation of sediment to reduce direct contact of burrowing organisms and bioturbation; (2) stabilization of sediment to reduce resuspension and transport to other sites; and/or (3) chemical isolation of sediment to reduce exposure from dissolved and colloidally bound contaminants. As of 2004, *in situ* capping (also referred to as subaqueous capping or sediment capping) has been selected as a component of the remedy at approximately fifteen Superfund sites (*136*). At some sites, capping has served as the primary treatment approach, while at other sites it has been combined with sediment removal (i.e., dredging or excavation) and/or MNA. Table 2.3 provides details from selected capping operations, compiled by Palermo et al. (*143*) in 1998, while a more comprehensive listing of over 100 capping sites is provided by the South and Southwest branch of the Hazardous Substance Research Center (HSRC-SSW) (*144*). Palermo (*145*) summarized design considerations for *in situ* capping and outlined

them at length in a technical document submitted to the USEPA (*143*). Examples of site conditions conducive to *in situ* capping are:

- Suitable types and quantities of cap material are readily available
- Anticipated infrastructure needs (e.g., piers, pilings) are compatible with cap
- Water depth is adequate to accommodate cap with anticipated uses
- Chances of cap-disrupting human behavior (e.g., anchoring) are low/controllable
- Long-term risk reduction outweighs habitat disruption, and/or habitat improvements are provided by the cap
- Hydrodynamic conditions not likely to compromise cap or can be designed for
- Groundwater flow rates are low and unlikely to create contaminant releases
- Sediment has sufficient strength to support cap
- Contaminants have low rates of flux through cap
- Contamination covers contiguous areas (e.g., to simplify capping)

The major advantage of *in situ* capping is that it can quickly reduce exposure to contaminants (*136*). A cap designed and placed properly should reduce the exposure of fish and biota to contaminated sediment faster than dredging, since contaminant residual at the cap-water interface should be none. Also, caps provide a clean habitat for recolonization by benthic organisms and more desirable environmental conditions (oxic) may be caused by changes in bottom elevation. Capping should also eliminate contaminant mixing via bioturbation, which typically extends 10 cm into the sediment, since *in situ* caps are generally designed to be 30 cm thick or greater. Another substantial advantage is that capping practically eliminates risks derived from resuspension,

Table 2.3. Summary of selected *in situ* capping projects. [a]

Project Location	Contaminants	Site Conditions	Cap Design	Construction Methods
Kihama Inner Lake, Japan	Nutrients	3,700 m^2	Fine sand 5 and 20 cm	-
Akanoi Bay, Japan	Nutrients	20,000 m^2	Fine sand 20 cm	-
Denny Way, Washington	PAHs, PCBs	3 acres nearshore with depths from 20 to 60 ft.	Avg 2.6 ft sandy sediment	Barge spreading
Simpson-Tacoma, Washington	cresote, PAHs, dioxins	17 acres nearshore with varying depth	4 to 20 feet of sandy sediment	Hydraulic pipeline with "sandbox"
Eagle Harbor, Washington	cresote	54 acres within embayment	3 ft of sandy sediment	Barge spreading and hydraulic jet
Sheboygan River, Wisconsin	PCBs	several small areas of shallow river/floodplain	sand layer with armor stone	Direct mechanical placement
Manistique River, Michigan	PCBs	20,000 ft^2 shoal in river with depths of 10-15 ft	40 cm plastic liner	Placement by crane from barge
Hamilton Harbor, Ontario	PAHs, metals, nutrients	10,000 m^2 portion of large, industrial harbor	0.5 m sand	Tremie tube
Eitrheim Bay, Norway	metals	100,000 m^2	geotextile and gabions	Deployed from barge
St. Lawrence River, Massena, New York	PCBs	75,000 ft^2	6 in sand/6 in gravel/ 6 in stone	Placed by bucket from barge

[a] reproduced from Palermo, M.R., Maynord, S., Miller, J., Reible, D.D. (*143*)

dispersion, and volatilization of contaminated materials during dredging/excavating operations. Relative to dredging and excavation, capping requires less infrastructure in terms of material handling, dewatering, treatment, and disposal. This is advantageous by allowing most capping projects to employ conventional equipment and locally available materials, with quicker implementation and with fewer costs. Capping is also perceived as a more aggressive treatment compared to MNA, and may carry additional public support.

The major limitation of *in situ* capping is that contaminants remain in the aquatic environment and can be re-dispersed if the cap is either significantly disturbed (i.e., scour) or if contaminants move through the cap. The general problem of contaminant re-mobilization is best alleviated if contaminant attenuation processes (e.g., biotransformations) occur below the cap. However, knowledge regarding natural attenuation processes below a cap remains largely unknown. To specifically prevent cap disturbances, cap designs have been proposed for high-energy environments which include armoring layers at the cap-water interface (*136*, *146*). Additionally, institutional controls can be imposed to limit activities in the water body and protect the cap from disturbances such as boat anchoring. To address the issue of eventual contaminant breakthrough of caps, research has focused on the development of active caps (see subsection 2.4.3.2). Another potential limitation of capping involves the physical placement of caps, which in some environments can cause compaction and disruption of the underlying sediment. For example, Zeman (*147*) discussed a field site where capping was expected to result in a 14 to 21 cm consolidation of underlying sediment. The consolidation can result in a transient, advective pulse of contaminated sediment

porewaters. Moo-Young et al. (*148, 149*) have attempted to experimentally simulate capping-induced sediment consolidation via centrifugation and modeled their results using an analytical solution for the advection-dispersion equation. Alshawabkeh et al. (*150*) developed a transient transport model to estimate mass flux following sediment consolidation and concluded that advective transport following cap placement accelerated contaminant breakthrough of a cap by orders of magnitude. The authors advocated active caps as a method of reducing dissolved contaminant flux. Another noted limitation of *in situ* capping may be the disruption of habitats which may not be adequately replaced by capping material (*136*). To provide erosion protection, it may be necessary to use coarse cap materials that are different from native soft bottom materials, which may alter the biological community. However, discussions of microbiological colonization of capping materials are not provided in the literature, while discussions of macrofaunal colonization are sparse and site-specific (*144*).

2.4.3.1. Traditional Capping Approaches

Traditional caps have generally been composed of uncontaminated granular materials, such as upland sand-rich soils or sandy sediment, which are resistant to scour and allow for cap placement via deposition. A review of over 100 capping sites (*144*) shows that sand (or sand-dominated natural sediments) has been the most common material employed for capping. The general availability and lower cost of natural sands is one notable advantage of their employment in capping operations. Sand caps have been estimated to reduce HOC breakthrough from sediments to overlying water by hundreds to thousands of years under purely diffusive conditions, depending on cap thickness (*151*). Bulk sand materials are typically regarded as possessing no significant

capabilities for contaminant sequestration and transformation. Therefore sand-based caps do not perform as well at sites where contaminant transport is not limited by diffusion, specifically when advection is present in the form of groundwater seeps or hyporheic flowpaths.

2.4.3.2. Active Capping Approaches

Active caps incorporate constituents designed to sequester or transform contaminants in the cap to provide a means of contaminant removal. Active caps should therefore eliminate the threat of contaminant breakthrough with time and can be utilized at locations dominated by advective flow (e.g., groundwater seeps). The transformation of contaminants within active caps also addresses concerns regarding long-term storage of contaminants in sediments. The development and demonstration of active cap amendments for contaminant sequestration and/or degradation has therefore been identified as a high research priority by SERDP and ESTCP (*152*). Constituents and materials proposed for active caps include phosphate minerals (*153*) and zeolites (*154*) for metals control, clays and cements (*155*) for permeability control, and organoclays, sorbents (*73, 156*), and reactive chemical species (*157*) for HOC control. Commercially available active capping technologies include AquaBlok™, a clay barrier distributed for capping applications by Adventus Americas, Inc. (www.aquablokinfo.com), organoclay materials from CETCO (www.sedimentremediation.com), and a suite of Reactive Core Mats (RCM) and liners also marketed by CETCO. Pilot-scale demonstration and performance monitoring of some of these materials (apatite, coke, AquaBlok™) is currently being conducted by HSRC-SSW (*158*).

The employment of physicochemical-based active caps has limitations, such as inherent ceilings for sorption and reaction, thus requiring replenishment of the active materials. Also, surface fouling of the sorptive/reactive constituents may occur and lead to lower treatment efficiencies (*158*). The employment of clay-based materials (e.g., organoclays, AquaBlok™) can also (intentionally or accidentally) divert flow patterns within sediments, leading to changes in contaminant attenuation processes. These limitations have stimulated the idea of a biologically-active (bioreactive) *in situ* cap in which contaminants are transformed to nontoxic products via microbially mediated reactions within the cap. Microorganisms can detoxify a range of environmental contaminants, including many HOCs (see subsection 2.3.4.2 above), and may provide a new arena of active cap development. Bioreactive caps, similar to physicochemically-active caps, could theoretically be placed at sediment sites subject to groundwater discharge for the treatment of both sediment contaminants (e.g., PCBs) and groundwater contaminants (e.g., chlorinated solvents). Research into the application of a bioreactive barrier at the SWI has not been previously reported. However, enhanced bioremediation approaches for groundwater aquifer remediation, specifically biostimulation and bioaugmentation, have been studied extensively and may provide insight for the development of a bioreactive cap. Biostimulation is the addition of substrate to the contaminated matrix to promote the activity of indigenous organisms capable of contaminant biotransformation. The addition of fermentable substrates as electron donors is the most commonly employed approach for biostimulation and often accompanies bioaugmentation. Bioaugmentation is the addition of exogenous organisms capable contaminant degradation into the contaminated matrix, and is generally

performed when the organism(s) required to degrade the contaminant is absent or present in low abundance. Many pilot- and field-scale studies have utilized enhanced bioremediation to successfully treat chlorinated solvent contamination in subsurface aquifers (*159-165*). However, none have investigated the application of a single-pass biobarrier placed at the SWI and the challenges associated with such a location. One such challenge is to design the cap to accommodate the biogeochemical response of native sediments following the perturbation of *in situ* cap placement, and ensuring that the resulting redox environments within the cap are conducive to a microbial community performing biotransformations of contaminants.

2.5 Characterization of Biogeochemical Processes within Sediments

Biogeochemical cycling of nutrients and elements near the sediment-water interface of aquatic sediments can be complex and dependent on a number of site-specific variables (e.g., hydrodynamics, bioturbation, organic matter deposition, anthropogenic contamination). Undisturbed aquatic sediments underlying oxic surface waters typically possess an aerobic layer extending only millimeters to centimeters into the sediment bed (*166*). Dissolved oxygen concentrations generally decrease linearly through a diffusive boundary layer (DBL) at the SWI; however, the DBL can be altered by the presence of photosynthetic organisms and light/dark cycling (*166, 167*). Meanwhile, the depth of oxygen penetration correlates inversely to organic carbon content of sediments (*56*). Examples of oxygen profiles at the SWI are provided in Figures 2.4A-B, which also demonstrate the effect of bioturbation. Beneath the aerobic layer exists a gradient of anaerobic biogeochemical processes, stratified according to thermodynamic yields

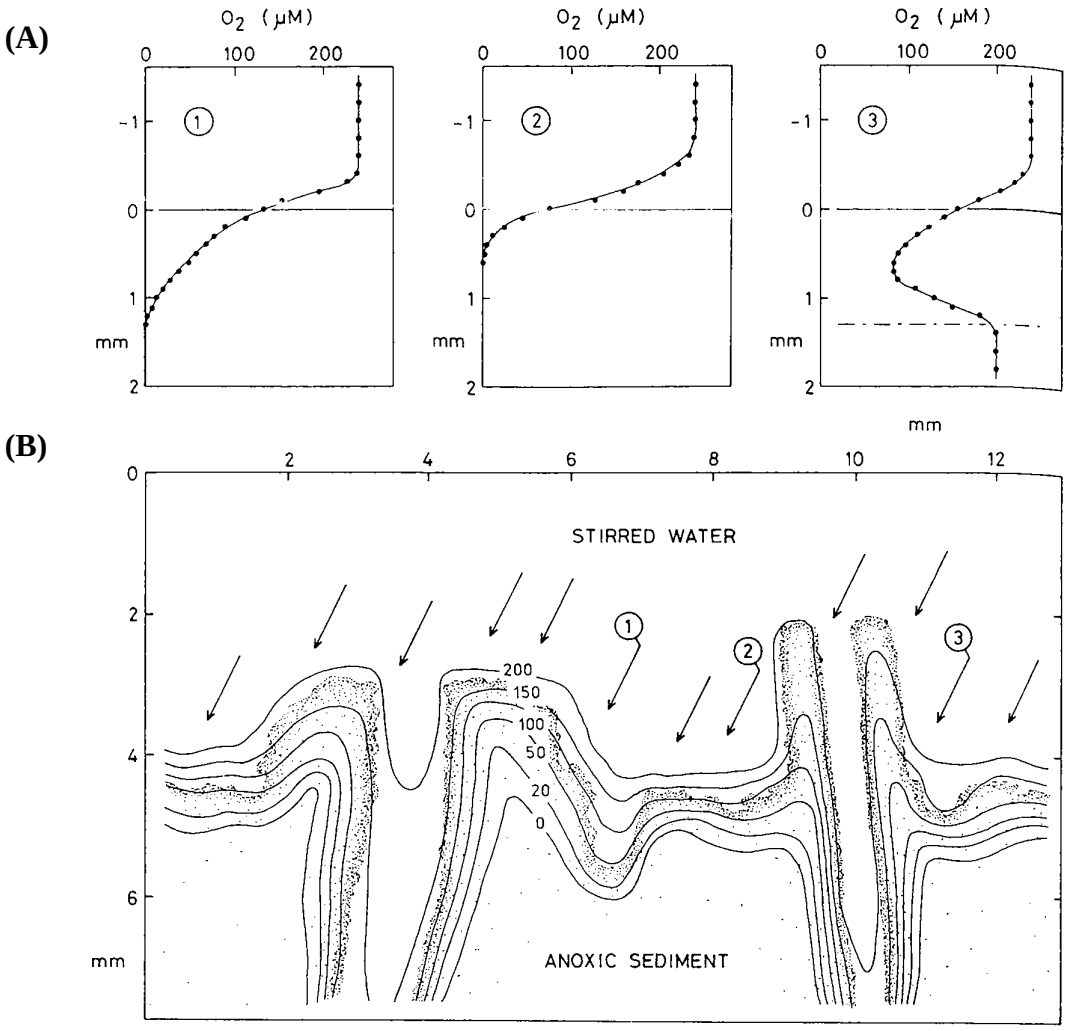

Figure 2.4A-B. Dissolved oxygen concentrations at the sediment-water interface of an organic-rich shallow water environment determined with microelectrodes. (A) Three plots displaying oxygen profiles corresponding to the numerically-marked locations in (B). (B) Isopleths representing dissolved oxygen concentrations (μmol liter^{-1}) at the sediment-water interface. The tubular structures are burrows from bioturbating polychaetes. Arrows indicate locations and trajectories of microprofiles, three of which are provided in (A). Figures are reproduced from Jørgensen and Revsbech (*166*).

corresponding to their terminal electron accepting processes (TEAPs) (*168*). Discussions redox stratification and the cycling of selected elements are the focus of the first subsection here, followed by section on analytical tools for biogeochemical monitoring.

2.5.1. Geochemical Stratification and Speciation of Redox-Sensitive Elements

Organic matter oxidation coupled to discrete regions of dissimilatory microbial reduction of nitrate (via denitrification and NO_3^- reduction), manganese, iron (freshwater), and sulfate (marine) are observed in redox stratified sediments. Figure 2.5, reproduced from Stumm and Morgan (*169*), gives equilibrium constants for redox processes in aquatic sediments. Figure 2.6A arranges terminal electron accepting processes from most favorable to least favorable, and a simple schematic illustrating redox stratification in sediments is presented in Figure 2.6B. This stratification is more commonly observed in systems containing excess organic matter. Fermentative and methanogenic conditions indicative of strongly reducing conditions occur at or below sulfate reduction (*169*). The relative sizes of redox zones are determined by factors including temperature, hydrology, mixing, and bioturbation activity, which together influence organic matter oxidation and TEAPs. For example, seasonal variations in sediment biogeochemistry and redox zonation, have been observed in sediments resulting from increased microbial activities during warmer spring and summer seasons (*170-172*). Also, Sell and Morse (*173*) demonstrated that changes in overlying oxygen concentrations can also impact the spatial distributions of iron- and sulfate-reducing zones. No previous research has investigated the impact of *in situ* capping on sedimentary redox processes and stratification. Chemical speciation and cyclings of nitrogen, manganese, iron, sulfur, and carbon within aquatic sediments are dependent on

Reaction		pε° (= log K)	pε° (W)[a]
(1) $\frac{1}{4}O_2(g) + H^+ + e^-$	$= \frac{1}{2}H_2O$	+20.75	+13.75
(2) $\frac{1}{5}NO_3^- + \frac{6}{5}H^+ + e^-$	$= \frac{1}{10}N_2(g) + \frac{3}{5}H_2O$	+21.05	+12.65
(3) $\frac{1}{2}MnO_2(s) + \frac{1}{2}HCO_3(10^{-3}) + \frac{3}{2}H^+ + e^-$	$= \frac{1}{2}MnCO_3(s) + H_2O$	—	+8.9[b,c]
(4) $\frac{1}{2}NO_3^- + H^+ + e^-$	$= \frac{1}{2}NO_2^- + \frac{1}{2}H_2O$	+14.15	+7.15
(5) $\frac{1}{8}NO_3^- + \frac{5}{4}H^+ + e^-$	$= \frac{1}{8}NH_4^+ + \frac{3}{8}H_2O$	+14.90	+6.15
(6) $\frac{1}{6}NO_2^- + \frac{4}{3}H^+ + e^-$	$= \frac{1}{6}NH_4^+ + \frac{1}{3}H_2O$	+15.14	+5.82
(7) $\frac{1}{2}CH_3OH + H^+ + e^-$	$= \frac{1}{2}CH_4(g) + \frac{1}{2}H_2O$	+9.88	+2.88
(8) $\frac{1}{4}CH_2O + H^+ + e^-$	$= \frac{1}{4}CH_4(g) + \frac{1}{4}H_2O$	+6.94	−0.06
(9) $FeOOH(s) + HCO_3^- (10^{-3}) + 2H^+ + e^-$	$= FeCO_3(s) + 2H_2O$	—	−0.8[b,c]
(10) $\frac{1}{2}CH_2O + H^+ + e^-$	$= \frac{1}{2}CH_3OH$	+3.99	−3.01
(11) $\frac{1}{6}SO_4^{2-} + \frac{4}{3}H^+ + e^-$	$= \frac{1}{6}S(s) + \frac{2}{3}H_2O$	+6.03	−3.30
(12) $\frac{1}{8}SO_4^{2-} + \frac{5}{4}H^+ + e^-$	$= \frac{1}{8}H_2S(g) + \frac{1}{2}H_2O$	+5.25	−3.50
(13) $\frac{1}{8}SO_4^{2-} + \frac{9}{8}H^+ + e^-$	$= \frac{1}{8}HS^- + \frac{1}{2}H_2O$	+4.25	−3.75
(14) $\frac{1}{2}S(s) + H^+ + e^-$	$= \frac{1}{2}H_2S(g)$	+2.89	−4.11
(15) $\frac{1}{8}CO_2(g) + H^+ + e^-$	$= \frac{1}{8}CH_4(g) + \frac{1}{4}H_2O$	+2.87	−4.13
(16) $\frac{1}{6}N_2(g) + \frac{4}{3}H^+ + e^-$	$= \frac{1}{3}NH_4^+$	+4.68	−4.68
(17) $H^+ + e^-$	$= \frac{1}{2}H_2(g)$	0.0	−7.00
(18) $\frac{1}{4}CO_2(g) + H^+ + e^-$	$= \frac{1}{24}(glucose) + \frac{1}{4}H_2O$	−0.20	−7.20
(19) $\frac{1}{2}HCOO^- + \frac{3}{2}H^+ + e^-$	$= \frac{1}{2}CH_2O + \frac{1}{2}H_2O$	+2.82	−7.68
(20) $\frac{1}{4}CO_2(g) + H^+ + e^-$	$= \frac{1}{4}CH_2O + \frac{1}{4}H_2O$	−1.20	−8.20
(21) $\frac{1}{2}CO_2(g) + \frac{1}{2}H^+ + e^-$	$= \frac{1}{2}HCOO^-$	−4.83	−8.33

[a]Values for pε° (W) apply to the electron activity for unit activities of oxidant and reductant in neutral water, that is, at pH = 7.0 for 25°C.

[b]These data correspond to $(HCO_3^-) = 10^{-3}$ M rather than unity and so are not exactly pε° (W); they represent typical aquatic conditions more nearly than pε° (W) values do.

[c]Alternatively one may consider the reaction.
$\frac{1}{2}MnO_2(s) + 2H^+ + e^- = \frac{1}{2}Mn^{2+}$ $(10^{-6}$ M) $+ H_2O$; pε° (W) = 9.8

[d]$Fe(OH)_3(am) + 3H^+ + e^- = (Fe^{2+})$ $(10^{-6}$ M) $+ H_2O$; pε° (W) = 1.0

Figure 2.5. Table of environmentally-relevant reductions and corresponding equilibrium constants, arranged from most favorable to least. Reproduced from Stumm and Morgan (*169*).

(A)

O_2 consumption (respiration)		
$\frac{1}{4}\{CH_2O\} + \frac{1}{4}O_2$	$= \frac{1}{4}CO_2 + \frac{1}{4}H_2O$	(1)
Denitrification		
$\frac{1}{4}\{CH_2O\} + \frac{1}{5}NO_3^- + \frac{1}{5}H^+$	$= \frac{1}{4}CO_2 + \frac{1}{10}N_2 + \frac{1}{2}H_2O$	(2)
Nitrate reduction		
$\frac{1}{4}\{CH_2O\} + \frac{1}{8}NO_3^- + \frac{1}{4}H^+$	$= \frac{1}{4}CO_2 + \frac{1}{8}NH_4^+ + \frac{1}{8}H_2O$	(3)
Production of soluble Mn(II)		
$\frac{1}{4}\{CH_2O\} + \frac{1}{2}MnO_2(s) + H^+$	$= \frac{1}{4}CO_2 + \frac{1}{2}Mn^{2+} + \frac{1}{8}H_2O$	(4)
Fermentation		
$\frac{3}{4}\{CH_2O\} + \frac{1}{4}H_2O$	$= \frac{1}{4}CO_2 + \frac{1}{2}CH_3OH$	(5)
Production of soluble Fe(II)		
$\frac{1}{4}\{CH_2O\} + FeOOH(s) + 2H^+$	$= \frac{1}{4}CO_2 + \frac{7}{4}H_2O + Fe^{+2}$	(6)
Sulfate reduction, production of H_2S		
$\frac{1}{4}\{CH_2O\} + \frac{1}{8}SO_4^{2-} + \frac{1}{8}H^+$	$= \frac{1}{8}HS^- + \frac{1}{4}CO_2 + \frac{1}{4}H_2O$	(7)
Methane fermentation		
$\frac{1}{4}\{CH_2O\}$	$= \frac{1}{8}CH_4 + \frac{1}{8}CO_2$	(8)

(B)

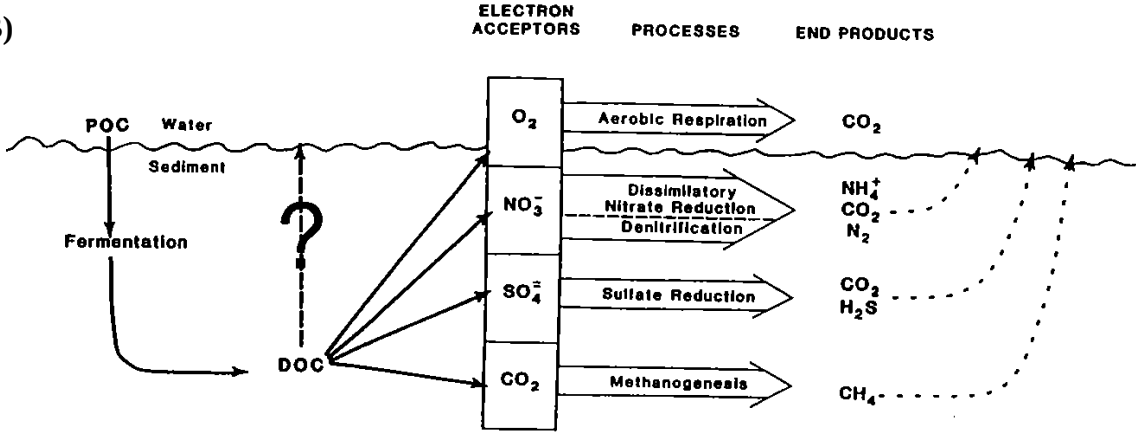

Figures 2.6A-B. (A) The sequence of redox reactions observed in a system with excess organic matter (CH_2O). Processes are listed from most favorable, at the top, to least favorable, at the bottom. Reproduced from Stumm and Morgan (*169*). (B) Schematic of stratified redox processes within a sediment bed following deposition of organic carbon (POC). Dissolved organic carbon (DOC) compounds are utilized by vertically separated terminal electron accepting processes in aquatic sediments. Solid arrows represent anaerobic metabolic pathways while dashed arrows indicate diffusive efflux of dissolved organic and inorganic compounds from the sediments to the overlying water. Reproduced from Carlton and Klug (*56*).

various abiotic and biological factors. Identifying the exact speciation of these elements can provide information regarding prevailing redox conditions, stratification, and biogeochemical processes at a particular location. (Use of the term species in this subsection refers to the form in which a molecule or ion is present in solution.)

2.5.1.1. Nitrogen. Multiple species and oxidation states of nitrogen exist within sediments, ranging from nitrate (NO_3^-; +5 oxidation state) to nitrogen gas (N_2; neutral oxidation state) to ammonium (NH_4^+; -3 oxidation state). In vertically stratified sediments, nitrate reduction typically occurs just below the aerobic layer after dissolved oxygen has been depleted. Nitrate is then reduced via denitrification to produce N_2 via NO_2^-, NO, and N_2O under reducing conditions. Partial denitrification is also observed, as well as nitrate reduction to ammonium (NH_4^+). Nitrogen speciation was not analyzed experimentally in studies comprising this dissertation.

2.5.1.2. Manganese. Manganese predominantly exists as solid Mn(IV) and Mn(II) in aquatic sediments, although some solid Mn(III) oxides can be formed. Reduction of Mn(IV) oxides and oxyhydroxides (collectively referred to as (hydr)oxides) occurs at lower redox potentials than nitrate, and slightly higher redox potentials than iron (hydr)oxides. Therefore, manganese-reducing redox zones are generally observed above iron reduction in vertically stratified sediments. In the aerobic sediment region, aqueous manganese is chemically stable only as solid oxides, such as $MnO_{2(s)}$, and are generally immobile. Reduced forms of manganese can also exist as solids, exemplified by $MnCO_{3(s)}$, and are also immobile.

During sediment burial, (reductive) dissolution of manganese solids occurs, releasing soluble Mn^{2+} up to 10^{-3} M (*169*). Manganese (hydr)oxides are also susceptible

to abiotic reduction reactions upon burial and exposure to anaerobic conditions. For example, Figure 2.7 demonstrates how the production of hydrogen sulfide can abiotically reduce $MnO_{2(s)}$ to produce Mn^{2+} (*174*). Relatively fast manganese reduction can also be achieved by ferrous iron (*175*), leading to Mn^{2+} production (see subsection 2.5.1.3 for further discussions). Soluble Mn^{2+} is also produced during dissimilatory microbial manganese reduction. Many microbial species have been identified from various environmental settings that can reduce oxidized manganese (*55*), including *Geobacter* spp. and *Shewanella* spp. (*55, 176*). Following manganese reduction, Mn^{2+} can be

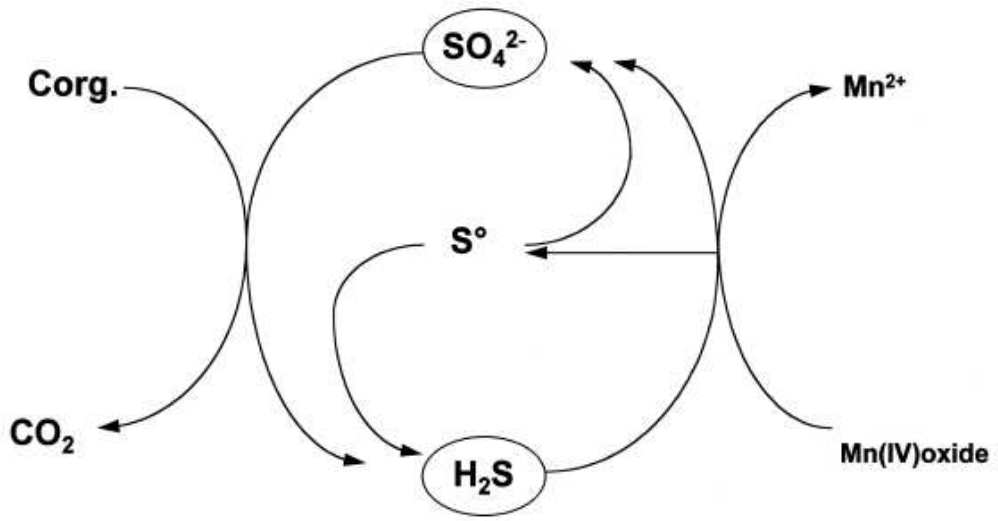

Figure 2.7. Simplified sedimentary sulfur cycle illustrating the role of bacterial sulfur disproportionation and the influence of Mn(IV)oxides. Reproduced from Böttcher and Thamdrup (*174)*.

removed from solution via multiple pathways. Free Mn^{2+} is susceptible to adsorption and precipitation, causing porewater concentrations of Mn^{2+} to generally be much smaller than solid Mn(II) (*177*). Reduced, soluble manganese in porewaters tends to diffuse back to the oxic/anoxic interface where it can be reoxidized and precipitated as (hydr)oxides. Abiotic oxidation of Mn^{2+} by dissolved oxygen is typically slow below pH 9 (*178, 179*), potentially leading to the release of Mn^{2+} to overlying waters. However microbially-catalyzed oxidation of reduced manganese can be rapid (*177*). A depletion of manganese from anoxic regions therefore occurs, with strong enrichment above the oxic/anoxic interface (*177*). More information on manganese (and iron) speciation and reduction is provided in reviews by Thamdrup (*177*) and Lovley et al. (*55*).

For detection of manganese-reducing redox zones, it should be emphasized that the presence of Mn^{2+} in porewater profiles indicates reducing conditions and is important for demonstrating manganese reduction.

2.5.1.3. Iron. Iron exists as ferric (III), ferrous (II), and elemental (Fe^0) forms in sediments, with the reduction of Fe(III) species at circumneutral pH is less energetically favorable than manganese reduction. Energy yields are dependent upon Fe(III) speciation and reduction potentials increase with decreasing pH (*177*). Iron is typically observed below manganese in vertically stratified sediments. Iron speciation and cycling is similar to manganese in some respects, since both have soluble reduced forms and insoluble (hydr)oxides in oxic conditions, but key differences also exist. The main oxidation product of iron is ferrihydrite (ferric (hydr)oxide) $Fe(OH)_3$, but many amorphous or poorly crystalline Fe oxides can also be formed. Canfield (*180*) surveyed U.S. rivers and found that, on average, 35% of iron found in particulates was composed

of crystalline and amorphous/poorly crystalline Fe, partitioned into roughly equal amounts. Similar ratios have been identified in marine surface sediments (*181*). This means that only about 20% of iron is in the amorphous/poorly crystalline form, which conventionally has been believed to be the available Fe form for microbial iron reduction. Recent studies have identified methods of crystalline iron reduction by microorganisms however (*182-186*). For instance, complexation of Fe(III) with organic ligands (organic-$Fe^{III}_{(aq)}$) can solubilize iron for microbial utilization. Multiple ligands are naturally present in organic matter which can form complexes with ferric iron (*187*). A detailed listing of known iron reducing species was provided by Lovley et al. (*55*) in 2004, which included strains of *Anaeromyxobacter*, *Geobacter*, and *Shewanella*. A more recent compilation of knowledge regarding microbial iron reduction and oxidation is available from Weber et al. (*188*).

Microbial iron reduction is a major biogeochemical process in many environments, however abiotic reductions of ferric iron can also be important. Ferric (hydr)oxides can be abiotically reduced by hydrogen sulfide (*189, 190*), producing Fe^{2+} and elemental sulfur as products, with reaction rates dependent on Fe(III) speciation. Free ferrous iron is less soluble and is reoxidized faster than the equivalent manganese species (Mn^{2+}). Many Fe(II) precipitates can be formed with carbonates, phosphates, and sulfides. Pyrite (FeS_2) is one of the most common forms of iron and is formed from ferrous sulfide when reduced sulfur is present (see subsection 2.5.1.4 for further discussions on iron sulfides). Pyrite and other solid iron sulfide precipitates serve to remove Fe^{2+} from the aqueous phase. Ferrous iron remaining in the aqueous phase can migrate to the anoxic/oxic boundary and become reoxidizied abiotically by manganese

dioxides (*175*) or oxygen (*191*) to produce iron (hydr)oxides. A schematic illustrating relative concentrations and cycling of Fe(II, III) at the anoxic/oxic interface is present in Figure 2.8. Oxidation of Fe^{2+} by nitrate is negligible at environmentally-relevant temperatures and aqueous conditions, however nitrate-reducing microorganisms are capable of enzymatic oxidation of Fe(II) and this process has been observed in several freshwater sediments [see (*188, 192*) and references therein]. Anaerobic microbial oxidation of ferrous iron can also occur by anaerobic photoautotrophs. Oxidation of ferrous iron by aerobes in the oxic sediment layer also occurs, but the contribution of this process to overall iron oxidation, in comparison to rapid abiotic oxidation, is under debate (*188*).

The detection of Fe^{2+} during porewater monitoring is a diagnostic indicator for iron reduction and anaerobic conditions. Additionally, peaks in Fe^{2+} concentration, as

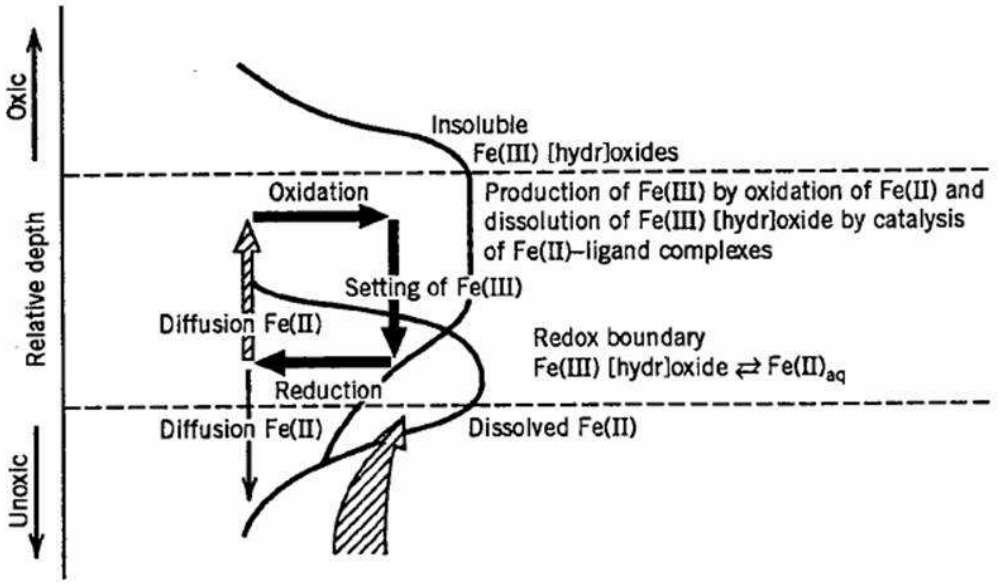

Figure 2.8. Transformation of Fe(II, III) at an oxic-anoxic boundary within sediments. Reproduced from Stumm and Morgan (*169*)

observed in Figure 2.8, indicate a redox zone dominated by iron reduction and typically underlie peaks in Fe(III) concentration (*169*).

2.5.1.4. Sulfur. Sulfur can exist in many different oxidation states, but sulfur cycling in anaerobic environments is dominated by sulfate reduction to sulfides (H_2S and HS^-). Sulfate reduction is restricted to reducing conditions with growth yield below those of nitrate, manganese, and iron (Figure 2.5, Figure 2.6B). Sulfate reduction is very common in marine and estuarine sediments and exceeds both iron and oxygen respiration processes in total organic carbon oxidation (*177*). Sulfate reduction is such a dominant process in marine sediments because oceanic concentrations of sulfate are 2,700 mg L^{-1} of seawater (at a salinity of 35 ‰), compared to 40 mg L^{-1} in terrestrial waters (*169*). Sulfate sources in freshwater systems include atmospheric deposition, groundwater and wastewater discharges (*193*).

Sulfate reduction in sediments typically produces sulfides as end products, but other forms of sulfur can also be formed, including sulfite (SO_3^{2-}), thiosulfate ($S_2O_3^{2-}$), and elemental sulfur (S^0). Sulfate reduction is performed primarily by microorganisms, with abiotic reductions largely being insignificant. It is possible for elemental sulfur to be formed during the dissolution of $CaSO_{4(s)}$ or as an intermediate or metastable phase (*169*). Coupling of sulfate reduction with methane oxidization has been observed at sulfate-methane redox interfaces; however, this processes is mediated by sulfate reducing prokaryotes (SRPs) and methanotrophic archaea, presumably interacting syntrophically (*194*, *195*). Microbial sulfate reduction is performed by phylogenetically diverse populations comprising many different prokaryotic phyla. Wagner et al. (*196*) provide a phylogenetic tree of all phyla known to contain SRPs (as of 2005). Also included is a

more detailed tree showing organisms containing the dissimilatory sulfite reductase (*dsr*) enzyme, an evolutionarily-conserved enzyme catalyzing (bi)sulfite reduction to sulfide (*196*). Sulfide (H_2S) formation, encoded by *dsr*, is the final step of sulfate reduction. Sulfide generally exists as the deprotonated anion (HS^-) at circumneutral pH and environmental conditions (*169*), with only very small portions of the conjugate base, S^{2-}, being formed (*197*). Microbial reductions of sulfite, thiosulfate and elemental sulfur are also documented to produce sulfide, but energy yields are smaller compared to complete sulfate reduction (*168*). Disproportionation of thiosulfate and elemental sulfur can also be microbially-catalyzed to yield sulfide and sulfate (*198*). More extensive reviews of microbial populations catalyzing redox reactions sulfur compounds are available elsewhere (*193, 196, 197*).

High sulfide concentrations can be toxic to microbes and benthic macrofauna, causing sulfide removal processes to be important mechanisms. A major sink for sulfides following sulfate reduction is precipitation with divalent metal cations, such as heavy metals (e.g., Cu^{2+}). Iron is the most abundant metal in sediments and in freshwater systems (i.e., sulfides not in excess) most hydrogen sulfide derived from sulfate reduction is bound to iron. Iron sulfide precipitation is more common in marine environments. Solid ferric (hydr)oxides can be reduced by sulfides to produce Fe^{2+} (*189, 190*), which then reacts immediately with excess hydrogen sulfide to yield ferrous iron precipitates (FeS). The precipitates are black-colored and are generally amorphous (*197*). Theberge and Luther (*199*) showed evidence of a transient, soluble intermediate in the precipitation of iron sulfide, however its stoichiometry has yet to be determined ($Fe_xS_{y(aq)}$). FeS can further react with S^0 or polysuflides (S_x^{2-}) to produce pyrite, FeS_2. Excess soluble

sulfides tend to diffuse towards the oxic/anoxic boundary. More extensive reviews of iron sulfide systems are available (*200*).

Oxidation of sulfides under both anaerobic and aerobic conditions presents additional sinks for the toxic sulfide species. Sulfides present in porewaters and drifting to the anoxic/oxic boundary can in turn be abiotically oxidized by oxygen and nitrate to form sulfate, by manganese dioxides to form elemental sulfur and sulfate, and by iron (hydr)oxides to form elemental sulfur (*201*). Interestingly, the oxidation of sulfide by MnO_2 and FeOOH to yield S^0 has been coupled with subsequent bacterial disproportionation of S^0 to H_2S and SO_4^{2-}. The sulfide product can reenter the cycle, while sulfate can be microbially reduced back to sulfide to reoxidize additional MnO_2 or FeOOH to S^0. This cycle is illustrated in Figure 2.7 and results in increased production of Mn^{2+} (from MnO_2 reduction) and FeS (from FeOOH reduction) (*174, 202*). Thiosulfate can also be a dominant product of free and iron-bound sulfide oxidation under both aerobic and anaerobic conditions (*203*). Also of note, anaerobic sulfide oxidation can be performed by purple sulfur bacteria (*197*). Upon sediment mixing and exposure to oxygen, pyrite (FeS_2) can be biologically oxidized to sulfate. In addition, solid iron monosulfide and pyrite can react with oxygen to form sulfate and ferric iron on the mineral surface (*201, 204*).

Redox zones dominated by sulfate reduction can be difficult to identify because of the precipitation of sulfides and the number of aqueous sulfur species potentially present (S^0, $S_2O_3^{2-}$, HS^-, $Fe_xS_{y(aq)}$). Qualitative indicators of sulfate reduction include the presence of black precipitates and the distinctive smell of hydrogen sulfide. Non-disruptive detection of sulfides in porewaters, along with microbial analysis, can provide

more quantitative analysis of sulfate-reducing zones. Targeting the dissimilatory sulfite reductase gene (*dsr*) is another option to gain information regarding the spatial distribution of SRPs.

2.5.1.5. Carbon. Carbon is generally deposited to the sedimentary environment through the water column in the form of solid detritus and organic matter. With the exception of methane, no organic solute present in natural sediments are thermodynamically stable (*169*). Heterotrophic organic carbon oxidation is coupled to microbial processes listed in Figure 2.6A. Carbon compounds can also be fermented to organic acids and alcohols, eventually producing acetate and methane. Methane is the carbon species that is most interesting for discussions regarding stratification of terminal electron accepting processes, since it is the least favorable redox process and occurs either below or concurrently with sulfate reduction in vertically-stratified sediments (*169*). All known methanogenic microorganisms belong to the Archaeal kingdom and are found in a large variety of environments, such as wetlands, soils, open oceans, sediments, digesters, and hydrothermal vents. Detailed information on methanogenic species is compiled by Madigan and Martinko (*205*), Vogels et al. (*206*), and Friedrich (*207*). Acetoclastic and hydrogen-oxidizing pathways (utilizing CO_2) comprise a majority of methanogenesis. Methanogens use a methyl group as their terminal electron acceptor, releasing methane as the final step in the metabolic process (*207*). The methyl-coenzyme M reductase (*mcr*) is the key enzyme of methanogenesis and catalyzes the final step of the process by reducing a coenzyme M-bound methyl group to methane (*207*). Genes encoding the alpha subunit of the *mcr* (*mcrA*) are evolutionarily conserved an provide and opportunity for targeting methanogenic populations using molecular techniques. A similar gene encoding *mcrA*

has been identified in anaerobic methane oxidizers performing reverse methanogenesis (*208, 209*). Anaerobic methane oxidation, found in strongly anoxic environments and proximal to methane gas hydrates, is syntrophically coupled to sulfate reduction (*194, 195*) yielding sulfide and bicarbonate. Therefore, analytical detection of *mcrA* indicates the presence of methanogenic and/or methane oxidizing organisms.

Methane can be oxidized in aerobic environments following (bubble) transport to the oxic sediment region. Aerobic methanotrophs, organisms that are able to grow using methane as their only source of carbon and energy, typically inhabit the sediment-water interface. Fortuitous biotransformations of environmental contaminants can occur when methane monoxygenase enzymes of aerobic methanotrophs are expressed (*132, 133*).

Detection of porewater methane can indicate strongly reducing, methanogenic redox conditions. Porewater sampling for methane concentrations can be challenging because of biogenic gas formation and subsequent bubble ebullition, increased spatial heterogeneity associated gas-phases present in sediment pores, and bulk methane release during sediment mixing and disruption. Delineating methanogenic redox zones using porewater sampling and molecular tools (e.g., targeting the *mcrA* gene) therefore provides complementary information. Analytical advances now provide high resolution detection of geochemical speciation, while also providing the quantification and characterization of microbial populations, allowing for the determination of biogeochemical responses to *in situ* capping.

2.5.2. Geochemical Characterization Tools

New analytical tools to measure aqueous geochemical species in sediment porewaters has allowed for clear mapping of redox zones at high vertical resolutions.

Traditional approaches to obtain porewater geochemical profiles, such as peepers and benthic chambers, can be disruptive to the environment upon deployment and collection. New techniques, specifically microelectrodes, provide sub-millimeter scale measurements of redox-important geochemical species near the SWI. Extensive reviews of electrochemical techniques for *in situ* measurements in aquatic sediments can be found in the literature (*210-213*), and discussion here will briefly summarize these reviews.

Microelectrodes are electrochemical sensors that have sensing tip diameters on the micron scale. A number of different microelectrodes have been developed for aquatic environmental research and can be categorized based on electrochemical operation. Amperometric electrodes measure reduction current at a single potential (i.e., single analyte), with the most commonly employed being the Clark electrode for the detection of oxygen. Other amperometric electrodes have been developed for detection of N_2O (*214*), NO_3^- (*215*) , H_2S (*216*), and CH_4 (*217*). Potentiometric electrodes measure the difference of potential between a reference electrode and an indicator electrode and can be used to measure pH (*218*), S^{2-} (*218, 219*), and pCO_2 (*220*), and ion selective electrodes for NO_3^-, NO_2^-, NH_4^+, Ca^{2+}, and CO_3^{2-} (*221*). The small size of microelectrodes allows for insertion into porous media (e.g., aquatic sediments) and *in situ* electrochemical analysis of porewaters with minimal disruption to the surrounding environment, leaving natural gradients of metabolites and substrates intact (*210*). Additionally, data acquisition can be rapid, providing quantitative information in real-time to guide subsequent sampling and analysis. However, since no sample preparation steps are taken during *in situ* measurements, amperometric and potentiometric microelectrode analyses

are susceptible to matrix interferences, lack of specificity or selectivity, problems of reversibility, fouling, and signal drift.

Voltammetric electrodes, described by Brendel and Luther (*222*) consisting of gold amalgam reactive tips of 100 μm housed within glass tubes with 400 μm outside diameter. were utilized in studies described herein and operate by ramping the potential between a working electrode and a reference electrode. At an appropriate potential, an analyte is oxidized or reduced at the working electrode and the current resulting from this reaction is measured at an auxiliary (counter) electrode. Advantages of voltammetric techniques are they can simultaneously measure many analytes present in sediment porewaters, they display low detection limits (μM), and they generally do not suffer from matrix problems (e.g., high salinity) (*210*). Voltammetric gold amalgam microelectrodes (*222*) were utilized in this research and have recently provided *in situ* measurements in estuarine sediments (*223*), salt marsh sediments (*224*), continental margin sediments (*225*), hydrothermal vents (*226*), and overlying water columns (*227*) among many other sites. Gold amalgam electrodes were recently employed to show that *Shewanella putrefaciens*, a model iron-reducing bacterium, excreted organic ligands to solubilize iron oxides for anaerobic Fe(III) respiration (*183*). The electrodes have not previously been used to monitor geochemical species during *in situ* capping applications.

2.5.3. Microbiological Characterization Tools

Microbial population enumeration and community characterization using culture-independent PCR-based techniques can provide complementary information for assessing biogeochemical processes within aquatic sediments. Several molecular biological tools for monitoring microbial populations within environmental samples are available and

were recently summarized during a expert panel workshop (*228*). Discussion here will focus on the application of qPCR and T-RFLP techniques to quantify microbial populations investigated herein.

Quantitative real-time PCR (qPCR) was initially described in the mid-1990's (*229*) and has since been used to detect and enumerate microbial populations from many environmental settings. Harms et al. (*230*) provide a schematic and brief description of qPCR techniques for environmental applications. The ability of qPCR to confirm the presence/absence of target microbial populations while also providing abundance values at relatively high sensitivity has led to its general replacement of direct and nested PCR approaches (*228*). Primers have been developed targeting the 16S rRNA gene to provide information at kingdom (e.g., bacteria (*230*)) to genera (e.g., *Dehalococcoides* (*231*)) levels of specificity. Analysis of total bacterial and archaeal populations using qPCR has been performed routinely in a variety of environmental samples, including municipal wastewater treatment plants (*230*), contaminated groundwater aquifers (*232*), and aquatic sediments (*233*). Likewise, qPCR analyses with primers to quantify bacteria implicated in iron reduction and bioremediation have been utilized to characterize subsurface environments and to examine spatial and temporal population changes (*234-237*). Primers targeting process-specific indicator genes (e.g., sulfate reduction (*196*)) have been developed to examine microbial functionality across phylogenetic groupings and can give information on specific pathways and biogeochemical niches. qPCR primers targeting functional genes encoding enzymes for sulfate reduction, dissimilatory sulfate reductase (*dsr*), and methanogenesis, methyl coenzyme-M reductase (*mcr*), have recently been utilized to examine spatial distributions of sulfate-reducing and methanogenic

prokaryotes in sediments (*233*, *238*). Due to the recent emergence of qPCR as a molecular biological tool, few studies have compiled multiple primers into one study to characterize biogeochemical distributions. Schippers and Neretin (*233*) provide one example, investigating microbial communities within a continental margin sediment and employing qPCR to enumerate Prokaryotes, Bacteria, Archaea, Eukaryotes, *Geobacter*, and *dsr* functional gene. Michalsen et al. (*232*) recently examined microbial changes at a radionuclide contaminated site by qPCR analysis for Eukaryotes, *δ-Protecobacteria*, *Geobacter* spp., *mcr* functional gene, and methanotrophs and denitrifyers using functional genes. All of the qPCR analyses by Michalsen et al. were commercially performed (Microbial Insights, Inc.), suggesting the potential for future applications of qPCR to characterize microbial communities indicative of specific redox zones.

Terminal-restriction fragment length polymorphism (T-RFLP) generates fragment patterns from a PCR amplified marker (e.g., 16S rRNA gene) and can facilitate differentiation of dominant community members. Complex fragment patterns produced by T-RFLP can be further analyzed to provide numerical estimates of community composition and diversity to allow for more quantitative comparison of patterns. Reviews and research articles in the literature cover T-RFLP origins, basics, and how T-RFLP can be used to assess community composition and dynamics (*239-242*). T-RFLP is not as commonly employed as qPCR for groundwater remediation applications, but has been used more often in ecological studies examining microbial community changes associated with redox changes (*243-245*). Pett-Ridge and Firestone (*246*), for example, analyzed T-RFLP fragment patterns of bacterial DNA extracted from sediments subject to different oxic conditions with a web-based phylogenetic assignment tool to observe

community changes based on oxygen exposure. The combined use of qPCR and T-RFLP to characterize microbial communities in soils and sediments has been utilized previously (*247-249*).

2.5.4. Coupling Geochemical and Microbiological Data

The ability of voltammetric microelectrodes to monitor *in situ* concentrations of $O_{2(aq)}$, Mn^{2+}, Fe^{2+}, ΣH_2S, organic-$Fe^{III}_{(aq)}$, and $Fe_xS_{y(aq)}$ indicates the presence of microbial heterotrophic oxidation processes; while coupling these measurements to qPCR and T-RFLP analyses can help confirm the presence of these speculations. Few peer-reviewed studies are available that thoroughly detail both geochemical and microbial process within an environmental sample. Previous attempts to combine sedimentary geochemical measurements and microbial populations have utilized couplings of: peepers and plate enumeration (*172*); core sectioning and wet chemical techniques combined with T-RFLP (*250*) or phospholipid fatty acid analysis (PLFA) (*251*); diffusive gradients in thin films (DGT) and denaturing gradient gel electrophoresis (DGGE) (*252*); and oxygen microelectrodes and T-RFLP (*243, 253*). Authors have reported general shifts in community profiles (e.g., T-RFLP, DGGE, PLFA) correlated to observed geochemical shifts, but characterization of specific bacterial groups with geochemical measurements has produced mixed results. Koretsky et al. (*172*) found no vertical separation among aerobic microorganisms, iron-, manganese-, and sulfate-reducing bacteria despite vertical geochemical stratification and attributed the lack of microbial segregation to high labile organic matter input and sediment mixing by bioturbating organisms. Braker et al. (*250*) reported little change in denitrifying populations in marine sediments despite steep redox gradients and also hypothesized that bioturbation resulted in little apparent differences in

community structure. However, a biogeochemical study of a hydrothermal sediment matched regions of increased Fe^{2+} and Mn^{2+} concentrations within a sediment core to increased cells of culturable iron- and manganese-reducing organisms in those regions (*254*). Others sequenced DGGE bands and reported microbial results consistent with chemical redox data from a lake sediment (*252*). Taillerfert et al. (*255*) performed wet chemical techniques and RNA hybridization to correlate δ-proteobacteria with manganese reduction in the waters of a stratified lake. Lowe et al. (*256*) also used wet chemical techniques, and found a positive correlation between amorphous Fe(III) oxides and culturable iron-reducing bacteria. Most recently, Wilms et al. (*238*) used qPCR to demonstrate that methanogenic (*mcr* gene) and sulfate-reducing prokaryotes (*dsr* gene) reflected methane and sulfate concentration profiles in a marine tidal flat. None of these studies, however, had the analytical sophistication or vertical resolution associated with gold amalgam voltammetric microelectrodes. The development of qPCR techniques to characterize population changes of microbes of known functional capacity, such as iron- and sulfate-reduction and methanogenesis, allows for the coupling of quantitative microbial data to measured redox gradients at unprecedented resolutions.

CHAPTER 3.

SPATIAL AND TEMPORAL EVOLUTION OF BIOGEOCHEMICAL PROCESSES FOLLOWING *IN SITU* CAPPING OF CONTAMINATED SEDIMENTS [a]

3.1. Abstract

In situ capping has recently emerged as a remedial method for contaminated sediments and involves placing a layer of clean material at the sediment-water interface. The biogeochemical response of native sediment following capping, as well as the redox environments that develop within the cap, are currently unknown. Column experiments were conducted and voltammetric microelectrodes used to characterize the spatial and temporal distribution of biogeochemical processes in capped sediments under stagnant and upflow conditions. Oxygen penetration into sand caps extended only a few centimeters, thus maintaining underlying sediment anaerobic. Chemical species indicative of heterotrophic organic matter degradation (Mn^{2+}, Fe^{2+}, organic-$Fe^{III}_{(aq)}$, $Fe_xS_{y(aq)}$, ΣH_2S) were observed in stratified zones below the oxic layer. The majority of the overlying cap was subject to iron-reducing conditions under stagnant flow, while upflow conditions led to a compression of the redox zones towards the cap-water interface. Controls confirmed that sediment capping induced an upward, vertical shift of biogeochemical processes into the overlying cap, with redox stratification conserved.

---

[a] The contents of Chapter 3 have been submitted to *Environmental Science & Technology* and have been reformatted here for consistency with the remainder of the dissertation. The citation is as follows: David W. Himmelheber, Martial Taillefert, Kurt D. Pennell, and Joseph B. Hughes. "Spatial and temporal evolution of biogeochemical processes following *in situ* capping of contaminated sediments." Submitted to *Environmental Science & Technology,* October, 2007.

The redox conditions within the cap, specifically the predominance of iron reduction, should allow for reductive contaminant attenuation processes to extend into the overlying cap. These findings improve our understanding of the dynamics of biogeochemical processes following capping of contaminated sediments.

3.2. Introduction

Many aquatic sediments are sufficiently contaminated to cause adverse effects on aquatic life and limit recreational and economic use, especially near urban and industrial settings (*2, 3, 257*). *In situ* capping has recently emerged as a remedial method for contaminated sediments and involves placing a layer of clean fill material at the sediment-water interface to isolate contaminants from the benthic community and overlying surface water. Clean sand has traditionally been the material employed for capping and can delay contaminant breakthrough considerably when diffusive transport dominates (*151*). A potential consequence of emplacing an *in situ* cap at the sediment-water interface is that it may induce considerable, abrupt restructuring of biogeochemical processes within the underlying sediment.

Biogeochemical restructuring within capped sediments can directly influence contaminant fate and transport, since aquatic sediments are capable of naturally attenuating a number of different contaminants through both abiotic and biotic processes. Examples of abiotic contaminant transformations and their associated redox conditions include nitroaromatic reduction during Fe^{III} reducing conditions (*95, 97*), the dehalogenation of chlorinated organics by iron sulfides (*98, 99*), naturally occurring zero-valent iron (*102*), and Fe(II) present at surfaces of iron-containing minerals (*95-97*),

metal and nutrient sequestration under oxic (*14*) and sulfidogenic (*258*) conditions, and hydrophobic organic contaminant sorption. Biogeochemical perturbations following sediment capping may also impact biologically-mediated contaminant transformations, which are especially dependent on proper redox conditions. Biogeochemical shifting induced by *in situ* capping could therefore alter natural attenuation processes and potentially lead to changes in contaminant fluxes.

Aquatic sediments underlying oxic surface waters typically possess an aerobic layer extending millimeters to centimeters into the sediment bed. Beneath this aerobic layer exists a gradient of terminal electron accepting processes (TEAPs), stratified according to thermodynamic yield (*168*). Previous characterizations of geochemical niches within capped sediments during laboratory- and field-scale capping operations have revealed only general trends. Liu et al. (*31*) measured redox potentials (E_h) at fixed locations via sideports in capped sediments under upflow conditions and found that sediment E_h drops following capping to values between 0 and 100 mV. Azcue et al. (*259*) examined a field-scale sediment site one year after capping and reported anoxic conditions beginning 4 cm below the cap-water interface (CWI). Both of these studies suggest that an aerobic/anaerobic transition forms within the cap, but elucidation of specific redox zones was not possible due to the limited number of sampling locations. Greater spatial resolution, in addition to temporal patterns and chemical speciation data are needed to assess changes in biogeochemical stratification and accurately predict contaminant fate and transport. The influence of advective flow on TEAP distribution within capped sediments should also be addressed since capping sites can be subject to groundwater seepage.

The objectives of this work were to characterize the spatial and temporal distribution of biogeochemical processes in aquatic sediments with high vertical resolution and monitor how these processes are altered by the emplacement of an *in situ* cap under stagnant and upflow conditions. Sediment columns were constructed from river sediment, capped with a clean sand, and monitored with voltammetric microelectrodes for geochemical species indicative of specific redox zones under stagnant and upflow conditions. Results from this study provide fundamental information regarding the dynamics of biogeochemical processes at the sediment-water interface during engineered remedial operations, allowing for better predictions of contaminant fate and transport.

3.3. Materials and Methods

3.3.1. Sediment Columns

Sediment from the Anacostia River was used for all experiments. The river is subject to tidal pumping and flows through Washington, D.C., USA. Sediment from the river has previously been reported to contain elevated levels of PCBs, PAHs, metals, and organic pesticides (*158*). Surficial wet sediment was homogenized after removal of large debris and shells and transferred to quart-sized, air-tight jars that were stored in the dark at 4 ºC until use. Physicochemical characterization of the homogenized sediment has been reported previously (*260*) Satellite imagery of the river is provided in Figure 3.1.

A sediment column was constructed with a glass chromatography column (20 cm long, 5.0 cm I.D.; Spectrum Chromatography) fitted with Teflon endplates. The column was packed with wet Anacostia sediment within an anaerobic glovebox (Coy Laboratory

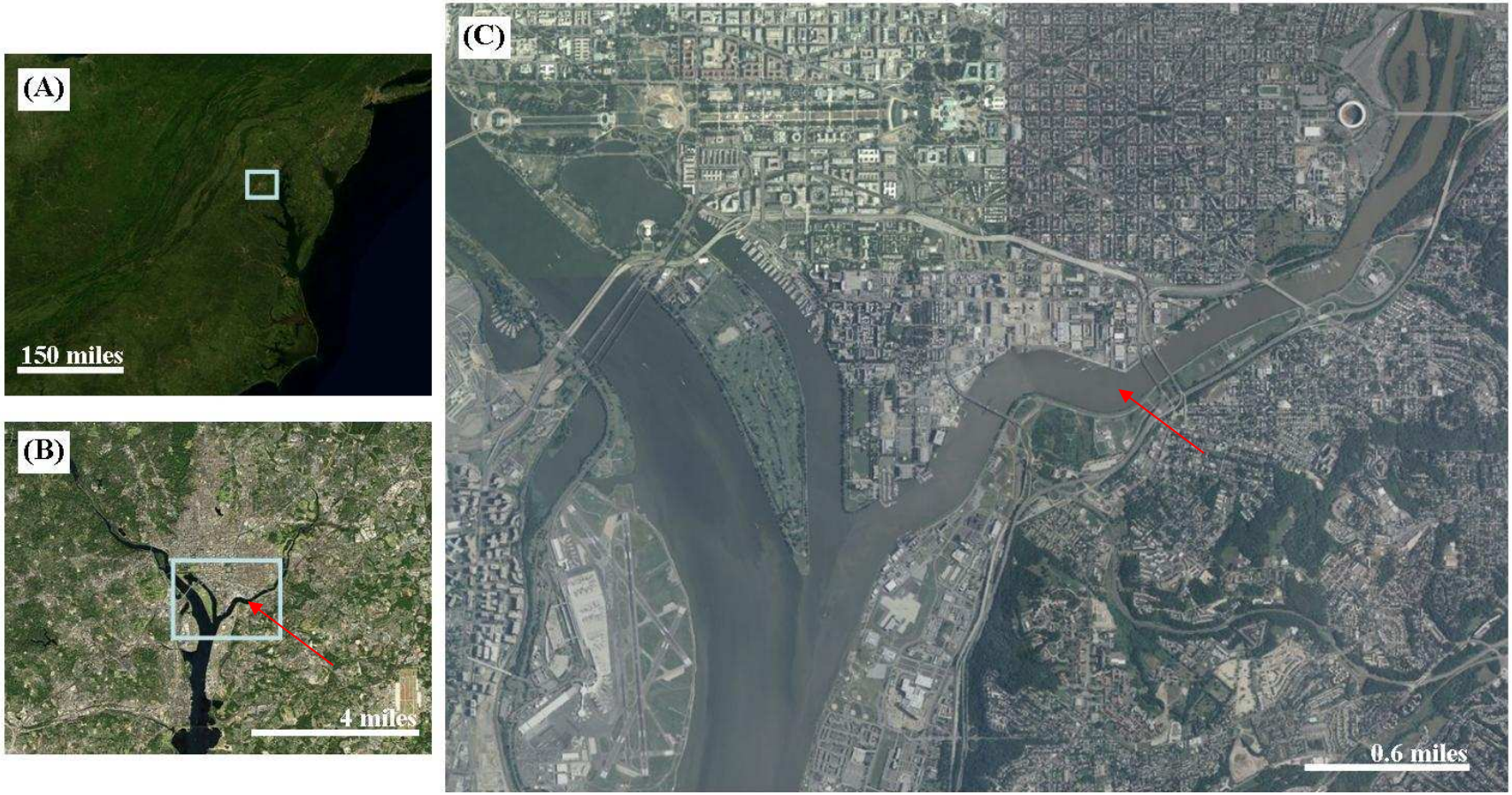

Figures 3.1A-C. Satellite images of the Anacostia River, Washington, D.C. (A) Eastern United States. The box approximates the boundaries of image (B). (B) Washington, D.C.. The red arrow indicates the Anacostia River. The box approximates the boundaries of image (C). Lower portion of the Anacostia River, indicated by the red arrow. Images captured from MSN Virtual Earth.

Products) under an atmosphere of 5% CO_2/ 5% H_2/ 90% N_2. The sediment column was kept in the dark and remained capped in the glovebox for one week to allow particle settling, creating a sediment depth (below the overlying waters) of 7 cm. The column was then removed from the glovebox, the top endplate disconnected, and incubated under atmospheric conditions at room temperature. Overlying water for the sediment column consisted of a solution prepared from nano-pure water (> 18.2 Ω) and contained only sodium chloride at a concentration matching the salinity of the Anacostia sediment porewater ($10^{-2.9}$ M NaCl). An overlying water depth of 4 cm was established above the sediment and maintained using a constant head reservoir. Appendix B provides a schematic and photograph of the column (Figures B.1A-B). An aeration tube placed above the water surface provided a stream of air to promote oxygen dissolution with minimal mixing. After incubation for 4 weeks, the sediment column was capped with dry, autoclaved ASTM C-33 concrete sand (U.S. Silica). The final thickness of the cap measured 7 cm and overlying water depth above the cap was maintained at approximately 4 cm. Porewater geochemical profiles of the capped sediment were analyzed at 2, 6, 8, and 13 weeks following capping.

After 13 weeks of stagnant incubation, upflow conditions were induced with a syringe pump at a flow rate of 2.0 $cm^3 \cdot hr^{-1}$, with a corresponding seepage velocity of 4.4 $cm \cdot day^{-1}$ (Darcy velocity = 2.4 $cm \cdot day^{-1}$) calculated from bulk sediment properties (*260*). The influent solution was the same as the overlying water solution ($10^{-2.9}$ M NaCl), but was sparged with UHP nitrogen gas (Airgas) for 30 minutes to remove dissolved oxygen. A constant head reservoir maintained overlying water levels at approximately 4 cm. Geochemical profiles of the capped sediment under upflow conditions were obtained at 1,

6, 13, and 16 weeks following the initiation of flow, corresponding to 14, 19, 26, and 29 weeks of total incubation (i.e., stagnant incubation plus upflow incubation). The upflow time-points represent approximately 4, 27, 58, and 71 pore volumes flushed through the sediment, respectively.

An uncapped sediment control column was similarly established but remained uncapped for the duration of the experiment. This uncapped control was intended to confirm that any redox changes observed in the experimental column were the result of capping. The uncapped control was constructed using a glass chromatography column (30 cm long, 4.8 cm I.D.; Kimble Kontes) with Teflon endplates. Wet sediment was loaded to a depth of 25 cm, with 4 cm of overlying water. A second control column was constructed with dry, autoclaved ASTM C-33 sand but without underlying sediment. This sediment-free sand control column was established to investigate the role of sediment on the redox conditions observed within the sand cap of the experimental column. The sediment-free control column was maintained in a glass beaker (600 mL), filled with sand to a depth of 7 cm, and 4 cm of overlying water ($10^{-2.9}$ M NaCl). Both control columns were maintained in the dark at room temperature with aeration tubes placed at each air-water interface. Geochemical profiles were obtained at parallel time points with the experimental column. Photographs of each control column are provided in Appendix B (Figures B.2A-B).

3.3.2. Porewater Geochemical Profiles

Aqueous geochemical species were analyzed electrochemically at discrete depths within the columns by inserting voltammetric microelectrodes into cap and sediment porewaters. All voltammetric measurements were performed using a platinum counter

electrode, an Ag/AgCl reference electrode, and an Au/Hg solid-state microelectrode fabricated as described by Brendel and Luther (*222*). The Au/Hg microelectrodes consisted of a 100 μm diameter gold wire housed in glass tubing filled with nonconductive epoxy and connected via copper conducting wire to a potentiostat. The gold surface was polished with diamond pastes of 15, 6, 1, and 0.25 μm (Buehler, Lake Bluff, IL), mercury plated at -0.1 V in a $Hg(NO_3)_2$ solution, then polarized at -9 V for 90 s to form the gold amalgam (*222*). The Au/Hg working microelectrodes are capable of simultaneously measuring $O_{2(aq)}$, H_2O_2, Fe^{2+}, Mn^{2+}, $S_2O_3^{2-}$, ΣH_2S [$=H_2S + HS^- + S^{2-} + S^0 + S_x^{2-}$], organic-$Fe^{III}_{(aq)}$, and $Fe_xS_{y(aq)}$ species (*187, 199, 222*).

Each Au/Hg microelectrode was tested for quality and calibrated for dissolved oxygen by linear sweep voltammetry in simulated freshwater (0.1M NaCl), and then for manganese by cathodic square wave voltammetry (CSWV) in degassed simulated freshwater. Both the O_2 and Mn^{2+} calibrations were run from -0.1 to -1.75 V with a scan rate of 200 $mV \cdot s^{-1}$. A preconditioning potential of -0.1 V for 10 s was applied to all O_2, Mn^{2+}, and Fe^{2+} measurements to clean the surface of the microelectrodes between measurements (*222*). When organic-$Fe^{III}_{(aq)}$, ΣH_2S, and $Fe_xS_{y(aq)}$ complexes were present, however, a cleaning step at -0.9 V for 10 seconds was added to remove any organic-Fe^{III}, ΣH_2S, or Fe_xS_y adsorbed at the electrode surface between measurements (*187, 199*). Concentrations of $Fe^{2+}$and ΣH_2S were determined from manganese calibration curves following the pilot ion method (*222*). Soluble ferric iron can be measured by voltammetry at circumneutral pH only if complexed by an organic ligand (*187*). The sensitivities of the organic-$Fe^{III}_{(aq)}$ complexes have yet to be determined, and their concentrations are therefore reported in units of current intensity (nA) (*187*). Similarly,

the stoichiometry of $Fe_xS_{y\,(aq)}$ is unknown and current intensities (nA) are also reported for these species (*199*).

Between three to ten voltammetric scans were obtained at each depth depending on the analytes detected. Mean values from each depth are reported. Relative standard deviations of each species for all profiles averaged 10% and are not included in the Figures with the exception of Figure 3.2B, which provides an example of standard deviations for oxygen at each depth. Voltammetric analyses were performed with a computer-operated DLK-100A potentiostat and a computer-operated micromanipulator capable of vertical movements at the sub-millimeter scale (Analytical Instrument Systems, Inc.). The small size of the working microelectrode, coupled with the precise control of vertical movement, allowed for data collection with high vertical resolution and for repeated profiling of sediment geochemistry while minimizing bulk sediment disturbance. Voltammograms were processed with a Matlab®-based program (*261*). Appendix A provides more information regarding the use of voltammetric microelectrodes for the determination of species concentrations.

3.4. Results and Discussion

3.4.1. Controls

The control columns provide the geochemical properties of the sediment and sand when not associated with capping: the uncapped sediment displayed an aerobic layer at the sediment-water interface above stratified anaerobic biogeochemical processes, while the sediment-free sand was completely aerobic. After 6 weeks of aerobic incubation, dissolved oxygen was present in the overlying water of the uncapped sediment control

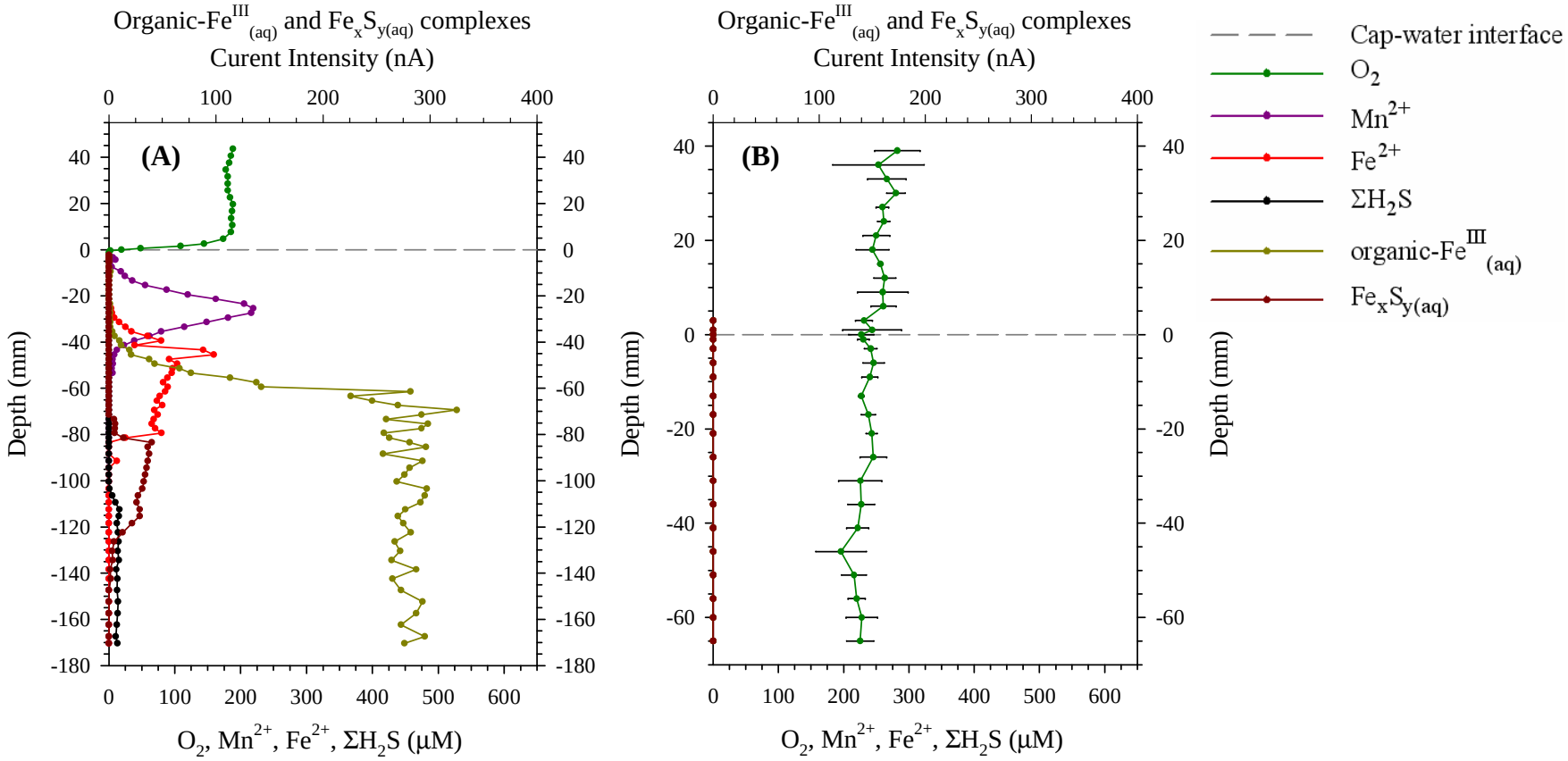

Figures 3.2A-B. Geochemical characterization of columns exposed to atmospheric conditions containing (A) uncapped Anacostia River sediment and (B) C-33 sand after 6 weeks of incubation. Note that the values for the organic-$Fe^{III}_{(aq)}$ and $Fe_xS_{y\,(aq)}$ complexes are reported as current intensity and referenced to the top x-axis. The concentrations of $O_{2(aq)}$, Fe^{2+}, Mn^{2+}, and ΣH_2S are referenced to the lower x-axis. The dashed line at y = 0 in each plot represents the sediment-water interface in (A) and the sand-water interface in (B). The data point at the most positive y-value was obtained at the air-water interface.

column at relatively constant concentrations (Figure 3.2A) and penetrated 1.4 mm below the CWI. The shape of the oxygen profile in Figure 3.2 is typical for aquatic sediments in the absence of photosynthetic O_2 production (*166*). Below the oxic layer, sequential regions dominated by Mn^{2+}, Fe^{2+}, organic-$Fe^{III}_{(aq)}$, $Fe_xS_{y(aq)}$, and ΣH_2S species were present, demonstrating stratification with depth corresponding to the thermodynamic yield of electron accepting processes. The spatial relationships among the stratified TEAPs observed in Figure 3.2 were maintained for the duration of the uncapped sediment control incubation (not shown). In contrast, the sediment-free sand control remained aerobic throughout the entire thickness of 7 cm after 6 weeks (Figure 3.2B), without any appearance of reduced species over the duration of the experiment (29 weeks). Bioturbation at the solid-water interface was not observed in the control or experimental columns. Appendix B provides all porewater profiles obtained from the control columns.

3.4.2. Capped Sediment

Oxygen profiles under both stagnant and upflow conditions are presented in Figure 3.3, while a quantitative summary of oxygen penetration at each time point is provided by Table 3.1. For each profile, oxygen concentrations in the overlying water column were relatively constant, however oxygen concentrations were lower during upflow compared to stagnant conditions and generally tended to decrease as a function of time during upflow, suggesting that anaerobic porewaters mixed with the overlying water. Variations in oxygen penetration between the first two measurements can be attributed to substrate utilization during aerobic respiration, while the presence of Fe^{2+} just below the aerobic layer (-8.4 mm in Figure 3.4B) limited oxygen penetration in subsequent profiles (Table 3.1). Under upflow conditions, decreased aerobic respiration

may have allowed oxygen penetration to increase until 16 weeks, when Fe^{2+} was located just below the CWI to reduce dissolved oxygen. Dissolved oxygen was not observed throughout the remaining depth of the cap nor within the sediment. The loss of oxygen in the cap can be attributed in part to the presence of reduced chemical species. For all

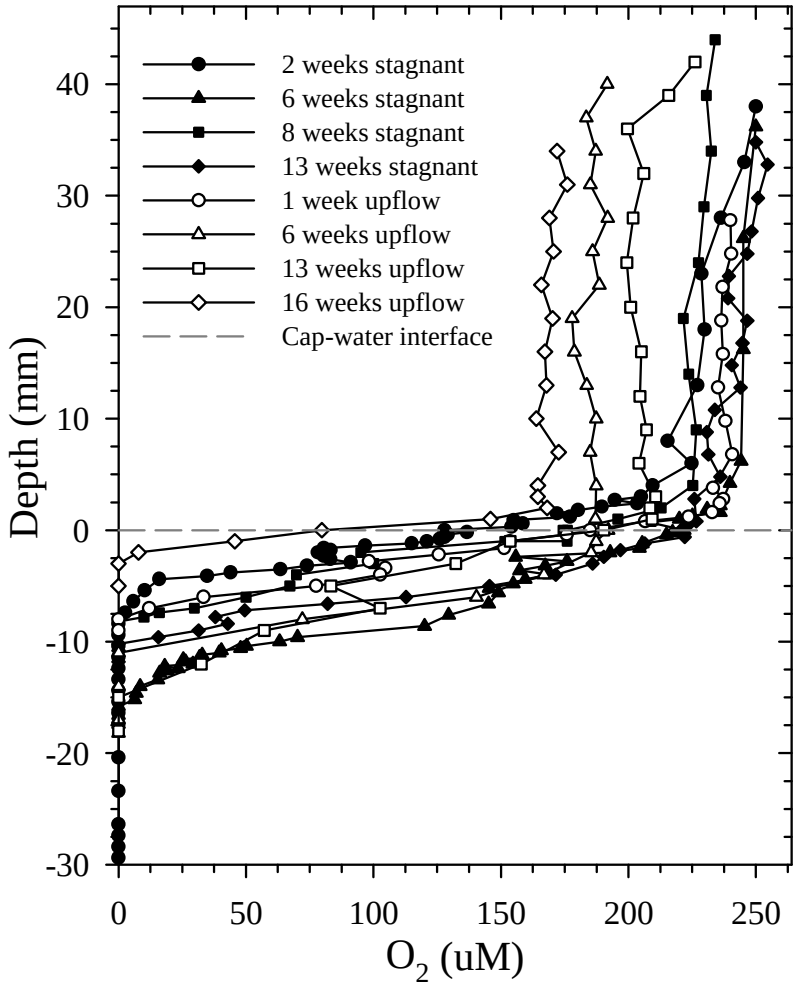

Figure 3.3. Oxygen penetration into upper portion of sand cap under stagnant and upflow conditions. The cap-water interface is defined at y = 0 mm, with the data point at the most positive y-value obtained at the air-water interface.

Table 3.1. Oxygen penetration characteristics for each porewater geochemical profile of the capped sediment column.

Profile incubation conditions and time	Average oxygen concentration in overlying water (μM) [a]	Diffusive boundary layer depth (mm)	Depth of oxygen penetration (mm) [b]
Stagnant – 2 weeks	232.17 ± 11.31	13.4	-9.4
Stagnant – 6 weeks	233.51 ± 12.56	15	-15.2
Stagnant – 8 weeks	227.89 ± 4.13	9.8	-7.8
Stagnant – 13 weeks	223.05 ± 7.32	9.6	-9.6
Upflow – 1 week	237.45 ± 6.04	9.2	-8.0
Upflow – 6 weeks	186.23 ± 3.94	9.0	-11.2
Upflow – 13 weeks	205.94 ± 8.11	11.0	-12.0
Upflow – 16 weeks	168.65 ± 3.60	4.0	-2.8

[a] Reported values of oxygen concentration are arithmetic mean ± one standard deviation.
[b] Depth of oxygen penetration is relative to the cap-water interface, defined at y = 0.

capped sediment profiles (Appendix B) , and similar to the uncapped sediment control, anaerobic processes were observed below the aerobic layer in sequential regions dominated by Mn^{2+}, $Fe^{2+}$and organic-$Fe^{III}_{(aq)}$, $Fe_xS_{y(aq)}$, and ΣH_2S and generally corresponding to theoretical TEAP stratification based on thermodynamic yield. Details of the geochemical profiles are described in the following sections.

3.4.2.1. Stagnant Incubation. Capping of contaminated sediment under stagnant flow conditions created a short aerobic layer at the CWI overlying stratified geochemical regions in the remainder of the cap and sediment. The geochemical profile after 6 weeks of stagnant incubation (Figure 3.4A) shows oxygen penetration into the upper cap, followed by the production of Mn^{2+} between -10 to -24.8 mm, at which point Fe^{2+} concentrations exceeded Mn^{2+} levels to become the dominant redox species within the cap from -24.8 mm to -55.8 mm. The loss of Fe^{2+} at -55.8 mm coincided with the appearance of $Fe_xS_{y(aq)}$, an intermediate in the formation of amorphous FeS (*262*), suggesting the formation of iron sulfides contributed to the loss of dissolved ferrous iron. Coexistence of the organic-$Fe^{III}_{(aq)}$ and $Fe_xS_{y(aq)}$ complexes, as observed at approximately -80 mm in Figure 3.4A, suggests that the soluble ferric iron species was reduced by traces of ΣH_2S to eventually form $FeS_{(s)}$ (*19*)

The geochemical profile after 13 weeks of stagnant incubation shows more developed redox zonation (Figure 3.4B). Reduced manganese diffused into the oxic zone and extended 12.8 mm above the CWI, indicating that Mn^{2+} flux from the sediment exceeded the rate of abiotic manganese oxidation by dissolved oxygen, the kinetics of which is slow below pH 9 (*178*). Interestingly, $Fe_xS_{y(aq)}$ was observed at -7.2 mm but was not anticipated, since this does not follow the traditional theory of redox stratification

based on thermodynamic yield. It is possible, however, that sulfate reduction occurred prior to iron reduction, which has been observed in natural environments and proven theoretically possible when pH conditions and iron oxide speciation make it thermodynamically favorable (*263*). Threshold sulfate concentrations for microbial sulfate reduction by both mixed and pure cultures have been reported between 5 to 40 μM (*264-268*). A previous upflow column experiment (*260*) utilizing the same Anacostia River sediment routinely measured effluent sulfate concentrations between 20 to 60 μM, with concentrations spiking up to 200 μM, thus exceeding threshold limitations. Sulfidogenesis below the oxic layer may have also reduced any manganese oxides in this region (*269*), supported by the increase in Mn^{2+} concentrations after 13 weeks compared to 6 weeks. Alternatively, microbial manganese oxide reduction could have been ongoing just below the CWI. The most marked difference between the stagnant profiles after 6 and 13 weeks, however, was the extent of the Fe^{2+}-dominated zone, which occupied the middle of the sand cap and peaked in the upper portion of the sediment (-81.8 mm) at week 13, coinciding with a peak for organic-$Fe^{III}_{(aq)}$ (-84.8 mm). Recently, it was discovered that *Shewanella putrefaciens*, a model iron-reducing bacterium, excretes organic ligands to solubilize iron oxides for anaerobic Fe(III) respiration (*183*). The prevalence of organic-$Fe^{III}_{(aq)}$ below the sediment-cap interface may indicate microbial iron reduction was occurring; however, verification that *Shewanella* or other iron-reducing bacteria were indeed present in the sediment requires further investigations. The accumulation of Fe^{2+} and organic-$Fe^{III}_{(aq)}$ also led to the depletion of ΣH_2S, previously observed at -70 mm after 6 weeks (Figure 3.4A). After 13 weeks, ΣH_2S was detected in the sediment at -87.8 mm (Figure 3.4B) at the onset of $Fe_xS_{y(aq)}$. The $Fe_xS_{y(aq)}$

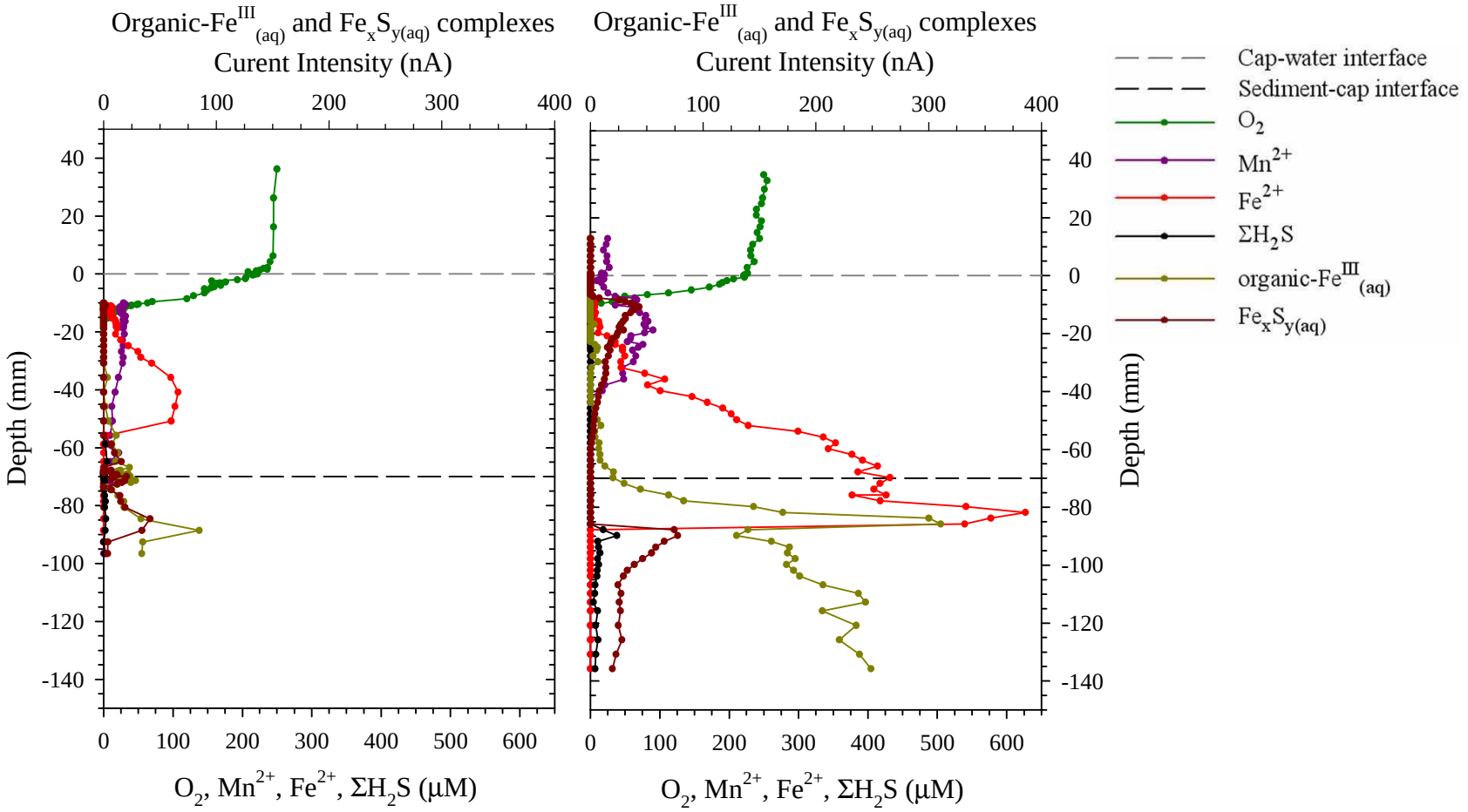

Figures 3.4A-B. Geochemical profiles of capped sediment under stagnant flow conditions (A) 6 weeks after capping and (B) 13 weeks after capping. Note that the values for the organic-$Fe^{III}_{(aq)}$ and $Fe_xS_{y\,(aq)}$ complexes are reported as current intensity and referenced to the top x-axis. The concentrations of $O_{2(aq)}$, Fe^{2+}, Mn^{2+}, and ΣH_2S are referenced to the lower x-axis. The cap-water interface is defined at y = 0 mm, with the sediment-cap interface at y = -70 mm. The data point at the most positive y-value was obtained at the air-water interface.

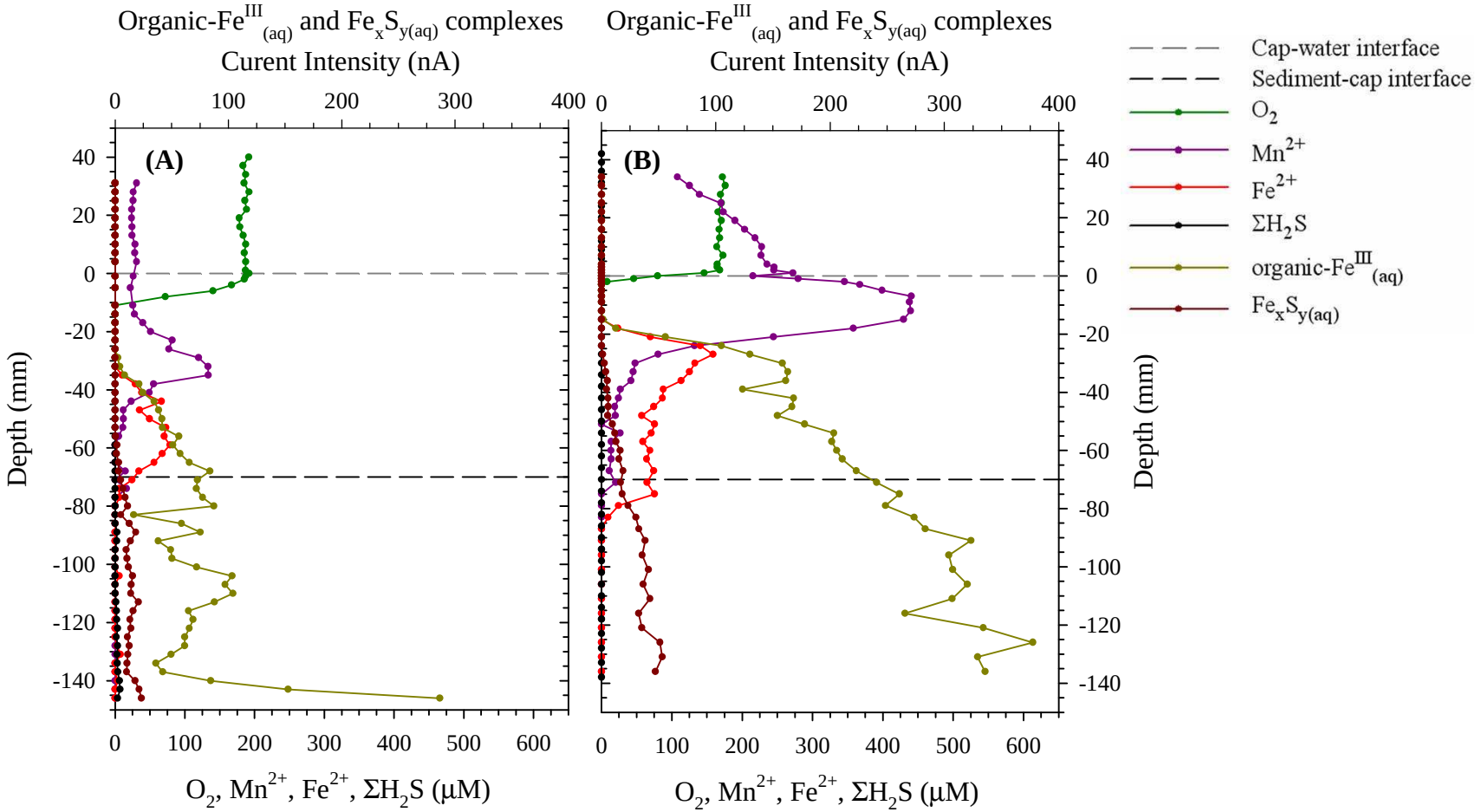

Figures 3.5A-B. Geochemical profiles of capped sediment under upflow conditions (A) 6 weeks after initiating flow and (B) 16 weeks after initiating flow. Note that the values for the organic-$Fe^{III}_{(aq)}$ and $Fe_xS_{y\,(aq)}$ complexes are reported as current intensity and referenced to the top x-axis. The concentrations of $O_{2(aq)}$, Fe^{2+}, Mn^{2+}, and ΣH_2S are referenced to the lower x-axis. The cap-water interface is defined at y = 0 mm, with the sediment-cap interface at y = -70 mm. The data point at the most positive y-value was obtained at the air-water interface.

complex was likely produced during the reduction of soluble organic-$Fe^{III}_{(aq)}$ by ΣH_2S and also contributed to the removal of Fe^{2+} (Figure 3.4B). Overall, results obtained under stagnant flow conditions suggest that manganese reduction was active in the upper cap; sulfate reduction occurred in the sediment, but not at substantial levels; and microbial iron reduction was a significant process just below the cap-sediment interface, vbgfghyindicated by the production of Fe^{2+} up to 600 μM and organic-$Fe^{III}_{(aq)}$.

3.4.2.2. Upflow Incubation. Upflow conditions resulted in a compression of biogeochemical processes toward the CWI while simultaneously conserving redox stratification. The compression of redox zones within the cap was caused by the movement of microbial iron reduction and possibly sulfate reduction into the cap, evidenced by observations from the upflow profiles (Figures 3.5A-B). Microbial iron reduction, indicated by organic-$Fe^{III}_{(aq)}$ production (*183*), was initially detected at -15 mm and dominated the cap and sediment after 16 weeks of upflow (Figure 3.5B). Despite the presence of microbial iron reduction, Fe^{2+} concentrations decreased compared to the stagnant profile obtained at 13 weeks (Figure 3.5B). One sink for Fe^{2+} is oxidation by dissolved oxygen, especially under upflow conditions which transports Fe^{2+} toward the CWI. Iron oxide formation is indirectly supported by decreases in dissolved oxygen concentrations in the overlying water under upflow conditions (170 μM, upflow week 16; Table 3.1) compared to stagnant conditions (220 μM, stagnant week 13; Table 3.1). A second Fe^{2+} removal mechanism is oxidation by manganese oxides (*175*), which probably contributed to the decrease in Fe^{2+} concentrations as well as the temporal increase of Mn^{2+} near the CWI (*270, 271*), especially under upflow conditions (90 μM stagnant week 6; 133 μM upflow week 6; 440 μM upflow week 16). Below -20 mm, Fe^{2+} may be

removed simultaneously with ΣH_2S to produce $Fe_xS_{y(aq)}$ complexes, which were detected at -21 mm after 16 weeks of upflow (Figure 3.5B). The source of the reduced sulfur within the cap and sediment is attributed to microbial sulfate reduction, however sulfur disproportionation is also a possible source (*202*). Reduced sulfur present near the CWI (e.g., -20 mm) can reduce manganese oxides (*269*) and contribute to increases in Mn^{2+} concentrations. Within the sediment, the initial decrease in organic-$Fe^{III}_{(aq)}$ under upflow conditions (Figure 3.5A) suggests ΣH_2S reduces ferric iron. Overall, the geochemical porewater profiles indicate that iron reduction is a major biogeochemical process within sediment caps under upflow conditions and the resulting ferrous iron can reduce dissolved oxygen and manganese oxides while also being utilized for $Fe_xS_{y(aq)}$ production. Microbial sulfate reduction shifts up into the overlying cap under upflow conditions and may provide the reduced sulfur for iron sulfide formation. Quantification of the iron- and sulfate- reducing bacteria within the cap and sediment will be addressed in further studies.

3.4.3. Implications for Capping

The results of the stagnant and upflow profiles, when compared to controls, demonstrate that redox stratification of heterotrophic processes is conserved within capped sediments but shifts vertically into the overlying cap, causing the cap and sediment to be dominated by anaerobic conditions. Results also show that flow conditions can influence the vertical size of TEAP regions. Similar vertical shifts in redox zonation have been observed in tidal sediments and marshes overlain by anoxic waters (*173, 272*), in tropical upland soils (*273*) and paddy soils (*243*) during flooding events, and within littoral sediments during periods of depressed photosynthetic activity

(*274*). The chemical species observed within the cap during this study appear to originate from the sediment, since the sand control column showed no such reduced species (Figure 3.2B). It is also possible that compression of the underlying sediment during cap placement led to an upwelling of sediment porewaters, a reported phenomenon during field placements of *in situ* caps (*147, 150*).

A vertical shift of biogeochemical processes within capped aquatic sediments could have numerous implications for contaminant fate and transport processes. One potential impact is the release of redox-sensitive metals and nutrients from the previously oxic upper sediment where manganese and iron oxyhydroxides tend to adsorb contaminants of concern. Results indicate the upper sediment turns anaerobic upon capping, potentially leading to the release of species which are mobile under anaerobic conditions (e.g., arsenic (*14*) and phosphate (*275*)). Alternatively, if ΣH_2S are in excess, the newly anaerobic sediment zone may provide increased opportunities for contaminants binding to sulfide precipitates, reducing the bioavailability of other metals (e.g., nickel (*258*) and zinc (*276*)). A second impact of an upward biogeochemical shift on contaminant fate and transport is that the increased size of the anaerobic zone could lead to increased opportunities for reductive transformations. Contaminants such as nitroaromatics (*95, 97*) and chlorinated organics (*95-99*) can be abiotically reduced by iron oxides and iron sulfides. A majority of the *in situ* cap was subject to iron reducing conditions, a redox regime which has been shown to be significant for the microbially-mediated reduction of radionuclides (*234, 277, 278*), petroleum hydrocarbons (*279-281*) and chlorinated ethenes (*53*). Microbial colonization of the cap corresponding with an upward biogeochemical shift may provide additional opportunities for reductive

biotransformations and extension of bioattenuation mechanisms from the sediment into the capping material (*260*). Finally, the outcomes of this study may aid in the implementation of active caps, which incorporate sorptive or reactive constituents into the cap to decrease contaminant bioavailability. Since anaerobic biogeochemical processes appear to naturally develop within sediment caps, active caps incorporating reductive contaminant transformations (e.g., reductive dechlorination) may be more favorable compared to oxidative processes (*282*) which would have to overcome oxygen demands to be successful.

The results of this study provide fundamental information on the redox conditions that develop within *in situ* caps and capped sediments following remedial action. Characterizing the redox environments contaminants are exposed to should improve predictions of contaminant fate and transport and ultimately predictions of contaminant flux to the benthic community and overlying water. This is especially important considering the increasing development and utilization of capping technology and the large degree of sediment contamination in populated, urban environments. This study also suggests that reductive *in situ* bio-reactive caps, in which microorganisms capable of reductive contaminant biotransformations are emplaced within caps, may be possible.

3.5. Acknowledgments

Members of the Taillefert research group at the Georgia Institute of Technology, especially Deidre Meiggs, assisted with voltammetric measurements. Much of this work was performed in the laboratory of Martial Taillefert, at the Georgia Institute of Technology.

CHAPTER 4.

MICROBIAL COLONZATION AND COMMUNITY CHARACTERIZATION FOLLOWING *IN SITU* CAPPING OF SEDIMENTS

4.1. Abstract

In situ capping of contaminated sediments is a promising management technique for contaminated aquatic sediments and involves placing a layer of clean fill material at the sediment-water interface. This work investigates the microbial colonization within a sand cap overlying aquatic sediment and couples microbial populations to high-resolution porewater geochemical profiles to monitor biogeochemical processes. Quantitative real-time PCR (qPCR) enumerated bacterial and archaeal populations in all dissected regions of the cap and sediment, and higher concentrations were generally observed in the sediment compared to the cap. New qPCR primers pairs were developed for *Anaeromyxobacter* and *Shewanellae* and accompanied published primer sets for δ-*Proteobacteria* and *Geobacteracea* to reveal iron-reducing bacteria were present throughout the cap and sediment, supporting geochemical measurements that indicated microbial iron reduction was a major terminal electron accepting process. Presence of the *dsrA* gene throughout the column suggests microbial sulfate reduction occurred, while detection of the *mcrA* gene demonstrated that anaerobic Archaea were also present within the cap. Canonical correspondence analysis of Terminal-Restriction Fragment Length Polymorphism (T-RFLP) patterns verified changes in bacterial community composition with depth and along Fe^{2+} and Mn^{2+} concentration gradients. Bacterial richness and diversity, estimated from T-RFLP fragment patterns, were correlated to qPCR results for total bacteria. Phylogenetic assignments inferred from T-RFLP data suggested

fermenting populations were present in the overlying cap and provided additional insight regarding community composition. The culture-independent microbial analyses confirm that microbial communities shift with biogeochemical processes and that microorganisms indigenous to aquatic sediments colonize an overlying sand cap. Implications for elemental biogeochemical cycling, contaminant fate and transport, and remedial design are discussed.

4.2. Introduction

Biogeochemical cycling at the sediment-water interface of aquatic sediments can be complex and subject to multiple site-specific variables such as organic carbon input, hydrodynamic flow patterns, bioturbation, and anthropogenic perturbation. Undisturbed aquatic sediments below oxic surface waters typically possess an aerobic layer extending millimeters to centimeters into the sediment bed (*166*). An abundant and diverse community of heterotrophic microorganisms inhabit the upper aerobic sediment layer due to the presence of oxygen and labile organic matter (*283*). Beneath this aerobic layer exists a gradient of anaerobic biogeochemical processes, stratified according to the thermodynamic yields of their respective terminal electron accepting processes (*168*). Microbial composition and functionality reflect this redox stratification and can impact contaminant bioattenuation mechanisms within sediments. For example, metal sequestration (*52*) and the microbial transformation of petroleum hydrocarbons (*284*, *285*), chlorinated solvents (*22*), polychlorinated biphenyls (PCBs) (*286*), and polyaromatic hydrocarbons PAHs (*110*) have all been documented within aquatic sediments under a variety of redox conditions.

Contaminated aquatic sediments can cause adverse effects on aquatic life and limit recreational and economic uses, especially in urban settings (*2*, *3*, *257*), necessitating remedial action. *In situ* capping has emerged as a remedial method for contaminated sediments and involves placing a layer of clean fill material at the sediment-water interface to prevent contaminant contact with benthic macrofauna and overlying surface water. Clean sand has traditionally been the material employed for capping and can delay contaminant breakthrough considerably when diffusive transport dominates (*151*). Recent efforts have focused on developing active cap technology, in which sediment caps are augmented with abiotic (*156*) or biological (*282*) constituents designed to remove or transform contaminants during transport through the cap. Chapter 3 of this work has demonstrated that emplacing an *in situ* cap at the sediment-water interface induces and upward, vertical shift of biogeochemical processes into the overlying cap while simultaneously conserving redox stratification. A majority of the cap was subject to anaerobic redox conditions, which promoted iron reduction. One issue that has not been addressed, however, is if microorganisms also shift from the sediment to inhabit the overlying cap.

Intrinsic microbial colonization of an *in situ* sediment cap can directly impact biogeochemical cycling and contaminant fate and transport within sedimentary environments. Studies described herein address the ability and degree to which microorganisms indigenous to sediments can colonize an overlying sand cap. Efforts are also made to examine populations implicated in metal reduction, sulfate reduction, and methanogenesis for comparison with geochemical gradients. To address the degree of microbial colonization and the impact on biogeochemical cycling and contaminant

biotransformation, target microbial populations were enumerated within a capped sediment column using quantitative real-time PCR (qPCR) and spatial changes in bacterial community composition were monitored with terminal-restriction fragment length polymorphism (T-RFLP) analysis. Total Bacterial and Archaeal cell numbers were quantified to gauge general microbial colonization and abundance in the various sections of the sand cap and sediment. The *δ-Proteobacteria* subclass was also analyzed with qPCR to provide a general indication of iron- and sulfate-reducing organisms, several of which are classified as *δ-Proteobacteria* (e.g., *Geobacter*, *Anaeromyxobacter*, *Desulfovibrio*, *Desulfuromonas*). To gain information on specific metal- and iron-reducing bacteria (DIRB), the bacterial genera of *Anaeromyxobacter*, *Geobacteraceae*, and *Shewanellae* were targeted. *Anaeromyxobacter* spp. are capable of respiration with oxygen, nitrate, nitrite, manganese, soluble and amorphous ferric iron, *ortho*-substituted halophenols, and U(VI) (*54*, *235*, *287-289*). *Geobacter* species are capable of reducing nitrate, metal oxides (e.g.., iron and manganese), sulfur, U(VI), and chlorinated ethenes while also oxidizing aromatic hydrocarbons (*53, 234*, *290-294*). S*hewanella* can also utilize a diverse suite of electron acceptors (e.g., oxygen, nitrite, nitrate, thiosulfate, ferric iron, Mn(IV), U(VI), and Cr(VI) (*55, 176, 295, 296*)), and previous geochemical profiling of the sediment (Chapter 3 of this work) has detected soluble organic-Fe^{III} complexes in anaerobic conditions, possibly indicating the presence of *Shewanella* species (*183*). Quantitative PCR was also used to gain further insight into sulfate reducing populations by targeting the functional gene encoding the alpha subunit of the dissimilatory (bi)sulfite reductase (*dsrA*). The *dsr* enzyme catalyses the final step of sulfate reduction (reduction of sulfite to sulfide) and has been shown to be evolutionarily

conserved among sulfate reducing prokaryote (SRPs) (*297*). Additionally, the functional gene encoding the alpha subunit of the methyl-coenzyme M reductase (*mcrA*) was quantified as an indicator for methanogenic Archaea. The *mcr* enzyme is conserved in all methanogens (*207*) and catalyzes the final step of the methanogenic pathway.

Combined results from the qPCR and T-RFLP studies provide detailed microbial community data coupled to geochemical characterization at very high resolution. Microbial populations colonized the sand cap from the underlying sediment with target populations performing specific terminal electron accepting processes generally correlated to geochemical zones. Statistically different populations were observed with depth and along Mn^{2+} and Fe^{2+} gradients.

4.3. Materials and Methods

4.3.1. Capped Sediment Column

A laboratory-scale sediment column was constructed to monitor biogeochemical changes induced by sediment capping with a layer of clean sand. Details of sediment column construction are reported in Chapter 3. Briefly, sediment from the Anacostia River was used as the sediment for the capped sediment column. The river is subject to tidal pumping and flows through Washington, D.C., USA. Sediment from the river has previously been reported to contain elevated levels of PCBs, PAHs, metals, and organic pesticides (*158*). The capped sediment column was established in a glass chromatography column (20 cm long, 5.0 cm I.D.; Spectrum Chromatography, Houston, TX) fitted with a Teflon bottom endplate. The column was packed with wet sediment to a depth of 7 cm then capped with 7 cm of dry, autoclaved ASTM C-33 concrete sand

(U.S. Silica, Mauricetown, NJ) for a total thickness of 14 cm. Overlying water consisted of nano-pure water (> 18.2 Ω) containing only sodium chloride ($10^{-2.9}$ M) to match the salinity of the Anacostia sediment porewaters and was maintained at 4 cm above the cap-water interface with a constant head reservoir. The capped sediment column was incubated under aerobic conditions in the dark at room temperature with static flow conditions for 13 weeks, then upflow conditions for 16 weeks. A syringe pump provided anoxic influent solution to the bottom of the column at a flow rate of 2.0 $cm^3 \cdot hr^{-1}$ (seepage velocity = 4.4 $cm \cdot day^{-1}$; Darcy velocity = 2.4 $cm \cdot day^{-1}$). The influent was equivalent to the overlying water solution but sparged for 30 minutes with nitrogen gas (Airgas, Atlanta, GA) to remove dissolved oxygen. Exogenous sources of mineral media, vitamins, carbon, and energy sources were not supplied by the influent solution to most accurately mimic environmental conditions. A constant head reservoir maintained overlying water levels at approximately 4 cm under upflow conditions. Multiple porewater geochemical profiles were obtained during stagnant and upflow conditions, with a final profile obtained 16 weeks after the onset of upflow conditions (29 weeks of total incubation; 71 pore volumes flushed).

4.3.2. Porewater Geochemical Profiles

Details of geochemical measurements are reported in Chapter 3, with only a brief description provided here. Voltammetric microelectrodes were used to analyze aqueous geochemical species. All voltammetric measurements were performed using a platinum counter electrode, an Ag/AgCl reference electrode, and an Au/Hg solid-state microelectrode fabricated as described by Brendel and Luther (*222*). The Au/Hg working microelectrodes are capable of simultaneously measuring $O_{2(aq)}$, H_2O_2, Fe^{2+}, Mn^{2+}, $S_2O_3^{2-}$

, ΣH_2S [$=H_2S + HS^- + S^{2-} + S^0 + S_x^{2-}$], organic-$Fe^{III}_{(aq)}$, and $Fe_xS_{y(aq)}$ species (*187, 199, 222*). Each Au/Hg microelectrode was tested for quality and calibrated for dissolved oxygen by linear sweep voltammetry in simulated freshwater (0.1M NaCl), and then for manganese by cathodic square wave voltammetry (CSWV) in degassed simulated freshwater. Concentrations of $Fe^{2+}$and ΣH_2S were determined from manganese calibration curves following the pilot ion method (*222*). The sensitivities of the organic-$Fe^{III}_{(aq)}$ complexes have yet to be determined, and their concentrations are therefore reported in units of current intensity (nA) (*187*). Similarly, the stoichiometry of $Fe_xS_{y\,(aq)}$ is unknown and current intensities (nA) are also reported for these species (*199*). All voltammetric analyses were performed with a computer-operated DLK-100A potentiostat and a computer-operated micromanipulator capable of vertical movements at the sub-millimeter scale (Analytical Instrument Systems). Voltammograms were processed with a Matlab®-based program (*261*).

4.3.3. Column Dissection

After 16 weeks of incubation under upflow conditions (29 weeks total), the capped sediment column was dissected specifically for microbiological analyses. Overlying surface water was first removed from the column with a sterile needle and syringe. A core sample was obtained from the center of the column using a zero contamination soil sampling tube (JMC Soil Samplers, Newton, IA), with the core encased within a PETG co-polyester liner measuring 30 cm long and 2.0 cm I.D. The liner containing the core was then removed from the sampling tube, capped with vinyl plugs, and stored at -20 °C until frozen. The intact core was simultaneously extruded from the liner and dissected while still frozen.

The first dissection was made 10 mm below the cap-water interface, with successive dissections at intervals of 12.5 mm until the cap-sediment interface was reached (Figure 4.1). A total of seven samples were obtained from the sand cap material (y=0 to -70 mm). Four sediment samples were obtained following dissections at 15 and 25 mm intervals (Figure 4.1). Dissected materials were immediately placed into sterile, 15 mL centrifuge tubes and stored at -20 °C. Dissected regions were labeled sequentially beginning with dissected region 1 at the cap-water interface and ending with dissected region 11 in the sediment (Figure 4.1). The final dissection region (Region 11) was not obtained aseptically following leakage from the core induced by gas voids within the sediment, and was thus not included in subsequent analysis.

Dissection regions were subject to different biogeochemical conditions according to the porewater geochemical profile: Region 1 included oxygen and manganese reduction; Region 2 displayed manganese reduction; Regions 3 and 4 contained iron and manganese reduction; Region 5 indicated iron reduction; Regions 6 through 8 displayed iron reduction and $Fe_xS_{y(aq)}$ formation; Regions 9 through 11 included iron reduction and $Fe_xS_{y(aq)}$ formation but no dissolved, free ferrous iron. Interpretation of the geochemical data of Chapter 3 also suggested the role of sulfate reduction as a minor process.

4.3.4. DNA Isolation

DNA was extracted from the solid and aqueous phases of each dissected region using the Ultraclean™ Soil DNA Isolation Kit (Mo Bio Laboratories, Inc., Solana Beach, CA). The manufacturer's protocol was followed, except that a Mini-beadbeater™

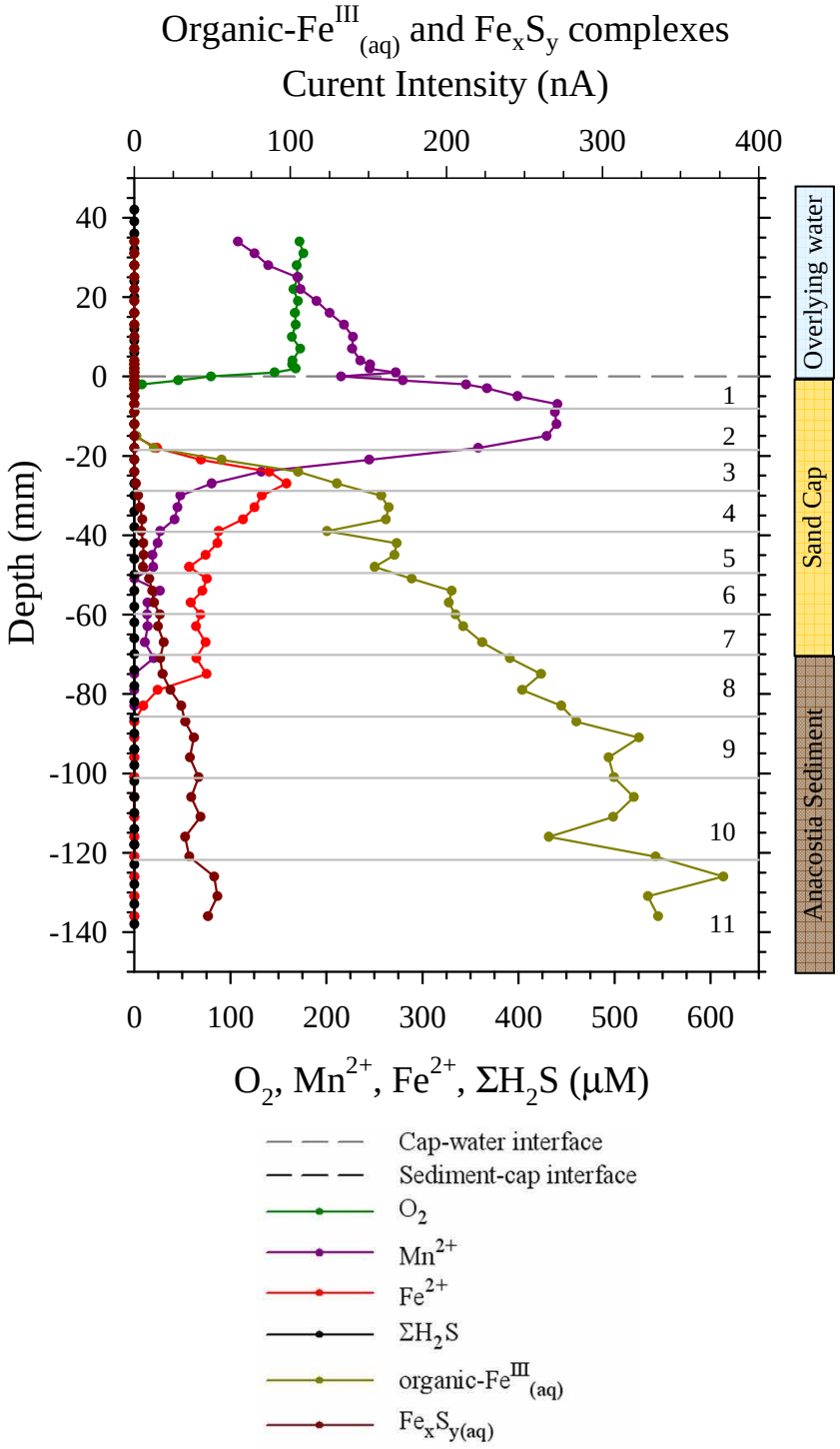

Figure 4.1. Porewater geochemical characterization of an Anacostia River sediment column capped with ASTM C-33 concrete sand. The values for the organic-$Fe^{III}_{(aq)}$ and $Fe_xS_{y\,(aq)}$ complexes are reported as current intensity and are referenced to the top x-axis. The concentrations of $O_{2(aq)}$, Fe^{2+}, Mn^{2+}, and ΣH_2S (µM)are referenced to the lower x-axis. Dissection locations are indicated by solid gray lines, with numbers corresponding to dissection regions.

(Biospec Products, Bartsville, OK) was used instead of a vortex for cell lysis. Extractions were performed on dissection regions 1 through 10. Four separate DNA extractions were performed on material from dissection region 1, with DNA from the replicate extractions combined. Six extractions were performed on material from each remaining region (Regions 2 through 10), with DNA from replicate extractions combined. DNA was also extracted from autoclaved, dry ASTM C-33 sand to examine if indigenous microbial populations were present in the sand prior to capping. Pooled samples were analyzed for DNA quality and concentrations ($ng \cdot \mu L^{-1}$) using a NanoDrop® ND-1000 UV/VIS spectrophotometer (NanoDrop Technologies, Wilmington, DE) and stored at -20 °C.

4.4.5. Primer Design

Specific qPCR primer pairs for *Shewanella* and *Anaeromyxobacter* spp. were designed with the Oligo Design and Analysis Tools (www.idtdna.com) based on the nearly complete 16S rRNA gene sequences available in GenBank. The 16S rRNA gene sequences were aligned using the MegAlign program of the Lasergene software package (DNA Star Inc., Madison, Wisconsin). The sequences of the selected primers are provided in Table 4.1. The forward primer for *Shewanellaea*-targeted qPCR was She211f as developed by Todorova et al. (*298*). The She211f primer was modified (i.e., reverse complement) to create reverse primer She220R (Table 4.1). The expected size of She112F/She220R amplicons is 108 bp, an acceptable size for qPCR. The *Anaeromyxobacter* primers were obtained using Applied Biosystems Primer Express™ software. A 200 bp section of the 16S rRNA gene sequence containing an *Anaeromyxobacter*-specific region was identified by analysis of the alignment and

entered into the Primer Express program to find a short region with a consistent melting temperature. The expected size of Amyx-399F/Amyx-466R amplicon is 67 bp. BLAST analysis suggested primer specificity to the target sequences.

4.3.6. Quantitative Real-Time PCR (qPCR) analysis

Target organisms, reaction chemistries, primer sequences, and standards for all qPCR analyses are provided in Table 4.1. Total Bacteria were quantified following qPCR conditions described by Ritalahti et al. (*231*). Total Archaea were quantified using primers and methods described by Da Silva et al. (*299*), with genomic DNA extracted from *Methanococcus maripaludis* as a standard. Quantification of *δ-Proteobacteria* was performed by Microbial Insights, Inc. (Rockford, TN) using primers and conditions described by Stults et al. (*293*). qPCR analysis for *Anaeromyxobacter*, *Geobacter*, and *Shewanella* spp. was performed using SYBR Green-based detection chemistry and the described primers (Table 4.1). The reaction mixture contained 15 µl of Power SYBR Green PCR master mix (Applied Biosystems), 300 nM of each primer, and 3 µl of template DNA in a total reaction volume of 30 µl. The qPCR temperature program was as follows: 2 min at 50 °C, 10 min at 95 °C, then 40 cycles of denaturation at 95 °C for 15 s and annealing at 60 °C for 1 min, with fluorescence measured after each annealing step. The *dsrA* gene was quantified under conditions utilized by Wilms et al. (*238*), with the exception that 2.5 µL of DNA was used with sterilized water filling the remaining volume. The standard for *dsrA* calibration was genomic DNA from *Desulfovibrio vulgaris* (ATCC 29579), whose genome has been sequenced and contains one copy of the *dsrA* gene, which matches the primers utilized here. The *mcrA* gene was quantified following a previously published protocol (*238*), except that the reverse primer was

modified such that a W replaced S at the ninth position to fully complement the original primers designed by Hales et al. (*300*). The standard for *mcrA* calibration was genomic DNA from *Methanosarcina mazei* (ATCC BAA-159), whose genome has been sequenced and contains one copy of the *mcrA* gene, matching the *mcrA* primers used here.

Extracted DNA was diluted 1:10 with elution buffer to minimize interferences from PCR inhibitors co-extracted from the column material. All qPCR was carried out with an Applied Biosystems 7500 Fast Real-Time PCR System and melting curve analysis was performed with the default settings of the ABI software from 67ºC to 95ºC following the completion of each qPCR. Standard curves were generated following the procedure outlined in Ritalahti et al. (*231*) and used a 10-fold dilution series of quantified plasmid (concentration determined spectrophotometrically at 260 nm) carrying a single copy of the 16S rRNA gene. The total length of the plasmid (3,931 bp) with the cloned 16S rRNA gene insert (1,534 bp) was 5,465 bp. When genomic DNA was used, genome sizes replaced plasmid size during calculations (*D. vulgaris*: 3,773,159 bp; *M. mazei*: 4,096,345 bp). For each set of standards and unknown samples (except *δ-Proteobacteria*), triplicate reactions were performed per experiment, with triplicate experiment means and standard deviations reported. Negative control reactions accompanied all qPCR analyses and consisted of nuclease-free water (Fisher Scientific) replacing the template.

Table 4.1. Conditions and primers employed during quantitative real-time PCR analysis.

Target Group	qPCR Chemistry	Primer/Probe Name	Sequence	Standards	References[a]
Total *Bacteria*	TaqMan®	Bac1055YF	5'-ATGGYTGTCGTCAGCT-3'	*Geobacter lovleyi SZ*	(*168*)
		Bac1392R	5'-ACGGGCGGTGTGTAC-3'		
		Bac1115Probe	5'-FAM-CAACGAGCGCAACCC-TAMRA-3'		
Total *Archaea*	TaqMan®	ARCH1-1369F	5'-CGGTGAATACGTCCCTGC-3'	*Methanococcus maripaludis*	(*230*, *231*)
		ARCH2-1369F	5'-CGGTGAATATGCCCCTGC-3'		
		PROK1541R	5'-AAGGAGGTGATCCTGCCGCA-3'		
		TM1389F	5'-FAM-CTTGTACACACCGCCCGTC-TAMRA-3'		
δ-Proteobacteria[b]	TaqMan®	361F	5'-AAGCCTGACGCASCAA-3'	*Geobacter bemidjiensis*	(*299*, *301*)
		685R	5'-ATCTACGGATTTCACTCCTACAC-3'		
		Eub1	5'-FAM-GTATTACCGCGGNTGCTGGC-TAMRA-3'		
Anaeromyxobacter spp.	SYBR Green I	Amyx-399F	5'-GCAACGCCGCGTGTGT-3'	*Anaeromyxobacter dehalogenans* str. 2CP-C	This study
		Amyx-466R	5'-TCCCTCGCGACAGTGCTT-3'		
		ME3 rev	5'-TGTGTGAAWCCKACDCCACC-3'		

Table 4.1 (continued).

Target Group	qPCR Chemistry	Primer/Probe Name	Sequence	Standards	References[a]
Geobacteracea spp.	SYBR Green I	Geo 564F	5'-CAAGTCGTACGAGAAACATATC-3'	*Geobacter lovleyi* SZ	(*293*)
		Geo 840R	5'-GAAGAGGATCGTCTTTCCACGA-3'		
Shewanellae spp.	SYBR Green I	She 120F	5'-GCCTAGGGATCTGCCCAGTCG-3'	*Shewanella oneidensis* MR1	This study
		She 220R	5'-CTAGGTTCATCCAATCGCG-3'		
Dehalococcoides spp.	TaqMan®	Dhc1200F	5'-CTGGAGCTAATCCCCAAAGCT-3'	*Dehalococcoides* sp. str. FL2	(*53*, *236*)
		Dhc1271R	5'-CAACTTCATGCAGGCGGG-3"		
		Dhc1240Probe	5'-FAM-TCCTCAGTTCGGATTGCAGGCTGAA-TAMRA-3'		
dsrA gene	SYBR Green I	dsr-1f	5'-ACSCACTGGAAGCACG-3'	*Desulfovibrio vulgaris* subsp. *vulgaris*	(*302*)
		dsr-500r	5'-CGGTGMAGYTCRTCCTG-3'		
mcrA gene	SYBR Green I	ME1 fwd	5'-GCMATGCARATHGGWATGTC-3'	*Methanosarcina mazei*	(*238*)
		ME3 rev	5'-TGTGTGAAWCCKACDCCACC-3'		

[a] original literature sources for primer/probe names and sequences
[b] performed by Microbial Insights, Inc, Rockford, TN

4.3.7. Terminal-Restriction Fragment Length Polymorphism (T-RFLP) Analysis

The dissected regions 1, 2, 3, 4, 6, 8, and 10 exhibited unique geochemical characteristics and were selected for T-RFLP analysis (Figure 4.1). Amplification of bacterial 16S rRNA genes from each selected region was performed using triplicate PCR reactions (100 μL each) with a HEX-labeled forward primer 8F (5'-AGAGTTTGATCCTGGCTCAG-3') and the unlabeled reverse primer 1541R (5'-AAGGAGGTGATCCAGCCGCA-3'). The PCR products were purified with the QIAquick PCR purification kit (QIAGEN, Valencia, CA), the replicates combined (90 μL total), then quantified using the NanoDrop® spectrophotometer. Enzyme digests (30 μL) were prepared with purified PCR products (200 ng DNA), reaction buffer (3 μL), and restriction enzyme (7.5 U). The restriction enzymes utilized in this study were *HhaI*, *MspI*, and *RsaI*. Each digest was performed at 35 °C for 3 h, followed by enzyme denaturing at 68 °C for 25 min. T-RFLP samples were analyzed at the University of Illinois Urbana-Champaign Core Sequencing Facility using a Prism 3730xl Analyzer (Applied Biosystems). The ROX-1000 size standard was used for calibration of fragment sizes. Data collection and analysis was performed using GeneMapper™ 3.7 software (Applied Biosystems). To generate T-RFLP profiles, each profile was normalized to the profile with the lowest total fluorescence (*239*). *Anaeromyxobacter dehalogenans* strain 2CP-C DNA was digested with each digestion enzyme to ensure that experimentally-derived T-RF digestion patterns matched predicted in silico patterns (data not shown).

Phylogenic assignment of T-RFLP peaks was inferred using an automated, web-based phylogenetic assignment tool (PAT) maintained by University of Wisconsin's North Temperate Lakes Microbial Observatory

(http://trflp.limnology.wisc.edu/index.jsp). The program compares T-RF sizes to the University of Idaho's Microbial Community Analysis database of fragments produced by known 16S rRNA gene sequences (*303*) to generate phylogenetic assignments from submitted T-RFLP profiles. Phylogenic assignments were performed for each dissection region (regions 1, 2, 3, 4, 6, 8, 10) using fragment patterns produced from the *HhaI*, *MspI*, and *RsaI* digests. Phylogenetic assignments were restricted to the Phylum-Class levels.

4.3.8. Data Analysis

T-RFLP profiles were statistically analyzed to elucidate significant changes in community composition and to provide more quantitative information regarding community diversity. For each statistical analysis, distinct fragment sizes (bp) represented individual species, with relative fluorescence (rfu) representing species abundance (*241*). Canonical correspondence analysis (CCA) was performed to determine if positive relationships existed between bacterial community patterns and environmental variables (*304*) (CANOCO 4.5 software, Microcomputer Power, Ithaca, NY, USA). Quantitative environmental variables tested were average depth values, and measured concentrations of Mn^{2+}, Fe^{2+}, organic-$Fe^{III}_{(aq)}$, and $Fe_xS_{y(aq)}$. Untransformed fragment patterns generated from *HhaI* enzyme digestions of Regions 1, 2, 3, 4, 6, 8, and 10 were used as input species data. To identify which variables were most effective at explaining community shifts, automatic forward selection of environmental variables followed by Monte Carlo permutation tests (≥1500) were performed within CCA, with significance defined at $p<0.05$ Combinations of environmental variables were also examined using

forward selection and Monte Carlo permutation tests. Results were summarized in ordination diagrams (CanoDraw 4.0).

Three independent species diversity indices were calculated from normalized *HhaI* T-RFLP fragment patterns to provide quantitative information on microbial diversity, composition, and health. The first indicator calculated was species richness (*S*), which equivalent to the amount of unique fragments in each region (i.e., distinct fragment sizes represent individual species) (*305*). The second indicator was Shannon's diversity index (*H*) and provides an estimate of diversity accounting for both species abundance and evenness in the estimate. Typical values are between 1.5 and 3.5 with higher values indicating a greater degree of diversity. Shannon index values and their associated error were calculated using StatsDirect Statistical Software (StatsDirect, Ltd, Altrincham, Cheshire, UK). The third indicator calculated was the Smith and Wilson evenness value (E_{var}), recommended by Blackwood et al. (*306*) to determine species parity from T-RFLP data. The value ranges from 0 (patchy or skewed) to 1 (even), and is equally sensitive to species with high or low abundance (*307*).

4.4. Results

4.4.1. Target Microbial Populations

Microbial populations were present and quantifiable in each dissected region of the sediment and overlying sand cap (Figures 4.2A-C). Bacteria cell numbers in the cap generally decreased in each subsequent region (Figure 4.2A), from 5.2×10^8 cells per mL porewater in Region 1 to 1.7×10^6 cells per mL porewater in Region 6, before an increase in Region 7 directly above the sediment-cap interface. Bacterial cells were relatively

constant within the sediment (Regions 8 to 10), with observed mean values between 5.9 x 10^8 and 6.8 x 10^8 cells per mL porewater. Neither Bacteria nor Archaea were detected in DNA extracted from dry, autoclaved ASTM C-33 sand.

Bacteria associated with dissimilatory metal reduction and potential contaminant biotransformations were detected in each region of the sediment and the overlying sand cap (Figure 4.2A). *δ-Proteobacteria* were detected throughout the column at levels similar to those of total Bacteria, suggesting sediment and cap populations are dominated by *δ-Proteobacteria*. Comparison of specific metal- and iron -reducing bacteria reveals that *Geobacter* spp., *Anaeromyxobacter* spp., and *Shewanella* spp., were all detected in each respective region. *Geobacter* cell numbers in the cap ranged from 10^5 to 10^6 cells per aqueous mL, and peaked at 6.7 x 10^7 cells per mL porewater in the sediment. *Anaeromyxobacter* cell numbers were most prominent in the upper cap layers (9.9 x 10^5 in Region 1) and in the sediment (1.8 x 10^7 in Region 9). The presence of *Shewanella* species, suspected following detection of the organic-$Fe^{III}_{(aq)}$ complex (*183*), was confirmed by the qPCR results and were most abundant in the upper cap layers (1.0 x 10^6 in Region 1), then stabilized to mean values between 10^4 and 10^5 cell per mL of porewater before increasing slightly in the sediment. In Region 1, DIRB (*Anaeromyxobacter*, *Geobacter*, *Shewanella*) accounted for only 0.4% of the total Bacteria (Table 4.2). Higher proportions of DIRB relative to total Bacteria were observed in the remainder of the cap and sediment, from 8.7% in Region 6 to 1.2% in Region 7. *Dehalococcoides* species were not detected in any region of the column, however the necessary electron acceptors to enrich their population (e.g., chlorinated ethenes) were not provided.

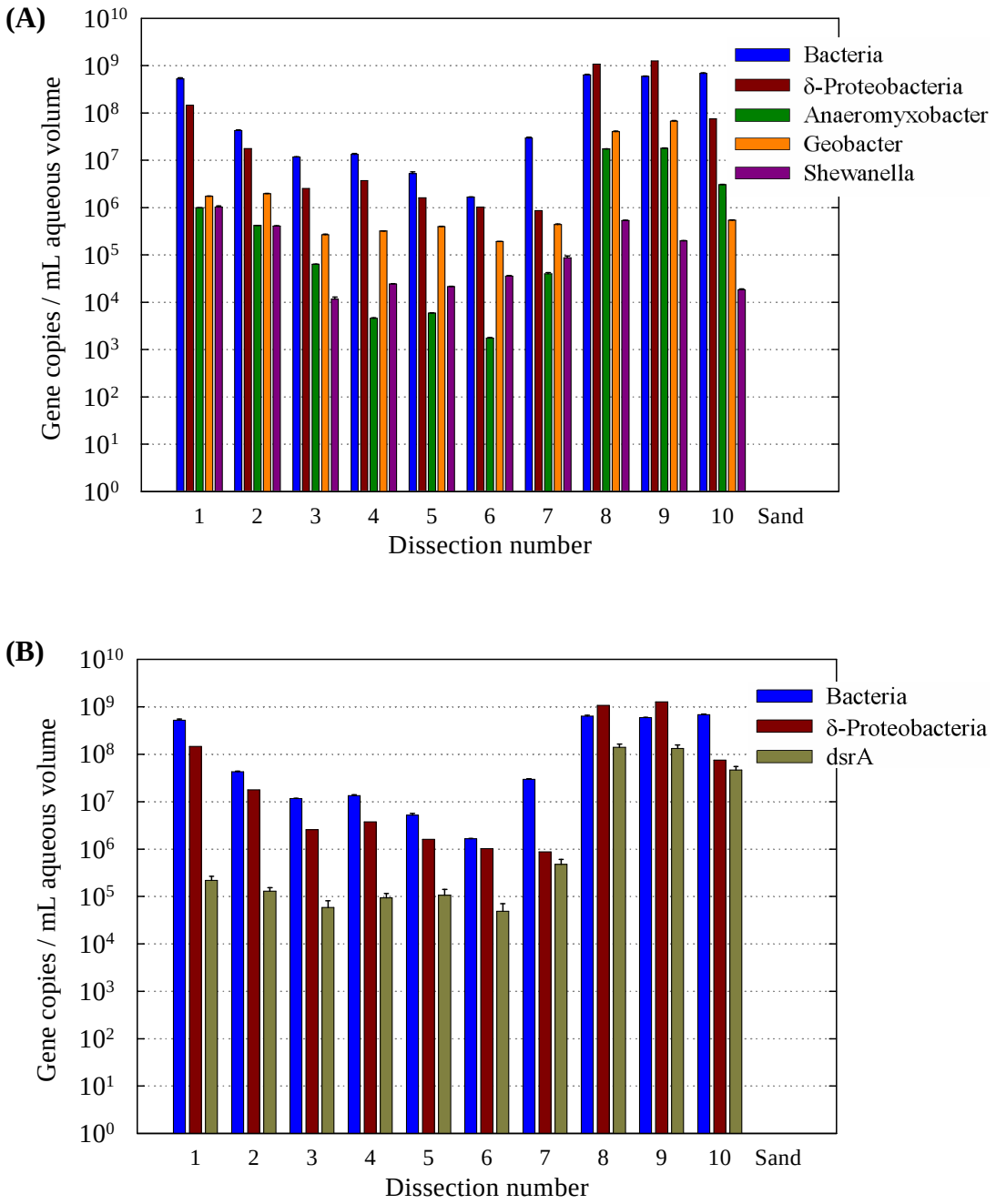

Figures 4.2A-C. Quantitative real-time PCR (qPCR) results for (A) Total Bacteria and populations implicated in metal reduction and bioremediation, (B) Total Bacteria and target genes indicating sulfate-reducing microbial populations, and (C) Total Archaea and *mcrA* functional gene copies.

(C)

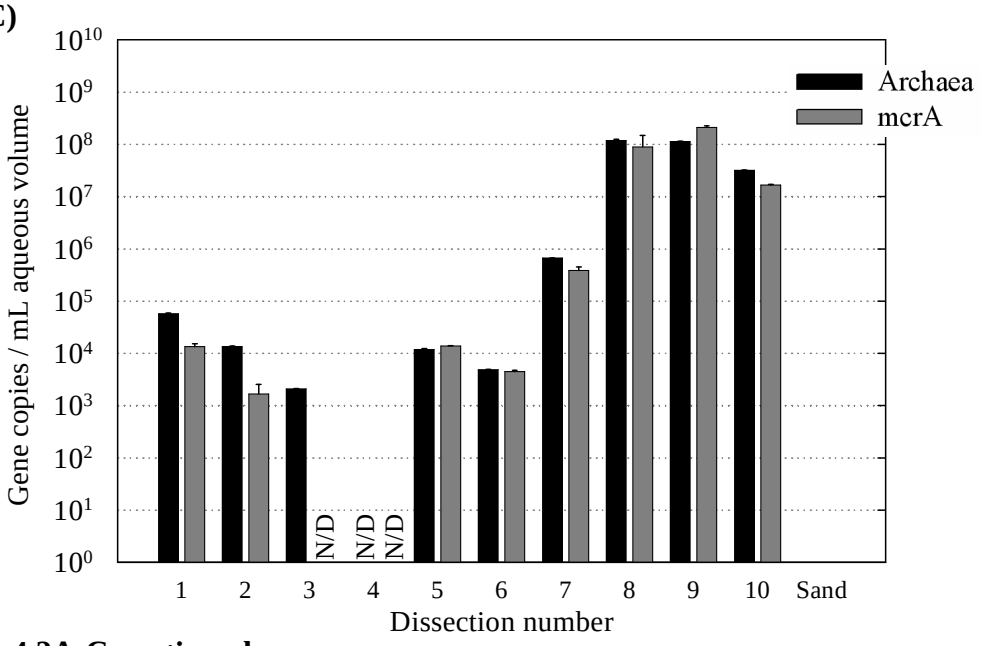

Figures 4.2A-C continued.

Table 4.2. Proportion (percent) of metal-reducing, sulfate-reducing, and methanogenic organisms to total organisms for each dissection region, calculated from qPCR results. All values are reported in percentages of gene copies to gene copies. The dashed line between regions 7 and 8 indicates the sediment-cap interface.

Dissection Region	Proportion of DIRB[a] to Bacteria	Proportion of *dsrA* to Bacteria	Proportion of Archaea to Bacteria	Proportion of *mcrA* to Archaea
1	0.4	<0.1	<0.1	23.4
2	4.0	0.3	<0.1	12.5
3	2.7	0.5	<0.1	N/A
4	4.1	0.7	N/A [b]	N/A
5	6.3	2.1	0.2	>100
6	8.7	2.9	0.3	92.5
7	1.2	1.6	2.2	57.9
8	3.8	22.2	18.5	75.9
9	6.9	22.3	19.1	>100
10	0.2	6.7	4.7	52.2

[a] Metal- and Iron- Reducing Bacteria, defined as the cumulative gene copies of *Anaeromyxobacter*, *Geobacter*, and *Shewanella*
[b] Calculation not able to be performed due to quantifications below detection limits.

The *dsrA* functional gene for sulfate reduction was detected in all sediment and cap regions, whereas the *mcrA* functional gene for methanogenesis was detected in most regions but was absent in Regions 3 and 4. The *dsrA* gene was detected in the capping layer at 10^4 to 10^5 cells per ml of porewater, but increased two to three orders of magnitude in the sediment (Figure 4.2B). Additionally, *dsrA* gene copies were more comparable (i.e., within one order of magnitude) to *δ-Proteobacteria* levels in the deeper sediment regions of the column (Regions 7 to 10) compared to most cap layers (Regions 1 to 6). The proportion of sulfate reducing prokaryotes (SRP) compared to total Bacteria generally increased with depth, increasing from less than 0.1% in Region 1 to 2.1% in Region 5 to 22.3% in Region 9.

Archaeal cell numbers displayed slightly greater abundance in the uppermost cap region compared with the underlying regions (Figure 4.2C). Archaeal cell numbers increased in Region 7 to 6.6 x 10^5 copies per mL porewater then increased again in the sediment to approximately 10^8 copies per mL of porewater. The ratio of archaeal to bacterial 16S rRNA gene copies ranged from less than 0.1% in Regions 1-3 to 19.1% in Region 9. The *mcrA* gene was detected in the upper two regions, but was not detected in Regions 3 and 4, respectively. Copy numbers of *mcrA* in the remaining layers (Regions 5 to 10) were comparable to those observed for *Archaea*, with the most *mcrA* gene copies detected in the sediment (2.1 x 10^8 in Region 9). The proportion of *mcrA* gene copies per mL porewater to Archaea gene copies ranged from 12.5% in Region 2 to greater than 100% in Region 9. A modified *mcr* gene has recently been identified in enrichments of anaerobic methane oxidizers (*207*) and may be involved in reverse methanogenesis under anoxic conditions (*208, 209*). Therefore, detection of *mcrA* indicated the presence of

methanogens and/or methane oxidizers, with both groups found in anaerobic environments.

4.4.2. Bacterial Community Analysis

Analysis of T-RFLP fingerprint patterns (Figure 4.3) indicated statistically significant changes in the bacterial community composition within each region. Monte Carlo permutation tests within CCA suggested that changes in T-RFLP patterns could be significantly correlated to the environmental variables of depth, Fe^{2+} and Mn^{2+} concentrations (μM). Average depth best explained changes in the T-RFLP data and was the only variable independently related to species data ($p=0.015$). The T-RFLP data were explained with the greatest degree of confidence ($p=0.008$) when average depth, Fe^{2+}, and Mn^{2+} concentrations were all considered, suggesting these three variables collectively influenced species niche separation. The ordination bi-plot presented in Figure 4.4 shows the relationship of each dissection region to gradients extracted from the species data when depth, Fe^{2+}, and Mn^{2+} concentrations were considered. Based on the CCA results, the hypothesis of no relation between organism and environment could be rejected due to significant species composition changes correlated to depth and concentrations of Mn^{2+} and Fe^{2+}.

Indices of bacterial diversity and evenness were generally constant across all regions analyzed with two exceptions: Region 6 had relatively low species richness and diversity, while Region 1 had patchy species evenness (Table 4.3). Most species richness values were between 95 and 132, indicating a complex community. Previous studies estimating richness from T-RFLP data classified values between 45 and 72 as indicating a high degree of complexity in community diversity (*305*). The maximum richness

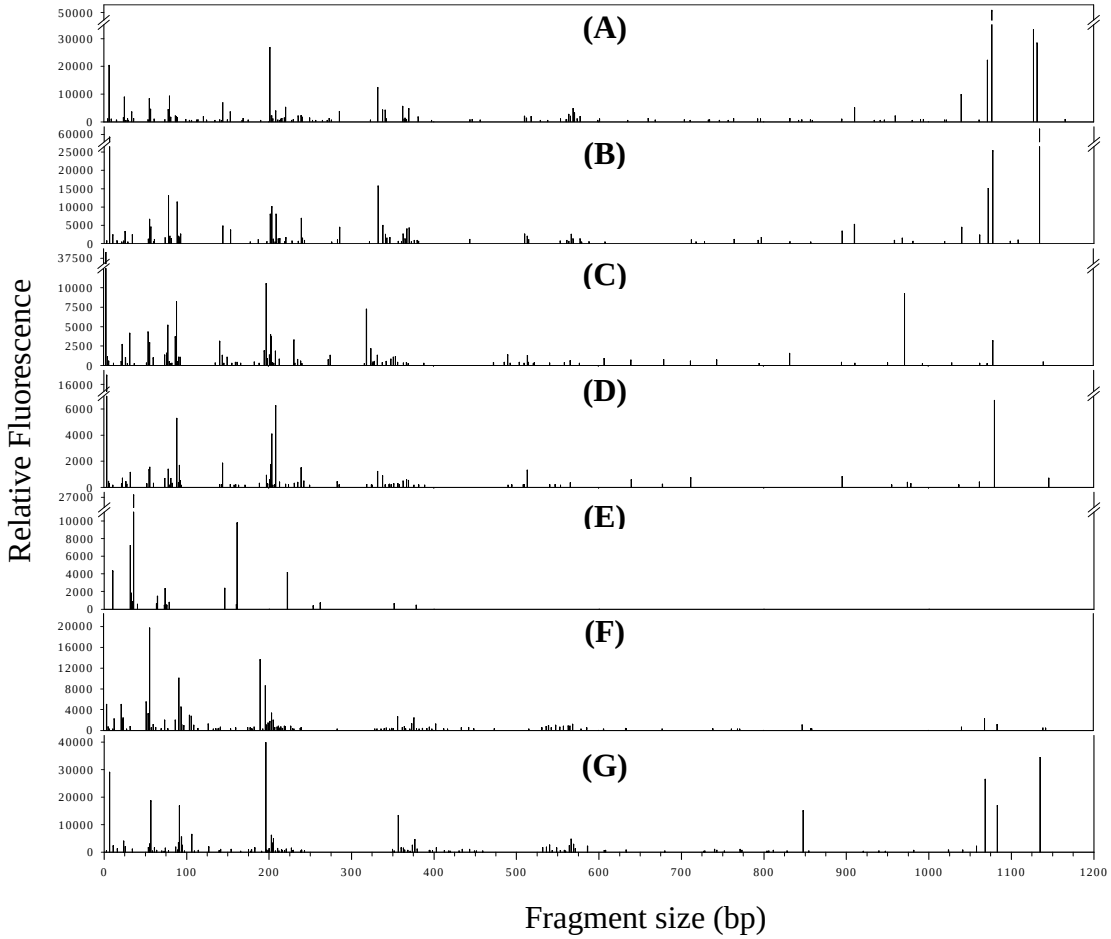

Figures 4.3A-G. Terminal-restriction fragment length polymorphism (T-RFLP) fragment patterns for *HhaI* enzyme at each dissection region. (A) Dissection Region 1, (B) Dissection Region 2, (C) Dissection Region 3, (D) Dissection Region 4, (E) Dissection Region 6, (F) Dissection Region 8, and (G) Dissection Region 10.

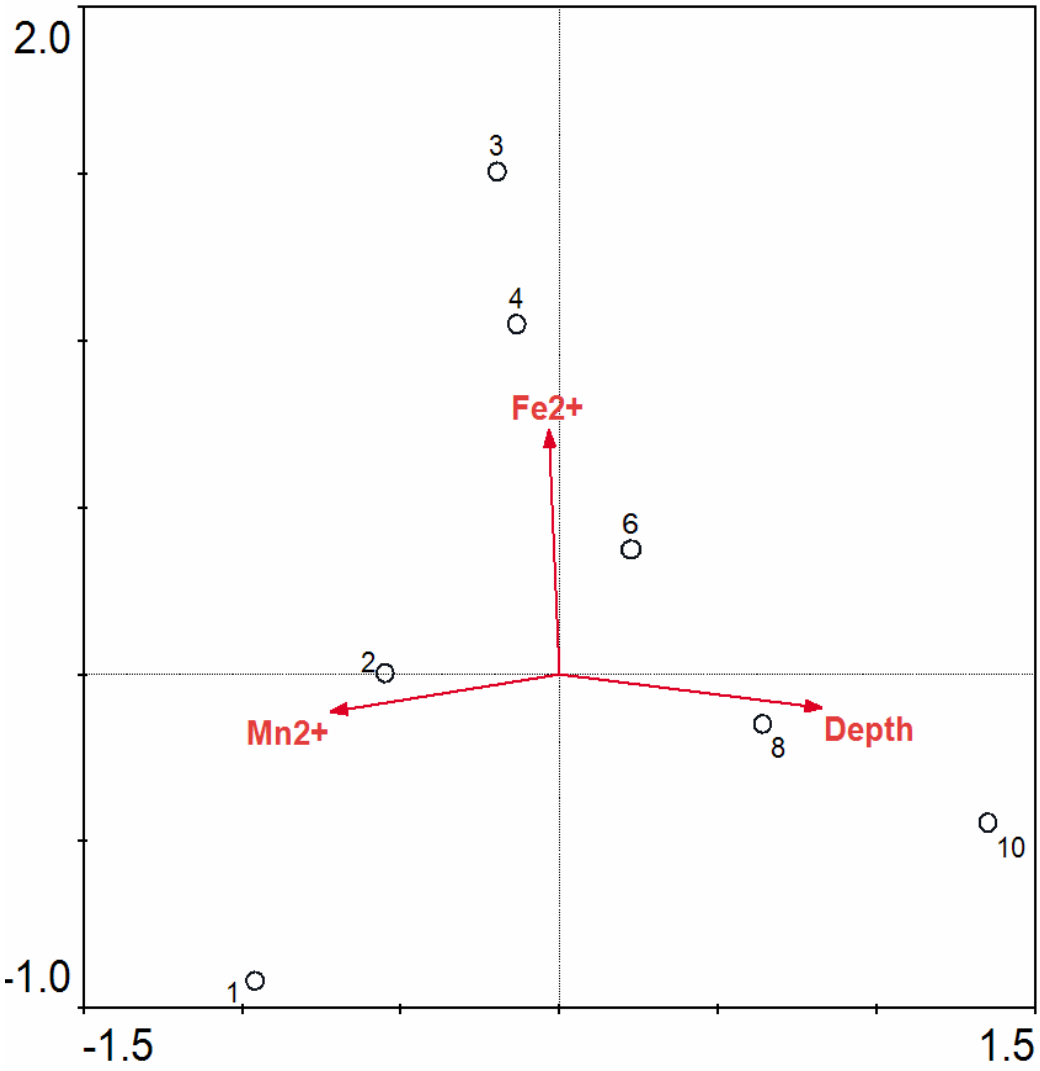

Figure 4.4. Ordination diagram based on canonical correspondence analysis of T-RFLP community profiles from dissection regions 1, 2, 3, 4, 8, and 10. The coordinates of the site points are the scores of each individual site on the two synthetic axes. Quantitative environmental variables are indicated by arrows, which point in the direction of maximum change in the value of the associated variable. The eigenvalues of axis 1 (horizontal) and axis 2 (vertical) are 0.696 and 0.497, respectively. The diagram accounts for 49% of the total inertia and 73% of the total variance.

value occurred in Region 1, which recorded relatively high bacterial numbers as determined by qPCR (Figure 4.2A); followed by Regions 8 and 10 (S=122 for each region), which was also characterized by high bacterial numbers. In fact, a moderate correlation between bacterial numbers and species richness (R^2=0.75) was observed. Region 6 had very low species richness (S=21) and modifications to the T-RFLP experimental protocol (e.g., further diluting the DNA prior to PCR amplification, increasing the volume of purified DNA in the digestion reactions) and replicate T-RFLP analyses yielded comparable results. Shannon index values were between 3.45 and 4.00 for most regions, with Region 6 being the exception (H=2.13), possibly indicating bacterial stress in this region. A modest correlation was detected between bacterial numbers and diversity (R^2=0.66). Smith-Wilson estimates of evenness suggested that species abundances within most regions were relatively similar, except for Region 1, which showed skewed abundance values (E_{var}=0.23).

Phylogenic assignment of T-RFLP peaks from *HhaI*, *MspI*, and *RsaI* digestions are summarized in Table 4.4. A total of 14 different taxonomic classes were identified, encompassing organisms characterized as phototrophs, heterotrophs, aerobes and anaerobes). Peaks that matched those of environmental clone sequences were placed into a separate category and comprised a large percent (up to 35%) of bacteria in each region. The *β-Proteobacteria* was the only identified class observed in all regions. Region 1 appeared to consist of a large percentage of *γ-Proteobacteria*, which includes aerobic methanotrophs and *Shewanellaea*. Regions 2 through 4 had large percentages of *β-Proteobacteria*, which are common organisms in soils and include aerobic, facultative, and nitrogen-fixing members. The highest phylogenic assignment in Region 6 belonged

Table 4.3. Indices of diversity and evenness calculated from *HhaI* T-RFLP fragment patters at each dissection region analyzed.

Dissection Region	Richness (*S*)	Shannon Diversity (*H*)	Smith-Wilson Evenness (E_{var})
1	132	3.87 ± 0.0023 [a]	0.23
2	95	3.45 ± 0.0025	0.43
3	105	3.63 ± 0.0037	0.48
4	93	3.52 ± 0.0052	0.51
6	21	2.13 ± 0.0049	0.40
8	122	4.00 ± 0.0033	0.53
10	122	3.73 ± 0.0029	0.45

[a] estimated value ± one standard deviation

to *Clostridia*, a bacterial class common in sediments with members capable of fermentation and cellulose degradation. Regions 8 and 10 had large amounts of environmental clone sequences and *β-Proteobacteria*. Surprisingly, the *δ-Proteobacteria* subclass did not comprise a large percent of the phylogenic assignments, in contrast to the qPCR results (Figure 4.2A). A BLAST analysis of the primers used for the *δ-Proteobacteria* class resulted in a large number of matches with uncultured *Geobacteracea*. The lack of *δ-Proteobacteria* in the phylogenic assignments may therefore be accounted for by large percentages in the uncultured bin.

4.5. Discussion

The microbial colonization of a laboratory-scale *in situ* sediment cap was evaluated using a coupled, culture-independent approach of qPCR to enumerate target microbial populations and T-RFLP to examine changes in bacterial community structure. qPCR analysis confirmed that Bacteria and Archaea colonized the cap at levels approaching those in the underlying sediment. Microorganisms colonizing the overlying sand cap originated from the sediment, since qPCR did not detect any indigenous microorganisms associated with the sand prior to cap emplacement. Statistical analysis with CCA demonstrated that changes in relevant environmental variables (depth, Fe^{2+}, and Mn^{2+}) were significantly related to changes in observed T-RF patterns, suggesting that collected microbial data did not simply reflect the elution of planktonic microorganisms from the sediment. If this were the case, then environmental variables would not adequately explain changes in T-RF fingerprint patterns. Bacterial cell numbers in the cap were greatest in the top layer, where aerobic processes occurred. It is common for aquatic sediments to have higher abundances of bacteria in the aerobic layer compared with the anaerobic portions attributed to the prevalence of labile organic matter and energy gained from aerobic respiration (*283*). This is supported by the increases of microbial numbers in Region 7, due to the elution of dissolved organic matter from the sediment into the cap, and within the sediment, where organic matter was present for utilization as carbon and energy sources.

Genera known to contain metal- and iron- reducing members (*δ-Proteobacteria*, *Anaeromyxobacter*, *Geobacter*, and *Shewanella* groups) were all detected in each region of the cap and sediment; thus confirming the hypothesis inferred from the geochemical

Table 4.4. Terminal-restriction fragment length polymorphism (T-RFLP) phylogenetic assignments from *HhaI*, *MspI*, and *RsaI* fragment patterns at each dissection region analyzed

	Percentage of Ribotypes Assigned per Dissection Region [a]						
Phyla/Class	Region 1	Region 2	Region 3	Region 4	Region 6	Region 8	Region 10
Actinobacteria	-	-	-	8	22	-	4
α-Proteobacteria	13	3	9	9	-	-	-
Bacilli	-	10	11	9	-	-	4
β-Proteobacteria	19	31	38	25	20	23	26
Chlorobia	-	5	-	-	-	5	-
Clostridia	-	-	-	-	28	-	9
Cyanobacteria	-	3	6	3	-	-	-
δ-Proteobacteria	-	-	3	-	2	18	-
Florideophyceae	6	2	2	-	-	-	-
Fusobacteria	-	-	2	-	-	-	-
γ-Proteobacteria	31	12	6	15	8	-	17
Kinetoplastida	-	-	-	-	-	5	-
Mollicutes	-	10	2	2	-	-	-
Sphingobacteria	-	2	4	3	-	18	5
Uncultured	31	22	17	26	20	31	35

[a] Phylogenic assignments performed using in silico assignment tool (http://trflp.limnology.wisc.edu/index.jsp).

data that microbial iron reduction was the major biogeochemical process in the system (Chapter 3). The discrepancy between cell numbers of *δ-Proteobacteria* and total Bacteria in Regions 8 and 9 may be due to non-universal amplification of the targeted region of the bacterial 16S rRNA gene, leading to under-representation. In Region 1, DIRB (*Anaeromyxobacter*, *Geobacter*, *Shewanella*) accounted for only 0.4% of the total Bacteria (Table 4.2), consistent with observed geochemical data indicating predominant oxygen reduction. Regions 2 through 9 displayed higher proportions of DIRB relative to total Bacteria, agreeing with the geochemical data which implied metal reduction in these regions. The drop in DIRB between the adjacent Regions 6 and 7 is attributed to dissolved organic matter eluting from the sediment and promoting the growth of both DIRB and other bacteria. This trend is also observed with the *dsrA* proportions (Table 4.2). It is possible that fermenting organisms such as *Clostridia*, identified in the T-RFLP profiles (Table 4.4), flourished in these regions and outcompeted DIRB and sulfate-reducers for fermentable substrates. *Geobacter* spp. consistently outnumbered the other DIRB within the cap. The relative concentrations of *Anaeromyxobacter* and *Shewanella* were higher in the upper regions compared to the rest of the cap, possibly due to their roles in oxygen and manganese reduction. *Geobacter* spp. have been shown to remain viable under aerobic conditions (*308*) or to participate in manganese reduction (*55*) and were also detected in Region 1. The abundance of *Geobacter* over *Shewanella* in environmental samples has been reported previously (*309-311*). *Anaeromyxobacter* levels were very low in the cap but were comparable to and even exceeded *Geobacter* cell numbers in the sediment.

The proportion of sulfate reducing prokaryotes (SRPs) compared to total Bacteria increased three to four orders of magnitude in the sediment compared to the cap (Table 4.2), complementing porewater geochemical profiles which indicated sulfate reduction in the sediment (Figure 4.1; Chapter 3). The detection of the *dsrA* gene in cap regions suggests that microbial sulfate reduction supplied the sulfide required for $Fe_xS_{y(aq)}$ formation, with the sulfide possibly also contributing to manganese oxide reduction in the upper cap (y=-20 mm; (*269*)). The detection of *dsrA* in the more oxidized regions of the cap (Regions 1 and 2) is not unfounded since certain SRBs withstand exposure to oxygen (*312-315*). The presence of iron and sulfate reducing processes lends support to the hypothesis that biogeochemical processes were compressed towards the cap-water interface under upflow conditions (Chapter 3). This hypothesis is additionally supported by the detection of the *mcrA* gene in the lower portion of the cap, suggesting the presence of methanogenic Archaea. It therefore appears that microbially-catalyzed elemental cycling processes for oxygen, manganese, iron, sulfur, and carbon shift vertically from the sediment into the overlying sediment cap. Aerobic and manganese respiration processes are confined to the upper portion of capping material. In active freshwater sediments, microbial iron reduction coupled to the oxidation of organic carbon (or hydrogen) will be a dominant biogeochemical process within the cap and sediment. In contrast, sulfate reduction may be a major process within caps in marine sediments, evidenced by the detection of SRP throughout the column in this study. The microbial colonization of the cap and development of discrete biogeochemical zones provide additional insight into the microbial community response following physical and geochemical perturbations to the sedimentary environment. Microbial populations

rapidly sense, respond, and adapt to redox changes at the sediment-water interface to create stratified, functional communities. Similar observations have been made in natural systems such as flooded tropical soils (*246*).

The microbial colonization of the cap will affect biotransformation of contaminants within *in situ* sediment caps. Hence, capping provides an intrinsic secondary level of treatment in addition to the physical isolation of the sediment contaminants. Organisms colonizing the overlying cap during this study (e.g., *Anaeromyxobacter*, *Geobacter*, *Shewanella*) are capable of transforming multiple classes of environmental contaminants including radionuclides (*234, 277, 278*), petroleum hydrocarbons (*279-281*) and chlorinated ethenes (*53*). Actively dechlorinating *Dehalococcoides* were previously observed to elute from enriched Anacostia River sediment under upflow conditions (*260*), suggesting they may also populate a sediment cap. This is significant considering *Dehalococcoides* have been linked to the reduction of chlorinated ethenes (*316*), PCBs (*114*), polybrominated diphenyl ethers (*127*), chlorophenols (*126*), and dioxins (*317*) among other chlorinated organics (*124, 317*). Additionally, nitroaromatics (*95, 97, 318*) and chlorinated organics (*95-99, 101*) can be reduced by biogenically-derived iron and sulfide minerals. In the aerobic region, methanotrophic bacteria have been linked to the cometabolic transformation of organic contaminants (*132, 133*) and are present at the solids-water interface, as indicated by the T-RFLP analysis. The presence of a diverse bacterial community at the cap-water interface also suggests that aerobic PAH mineralization may continue to occur if oxygen penetration is sufficient (*110*). If additional contaminant biotransformations are sought, the natural colonization of an *in situ* cap suggests that microbial viability following

bioaugmentation of caps may be feasible (*132*, *133*). This strategy of enhanced bioremediation may overcome the lack of bacterial diversity and apparent stress within the cap region (Region 6; Table 4.3), possibly due to limited substrate availability (*260*). Exogenous amendments may therefore be required to sustain contaminant biotransformations following intrinsic colonization or bioaugmentation of the capping material. The presence of microorganisms within subaqueous sediment caps can also have negative implications that should be considered. Biogenic gas production (e.g., methanogenesis) within the sediment and cap could lead to contaminant partitioning and transport in the gas phase (*282*) as well as physical instability of the cap (*272*, *319*). Additional research is needed to optimize cap design and emplacement to fully exploit microbial activities in caps and to ensure long-term function.

4.6. Acknowledgments

Sara Thomas performed the primer design portion of this work and provided many helpful discussions and insight regarding qPCR and T-RFLP analyses. Some primers and standards for PCR and qPCR analysis were supplied by the Löffler lab at the Georgia Institute of Technology. Claribel Cruz-Garcia provided helpful discussions regarding *dsrA* genes and qPCR analysis. Rebecca Daprato and Laura Guest provided helpful discussions and assistance with T-RFLP analysis. John Fortner provided laboratory assistance during column dissection. Some of this work was performed in the laboratories of Frank Löffler and Martial Taillefert, at the Georgia Institute of Technology.

CHAPTER 5.
THE EFFECT OF ADVECTIVE FLOW DIRECTION ON REDOX ENVIRONMENTS WITHIN IN SITU SEDIMENT CAPS

5.1. Abstract

Aquatic sediments are subject to multiple hydrodynamic forces and transient flows which can influence biogeochemical processes and redox environments. Redox conditions within an *in situ* cap overlying contaminated aquatic sediments may also be altered by flow direction and can impact contaminant transformations. The effect of advective flow direction on redox conditions within capped sediment columns was therefore examined. Marine sediment cores obtained from the Satilla River, GA were extruded into laboratory-scale columns and subject to one of three flow conditions: static flow, upflow to simulate a groundwater seep, or downflow to simulate tidally-induced recharge. Each column was capped with sand and monitored for porewater geochemistry with voltammetric microelectrodes to observe spatial and temporal trends. Porewater profiles of uncapped sediment cores revealed only limited oxygen penetration under each flow condition, with sediment cores generally dominated by manganese reduction. The sand cap of the static flow core maintained aerobic conditions after 5 weeks, but then became anaerobic before 13 weeks. The upflow core and overlying cap became completely anaerobic much faster, after only one week of incubation, and maintained those conditions for 13 weeks. Under conditions of downflow, however, dissolved oxygen penetration into the cap increased with time until completely aerobic conditions were observed after 13 weeks. Results demonstrate that flow direction has a marked impact on redox environments within an overlying cap and can contribute to the location

of the aerobic/anaerobic transition. Additionally, the movements of a macroinvertebrate present in the upflow sediment core were tracked to examine the potential for recolonization following capping. After 14 weeks, the suspected nematode was unable to relocate from the previously oxic sediment-cap interface to the newly formed cap-water interface.

5.2. Introduction

Many aquatic sediments underlying surface waters are sufficiently contaminated to cause adverse effects on aquatic life and limit recreational and economic use (*2, 3, 257*). *In situ* capping has recently emerged as a remedial method for contaminated sediments and involves placing a layer of clean material at the sediment-water interface to isolate contaminants from the benthic community and overlying surface water. Clean sand has traditionally been the material employed for capping and can delay contaminant breakthrough considerably when diffusive transport dominates (*151*). A potential consequence of emplacing an *in situ* cap at the sediment-water interface is that it may induce considerable, abrupt restructuring of biogeochemical processes within the underlying sediment.

Biogeochemical restructuring within capped sediments can directly influence contaminant fate and transport, since aquatic sediments are capable of naturally attenuating a number of different contaminants through both abiotic and biotic processes. Examples of abiotic contaminant transformations and their associated redox conditions include nitroaromatic reduction during Fe^{III} reducing conditions (*95, 97, 318*), and the dehalogenation of chlorinated organics by iron sulfides (*98, 99*), naturally occurring zero-

valent iron (*101*), and Fe(II) present at surfaces of iron-containing minerals (*95-97*). In addition to these processes, alternative abiotic contaminant attenuation mechanisms within sediments include metal and nutrient sequestration under oxic (*14*) and sulfidogenic (*258*) conditions, and hydrophobic organic contaminant (HOC) sorption. Biogeochemical shifts following sediment capping may also impact biologically-mediated contaminant transformations, which are especially dependent on proper redox conditions. Biogeochemical restructuring within sediments following *in situ* capping could therefore alter natural attenuation processes and potentially lead to changes in contaminant flux.

Aquatic sediments underlying oxic surface waters typically possess an aerobic layer extending millimeters to centimeters into the sediment bed. Beneath this aerobic layer exists a gradient of terminal electron accepting processes, stratified according to thermodynamic yield (*168*). Previously reported results in Chapter 3 have demonstrated that *in situ* capping under stagnant and upflow conditions results in a vertical shift of stratified biogeochemical processes into the overlying cap. Data from the previous study also show that flow direction can impact the size of the stratified biogeochemical regions as well as the concentrations of the reduced metabolites within those regions. The effect of flow direction on biogeochemical processes within capped sediments merits further investigation since many contaminated aquatic sediments are subject to both steady and transient advective flows induced by cross flow, tidal pumping, and groundwater discharge. Such is the dynamic nature of rivers that both upwelling and downflow exchange between surface and subsurface waters have been observed only meters apart (*320*). Additionally, the presence of hyporheic flow paths has been linked with changes

in sediment biogeochemistry (*321*). Understanding the effect of advective flow on biogeochemical processes, and consequently contaminant fate and transport, is especially important considering that 75% of Superfund and RCRA sites are located within a half-mile of surface water and 50% of the Superfund sites report communication between the contaminated groundwater and surface water (*20*). The efficiency of active sediment caps, designed to remove contaminants from the aqueous phase during transport through the cap, may also depend on proper flow and redox conditions.

The objective of this work was to characterize the spatial and temporal development of biogeochemical processes in capped aquatic sediments subject to advective upflow and downflow. Sediment cores were collected, capped with a clean sand, and monitored with voltammetric microelectrodes for geochemical species indicative of specific redox zones. Results from this study demonstrate that advective flow direction has a direct impact on biogeochemical processes within *in situ* sediment caps.

5.3. Materials and Methods

5.3.1. Sediment Cores

The Satilla River, GA, USA drains a watershed of 9,140 km^2 in the coastal plain of Georgia (*322*) before discharging into the Atlantic Ocean (Figure 5.1). The river runs 420 km long with measured tidal influences extending 106 km upstream, with a semidiurnal tidal range near the ocean from 2 to 3 meters at neap and spring tides. The river has a heterogeneous distribution of bed sediments, possessing both sand- and clay-dominated sediments. Land use surrounding the Satilla River is dominated by undeveloped wetland vegetation. The lack of development adjacent to the Satilla River

and within the Satilla watershed has prevented significant anthropogenic contamination of the sediment (*322*).

Sediment cores were retrieved in October, 2006 near the mouth of the Satilla River (31° 4.72”N; 81°26’0.51”W). Salinity values recorded at the time of collection were 35 ppt and overlying water temperature was 24 °C. Sediment cores and overlying water were covered with aluminum foil and stored upright at room temperature during transportation to the laboratory. Overlying water was removed and the sediment cores were carefully extruded into 30 cm long, 4.8 cm I.D. glass chromatography columns (Kimble Kontes, Vineland, NJ) with Teflon endplates for experimental manipulation. The upper 12 cm of each core was extruded into the glass columns. Overlying water for each column consisted of Satilla River water obtained at the time of core collection. Three separate cores were extruded into three columns, each column dedicated to a different flow regime: stagnant, upflow, and downflow. The stagnant column was constructed such that the bottom endplate was plugged while the top endplate was detached. An aeration tube placed at the air-water interface provided a stream of air to promote oxygen dissolution in the overlying water column. The upflow column was constructed similarly but a syringe pump provided influent solution at a rate of 0.5 $mL \cdot hr^{-1}$. The influent solution consisted of Satilla River water and sparged with UHP nitrogen for 30 minutes to remove dissolved oxygen. To account for evaporation and salt accumulation in the overlying waters of the stagnant and upflow columns, deionized freshwater was added periodically to maintain salinity values at 35. The downflow column was fitted with a flow-adapter (Kimble Kontes) as the top endplate to induce flow through the overlying water column and through the sediment. Oxic Satilla

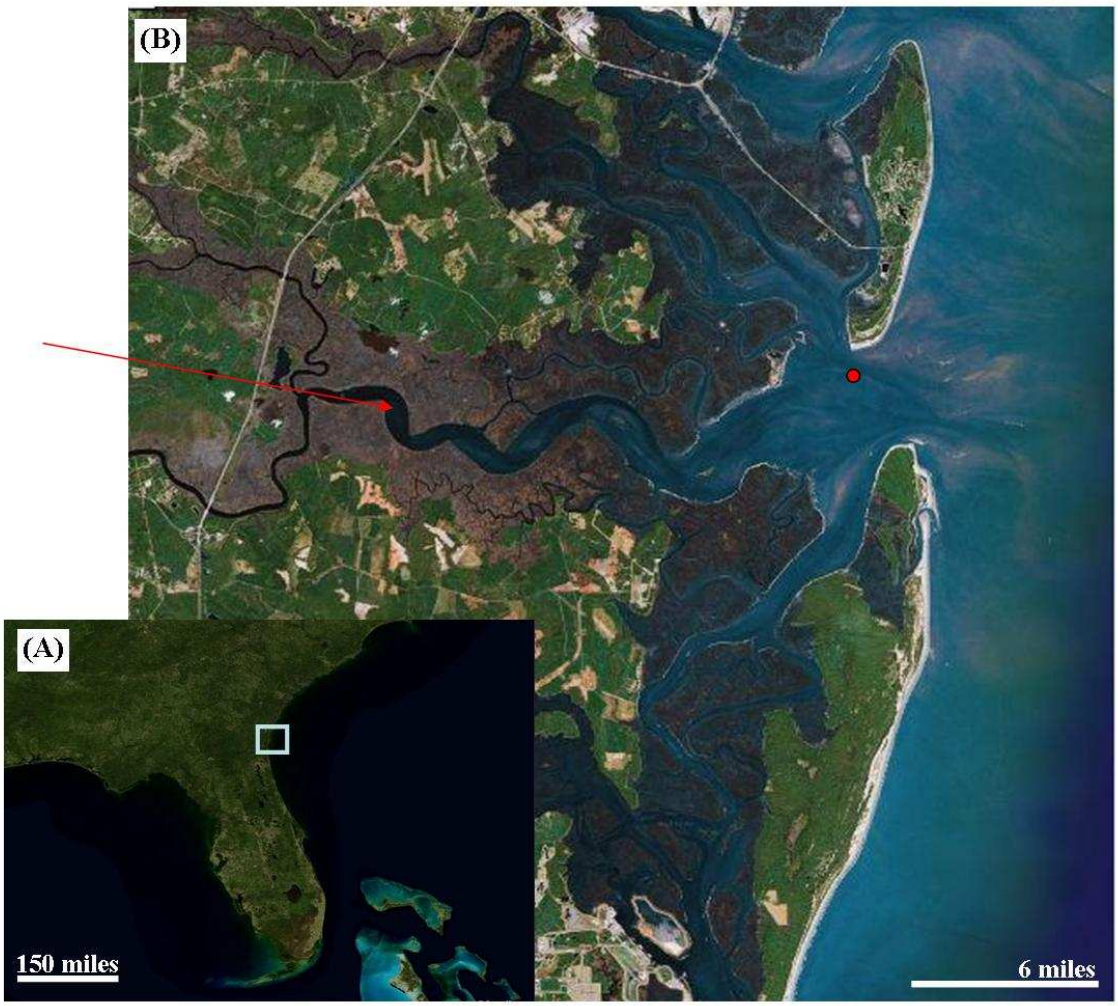

Figure 5.1. Satellite images of the Satilla River, GA. (A) Southeastern United States. The box in approximates the boundaries of image (B). (B) Satilla River, indicated by the red arrow. Sediment cores were collected at 31° 4.72”N; 81°26’0.51”W, indicated by the red, circular symbol. Images captured from MSN Virtual Earth.

River water was provided with a syringe pump at 0.5 $mL \cdot hr^{-1}$. Effluent from the bottom of the downflow column was captured in a sterile 120 mL syringe connected to the bottom endplate. Photographs of each control column are provided in Appendix C (Figures C.1A-C).

All columns were incubated under aerobic conditions in the dark at room temperature for one week to allow for equilibration following establishment in the glass columns. Flow was then induced through the sediment in the upflow and downflow columns for 3 weeks to obtain porewater geochemical profiles and baseline data. After this initial uncapped phase, each column was capped with dry, autoclaved ASTM C-33 concrete sand. The cap depths measured 11.2, 11.0, and 12.0 cm for the stagnant, upflow, and downflow columns, respectively. Oxic Satilla water was again provided as overlying water for the stagnant and upflow columns. Flow was immediately re-established in the upflow and downflow columns once the cap was emplaced. Porewater geochemical profiles of all capped sediment columns were obtained 1, 5, and 13 weeks following capping. Flow was temporarily ceased while obtaining porewater geochemical profiles of the upflow and downflow columns.

5.3.2. Porewater Geochemical Profiles

Geochemical species were analyzed electrochemically at discrete depths within the columns using voltammetric microelectrodes. All voltammetric measurements were performed using a platinum counter electrode, an Ag/AgCl reference electrode, and an Au/Hg solid-state microelectrode fabricated as described by Brendel and Luther (*222*). The Au/Hg microelectrodes consisted of a 100 μm diameter gold wire housed in glass tubing filled with nonconductive epoxy and connected via copper conducting wire to a

potentiostat. The gold surface was polished with diamond pastes of 15, 6, 1, and 0.25 μm (Buehler, Lake Bluff, IL), mercury plated at -0.1 V in a $Hg(NO_3)_2$ solution, then polarized at -9 V for 90 s to form the gold amalgam (*222*). The Au/Hg working microelectrodes are capable of simultaneously measuring $O_{2(aq)}$, H_2O_2, Fe^{2+}, Mn^{2+}, $S_2O_3^{2-}$, ΣH_2S [$=H_2S + HS^- + S^{2-} + S^0 + S_x^{2-}$], organic-$Fe^{III}_{(aq)}$, and $Fe_xS_{y(aq)}$ species (*187, 199, 222*).

Each Au/Hg microelectrode was tested for quality and calibrated for dissolved oxygen by linear sweep voltammetry in simulated freshwater (0.1M NaCl), and then for manganese by cathodic square wave voltammetry (CSWV) in degassed simulated freshwater. Both the O_2 and Mn^{2+} calibrations were run from -0.1 to -1.75 V with a scan rate of 200 $mV \cdot s^{-1}$. A preconditioning potential of -0.1 V for 10 s was applied to all O_2, Mn^{2+}, and Fe^{2+} measurements to clean the surface of the microelectrodes between measurements (*222*). When organic-$Fe^{III}_{(aq)}$, ΣH_2S, and $Fe_xS_{y(aq)}$ complexes were present, however, a cleaning step at -0.9 V for 10 seconds was added to remove any organic-Fe^{III}, ΣH_2S, or Fe_xS_y adsorbed at the electrode surface between measurements (*187, 199*). Concentrations of Fe^{2+}, Mn^{2+}, and ΣH_2S were determined from manganese calibrations following the pilot ion method (*222*). Soluble ferric iron can be measured by voltammetry at circumneutral pH only if complexed by an organic ligand (*187*). The sensitivities of the organic-$Fe^{III}_{(aq)}$ complexes have yet to be determined, and their concentrations are therefore reported in units of current intensity (nA) (*187*). Similarly, the stoichiometry of $Fe_xS_{y\,(aq)}$ is unknown and current intensities (nA) are also reported for these species (*199*).

Between three to ten voltammetric scans were obtained at each depth depending on the analytes detected. Mean values from each depth are reported. Relative standard deviations of each species for all profiles averaged less than 10% and are not included in the Figures. Voltammetric analyses were performed with a computer-operated DLK-100A potentiostat and a computer-operated micromanipulator capable of vertical movements at the sub-millimeter scale (Analytical Instrument Systems, Flemington, NJ). The small size of the working Au/Hg microelectrode, coupled with the precise control of vertical movement, allowed for data collection with high vertical resolution and for repeated profiling of sediment geochemistry while minimizing bulk sediment disturbance. Voltammograms were processed with a Matlab® program (*261*). Appendix A provides more information regarding the use of voltammetric microelectrodes for the determination of species concentrations.

5.4. Results and Discussion

5.4.1. Porewater Geochemical Profiles

Each of the sediment cores were successfully extruded into the glass columns and appeared to remain intact. Some streaking of the sediment occurred along the sides of the glass, and microelectrodes insertion for geochemical profiling was restricted towards the center of each column. The sediment was dark black in each column, indicative of strongly anaerobic conditions and consistent with previous descriptions of the Satilla as a black water river with high levels of dissolved organic carbon (*323*). Following one week of equilibration, the stagnant core was profiled and showed mostly reducing conditions within the sediment (Figure 5.2A). Oxygen from the overlying water reached

non-detectable levels immediately at the sediment-water interface (SWI) at -112 mm. Beneath the oxic layer, concentrations of Mn^{2+} increased steadily with depth, while modest concentrations of organic-$Fe^{III}_{(aq)}$ concentrations were observed. The detection of organic-$Fe^{III}_{(aq)}$ in the sediment suggests microbial iron reduction was occurring. Taillefert et al. (*183*) recently described how *Shewanella putrefaciens* excretes an organic ligand to solubilize Fe(III) oxides and allow for microbial Fe(III) assimilation and respiration. The geochemical profile obtained in the stagnant column after one week was also believed to be representative of the sediment in the upflow and downflow columns. Flow was initiated in the upflow and downflow columns successfully without any indication of porewater blockage or excessive back-pressure.

Porewater geochemical profiles of Satilla sediment capped with C-33 sand showed that flow direction has a direct impact on redox conditions within the overlying cap. The capped sediment column under stagnant flow was dominated by manganese reduction within the sediment but showed interesting temporal trends following capping. After 4 weeks of uncapped incubation (Figure 5.2B) the sediment was still largely anaerobic, with oxygen penetrating only 1 mm below the SWI, and resembled the uncapped profile obtained after one week of incubation (Figure 5.2A). Emplacement of the sand cap onto the sediment induced noticeable changes in the porewater profile. The sand cap was still subject to aerobic conditions after 5 weeks of capped incubation, with Mn^{2+} being the only other quantified species present within the cap at approximately 175 μM (Figure 5.2C). The coexistence of oxygen and reduced manganese is not unexpected, since the kinetics of manganese oxidation via dissolved oxygen are relatively slow (*178*). Interestingly, the aerobic layer of the sediment increased after capping, extending 12 mm

below the sediment-cap interface (-124 mm). The cause for this remains uncertain, but may be due to physical mixing following capping or due to the consumption of chemical oxygen demands at the interface since oxygen was continuously provided to the water column from the aeration tube. Within the sediment, organic-$Fe^{III}_{(aq)}$ levels increased relative to previous porewater profiles, possibly indicating the oxidation of ferrous in the presence of organic ligands. An alternative explanation is the increase in microbial iron reduction to produce the organic-$Fe^{III}_{(aq)}$, supported by the detection of Fe^{2+}. By week 13, however, the cap was largely anaerobic and dominated by Mn^{2+} (Figure 5.2D). Oxygen penetrated just 4 mm past the cap-water interface (CWI). The lack of oxygen in the cap is consistent with previous studies examining biogeochemical processes during sediment capping (*259*). Ferrous iron was not observed in the cap or sediment during week 13, however the porewater profile did not extend as deep into the sediment compared to week 5 (Figure 5.2C). Regardless, the sediment cap overlying intact Satilla River sediment subject to stagnant flow conditions was anaerobic after 13 weeks of incubation.

The capped sediment core subject to upflow conditions also exhibited anaerobic conditions within the cap but required less time to achieve such conditions compared to the stagnant column (Figure 5.3). The uncapped sediment exhibited a mix of biogeochemical processes within the sediment when subject to upflow conditions for 3 weeks (Figure 5.3A). Oxygen penetration into the sediment was insignificant, while manganese reduction, iron reduction, and sulfidogenesis all appeared to be occurring within the sediment; stratification of biogeochemical processes, however, was not apparent. Upon capping, the reduced chemical species were advectively transported into the cap and oxygen penetration was limited to only 2 mm below the CWI after one week

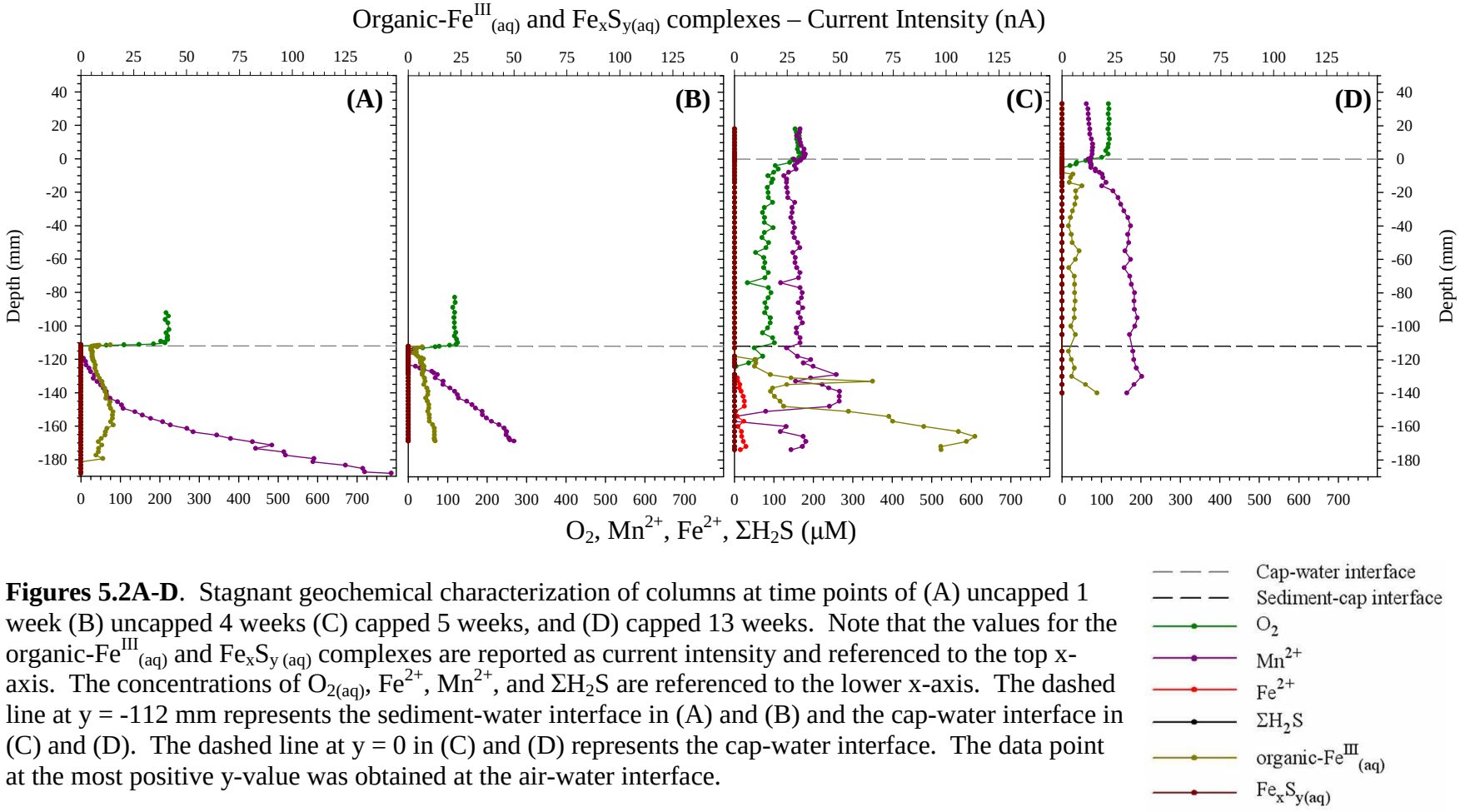

Figures 5.2A-D. Stagnant geochemical characterization of columns at time points of (A) uncapped 1 week (B) uncapped 4 weeks (C) capped 5 weeks, and (D) capped 13 weeks. Note that the values for the organic-$Fe^{III}_{(aq)}$ and $Fe_xS_{y\,(aq)}$ complexes are reported as current intensity and referenced to the top x-axis. The concentrations of $O_{2(aq)}$, Fe^{2+}, Mn^{2+}, and ΣH_2S are referenced to the lower x-axis. The dashed line at y = -112 mm represents the sediment-water interface in (A) and (B) and the cap-water interface in (C) and (D). The dashed line at y = 0 in (C) and (D) represents the cap-water interface. The data point at the most positive y-value was obtained at the air-water interface.

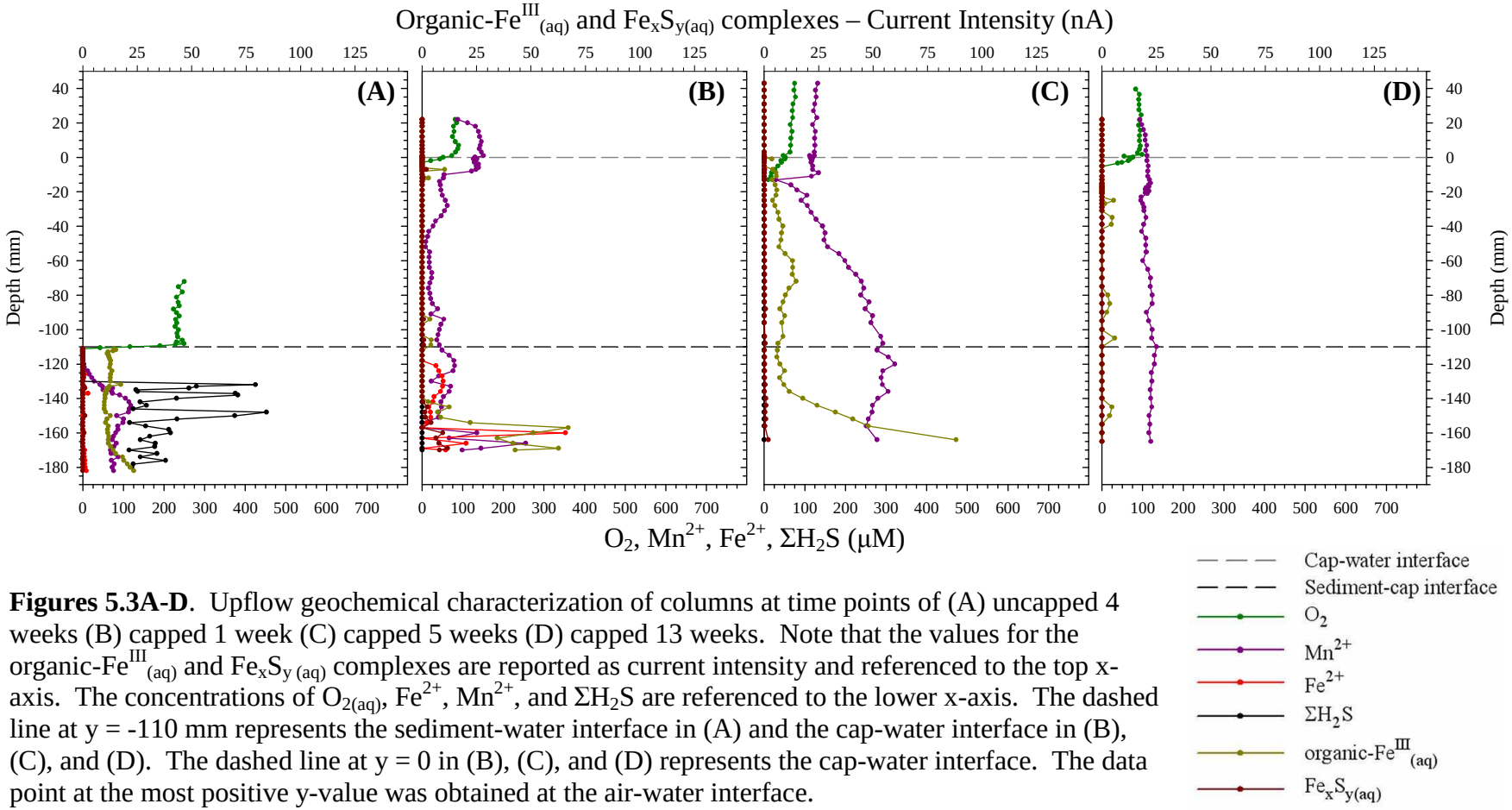

Figures 5.3A-D. Upflow geochemical characterization of columns at time points of (A) uncapped 4 weeks (B) capped 1 week (C) capped 5 weeks (D) capped 13 weeks. Note that the values for the organic-$Fe^{III}_{(aq)}$ and $Fe_xS_{y\,(aq)}$ complexes are reported as current intensity and referenced to the top x-axis. The concentrations of $O_{2(aq)}$, Fe^{2+}, Mn^{2+}, and ΣH_2S are referenced to the lower x-axis. The dashed line at y = -110 mm represents the sediment-water interface in (A) and the cap-water interface in (B), (C), and (D). The dashed line at y = 0 in (B), (C), and (D) represents the cap-water interface. The data point at the most positive y-value was obtained at the air-water interface.

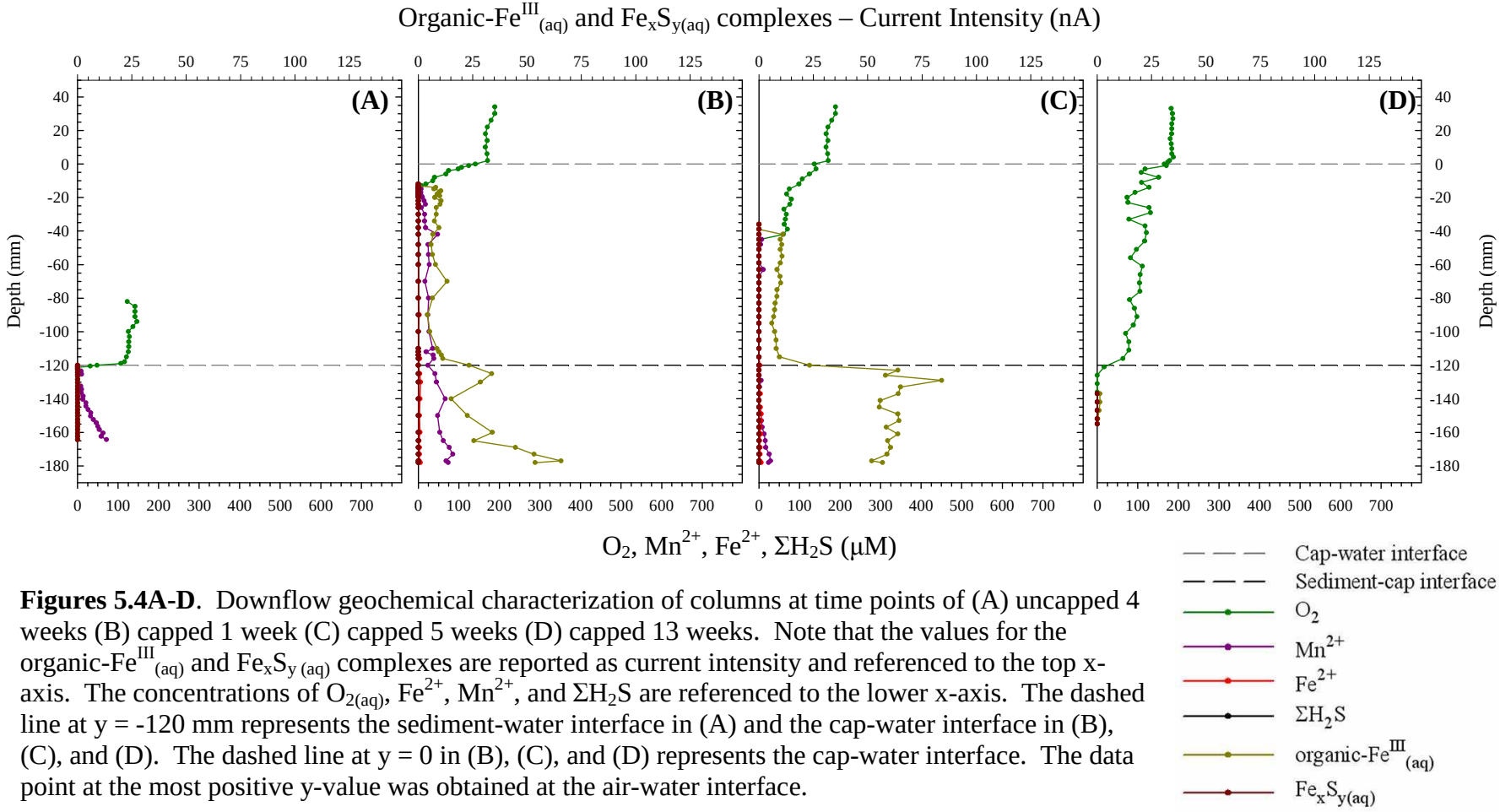

Figures 5.4A-D. Downflow geochemical characterization of columns at time points of (A) uncapped 4 weeks (B) capped 1 week (C) capped 5 weeks (D) capped 13 weeks. Note that the values for the organic-$Fe^{III}_{(aq)}$ and $Fe_xS_{y\,(aq)}$ complexes are reported as current intensity and referenced to the top x-axis. The concentrations of $O_{2(aq)}$, Fe^{2+}, Mn^{2+}, and ΣH_2S are referenced to the lower x-axis. The dashed line at y = -120 mm represents the sediment-water interface in (A) and the cap-water interface in (B), (C), and (D). The dashed line at y = 0 in (B), (C), and (D) represents the cap-water interface. The data point at the most positive y-value was obtained at the air-water interface.

(Figure 5.3B). Free ferrous iron was detected in the sediment after one week of capping while sulfide was no longer present. After 5 weeks of capping it appeared that Mn^{2+} and organic-$Fe^{III}_{(aq)}$ were being advectively transported from the sediment into the cap with little or no apparent production of these species within the capping region (Figure 5.3C). The porewater geochemical profile obtained after 13 weeks of capping (Figure 5.3D) is similar. The capped upflow core appeared to reach steady-state in regards to redox conditions (i.e., the overlying cap being mostly anaerobic) one week after capping.

The downflow core exhibited aerobic conditions within the overlying cap after 13 weeks of flow, demonstrating that flow direction has a large impact on bulk geochemical conditions. After 3 weeks of downflow incubation, oxygen penetrated only 0.6 mm below the SWI of the uncapped sediment (Figure 5.4A). The lack of significant oxygen penetration indicates a high degree of oxygen demand in the sediment, again consistent with previous descriptions of the Satilla River possessing high levels of dissolved organic carbon (*323*). Under the brief aerobic layer only manganese reduction was observed. One week after capping the cap appeared to be mostly reducing as evidenced by the detection of Mn^{2+} and organic-$Fe^{III}_{(aq)}$ beginning at -13 mm (Figure 5.4B). The detection of these reduced species in the cap despite downflow conditions is attributed to upwelling of sediment porewaters induced by compression of sediment following cap placement, a reported phenomenon during field placements of *in situ* caps (*147*, *150*). Reduced manganese was not observed in the cap after 5 weeks (Figure 5.4C) nor in subsequent porewater profiles. The organic-$Fe^{III}_{(aq)}$ species was observed in the cap after 5 weeks, however, and the increased current intensity of the species in the sediment compared to the previous profile (Figure 5.4B) suggests iron reduction was occurring.

Oxygen penetrated deeper into the cap after 5 weeks, reaching -42 mm before measuring non-detectable levels (Figure 5.4C), suggesting downflow may result in an aerobic capping layer if provided enough time. This hypothesis was confirmed after 13 weeks of downflow conditions, when the cap displayed completely aerobic redox conditions (Figure 5.4D). Oxygen rapidly approached non-detectable levels below the sediment-cap interface. No other analytes were detected in the 13 week profile, perhaps due to transport of soluble species towards the bottom of the column and away from the regions profiled with the electrodes. The aerobic nature of the cap, when subject to downflow conditions, demonstrates that flow direction and the advective transport of dissolved oxygen to reducing regions can dictate redox environments within sediment caps.

5.4.2. Macroinvertebrate Recolonization

The Satilla sediment core dedicated to upflow conditions contained a macroinvertebrate located near the sediment-water interface at the time of collection. The activity and visual health of the macroinvertebrate was monitored following core extrusion and capping. One potential advantage of *in situ* sediment capping over remedial alternatives is the suspected ability of the benthic macrofauna to relocate from the previous sediment-water interface to the new cap-sediment interface. After core extrusion and equilibration, a tube produced by the macroinvertebrate was observed protruding from the sediment-water interface (Figure 5.5A). The tube was hollow and meandered approximately 5 cm below the SWI and may have provided overlying, oxic water into the sediment (*41*). This role is supported by the light brown sediment surrounding the tube in Figure 5.5A, indicative of less reducing conditions. Upon capping the tube was completely covered with autoclaved, dry C-33 sand. According to

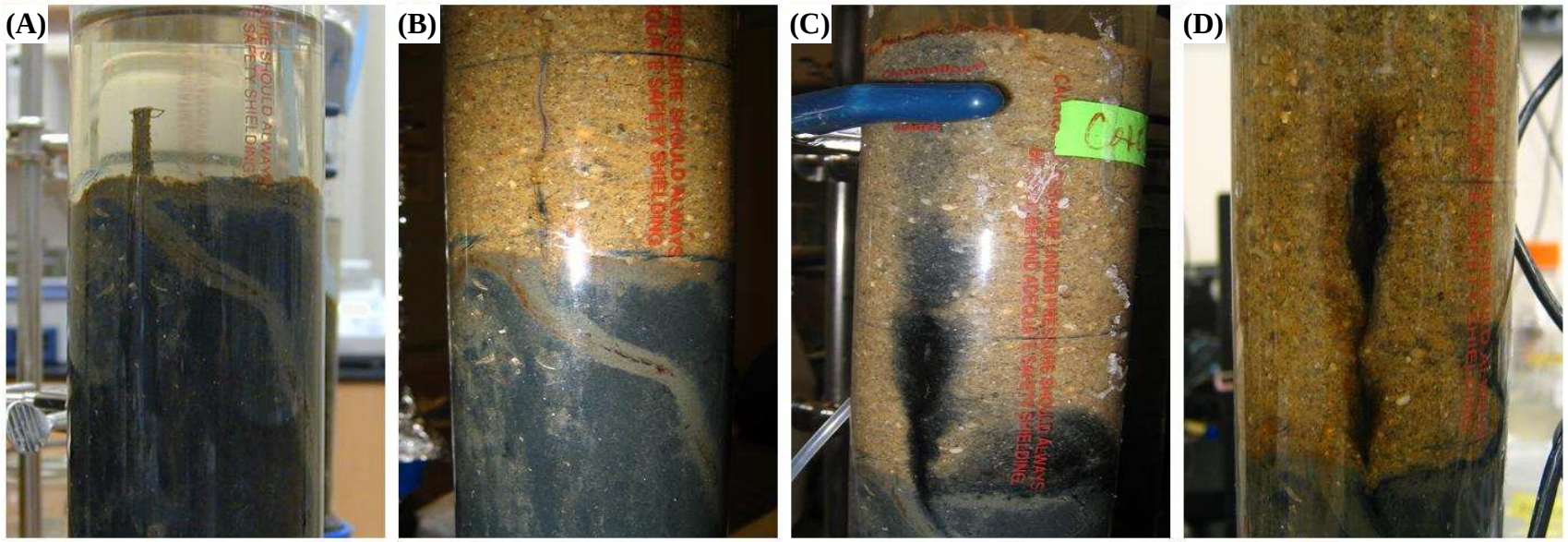

Figures 5.5A-D. Photographs of a macroinvertebrate native to the Satilla River core dedicated to upflow conditions (A) uncapped after 7 days, no flow (B) capped 3 days (C) capped 21 days (D) capped 97 days. The distance between the sediment-water and water-air interfaces in (A) is 4 cm. The distance between the sediment-cap interface and the marked line on the face of the column in photos (B), (C), and (D) is 4 cm.

porewater geochemical profiles, the sediment-cap interface was subject to reducing conditions within one week (Figure 5.3B). Three days after capping the macroinvertebrate had ascended approximately 4 cm past the sediment-cap interface inattempt to reach the oxic, overlying water and (Figure 5.5B). At this time the macroinvertebrate was visible at the glass wall of the column and appeared to be species of nematode, which are ubiquitous in freshwater and marine sediments. The macroinvertebrate did not appear to move further towards the cap-water interface with time, but a black substance was observed along its path after 21 days (Figure 5.5C). The black substance was most concentrated immediately adjacent to the macroinvertebrate and was transported into the overlying water with the advective upflow. Porewater geochemical profiles along this region, immediately adjacent to the walls of the column, were unable to identify the substance. After 97 days, however, the black substance was no longer present and the macroinvertebrate had not ascended significantly further than 4 cm above the sediment-cap interface. It appears that capping was involved in the loss of macroinvertebrate activity in this case. Specific causes for the loss of macroinvertebrate activity remain unclear, but possibilities include: the reduced environment and lack of oxygen within the cap may have prevented respiration; the sand may not have provided adequate organic matter and minerals; the weight of the overlying cap may have precluded tunneling towards the cap-water interface. In this example, capping was detrimental to one representative benthic macroinvertebrate. It may be hypothesized that lateral relocation of benthic communities, (i.e., from uncapped to capped regions of the sediment bed) may be more favorable than vertical relocation (i.e., from underlying

sediment to overlying cap). However, more thorough investigations and analyses from field capping scenarios are required to formulate general conclusions.

5.4.3. Implications for Capping

Aquatic sediments can be subject to changes in bulk advective motion, especially river sediments subject to tidal fluctuations. Porewater geochemical profiles obtained in this study demonstrate that alterations and reversals of flow patterns, which can introduce fresh solutes into the sediment, can strongly influence redox conditions within an *in situ* sediment cap. The stagnant and upflow profiles reported here verify previous results (Chapter 3) indicating that sediment caps under such conditions are largely anaerobic. The downflow column shows that advective downflow carrying dissolved oxygen was able to completely aerate the overlying cap. The temporal patterns of the downflow geochemical profiles observed in this study suggest that oxygen penetration may require weeks before complete aeration of the cap occurs; however, greater advective flow rates may have more pronounced effects. Therefore, at capping sites where flow reversals are common (e.g., semidiurnal tidal flushing), redox conditions within the overlying cap (and sediment) may be dependent on transient flow patterns and may never truly be at equilibrium.

The effect of flow direction on the spatial distribution of redox environments is significant with respect to nutrient and elemental cycling, the fate and transport of sedimentary contaminants, and remedial design. It appears the cycling of certain elements and nutrients will be spatially-dependent upon flow direction. For instance, in caps subject to upflow conditions, the oxidation of Mn^{II} to Mn^{IV} would be expected to

occur near the cap-water interface since Mn^{2+} was observed to discharge into the overlying, oxic water. However, manganese oxidation under downflow conditions would probably occur in the sediment. The location of elemental and nutrient cycling can indirectly impact microbial processes associated with anaerobic heterotrophic organic matter degradation, which utilize oxidized compounds as electron acceptors. The location of elemental cycling and microbial processes influences the fate and transport of sedimentary contaminants such as metals and hydrophobic organics. In aerobic sediment layers, manganese and iron oxyhydroxides tend to adsorb metals and nutrients prior to release into overlying waters (e.g., arsenic (*14*) and phosphate (*275*)). The formation of oxyhydroxides may be relocated to the CWI under stagnant and upflow conditions, thus releasing metals from the sediment into the cap. Under downflow conditions, however, oxyhydroxides should remain spatially stable due to the input of oxygen. In reducing environments, contaminants such as nitroaromatics (*95, 97, 318*) and chlorinated organics (*95-99, 101*) can be transformed via biological and abiotic processes. Specifically, iron-reducing bacteria are involved in the microbially-mediated reduction of radionuclides (*234, 277, 278*), petroleum hydrocarbons (*279-281*) and chlorinated ethenes (*53*). The reducing conditions within sediment caps during upflow and static flow could extend these (bio)attenuation processes from the sediment into the cap, which could allow for continued contaminant attenuation (*260*). Results presented here suggest these reductive (bio)transformations will not occur within a sand-based sediment cap subject to constantly downflowing conditions. If sediment contaminants overcome advective forces and are introduced in the overlying cap during downflow conditions, then oxidative contaminant attenuation processes may be promoted (*282*). These findings can aid in the

design of active caps, which decrease contaminant bioavailability during transport through the cap by sorption or transformation. Prediction of redox environments within sediment caps can increase the efficiency of active caps and allow for the incorporation of contaminant attenuation pathways that will be most favorable. The information provided in this study, which addresses redox conditions within *in situ* caps and capped sediments during environmentally relevant conditions, should improve our understanding of biogeochemical processes and contaminant behavior within engineered environments at the sediment-water interface. This is especially important when considering the increasing development and utilization of capping technology and the large degree of sediment contamination in populated, urban environments.

5.5. Acknowledgments

Time aboard the R/V Savannah was courtesy of Martial Taillefert. Crew members of the R/V Savannah collected cores. Denise Himmelheber and John Fortner provided laboratory assistance during core extrusion. This work was performed in the laboratory of Martial Taillefert, at the Georgia Institute of Technology.

CHAPTER 6.
NATURAL ATTENUATION PROCESSES DURING *IN SITU* CAPPING [a]

6.1. Abstract

Chlorinated solvents are common groundwater contaminants that threaten surface water quality and benthic health when present in groundwater seeps. Aquatic sediments can act as natural biobarriers to detoxify chlorinated solvent plumes via reductive dechlorination. *In situ* sediment capping, a remedial technique in which clean material is placed at the sediment-water interface, may alter sedimentary natural attenuation processes. This research explores the potential of Anacostia River sediment to naturally attenuate chlorinated solvents under simulated capping conditions. Results of microcosm studies demonstrated that intrinsic dechlorination of dissolved-phase PCE to ethene was possible, with electron donor availability controlling microbial activity. A diverse microbial community was present in the sediment, including multiple *Dehalococcoides* strains indicated by the amplification and quantification of the reductive dehalogenases *tceA*, *vcrA*, and *bvcA*. An upflow column simulating a capped sediment bed subject to PCE-contaminated groundwater seepage lost dechlorination activity and only achieved complete dechlorination when microorganisms present in the sediment were provided electron donor. Increases in effluent chloroethene concentrations during the period of biostimulation were attributed to biologically-enhanced desorption and the formation of

[a] The contents of Chapter 6 have been published in *Environmental Science & Technology* and have been reformatted here for consistency with the remainder of the dissertation. The citation is as follows: David W. Himmelheber, Kurt D. Pennell, and Joseph B. Hughes (2007). "Natural Attenuation Processes During *In Situ* Capping". *Environmental Science and Technology*, 41, (15): 5306-5313.

less sorptive dechlorination products. These findings suggest that *in situ* caps should be designed to account for reductions in natural biobarrier reactivity and for the potential breakthrough of groundwater contaminants.

6.2. Introduction

It is estimated that 75% of Superfund and RCRA sites are located within one half-mile of surface water bodies, with half of the Superfund sites reporting interaction between contaminated groundwater and surface water (*20*). Contaminants present in groundwater seeps threaten water quality and present dangers to the benthic community as well as to fish and humans. The chlorinated solvents tetrachloroethene (PCE) and trichloroethene (TCE) are common groundwater contaminants (*21*) whose plumes can extend considerable distances from their source to potentially discharge into surface water bodies (*22-26*).

Aquatic sediments, due to their inherently anaerobic conditions and abundant carbon and energy sources, tend to have ample microbial mass and diversity to serve as natural biobarriers to detoxify chlorinated solvent plumes. PCE can be biologically transformed under anaerobic conditions through reductive dechlorination to nontoxic ethene and ethane, with corresponding production of hydrogen and chloride ions. During this process, dissolved-phase chloroethenes serve as electron acceptors for the dechlorinating organisms while the source of electrons is typically hydrogen (*120, 121*), supplied from the oxidation of organic substrates by fermenting microbial communities (*122, 123*). Multiple dechlorinating organisms have been detected in enrichments originating from river sediments (*128-130*), including *Dehalococcoides* strains, which possess the unique ability to dechlorinate dichloroethenes (DCEs) and vinyl chloride

(VC) (*115-119*). The accumulation of DCEs and VC at contaminated sites is commonly observed, however.

In situ capping is a remedial option for contaminated sediments in which clean material is placed at the sediment-water interface to prevent contact between sediment contaminants and the overlying benthic community and surface water. Sand is the traditional material employed for capping, with reactive caps recently designed to sequester or transform sediment contaminants (*73, 154, 156, 324*). The presence of an *in situ* cap shifts the deposition of labile organic matter to the newly-formed cap-water interface, thus removing a source of carbon and organic substrates from the biologically-active sediment where biotransformations are most likely to occur. In addition, the employment of some synthetic capping materials have been reported to disrupt groundwater seepage patterns due to low hydraulic conductivities (~10^{-9} cm/s versus for ~10^{-7} for clayey/silt sediments), creating flow bypassing around the caps and localized zones of discharge with increased flow rates (*158, 325*). The effect of reduced organic substrate levels, coupled with elevated flow rates, on natural bioattenuation processes in capped sediments is unknown. Such fundamental information is needed for accurate reactive transport modeling and to aid in the design of *in situ* caps subject to advective flows.

Here we present a series of laboratory experiments designed to evaluate the effect of *in situ* capping on the natural bioattenuation of PCE in a natural river sediment. Batch microcosm tests were preformed to evaluate the capacity of the sediment to intrinsically dechlorinate PCE to nontoxic products. Electron donor was added to select microcosms at increasing concentrations to examine its effect on dechlorination. Dechlorination and

methane production were monitored within the microcosms, followed by characterization of the dechlorinating microbial community. A sediment column operating with advective flow simulating a groundwater seep was constructed to observe PCE dechlorination within the anaerobic sediment under dynamic conditions. The column influent consisted of only simulated groundwater and dissolved-phase PCE to mimic environmental conditions. Electron donor was again added during the course of the experiment to address limitations on dechlorination. Effluent samples were analyzed for dechlorination products and other geochemical indicators of microbial activity.

6.3. Materials and Methods

6.3.1. Chemicals

PCE (99+%, Sigma-Aldrich, St. Louis, MO), TCE (99.5%, Sigma-Aldrich), *cis*-DCE (97%, Acros Organics, Morris Plains, NJ), *trans*-DCE (99.7%, Acros Organics), and 1,1-DCE (99.9%, Acros Organics) were obtained in neat liquid form. Vinyl chloride (8%/ N_2 balance), ethene (99.5%), ethane (99.5%), and methane (99%) were obtained from Matheson Tri-gas (Parsippany, NJ). Sodium bicarbonate, potassium chloride, magnesium chloride, calcium chloride, sodium lactate syrup (60% vol/vol), ferric chloride, ferrozine (98+%), and potassium bromide were all purchased from Fisher Scientific. Hydrogen gas was purchased from Airgas (Atlanta, GA) and glacial acetic acid (ACS grade) was obtained from Acros Organics.

6.3.2. Sediment

Surficial sediment from the Anacostia River, Washington, D.C., was used as the sediment for all experiments. Satellite images of the river are provided as Figure 3.1A-C.

Sediment from the river has previously been characterized and found to contain elevated levels of PCBs, PAHs, metals, and organic pesticides (*325*). The wet sediment was homogenized in the laboratory by mechanical mixing after removal of large debris and shells and transferred to quart-sized mason jars that were stored in the dark at 4º C.

6.3.3. Microcosm Construction

Microcosms were constructed in duplicate by loading serum bottles (70 mL) with wet river sediment and simulated groundwater under anaerobic conditions (5% CO_2/ 5% H_2/ 90% N_2) in a glove-box (Coy Laboratory Products, Grass Lake, MI). The ratio of wet sediment to groundwater in the microcosms was 1:1.5 (v/v), following the method of Lorah and Voytek (*26*). The composition of the simulated groundwater was slightly modified from that described by Dries et al. (*326*), and consisted of 3.5 mM $NaHCO_3$, 0.1 mM KCl, 0.25 mM $MgCl_2$, and 0.75 mM $CaCl_2$. The microcosms were sealed with Teflon-lined butyl rubber stoppers and aluminum crimp caps. Neat PCE was introduced into the microcosms with a 10 µL syringe and the microcosm mass difference was recorded following injection to determine the mass of PCE loaded. The target aqueous-phase PCE concentration was approximately 0.08 mM after partitioning among gas, solid, and aqueous phases.

Microcosms were supplied with dissolved acetate and hydrogen gas ranging at concentrations from 0 to 2.5 mmoles reducing equivalents to test their effect on the times and extent of reductive dechlorination (Table 6.1). Acetate was added from an anaerobic, sterile stock solution of acetic acid in simulated groundwater. Target hydrogen concentrations were achieved by sparging the microcosm headspace with nitrogen gas then supplying hydrogen gas directly to the microcosm. When dechlorination was

complete (i.e., conversion to ethene/ethane), the microcosms were sparged with N_2, recapped under anaerobic conditions, and respiked with the appropriate amount of electron donor and neat PCE. The addition of mineral media, carbon sources (with the exception of the acetate microcosms), and vitamins to the microcoms was avoided to replicate environmental conditions. Duplicate active control microcosms were established without PCE to ensure that all observed ethenes were experimentally derived. Bioaugmented microcosms were also constructed with a 5% inoculum of a PCE to ethene mixed culture (*327*) to test the effect of excess dechlorinating cells on dechlorination times. Sterilized microcosms were prepared as described above but autoclaved at 121º C for 1 hour on two consecutive days prior to PCE addition to ensure that reductive dechlorination observed in the active reactors was not the result of abiotic transformation processes (*101, 328, 329*). All microcosms were wrapped in foil and incubated at 20º C on an orbital shaker at 150 rpm. Chlorinated ethenes, ethene, ethane, and methane concentrations were determined from headspace samples of the microcosms.

6.3.4. DNA Extraction and PCR Conditions

Partial characterization of the dechlorinating community was performed on an active PCE to ethene dechlorinating microcosm supplied PCE, acetate, and hydrogen. DNA was extracted from five separate one-gram samples of wet sediment (5.04 g total) using the Ultraclean™ Soil DNA Isolation Kit (Mo Bio Laboratories, Inc., Solana Beach, CA). Procedures of DNA extraction and PCR reactions have been described previously (*327*). Chromosomal DNA from *Dehalobacter restrictus*, *Desulfuromonas michiganensis* strain BB1, *Desulfomonile tiedjei*, and *Geobacter lovleyi* strain SZ were used as positive controls during PCR reactions and gel electrophoresis. The primer

sequences for the target 16S rRNA genes have previously been reported and are provided in the Supporting Information (Table 6S.3). Negative control reactions accompanied all PCR analyses and consisted of nuclease-free water (Fisher Scientific).

6.3.5. Quantitative Real-Time PCR (qPCR) Conditions

Detection of *Dehalococcoides* and reductive dehalogenase genes (RDases) *tceA* (*330*), *vcrA* (*331*), and *bvcA* (*332*) was performed using qPCR. The qPCR reactions for *Dehalococcoides* 16S rRNA genes and the *tceA*, *bvcA*, and *vcrA* genes were performed as described by Ritalahti et al. (*231*). Standard curves for qPCR analysis were prepared with a dilution series of quantified genomic DNA from *Dehalococcoides* sp. strain FL2 or from plasmids carrying a single *Dehalococcoides* RDase gene. The linear quantification range for *Dehalococcoides* sp. strain FL2 was $10^2 – 10^{10}$ gene copies·mL^{-1} ($r^2 = 0.999$). The linear range for the target RDases was $10^2 – 10^{10}$ gene copies·mL^{-1} ($r^2 = 0.995$), $10^1 – 10^{10}$ gene copies·mL^{-1} ($r^2 = 0.997$), and $10^1 – 10^8$ gene copies·mL^{-1} ($r^2 = 0.990$) for *tceA*, *vcrA*, and *bcvA*, respectively. The gene copy numbers were calculated as described previously (*231*). Genetic and genomic analyses show these 16S rRNA and the RDase genes exist as single copy genes on *Dehalococcoides* genomes (*231*, *333*, *334*).

6.3.6. Sediment Column Construction

An upflow sediment column was assembled to simulate an anaerobic sediment bed modified with an *in situ* cap. The column was constructed using a 2.5 cm I.D. glass chromatography column 30 cm in length (Spectrum Chromatography, Houston, TX) with custom-built stainless steel end plates. A 2.5 cm diameter disc of 80 mesh stainless steel (Small Parts, Inc., Miami Lakes, FL) and a second 2.5 cm diameter disc of finer mesh (5 μM opening; TWP Inc., Berkeley, CA) were placed in series within the end plates to help

distribute flow and prevent the loss of sediment particles. A glass reservoir (15 mL; 0.1 pore volumes) fitted with a stopcock was placed at the column effluent to allow for aqueous sampling. The column was packed with wet, homogenized sediment in a fume hood under a constant stream of N_2 and wrapped in foil. Estimates of porosity and water content were obtained from bulk sediment properties (Supporting Information, Table 6S.1) and column mass difference before and after packing.

Column influent composed of simulated groundwater spiked with dissolved-phase PCE (ranging from 31.4 ± 11.3 μM to 134.7 ± 47.1 μM; Supporting Information, Figure 6S.2) was supplied to the column by a syringe pump at a rate of 5.5 $mL \cdot hr^{-1}$ to produce a hydraulic residence time of one day and a seepage velocity of 47.0 $cm \cdot day^{-1}$ (Darcy velocity = 25.8 $cm \cdot day^{-1}$). The flow rate was selected to simulate elevated seepage velocities associated with flow bypassing potentially caused by *in situ* capping with relatively low permeability caps. The column seepage velocity of 47.0 $cm \cdot day^{-1}$ is on the upper end of the range of observed field velocities of groundwater seeps (0.0026 to 720 $cm \cdot day^{-1}$ (*31*)). The simulated groundwater was autoclaved at 121º C for 30 minutes and sparged with N_2 gas for 45 minutes prior to use. Periodic measurements of the influent indicated that dissolved oxygen levels were routinely below 0.5 $mg \cdot L^{-1}$ and always below 1 $mg \cdot L^{-1}$ (data not shown). The pH of the sparged groundwater was adjusted to circumneutral by the addition of carbon dioxide gas. Dissolved-phase PCE, obtained from a saturated stock solution of neat PCE in anaerobic, sterile simulated groundwater, was added to the influent syringe immediately preceding connection to influent tubing. The column lifetime was divided into three separate phases based on influent conditions: Phase I from 0 to 108 pore volumes; Phase II from 108 to 146 pore volumes; and Phase

III from 146 pore volumes until the conclusion of the experiment 180 pore volumes. Phase I was defined by an influent composed of only simulated groundwater and PCE with the goal of obtaining baseline transport and biotransformation data. Phase II was characterized by the addition of 5 mM lactate to the influent from an anaerobic, sterile stock solution intended to stimulate the microbial community. In Phase III, the influent was returned to the initial Phase I conditions, containing only simulated groundwater and aqueous phase PCE.

Influent concentrations of PCE were routinely measured due to variability in the concentration of the aqueous PCE stock and to ensure that no PCE transformations occurred before introduction into the column. Aqueous effluent samples were obtained from the sampling reservoir and transferred to a sealed serum bottle that had an equivalent volume of gas-phase removed immediately prior to injection. Chlorinated ethenes, ethene, ethane, methane, and hydrogen concentrations were determined from headspace samples of these serum bottles. Aqueous samples were obtained from these serum bottles to measure effluent anion concentrations. Colorimetric iron analysis was performed on reservoir samples transferred directly to cuvettes.

6.3.7. Analytical Methods

Chloroethenes, ethene, ethane, and methane were separated via gas chromatography (GC) and analyzed with an FID detector, as described previously (*122*). Hydrogen concentrations were determined from headspace samples using a GC equipped with a reducing gas analyzer (*335*). Iron measurements were conducted using a modified ferrozine method (*336*) with colorimetric determination of ferrous and total iron by a Cary 300 UV-VIS spectrophotometer. Anions were separated using a Dionex DX-100

ion chromatograph equipped with a Dionex AG4A IonPac guard column and Dionex AS4A IonPac column.

6.4. Results and Discussion

6.4.1. Microcosms

PCE was successfully dechlorinated to the end products of ethene and ethane under methanogenic conditions in all biologically active microcosms. Figure 6.1 shows a a representative microcosm following the three initial PCE dechlorination cycles. This microcosm was supplied with acetate and hydrogen, resulting in 1.3 mequiv of electrons (electron donor to PCE ratio = 16.6). Temporary stalling of dechlorination at *cis*-DCE occurred during the first dechlorination cycle in most microcosms. The loss of ethene mass balance in the representative microcosm during the first spike was attributed to leakage through the septa after multiple punctures, as evidenced by the loss of methane after approximately 40 days. It is also possible that anaerobic oxidation within the microcosms contributed to the loss of the species (*337*), however this pathway was not monitored. During the subsequent dechlorination cycles, rapid dechlorination and ethane production occurred. Interestingly, a concurrent increase in methanogenesis was observed during conversion of ethene to ethane, which has been reported previously (*338, 339*).

The effect of exogenous electron donor supply on the time required for complete dechlorination is presented in Table 6.1, along with the amount of reducing equivalents provided. It was generally observed that increasing amounts of reducing equivalents (i.e., increasing the electron donor to PCE ratio) decreased the time necessary for complete

Table 6.1. Reducing equivalents added to PCE microcosms and time required to achieve complete dechlorination of PCE to ethene for the initial three dechlorination cycles. Reducing equivalents were added in the form of hydrogen and acetate, where indicated.

Microcosm Name	Reducing Equivalents Added (meq total)[a]	ED to PCE Ratio[b]	Tme Required for Complete Dechlorination (days)[c]		
			First Dechlorination Cycle	Second Dechlorination Cycle	Third Dechlorination Cycle
No H_2	0.0	0.0	82	24	20
minimal H_2	0.1	1.4	80	19	26
acetate + H_2	1.3	16.6	76	15	10
excess H_2	2.5	31.3	56	12	6
bioaugmented[d]	0.1	1.4	33	16	21

[a] Reducing equivalents were calculated based on 2 equivalents per 1 mole H_2; 4 equivalents per 1 mole acetate (*340*). "Minimal H_2" and "Acetate + H_2" microcosms had 3.5 % H_2 in microcosm headspace and "Excess H_2" microcosms had 80% H_2 in microcosm headspace. [b] Electron donor (ED) to PCE ratio was calculated based on 8 reducing equivalents required for PCE to be reductively dechlorinated to ethene, all chloroethene mass being bioavailable, and no loss of reducing equivalents to competing biotic and abiotic processes. [c] Times required for complete dechlorination are averages of duplicates. [d] Bioaugmented microcosms were supplied with a 5% inoculum (volume culture/aqueous volume microcosm) of a PCE to ethene mixed culture (Owls - (*327*)) sparged with N_2 prior to addition.

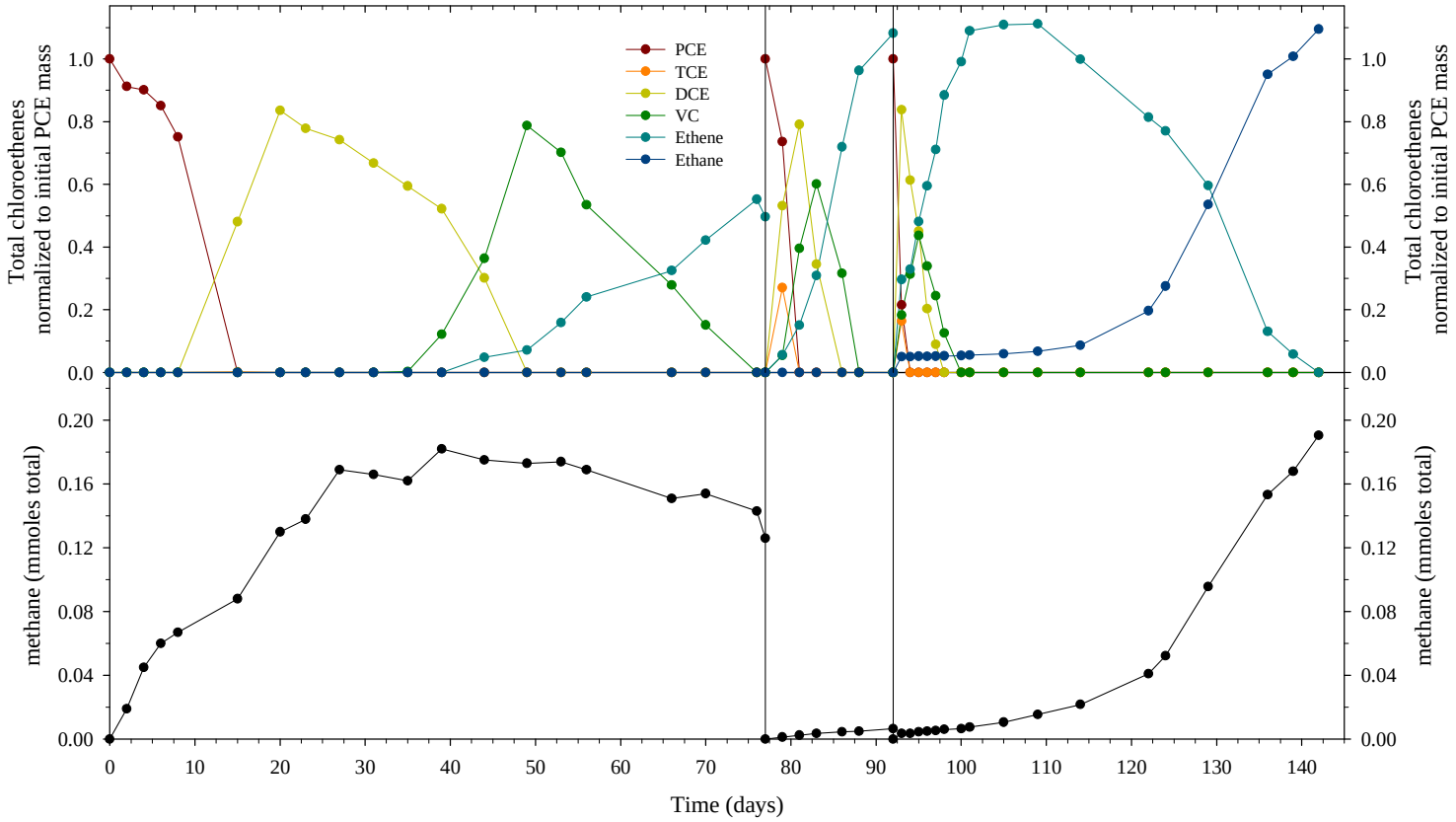

Figure 6.1. Representative example of the initial three dechlorination cycles and associated methane production for an active PCE microcosm. The example microcosm shown was provided 5 mM acetate and 3.5 % H_2 in microcosm headspace, resulting in an electron donor to PCE ratio of 16.6. Chloroethene concentrations are plotted as the total mmoles of chloroethene species present in the microcosm (i.e., sum of solid, aqueous, and gas phases) normalized to initial mmoles of PCE introduced into the microcosm. Methane concentrations are plotted as total mmoles within the microcosm (i.e., sum of solid, aqueous, and gas phases). Black vertical lines represent microcosm headspace sparging with nitrogen gas and respike with PCE.

conversion of PCE to ethene, especially after the second and third PCE additions. Notably, complete dechlorination was observed in microcosms not provided with additional reducing equivalents. These results are in agreement with previous studies reporting that in the absence of nutrient and substrate amendments, sediment can serve as a nutrient source with the system as a whole being electron donor limited (*341, 342*). The bioaugmented control did not perform substantially better than other microcosms after the initial dechlorination cycle, suggesting dechlorination was not limited by cell numbers. PCE transformation was not observed in the autoclaved control microcosm, with the disappearance of PCE over time attributed to sorption (Supporting Information, Figure 6S.1). A lumped rate coefficient describing neat PCE dissolution into the aqueous phase, partitioning into the headspace, and sorption by the sediment was obtained in the sterilized controls using a nonequilibrium mass-transfer model, which was used to estimate PCE sorption by the solid phase for mass balance calculations. The organic carbon distribution coefficient (K_{oc}) for PCE onto the sediment was measured to be 312 $mL \cdot g^{-1}$, which is similar to a reference value of 265 $mL \cdot g^{-1}$ (*343*).

6.4.2. Microbial Analysis

Partial characterization of the dechlorinating microbial community summarized by Table 6.2 indicated that multiple organisms were potentially responsible for the observed PCE dechlorination in Anacostia River sediment. *Dehalobacter* spp., *Desulfuromonas* spp., and *Desulfomonile* spp. were detected in the sediment, all of which are capable of dechlorinating PCE to DCE (*128-130*). *Dehalococcoides* and the target reductive dehalogenase genes *tceA*, *vcrA*, and *bvcA* were all amplified from the extracted DNA at concentrations provided in Table 6.2. Comparison of cell numbers provided by

Table 6.2. Partial characterization and quantification of dechlorinating microorganisms within a microcosm supplied wet sediment, simulated groundwater, PCE, acetate, and hydrogen.

Target Microorganism or Gene	Dechlorination Activity	Presence	Quantification (gene copies·mL^{-1})
Dehalobacter spp.	PCE → DCE	+	
Desulfuromonas spp.	PCE → DCE	+	*Not Performed*
Desulfomonile spp.	PCE → DCE	+	
Geobacter sp. strain SZ	PCE → DCE	N/D [a]	
Dehalococcoides spp.	PCE → Ethene DCEs →Ethene	+	$5.2 \times 10^8 \pm 2.3 \times 10^7$ [b]
tceA (*Dehalococcoides* sp. strain 195 or strain FL2)	TCE → VC	+	$8.3 \times 10^7 \pm 2.9 \times 10^6$
vcrA (*Dehalococcoides* sp. strain VS or strain GT)	DCEs →Ethene	+	$2.1 \times 10^8 \pm 2.1 \times 10^7$
bvcA *(Dehalococcoides* sp. strain BAV 1)	VC → Ethene	+	$2.8 \times 10^7 \pm 1.1 \times 10^5$

[a] N/D = not detected with PCR (nested or direct). [b] Quantification of *Dehalococcoides* and RDase numbers are average of triplicates ± one standard deviation.

qPCR should be made with caution due to inherent analytical uncertainty (*237, 344*), however the technique was successful in identifying which *Dehalococcoides* strains were present, which was the goal of the procedure. Amplification of the *tceA* gene suggests the presence of a 195-type (*330*) and/or FL2-type (*345*) organism, while the presence of the *vcrA* gene suggests either a *Dehalococcoides* sp. strain VS-type (*331*) and/or GT-type (*117*) organism. Detection of the *bvcA* gene suggests the presence of a BAV1-type (*332*) organism. It is interesting that such an active dechlorinating community was detected in the sediment despite the lack of chloroethenes detected in the unamended sediment. This can be attributed to the diverse metabolic capabilities of the organisms, which have been shown to dechlorinate more common sediment contaminants such as chlorobenzenes (*124*), dioxins (*125*), and PCBs (*114, 317, 346, 347*).

6.4.3. Sediment Column

Results of the 1-D sediment column are presented in Figures 6.2A-B and 6.3A-B. A total of 180 pore volumes of simulated groundwater supplemented with dissolved-phase PCE were flushed through the column at a one day retention time. Methanogenesis (Figure 6.3A), iron sulfide precipitation (Figure 6.3B), and phosphate elution (Figure 6.3B) were observed shortly after flow was initiated, all indicators of reducing conditions. Non-ideal flow patterns and physical nonequilibrium conditions (e.g., dead end pores) were revealed by non-reactive tracer tests conducted at 5 and 96 pore volumes (Supporting Information, Table 6S.2). The high degree of dispersion, as indicated by very low fitted Peclet numbers, was attributed to a combination of biogenic gas production and the inherent heterogeneity of natural sediments.

6.4.3.1. Phase I. Figure 6.2A shows the effluent concentrations of PCE and its dechlorination products, while normalized product distribution at selected pore volumes is presented in Figure 6.2B. The sorption and partial dechlorination of chloroethenes, along with the loss of methanogenesis, were observed during Phase I of the column experiment. The cause for the scattering of chloroethene effluent concentrations in Figure 6.2A is unknown, and assessment of column plumbing (e.g., leaks), sampling procedures (e.g., replicate samples, increasing sampling frequency, changing sampling vial), and calibration curves yielded no experimental nor analytical reasons for the scattering. One possible explanation is that the creation of preferential flow patterns within the hydraulically dynamic sediment caused pulsed elution of chloroethene mass. Conant et al. (*22*) characterized a chloroethene plume discharging into a river and reported complex porewater concentration distributions over relatively small lateral distances due to the presence of preferential flow patterns.

Examination of Figure 6.2A reveals that effluent *cis*-DCE molar concentrations, beginning at 46 pore volumes, were markedly below the corresponding influent PCE concentrations (Supporting Information, Figure 6S.2), which was attributed to sorption of chloroethenes by the solid phase. The appearance of PCE and TCE in the column effluent began at approximately 85 pore volumes, and corresponded to an increase of influent PCE concentrations combined with a loss of microbial activity, indicated by methane concentrations approaching non-detect levels beginning at 45 pore volumes (Figure 6.3A). It was hypothesized that the loss of dechlorination and methanogenic activity was due to a lack of available electron donor, and the addition of lactate to the influent was initiated to test this hypothesis.

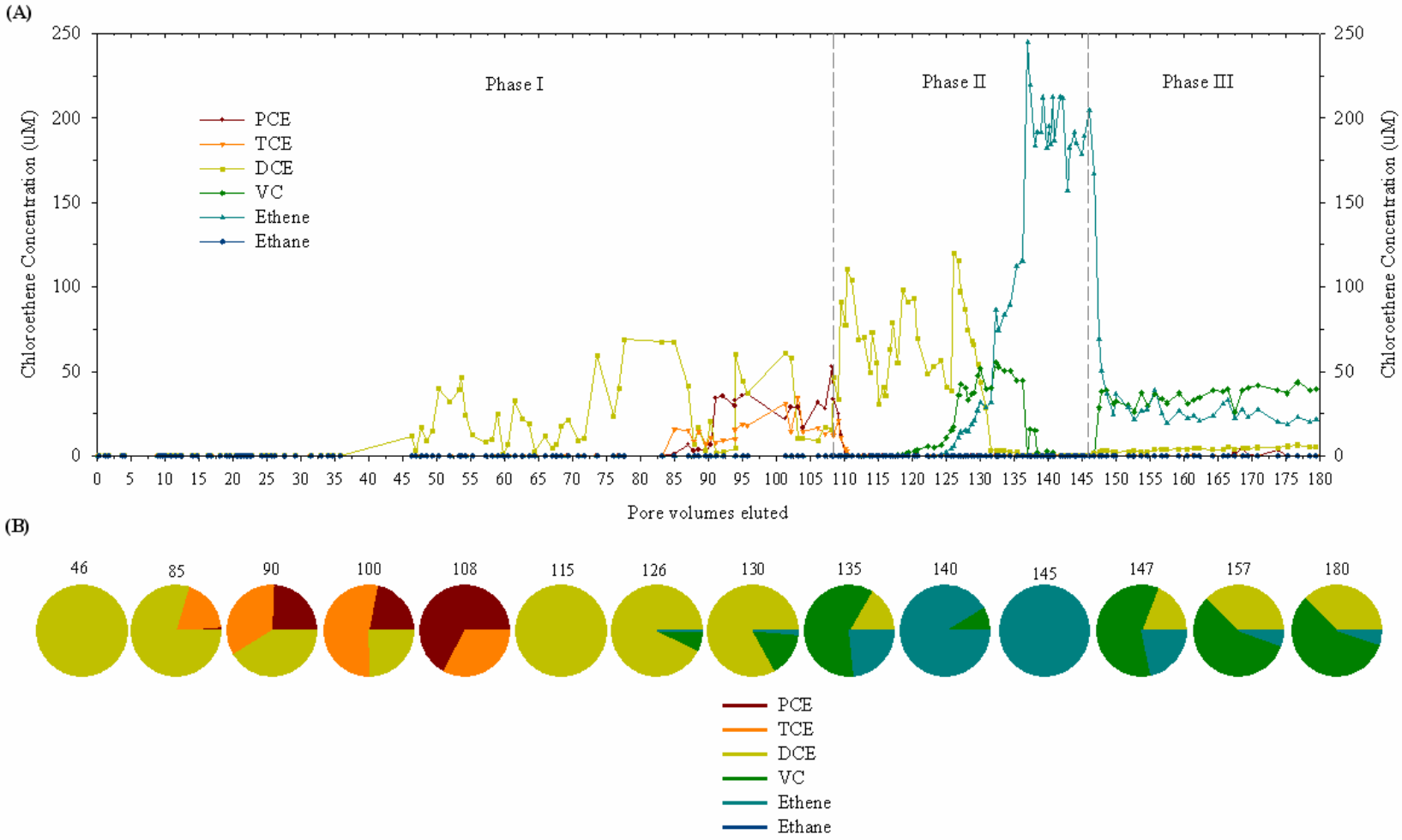

Figures 6.2A-B. Sediment column aqueous phase effluent concentrations of PCE and its dechlorination products. (A) Effluent concentration of PCE and dechlorination products (μM). The vertical dashed lines indicate Phase II of the experiment, when lactate was supplied to the influent along with dissolved phase PCE and simulated groundwater. (B) Effluent PCE dechlorination product distribution at selected pore volumes, indicated above each pie chart. Dechlorination products were normalized to the total amount of ethenes and ethane eluted.

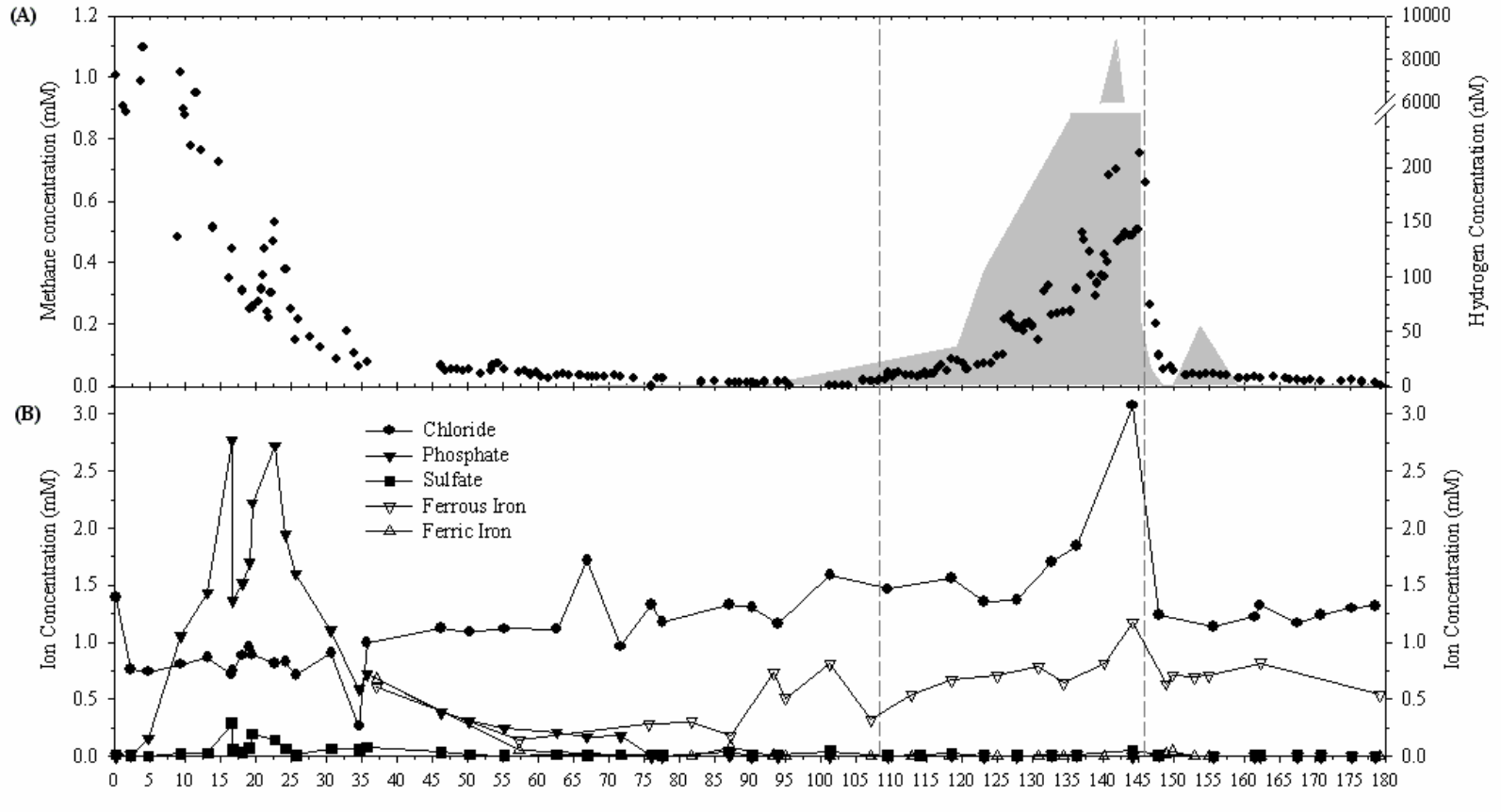

Figures 6.3A-B. (A) Effluent aqueous methane concentrations (mM – left axis) and aqueous hydrogen concentrations (nM – hatched area). (B) Selected ions in sediment effluent (mM). The vertical dashed lines indicate Phase II of the experiment, when lactate was supplied to the influent along with dissolved phase PCE and simulated groundwater.

6.4.3.2. Phase II. The addition of 5 mM lactate during pore volumes 108 to 146 stimulated the microbial community, evidenced by the revival of dechlorinating and methanogenic activities and a spike in hydrogen concentrations. Effluent chloroethene distribution shifted from a mix of PCE, TCE, and *cis*-DCE prior to lactate addition to solely *cis*-DCE almost immediately following lactate addition (Figure 6.2B). When *cis*-DCE was the predominant product during Phase II (pore volumes 111 to 124), total chloroethene effluent concentrations averaged 68.6 ± 22.0 μM, similar to influent PCE concentrations of 68.9 ± 16.7 μM during this period. The appearance of VC and ethene began at approximately 118 and 124 pore volumes, respectively, with ethene eventually becoming the dominant product (Figures 6.2A-B). Interestingly, between pore volumes 127 to 147 ethene concentrations averaged 172.2 ± 34.3 μM, approximately 2.5 times greater than influent PCE concentrations during this period. The increase in dechlorinating activity is accompanied by an increase in chloride at 144 pore volumes (Figure 6.3B). Additionally, active dechlorinating cells including *Dehalococcoides* eluted from the column during Phase II (Supporting Information, Figure 6S.3A). Two possible causes for the observed increase in total chloroethene effluent concentrations are the induction of biologically-enhanced desorption and the formation of decreasingly sorptive products during the PCE dechlorination pathway. The stimulation of the dechlorinating community removed chloroethenes from the aqueous phase, inducing chloroethene desorption to maintain equilibrium conditions. PCE dechlorination products are also less sorptive (i.e., lower K_{oc} values), allowing for greater aqueous phase concentrations. The combination of these processes may have contributed to the elevated effluent chloroethene concentrations observed during Phase II.

Stimulation of the non-dechlorinating microbial community during Phase II is supported by the increase in effluent concentrations of methane, hydrogen, and ferrous iron. Methane concentrations approached non-detect levels prior to lactate addition, but approached initial levels at the conclusion of Phase II (Figure 6.3A). Figure 6.3A shows effluent hydrogen concentrations at non-detect during Phase I then significantly elevated during Phase II. A substantial increase in hydrogen was observed at 142 pore volumes, almost 3 orders-of-magnitude greater than levels associated with minimum hydrogen thresholds for dechlorinators (*120, 335*), suggesting that much of the hydrogen being produced was eluting from the sediment column. A modest spike in ferrous iron at approximately 142 pore volumes (Figure 6.3B) suggests that iron-reducing bacteria were also stimulated within the sediment by lactate addition. Although the addition of electron donor successfully stimulated the microbial community within the sediment, it was unclear whether this activity would be sustained after lactate addition ceased. It was hypothesized that fermentation of organic matter would maintain the observed VC and ethene production during Phase II, and this was tested during Phase III.

6.4.3.3. Phase III. The lack of exogenous electron donor supply during Phase III caused an immediate decrease in microbial activity, demonstrated by the simultaneous reductions of dechlorinating activity, methanogenesis, and hydrogen production. Chloroethene product distributions shifted from complete dechlorination to a mixture of *cis*-DCE, VC, and ethene for the remainder of the experiment (Figures 6.2A-B). Total chloroethene concentrations immediately decreased from the end of Phase II (172.2 ± 34.3 μM) to the beginning of Phase III (67.9 ± 10.8 μM) to match influent concentrations (68.9 ± 16.7 μM). In addition, active *cis*-DCE and VC dechlorinators were not eluting

from the sediment during Phase III, suggesting a decrease in the active population within the sediment (Supporting Information, Figure 6S.3B). These reductions, concomitant with the removal of electron donor from the influent, confirm that elevated chloroethene effluent concentrations observed during Phase II were caused by stimulation of the microbial community. This observation may have ramifications for historically-contaminated sites with large amounts of sorbed-phase mass that are to be treated using biologically based remediation. Dechlorination of previously sorbed chloroethene mass may occur during the onset of microbial stimulation, leading to a burst of dechlorination products (*159*). Methanogenesis also diminished immediately after the cessation of lactate addition, and approached non-detect levels. Hydrogen concentrations declined to non-detect levels, despite an observed peak at 154 pore volumes, while ferrous iron returned to previous concentrations without any notable spikes in concentration.

Reducing equivalents from the oxidation of organic matter apparently were not able to maintain microbial activity in the sediment column experiment, perhaps due to the combined effects of organic matter recalcitrance, electron donor washout, and preferential flow path formation. In natural settings labile organic matter is quickly oxidized at the sediment-water interface, leaving more refractory organic matter subject to burial (*108*). This process may have occurred throughout the sediment column, since the sediment was homogenized and labile organic matter was evenly distributed. In addition, elution of fermentation products from the column removed electron donor from the system prior to utilization. This explanation is supported by the large hydrogen peak observed during Phase II. Finally, the presence of preferential flow paths may have reduced or eliminated contact between dissolved-phase chloroethenes and occluded

regions of sediment, effectively decreasing the amount of reducing equivalents available for dechlorinating microbes in the vicinity of the contaminants. Due to the limited availability of electron donor, biostimulation was necessary to achieve complete dechlorination under the operating conditions for the sediment column experiment.

These findings are relevant to *in situ* capping scenarios where contaminated groundwater seeps are present. Our experiments addressed how capped sediment responded to the introduction of new contaminants, but the outcomes should also be applicable in cases when the capped sediment is subject to previous contamination, since reductions in electron donor availability may still occur, leading to subsequent reductions in natural bioattenuation. The observed loss of sedimentary bioattenuation processes suggests that groundwater contaminants can be transported through sediments without substantial biotransformation and discharge into *in situ* caps and surface waters. Therefore, it appears that *in situ* caps should be designed to account for the potential loss of natural biobarrier reactivity and for the breakthrough of groundwater contaminants. The use of reactive caps, whether physico-chemical or biologically-based, may be a viable solution to changes in natural reductive dechlorination capacity.

6.5. Acknowledgments

Rebecca Daprato assisted with molecular analysis techniques. Some primers and standards for PCR and qPCR analysis were supplied by the Löffler lab at the Georgia Institute of Technology. Kurt Pennell provided many helpful discussions regarding data analysis and interpretation.

6.6. Supporting Information

6.6.1. Sorption of PCE to sediment. The sorption of PCE to wet Anacostia sediment was observed in a microcosm constructed within a serum bottle (70 mL) loaded with wet sediment, simulated groundwater, and neat PCE. The sediment was sterilized by autoclaving for one hour on two consecutive days prior to PCE addition. The normalized equilibrium aqueous phase PCE concentration, normalized by the mass of PCE introduced, was estimated to be 0.178 based on partitioning among gas, aqueous, and solid phases and the known mass of PCE added to the microcosm. Partitioning into the gas phase was predicted from the volume of microcosm headspace and Henry's coefficient for PCE, 0.723 (*348*). Sorption by the solid phase was modeled using the mass of solid sediment material and the linear distribution coefficient (K_D) for PCE, which was calculated to be 13.25 $mL \cdot g^{-1}$ from the product of the measured organic carbon content of the sediment (5.22%; Table 6S.1) and an average literature K_{oc} for PCE (265 $mL \cdot g^{-1}$ (*343*)). Nonequilibrium sorption was described using a one-site chemical nonequilibrium model:

$$C_{w,t} = C_{w,eq} - (C_{w,eq} - C_{w,0}) \exp^{(-kt)}$$

where $C_{w,t}$ is the aqueous phase concentration ($mg \cdot L^{-1}$) at time t (hr), $C_{w,eq}$ is the calculated equilibrium concentration ($mg \cdot L^{-1}$), $C_{w,0}$ is the initial aqueous phase concentration ($mg \cdot L^{-1}$), and k is the sorption rate coefficient (hr^{-1}) (*79, 81*). The value of k was fitted to minimize the root mean square error between the model and the observed data at each sampling point. The rate coefficient k incorporates the dissolution of neat PCE into the aqueous phase, volatilization of PCE into the headspace, and the sorption of

aqueous PCE onto the sediment. The model was used to estimate solid phase PCE concentrations during mass balance calculations of the biologically active microcosms.

Equilibrium PCE sorption data showed good agreement with the estimated value after 41 days, and no further disappearance of PCE occurred after this time (Figure 6S.1). The measured K_{oc} value after 41 days was calculated from the change in aqueous phase concentration and found to be 312 $mL \cdot g^{-1}$, which is similar to the reference value of 265 $mL \cdot g^{-1}$. The fitted sorption rate coefficient (k) for the nonequilibrium sorption model was calculated to be -5.48×10^{-3} hr^{-1}, as shown in Figure 6S.1.

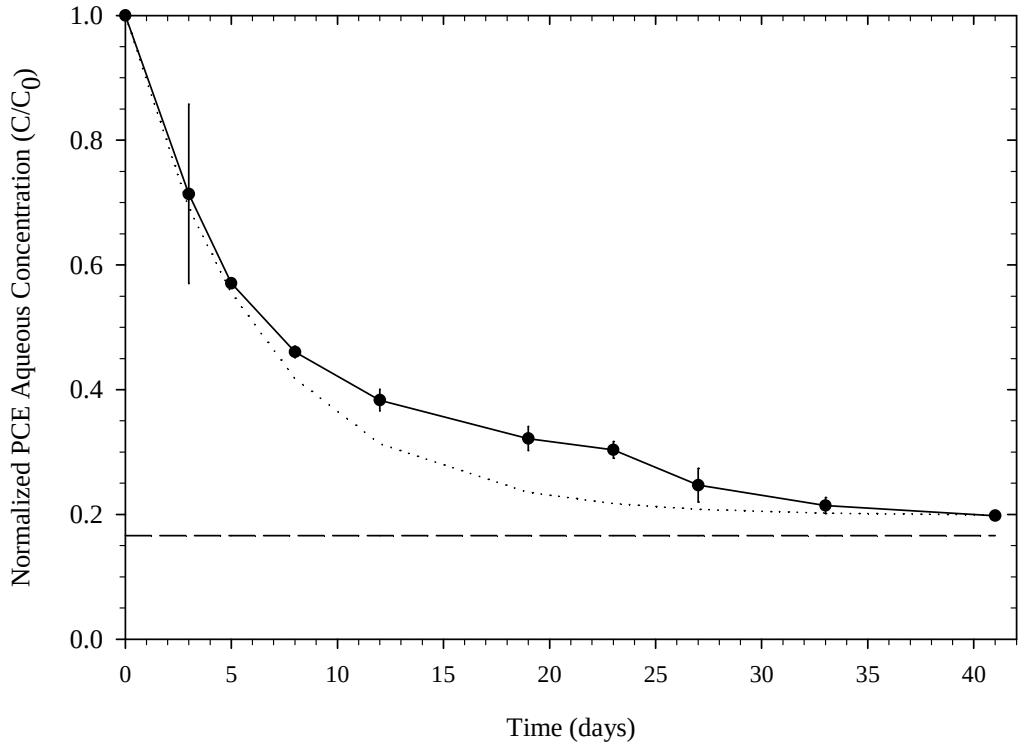

Figure 6S.1. Aqueous phase concentration of PCE in sterilized microcosms normalized to initial PCE mass introduced. Measured values of aqueous phase PCE concentration are the average of duplicates, and error bars represent ± one standard deviation. The dashed line (– – – –) at $C/C_0 = 0.178$ is an estimate of equilibrium concentration of PCE based on partitioning among gas, aqueous, and solid phases. The dotted line (····) corresponds to the fitted one-site chemical nonequilibrium model with $k = -5.48 \times 10^{-3}$ hr^{-1}.

Table 6S.1. Results of the sediment characterization. The values of wet bulk density, particle density, and gravimetric water content were used to estimate the mass-volume relationships of solid, aqueous, and gas phases during microcosm and column construction. The particle size analysis was classified according to the Wentworth classification system (*349*). The fraction organic was determined from dried sediment with a Shimadzu TOC-5050A Total Carbon Analyzer (Shimadzu Scientific Instruments, Inc., Columbia, MD) equipped with non-dispersive infrared detector with catalytic combustion at 680º C.

Sediment Property	Measured Value
Wet bulk density	1.36 $g \cdot mL^{-1}$
Particle density	2.44 $g \cdot mL^{-1}$
Gravimetric water content	55 %
Fraction organic carbon	5.22 %
Porewater salinity	0.25 ppt
Particle size analysis	
Medium silt and smaller	33.7 %
Coarse silt	19.8 %
Fine sand	19.6 %
Medium sand	20.8 %
Coarse sand	6.20 %

Table 6S.2. Summary of tracer experiments conducted on sediment column using bromide as a nonreactive tracer. Bromide was supplied to the influent at a concentration of 100 $mg \cdot L^{-1}$ (1.25 mM) from an anaerobic, sterile stock of potassium bromide in simulated groundwater. A fraction collector captured tracer effluent, with volatile effluent species (e.g., dechlorination products) not measured during fraction collecting. The Peclet number is an indicator of dispersion within the sediment; beta represents the dimensionless fraction of mobile pore volumes within the column; omega represents a dimensionless rate constant; and alpha is a calculated mass transfer coefficient (hr^{-1}).

Property	Tracer 1	Tracer 2
Period of tracer effluent collection (pore volumes)	5 to 8	96 to 101
Peclet number[a]	37.29	2.28
Beta[a]	0.793	0.358
Omega[a]	0.547	0.409
Alpha (hr^{-1})	0.0197	0.0.0147

[a] Fitted parameters were obtained with the CFITM3 break through curve fitting program under physical nonequilibrium constraints.

Table 6S.3. Primers and probes used for identifying organisms and reductive dehalogenase genes.

Target Group	Primer Name	Sequence	Specificity	References
Dehalobacter sp.	deb179f	5'-TGTATTGTCCGAGAGGCA-3'	*Dehalobacter sp.*	(*350*)
	deb1007R	5'-ACTCCCATATCTCTACGG-3'		
Desulfuromonas spp.	Desulf for	5'-AACCTTCGGGTCCTACTGTC-3'	*Desulfuromonas michiganensis* strain BB1, *D. acetoxidans* and *D. chloroethenica*	(*351*)
	Desulf rev	5'-CGGCAACTGACCCCTATGTT-3'		
Desulfomonile spp.	Dt1	5'-CAAGTCGTACGAGAAACATATC-3'	*Desulfomonile tiedjei*	(*352*)
	Dt2	5'-GAAGAGGATCGTCTTTCCACGA-3'		
Geobacter lovleyi strain SZ	Geo 169F	5'-GAATATGCTCCTGATTC-3'	*Geobacter lovleyi* strain SZ	(*53*)
	Geo 999R	5'- ACCCTCTACTTTCATAG-3'		
bvcA gene	Bvc925F	5'-AAAAGCACTTGGCTATCAAGGAC-3'	*Dehalococcoides* sp. strain BAV1	(*231, 332*)
	Bvc1017R	5'-CCAAAAGCACCACCAGGTC-3'		
	Bvc977Probe	5'-FAM-TGGTGGCGACGTGGCTATGTGG-TAMRA-3'		
tceA gene	TceA1270F	5'-ATCCAGATTATGACCCTGGTGAA-3'	*Dehalococcoides* sp. strains 195, FL2	(*231, 330, 353*)
	TceA1336R	5'-GCGGCATATATTAGGGCATCTT-3'		
	TceA1294Probe	5'-FAM-TGGGCTATGGCGACCGCAGG-TAMRA-3'		
vcrA gene	Vcr1022F	5'-CGGGCGGATGCACTATTTT-3'	*Dehalococcoides* sp. strains, VS[a], GT	*(117, 119, 231, 354)*
	Vcr1093R	5'-GAATAGTCCGTGCCCTTCCTC-3'		
	Vcr1042Probe	5'-FAM-CGCAGTAACTCAACCATTTCCTGGTAGTGG-TAMRA-3'		
Dehalococcoides sp. 16S rDNA	Dhc1200F	5'-CTGGAGCTAATCCCCAAAGCT-3'	All *Dehalococcoides* sp. strains	(*231, 302*)
	Dhc1271R	5'-CAACTTCATGCAGGCGGG-3'		
	Dhc1240Probe	5'-FAM-TCCTCAGTTCGGATTGCAGGCTGAA-TAMRA-3'		

[a] Characterized in mixed culture

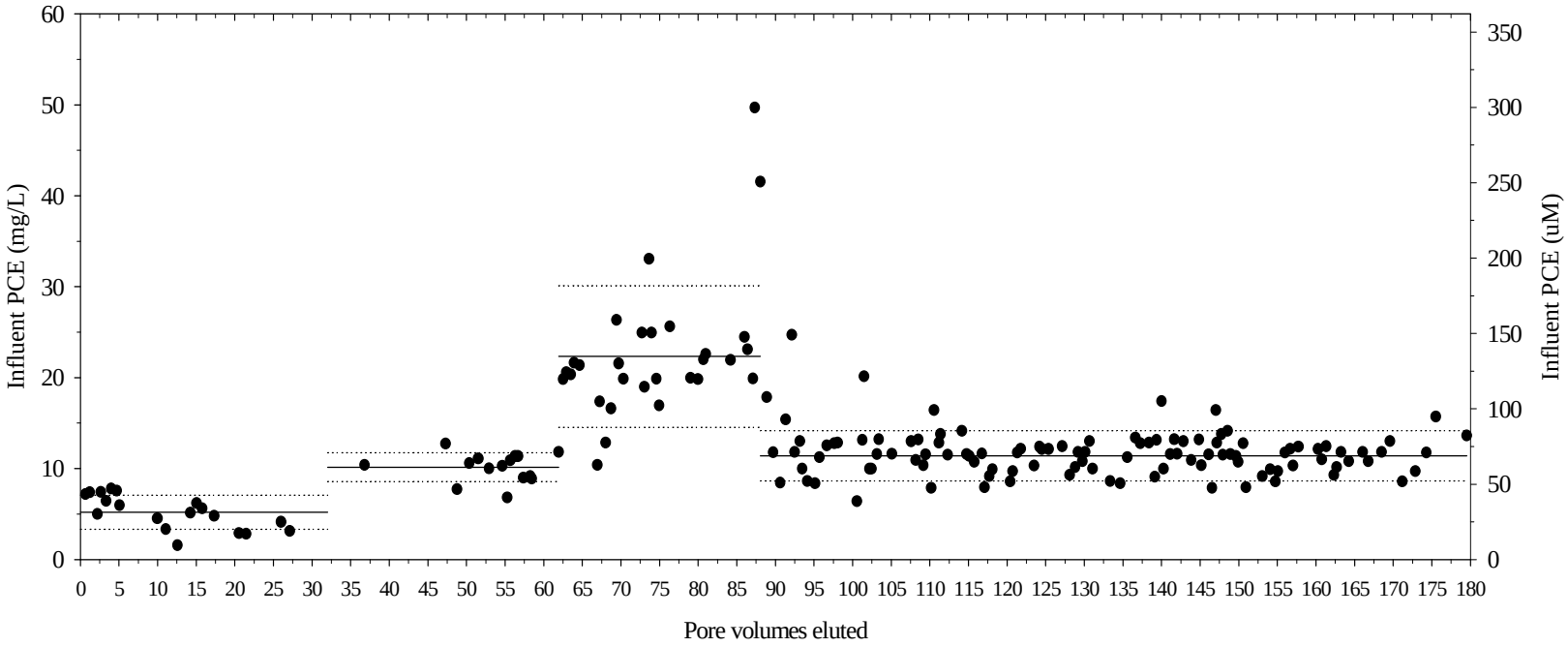

Figure 6S.2. Measured influent PCE concentrations provided to sediment column. Solid black lines are the average PCE concentration during the influent regime, with the dotted lines indicating one standard deviation. Four separate influent regimes were intentionally created based on PCE concentrations. The initial regime was from 0 to 32 pore volumes and had an average PCE concentration of 31.4 ± 11.3 μM. The second regime was from 32 to 62 pore volumes and had an average PCE concentration of 61.2 ± 9.6 μM. The third regime was from 62 to 88 pore volumes and had an average PCE concentration of 134.7 ± 47.1 μM. The fourth regime was from 88 to 180 pore volumes and had an average PCE concentration of 68.9 ± 16.7 μM.

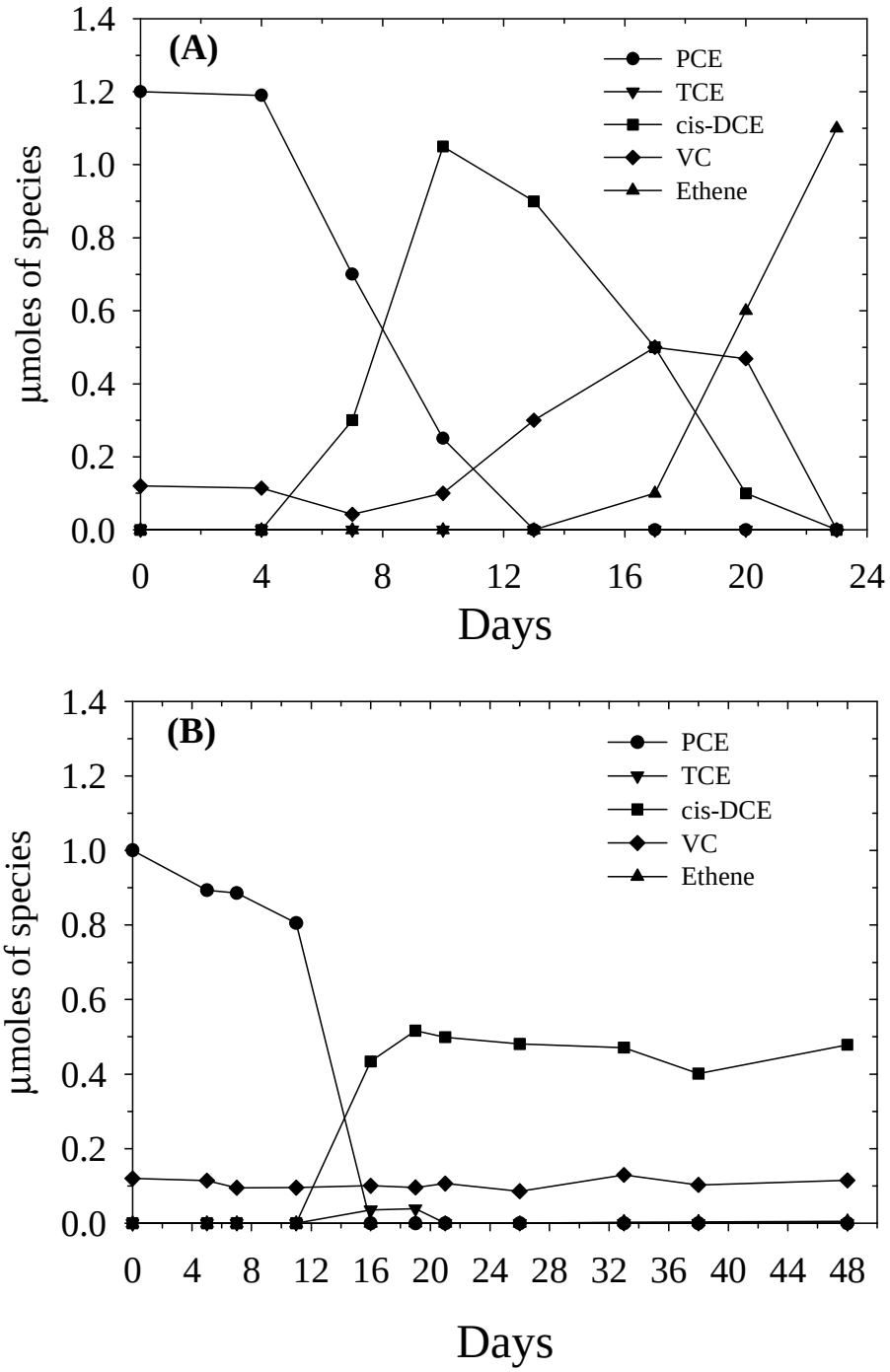

Figures 6S.3A-B: Dechlorination of PCE and VC in microcosms inoculated with an aqueous sample of sediment column effluent obtained during (A) Phase II of column operation and (B) Phase III of column operation. The microcosms contained reduced mineral media supplemented with Wolin vitamins, lactate (5 mM), and hydrogen (20 % headspace). Both PCE and VC were added to the microcosm as electron acceptors to support the activity of all dechlorinating organisms (i.e., PCE to DCE species and VC to ethene species). Concentrations of dechlorination products are plotted as µmoles of species total (sum of aqueous and gas phase concentrations).

CHAPTER 7.

DEVELOPMENT OF A LABORATORY-SCALE BIOREACTIVE *IN SITU* CAP FOR THE TREATMENT OF GROUNDWATER CONTAMINANTS

7.1. Abstract

The development of a bioreactive *in situ* sediment cap, in which microorganisms capable of contaminant transformation are placed within the cap, provides an active cap design that can continuously treat sediment and groundwater contaminants as they are transported through the cap. Sediment effluent eluting into the overlying cap may need to be augmented with certain amendments to maintain microbial activity, however. The goal of this study was to identify limitations on the dechlorinating activity of a mixed consortium within a sand-based cap. Batch experiments demonstrated that the OW culture, a tetrachloroethene (PCE)-to-ethene mixed consortium, was able to completely dechlorinate dissolved-phase PCE to ethene when supplied only sediment effluent. To simulate a bioreactive cap, laboratory-scale sand columns inoculated with the OW culture were placed in series with an upflow sediment column and directly supplied sediment effluent and dissolved-phase *cis*-dichloroethene (DCE). Dechlorination activity and methanogenesis were monitored by aqueous sampling of sand column effluent. The mixed consortium was unable to sustain dechlorination activity at a one day retention time without amendments to the sediment effluent, evidenced by the rapid loss of *cis*-DCE dechlorination to vinyl chloride. When lactate was augmented to the sediment effluent, complete dechlorination of *cis*-DCE to ethene was observed at retention times as fast as 0.5 days, demonstrating that sediment effluent lacks suitable electron donors to

maintain an active microbial community within a sediment cap. Electron donor additions to the bioreactive cap therefore appear to be required to maintain cap reactivity and prevent contaminant breakthrough. Increased contaminant fluxes also limited performance of the dechlorinating consortium within the cap, suggesting the need to reduce contaminant concentrations or flow rates entering the bioreactive cap.

7.2. Introduction

When aquatic sediments are sufficiently contaminated such that it causes adverse effects on aquatic life and limits recreational and economic use, remedial action is often necessary and sometimes legally required. The remedial treatment of contaminated sediment sites with *in situ* subaqueous caps can have both cost and technical advantages over alternative methods such as dredging and monitored natural attenuation (*142*). Traditional *in situ* caps have been composed of sand but can have shortcomings, however, such as eventual contaminant break through and preclusion of their application in regions subject to groundwater seepage. Research efforts have therefore focused on the development of "active" caps, which incorporate reactive an/or sorptive constituents designed to reduce contaminant bioavailability during transport through the cap (*154, 156, 158, 282, 355*). The use of active caps ideally eliminates the threat of contaminant break through with time and allows for their use at groundwater seeps, provided adequate hydraulic control.

The employment of physicochemical-based active caps has limitations, however, such as inherent ceilings for sorption and reaction, thus requiring replenishment of the active materials. Also, surface fouling of the sorptive/reactive constituents may occur and lead to lower treatment efficiencies. These limitations have stimulated the idea of a

bioreactive *in situ* cap in which contaminants are transformed to nontoxic products via microbially mediated reactions within the cap (*282*). An advantage of biologically-based active caps over physicochemical-based caps is that bioreactive caps should not lose reactivity with time provided that necessary metabolic requirements are available. Chapter 4 of this work has demonstrated that microorganisms indigenous to underlying sediment are capable of colonizing the overlying cap, with significant changes in community composition observed with depth. These results indicate that microbial populations naturally inhabit an overlying cap, remain active, and can possibly participate in natural contaminant bioattenuation processes. If intrinsic contaminant biotransformation is not sufficient to completely detoxify contaminants within the cap, amendments or bioaugmentation with a microbial consortium can help ensure desired endpoints.

Previous research addressing biogeochemical conditions and contaminant (bio)attenuation within capped sediments has provided fundamental information to aid in the development of a laboratory-scale bioreactive cap. Studies in Chapters 3 and 5 of this work have thoroughly mapped geochemical conditions within capped sediments to demonstrate that anaerobic processes dominate caps subject to stagnant and upflow conditions. These results suggest that reducing bioattenuation processes should be pursued within a bioreactive cap under these flow conditions. The presence of groundwater seeps at sediment capping sites has been documented (*20, 158*) and could potentially be a source of contaminants to the sedimentary environment. The chlorinated solvents tetrachloroethene (PCE) and trichloroethene (TCE) are common groundwater contaminants (*21*) whose plumes can extend considerable distances from their source to

discharge into surface water bodies (*22-26*). Laboratory research investigating the reductive dechlorination of PCE in a sediment column simulating capping conditions concluded that intrinsic bioattenuation processes within capped sediments may be reduced following capping (*260*). It is therefore expected that contaminated groundwater seeps will carry parent contaminants (i.e., subject to minimal bioattenuation processes) into an overlying cap where anaerobic, reducing biogeochemical processes are present; thus providing an opportunity for treatment with a bioreactive cap designed to perform reductive biotransformations.

Metabolic limitations on bioreactivity within *in situ* caps have not been previously addressed, however, and investigations are needed to identify if amendments are necessary to sustain an active microbial community performing reductive biotransformations (e.g., reductive dechlorination) within an overlying cap. Effluent from a sediment column/bed may have a different composition than sediment porewaters, and may not necessarily be successful at sustaining a dechlorinating community. The objective of this work was to maintain an actively dechlorinating microbial consortium within a sand column simulating an overlying cap and determine how amendments affected contaminant flux from the cap. Results allow for further development of bioreactive sediment caps performing reducing biotransformations and research into amendment delivery mechanisms.

7.3. Materials and Methods

7.3.1. Chemicals

PCE (99+%, Sigma-Aldrich, St. Louis, MO), TCE (99.5%, Sigma-Aldrich), *cis*-DCE (97%, Acros Organics, Morris Plains, NJ), *trans*-DCE (99.7%, Acros Organics),

and 1,1-DCE (99.9%, Acros Organics) were obtained in neat liquid form. Vinyl chloride (8%/ N_2 balance), ethene (99.5%), ethane (99.5%), and methane (99%) were obtained from Matheson Tri-gas (Parsippany, NJ). Sodium bicarbonate, potassium chloride, magnesium chloride, and calcium chloride were used in the preparation of simulated groundwater and were purchased from Fisher Scientific. Sodium lactate syrup (60% vol/vol, Fisher Scientific) was used during the preparation of stock lactate solutions. Potassium bromide, calcium sulfate, and potassium phosphate were purchased from Fisher Scientific and used for IC standards and tracer studies.

7.3.2. Batch Reactors

Batch reactors were established in triplicate consisting of sediment effluent, dissolved-phase PCE, and a mixed, PCE to ethene dechlorinating consortium to confirm that a microbial culture could successfully dechlorinate PCE completely to ethene when provided only sediment effluent. The recently characterized PCE-to-ethene dechlorinating mixed consortia referred to as OW (*327*) served as the inoculum. The OW culture was originally enriched from contaminated groundwater site in Texas and is maintained in a large bioreactor and provided PCE, reduced mineral media, and methanol daily (*327*). The OW consortia is capable of complete PCE dechlorination to ethene via reductive dechlorination and has been found to contain multiple dechlorinating microorganisms, including *Dehalococcoides* species and known reductive dehalogenases.

Three 25 mL aliqouts of OW culture were collected in 70 mL serum bottles that were pre-capped with teflon-faced butyl septa and sparged with nitrogen for 15 minutes to remove oxygen. The OW aliquots were then sparged with nitrogen for 15 minutes to remove residual chloroethenes and methanol from the batch reactors. Sediment effluent

was collected from an upflow sediment column supplied only with simulated groundwater and dissolved-phase PCE (*260*). The composition of the simulated groundwater was slightly modified from that described by Dries et al. (*326*) and consisted of 3.5 mM $NaHCO_3$, 0.1 mM KCl, 0.25 mM $MgCl_2$, and 0.75 mM $CaCl_2$. No chloroethenes were detected in the sediment effluent during time of collection (i.e., prior to 45 pore volumes in (*260*)). Sediment effluent was collected anoxically and 25 mL was directly added to the OW aliquots in the batch reactors. Dissolved-phase PCE was obtained from a saturated stock solution of neat PCE (i.e., NAPL present) in anaerobic, sterile simulated groundwater. Stock PCE concentrations were checked immediately prior to injection into the batch reactors. Reactor mass difference was recorded following injection to determine the mass of PCE loaded. Approximately 16 μmoles of dissolved-phase PCE was added to each microcosm with a 10 μL Hamilton glass syringe. All reactors were wrapped in foil and incubated at 20º C on an orbital shaker at 150 rpm. Chlorinated ethenes, ethene, ethane, and methane concentrations were determined from headspace samples of the microcosms.

7.3.3. Sand Column Operation

Two 1-D upflow sand columns (designated herein as Sand Column A and Sand Column B) were constructed using 2.5 cm I.D. glass chromatography columns 30 cm in length (Spectrum Chromatography, Houston, TX) with custom-built stainless steel end plates (Dutton & Hall, Atlanta, GA). A 2.5 cm diameter disc of stainless steel 80 mesh (Small Parts, Inc., Miami Lakes, FL) was placed within the column end plates to help distribute flow and to prevent loss of sand particles from the column. Stainless steel was used for all fittings and tubing. A glass reservoir (15 mL) fitted with a stopcock was

fabricated and placed at the column effluent to allow for aqueous effluent sampling. The columns were packed with ASTM C-33 grade concrete sand obtained from U.S. Silica (Mauricetown, NJ). The sand grade was selected due to its employment as a traditional cap in the Anacostia River Capping Demonstration Project performed by the Hazardous Substance Research Center – South and Southwest (*356*). The sand has a heterogeneous particle size distribution ranging from 0.15 to 4.75 mm in diameter and is composed mostly of medium to large sized particles and pebbles. The sand was used as received with the exception of autoclaving prior to application. An elemental analysis of the sand was performed at the University of Georgia Laboratory for Environmental Analysis (Table 7.1). The dry, autoclaved sand was packed into both columns under aerobic conditions and mixed every 5-cm of packing by vibration along the wall of the column. Downward pressure was applied to the top of the sand during mixing to prevent preferential settling of larger particles toward the outer region of the columns. Following column packing, nitrogen gas was flushed through the columns for 15 minutes to remove oxygen, followed by carbon dioxide gas for 15 minutes to displace the nitrogen and allow for complete dissolution of the gas phase within the columns. Three pore volumes of sparged, autoclaved simulated groundwater were then passed through the columns to check for leakage and to ensure anaerobic conditions. The columns were then inoculated with the OW via upflow flushing of the columns (see details provided in following sections).

Table 7.1. Elemental analysis of C-33 sand utilized as the capping material. A 5 g sample of sand was refluxed with 10mL HNO_3, followed with 5 mL H_2O_2, then taken up to 100 mL. All analysis was performed at the University of Georgia Laboratory for Environmental Analysis.

Element	Concentration (ppm)
Na	25.08
Mg	4.16
Al	134.2
K	6.64
Ca	5.43
Si	5050
Mn	0.95
Fe	490
S	0.15 [a]
Total C	< 0.02 [a]
Inorganic C	< 0.02 [a]
Total N	< 0.02 [a]
Sand	98.5 [a]
Silt	< 0.5 [a]
Clay	2.0 [a]

[a] reported as percent

Following inoculation, both sand columns were wrapped in foil to avoid exposure to light then connected in series with an upflow column packed with Anacostia River sediment (*260*). A schematic of the laboratory set-up is shown in Figure 7.1. The sediment column effluent served as the influent for the sand columns. The sediment column was provided only simulated groundwater and dissolved-phase PCE. The influent of the sand columns therefore consisted of sediment effluent and a mixture of partial PCE-dechlorination products. Table 7.1 provides a summary of experimental conditions for each sand column, with details for each column provided in the following sections.

7.3.3.1. Sand Column A. Prior to inoculating the Sand Column A, a tracer test was conducted with 100 $mg \cdot L^{-1}$ (1.25 mM) bromide obtained from an autoclaved, sparged stock solution of potassium bromide in simulated groundwater. A total of 1.2 pore volumes were flushed through the column, collected with a fraction collector, and analyzed via ion chromatography. Three pore volumes of simulated groundwater were flushed through the column following the tracer test to remove residual bromide prior to inoculation. A 200 mL aliquot of aqueous OW culture was obtained for inoculation and stored in a 160 mL serum bottle that had previously been capped with a teflon-faced butyl septum and sparged with nitrogen for 15 minutes to remove oxygen. The 200 mL aliquot was tested for its dechlorination ability in batch conditions by spiking with PCE and methanol. After successfully dechlorinating PCE to ethene, 1.5 pore volumes were fed to the column at a flow rate of 2.2 $mL \cdot hr^{-1}$ (1-day residence time). Following a 24-hour attachment period during which there was no flow, Sand Column A was emplaced

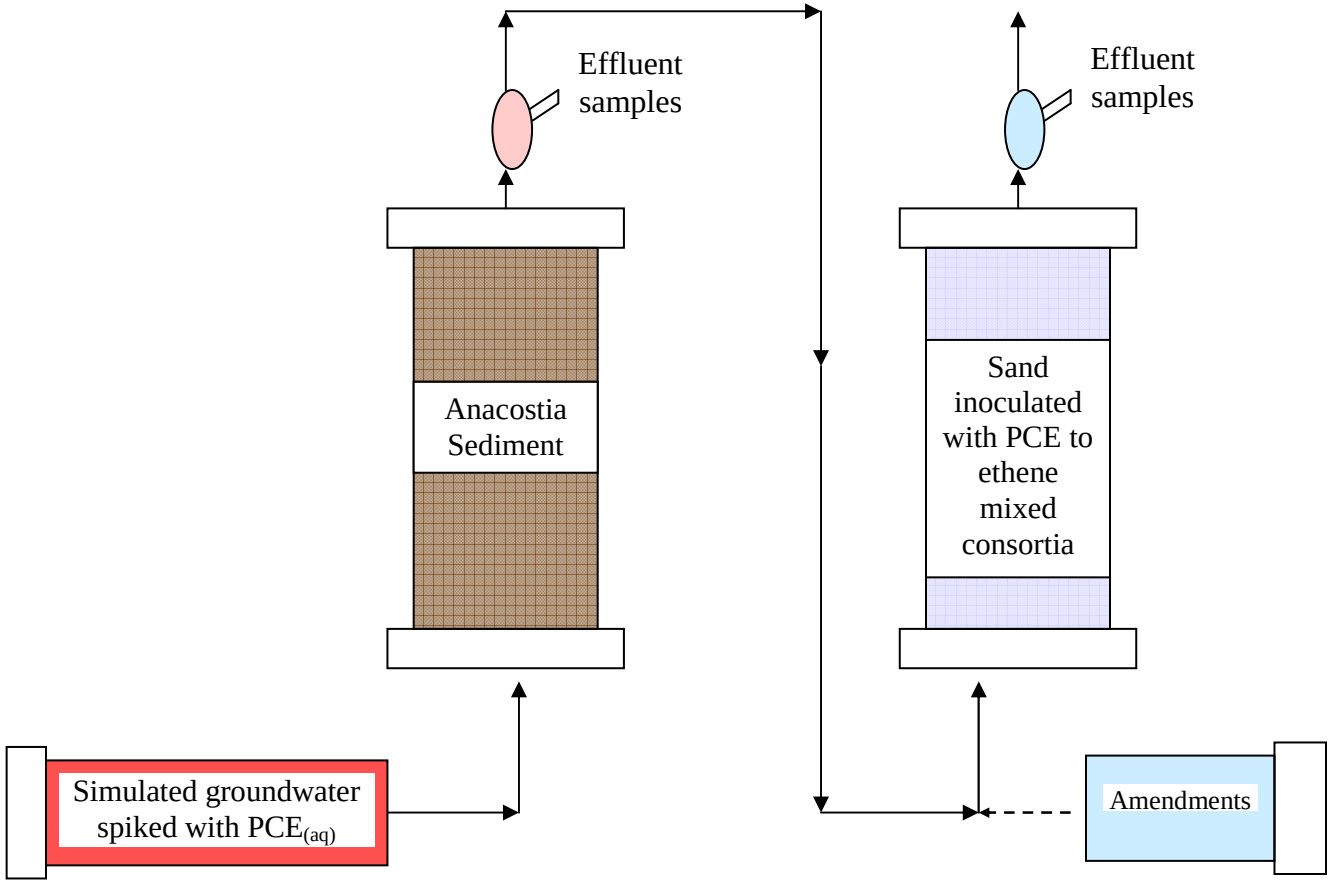

Figure 7.1. Schematic of laboratory simulation of a bioreactive sand cap placed in series with an anaerobic sediment bed subject to a PCE contaminated groundwater seep. *cis*-DCE was added to the influent from 0 to 3.4 pore volumes. Lactate was added to the influent of Sand Column B from 0 to 13.3 pore volumes.

in series with the sediment column from 67 to 83 sediment pore volumes (*260*). The unamended sediment column effluent served as the influent for the duration of the Sand Column A experiment. The effluent product distribution from Sand Column A therefore reflects the capacity of sediment effluent to maintain an external dechlorinating community, in this case simulating a bioreactive cap inoculated with a mixed dechlorinating consortia and operating under reducing conditions.

7.3.3.2. Sand Column B. The Sand Column B experiment was also designed to simulate a dechlorinating bioreactive cap operating under reducing conditions, but influent for this experiment was spiked with amendments. A tracer test was not initially performed on this column, but it was packed identically to Sand Column A. An aliquot of OW culture was retrieved and sparged with nitrogen prior to inoculation as described above for Sand Column A. The aliquot of OW culture again demonstrated the ability to completely dechlorinate PCE to ethene in batch culture. A total of 1.7 pore volumes of OW culture were then supplied to the column at a flow rate of 2.6 $mL \cdot hr^{-1}$ (1-day residence time). Sand Column B was not immediately connected to the sediment column effluent in order to perform positive-control experiments to ensure the inoculated column could completely dechlorinate *cis*-DCE to ethene when provided DCB-1 media, Wolin vitamins, and 5 mM lactate as an electron donor and carbon source. Following this demonstration of complete dechlorination, one pore volume of anaerobic simulated groundwater was flushed through the column to remove these constituents from the system prior to the introduction of sediment effluent. Sediment column effluent was obtained from 146 to 180 sediment pore volumes (*260*) to serve as Sand Column B influent.

For Sand Column B, sediment column effluent was captured anoxically by connecting an empty, gas-tight syringe to sediment effluent tubing and allowing the aqueous flow to gradually fill the syringe at the same rate of sediment column influent (5.5 $mL \cdot hr^{-1}$; (*260*)). Once the effluent syringe had been filled, it was transferred to a separate syringe pump and introduced into the sand column as the influent. This method allowed for manipulation of flow rates within the sand column and for addition of electron donor and acceptor to the influent prior to connection with the sand column. The electron donor used for this study was lactate, which was obtained from a 100 mM stock solution in autoclaved, sparged simulated groundwater. Lactate was supplied to the influent at a concentration of 5 mM from 0 to 13.3 sand pore volumes. Aqueous *cis*-DCE was briefly added to the influent as an electron acceptor and was obtained from a saturated stock solution of *cis*-DCE (i.e., NAPL present) in autoclaved, sparged simulated groundwater and supplied to the influent at a concentration of 200 ± 42 μM from 0 to 3.4 sand pore volumes.

The experimental conditions of Sand Column B were designed to gradually decrease aqueous residence times as well as electron donor concentrations to determine limitations on dechlorination. The experimental conditions are summarized in Table 7.2, and Figure 7.4A displays flow rates and lactate concentrations corresponding to effluent results. The influent flow rate for Sand Column B was increased step-wise from 1.3 $mL \cdot hr^{-1}$ (2-day retention time), to 2.6 $mL \cdot hr^{-1}$ (1-day retention time) to 5.5 $mL \cdot hr^{-1}$ (0.47-day retention time). The flow rate of 5.5 $mL \cdot hr^{-1}$ corresponds to the flow rate exiting the sediment column (*260*). From 0 to 3.4 sand pore volumes, additional *cis*-DCE was provided to the influent to ensure chlorinated ethenes were present due to complete

dechlorination of PCE to ethene in the sediment column effluent prior to connecting Sand Column B). After 3.4 pore volumes, however, the only source of chloroethenes was sediment effluent. Lactate was provided from 0 to 13.3 pore volumes, at which point it was removed from the influent. The effluent product distribution from Sand Column B should reflect the impact of flow rate and the presence of reducing equivalents on the capacity of the sediment column effluent to maintain an external dechlorinating community.

7.3.4. Analytical Methods

PCE, TCE, DCE isomers**,** VC, ethene, ethane, and methane concentrations were determined from the headspace of 5 mL aqueous effluent samples into and analyzed on a GC equipped with an FID, as described previously (*122*). Bromide was measured using a Dionex DX-100 ion chromatograph with a Dionex AG4A IonPac guard column and Dionex AS4A IonPac column at a flow rate of 1.5 mL/min and an ED40 electrochemical detector.

7.4. Results and Discussion

The results of the elemental analysis (Table 7.1) indicate that most of the particles within the C-33 concrete grade sand were classified as sand-sized particles, with approximately 2 percent classified as clay-sized particles. Silicon, iron, and aluminum had the greatest elemental concentrations. Carbon and nitrogen were not detected to any significant amount (< 0.02 %).

7.4.1. Batch Reactors

The OW culture successfully dechlorinated PCE to ethene when provided only sediment effluent and dissolved-phase PCE (Figure 7.2). Complete PCE dechlorination

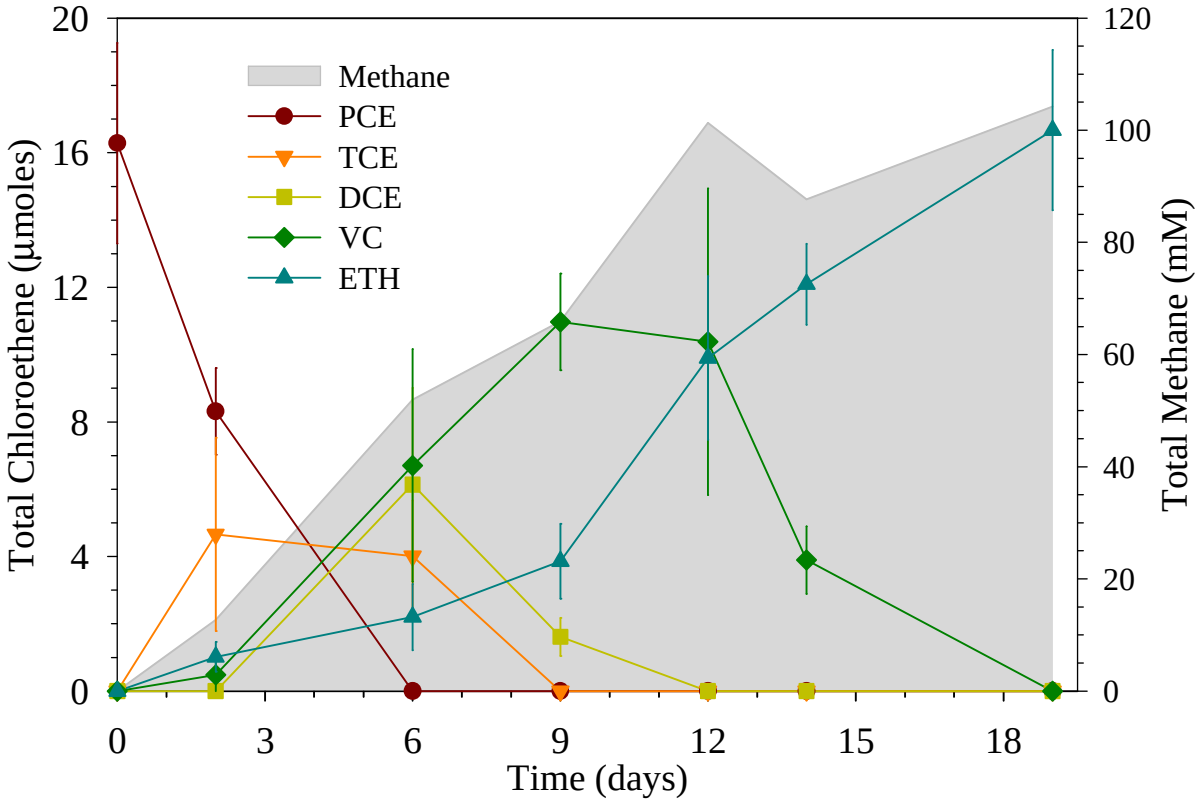

Figure 7.2. Batch microcosm results of OW culture provided only PCE and sediment effluent. Chloroethenes are reported as the sum of aqueous and gas phases within the microcosms. Error bars represent one standard deviation calculated from triplicate reactors. The shaded background area corresponds to methane production (mM) at each time point and is referenced to the right vertical axis. Total methane is calculated as the sum of aqueous and gas phase methane.

to ethene was achieved at 19 days of incubation. Chloroethene mass balance was acceptable (i.e., within 10%) for each time point except day 12, when chloroethene mole totals were 124% of the initial PCE introduced. This discrepancy arose because one of the triplicate reactors recorded unusually high concentrations of VC, despite typical ethene concentrations. This is reflected in the relatively high standard deviation of VC at day 12. Duplicate GC-FID analysis yielded similar results. This anomaly was not observed at any other time-point during the experiment. The results suggest dechlorinating species within OW, specifically *Dehalococcoides*, were able to remain active for at least one dechlorination cycle when provided only sediment effluent and dissolved phase electron acceptor. The sources of carbon, electron donor, and micronutrients presumably were provided by the sediment effluent.

Methane concentrations rose steadily during the dechlorination of PCE (Figure 7.2), indicating that methanogenic populations were also able to remain active when provided only sediment effluent. This suggests that dechlorinating species within a bioreactive cap inoculated with a methanogenic mixed consortia may have to compete with methanogens for electron donors, which may decrease dechlorination efficiency with time.

7.4.2. Sand Column A.

The void volume for Sand Column A was estimated to be 62.7 mL from differences between wet and dry column mass and assuming complete water saturation. The tracer test at the onset of Sand Column A operation resulted in a symmetrical break through curve, estimated to have a Peclet number of approximately 81 using CFITM3

Table 7.2. Summary of experimental conditions for sand column experiments.

Parameter	Sand Column A	Sand Column B
Void Volume[a] (mL)	62.72	61.82
Porosity[a] (cm^3 void·(cm^3 total)$^{-1}$)	0.413	0.407
Connected In Series to Sediment Column (sediment pore volumes)	67.02 to 83.21	145.96 to 180.00
Experimental Flow Rate(s) ($mL \cdot hr^{-1}$)	5.4642	1.2879; 2.5758; 5.4642
Seepage Velocity ($cm \cdot day^{-1}$) (Darcy Velocity ($cm \cdot day^{-1}$))	62.67 (25.88)	14.99; 29.98; 63.59 (6.10); (12.20); (25.88)
Peclet Number[b] (dimensionless)	80.48	*N/A*
Alterations to Influent	None	Addition of Lactate Addition of *cis*-DCE Decrease of Flow Rate
Influent Chloroethene Concentration (μM total chloroethenes)	16.19 ± 11.06[c]	0 to 3.44 pv: 200 ± 42[c] 3.44 pv to end : 34 ± 3.6[c]

[a] Estimated from mass difference between dry and wet packed columns.
[b] Obtained with the CFITM3 break through curve fitting program under equilibrium constraints. [c] Average ± one standard deviation.

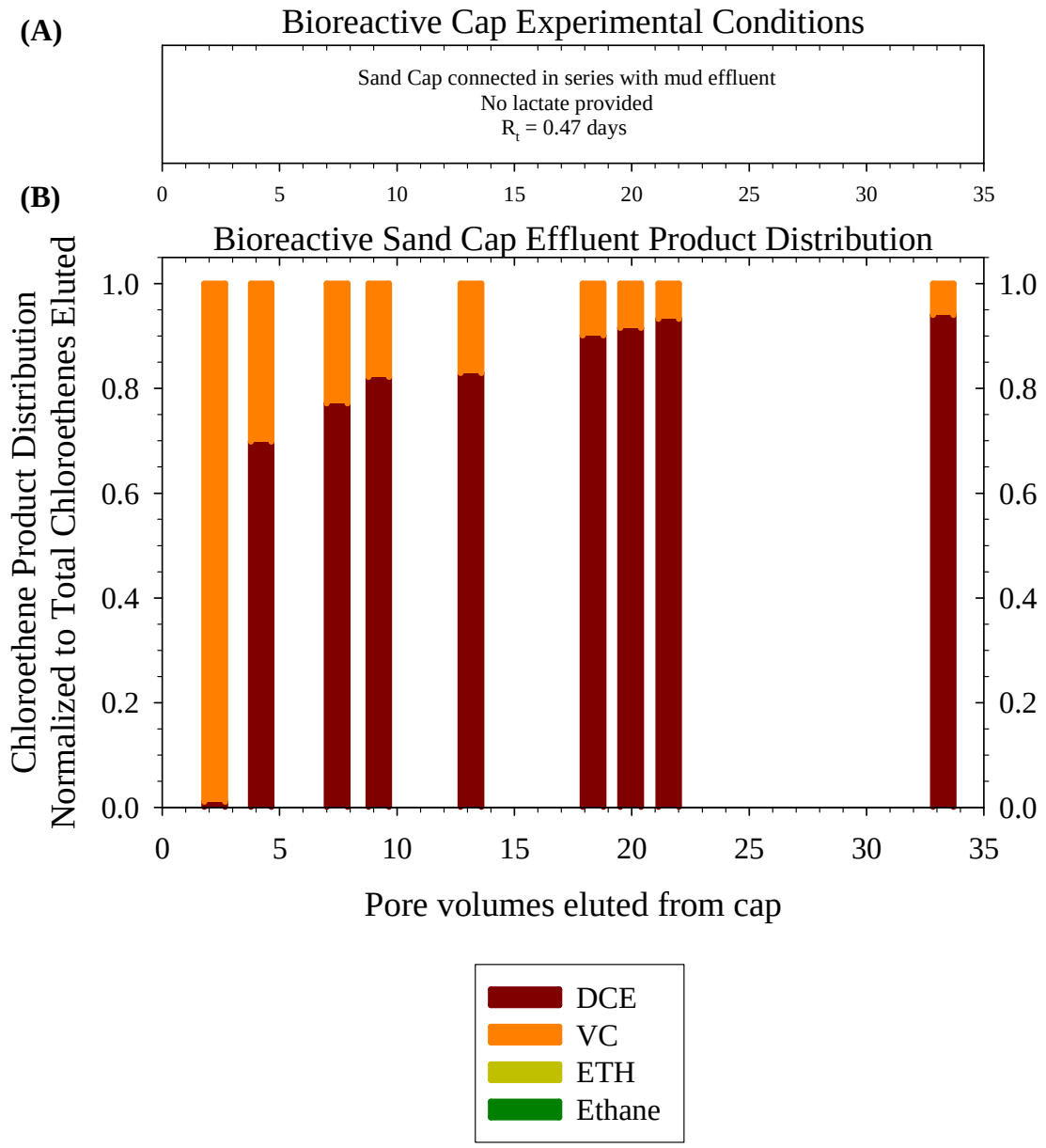

Figures 7.3A-B. (A) Operating conditions for Sand Column A. The effluent of the sediment column served as the influent of the sand column and was not amended with exogenous electron donors, electron acceptors, carbon sources, minerals, nor vitamins. (B) Effluent product distribution of Sand Column A inoculated with a PCE to ethene dechlorinating mixed consortia and connected in series with sediment column effluent between 68 and 83 sediment pore volumes.

software. This Peclet number is relatively low for a sand column, possibly reflecting the heterogeneous size distribution, and indicates solute dispersion within the column may be an important process. The normalized chloroethene effluent product distribution of Sand Column A is shown in Figure 7.3B. The 5.5 $mL \cdot hr^{-1}$ flow rate of the column corresponded to a residence time of 0.47 days. When Sand Column A was connected in series to the sediment column, *cis*-DCE was the predominant product in the sediment effluent (*260*), and thus was the predominant chloroethene in the sand column influent. The sand column was initially able to dechlorinate *cis*-DCE to VC, but ethene was not detected (Figure 7.3B). This reactivity quickly disappeared prior to 5 pore volumes, and eventually only 5% of the *cis*-DCE was being dechlorinated to VC, indicating that *Dehalococcoides* activity was impaired. Methane data collected during Sand Column A reveal that microbes other than dechlorinators also lost activity, suggesting a limitation in the system as a whole and not just for the dechlorinators (data not shown).

Based on data presented in Figure 7.3B, it appears as though sediment column effluent could not sustain a dechlorinating culture without additional amendments. Previous research (*260*) demonstrated that microbial activity in the sediment column was limited by electron donor availability. It was hypothesized that a lack of electron donor eluting from the sediment column effluent prevented the dechlorinating community in the sand cap from being fully active. Another possibility was that the high flow rates through the sand column precluded complete dechlorination by not allowing sufficient contact time between the contaminants and the dechlorinating community. These hypotheses were addressed during Sand Column B operation.

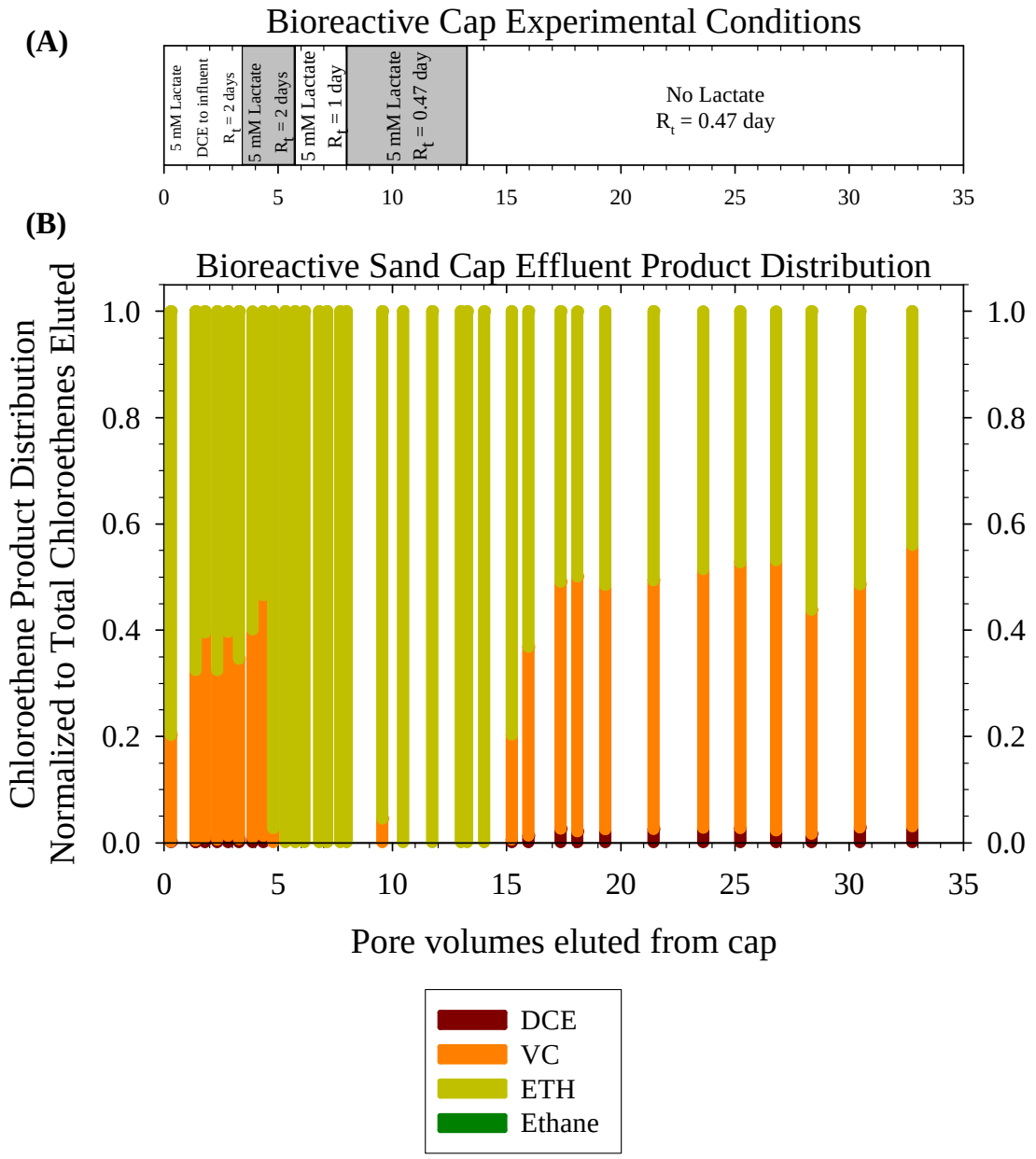

Figures 7.4A-B. (A) Operating conditions for Sand Column B. The effluent of the sediment column served as the influent of the sand column and was not amended with minerals nor vitamins. Exogenous electron donor (lactate), carbon sources (lactate), and electron acceptor (*cis*-DCE) were added where indicated. (B) Effluent product distribution of Sand Column B inoculated with a PCE to ethene mixed dechlorinating consortia and connected in series with sediment column effluent between 146 and 185 sediment pore volumes.

7.4.3. Sand Column B.

The experimental conditions associated with Sand Column B are presented in Figure 7.4A, with the normalized chloroethene product distribution displayed by Figure 7.4B. The void volume for Sand Column B was estimated to be 61.8 mL from differences between wet and dry column mass and assuming complete water saturation. Prior to feeding with sediment effluent, the inoculated column completely dechlorinated *cis*-DCE to ethene when provided electron donor, carbon sources, vitamins, and reduced media; confirming the ability of the OW culture to achieve complete dechlorination within the column (data not shown). After one pore volume of simulated groundwater, sediment effluent was supplied to Sand Column B beginning at pore volume 0 as shown in Figures 7.4A-B. The influent for Sand Column B was the sediment effluent from 146 to 180 sediment pore volumes and consisted of a mixture of *cis*-DCE, VC, and ethene (*260*). The influent of Sand Column B was initially augmented with *cis*-DCE and lactate while operating under a residence time of 2 days. Incomplete dechlorination was observed during this period, with a mix of VC and ethene in the sand column effluent. From 3.4 to 5.7 sand pore volumes, only lactate was provided to the influent (i.e., no *cis*-DCE was added) with the sediment effluent serving as the sole source of chloroethenes. The sand column successfully achieved complete dechlorination to ethene during this period, demonstrating that with lactate addition the sand cap could detoxify the flux of chloroethenes exiting the sediment column. This result, coupled with the lack of complete dechlorination during the previous condition (0 to 3.4 sand pore volumes) when additional *cis*-DCE was provided to the influent, suggests that chloroethene concentrations entering the sand column can limit the extent of dechlorination.

Therefore, measures may be needed to either increase microbial biomass or reduce contaminant flux within the cap in order for the dechlorinating caps to successfully detoxify chloroethenes.

Results from Sand Column B also indicate that electron donor concentrations within the cap can impact dechlorination activity. Complete dechlorination was observed between 8.0 and 13.3 pore volumes when lactate was provided to the sand column, despite relatively fast flow rates (0.47 residence time). When lactate was removed from the influent at 13.3 pore volumes, however, a mixture of chloroethenes was observed in the effluent, indicating the importance of supplying external reducing equivalents to the sand column. The supply of external electron donor is a common technique to stimulate and enhance reductive dechlorination in groundwater aquifers (*159, 234, 357, 358*) and may be necessary for bioreactive caps.

The results from the batch study and the two sand columns suggest that sediment effluent alone cannot achieve complete dechlorination in a bioreactive cap at the residence times examined. The batch results showed complete dechlorination occurred after 19 days when the OW consortium was provided only sediment effluent, certainly too long for the 2 day retention times utilized for the column studies. A bioreactive cap supplied sediment effluent exclusively may be successful only at sites with stagnant or minimal groundwater seep rates. Electron donor may be required at alternative sites with greater seepage rates (i.e., lower contaminant residence times) to stimulate and enhance microbial activity. This is consistent with data from Chapter 4 investigating the microbial colonization of an overlying sand cap. Bacterial diversity was lowest in the cap just a few centimeters above the sediment-cap interface, suggesting the community

was stressed in that location. A lack of suitable electron donors may limit bacterial community health and function. Therefore, a successful reducing bioreactive *in situ* cap for the treatment of groundwater and sediment contaminants appears to require the incorporation of electron donor to maintain the dechlorinating community. Further research is required to investigate the best means of electron donor delivery and deployment in the sedimentary environment. This knowledge is significant for the continued design and development of biologically active sediment caps.

CHAPTER 8.
CONCLUSIONS

This work has attempted to address unknown issues related to the *in situ* capping of contaminated sediments. The specific objectives of this work were: (1) to understand how capping impacts biogeochemical processes at the sediment-water interface, (2) to determine the ability and degree to which microorganisms indigenous to sediment colonize an overlying cap, (3) to assess the effects of flow direction on redox conditions within an emplaced cap, (4) to determine how *in situ* capping impacts natural bioattenuation processes occurring within the underlying sediment, and (5) to identify limitations on microbial activity within bioreactive *in situ* caps. Specific conclusions and findings are listed under each specific objective according to their merit, with the most definitive conclusions first and the more tentative conclusions last. A one-paragraph summary of overall conclusions is provided at the end of this chapter.

8.1. Biogeochemical Processes

- Capping of Anacostia sediments with clean sand induced an upward, vertical shift of reduced geochemical species from the sediment into the overlying cap (additionally supported by flow direction studies).
    - The previously oxic sediment-cap interface become anaerobic.
    - Oxygen penetration into the cap was limited by the presence of reduced, dissolved chemical species and did not extend past a few centimeters.

    - Reduced, dissolved phase geochemical species migrated from the sediment into the overlying cap porewaters.
- Existing redox stratification was conserved during the upward biogeochemical shift.
- Upflow conditions compressed stratified redox zones toward the cap-water interface.
    - Terminal electron accepting processes associated with more anaerobic conditions (i.e., iron reduction, sulfate reduction) extended upward into the emplaced cap from the sediment.
    - The formation of iron sulfides occurred within the cap.
- Manganese oxide reduction occurred to a greater extent in the cap material compared to the underlying sediment.
- Iron reduction was the predominant terminal electron accepting process within the capped sediment column, originating from the Anacostia River sediment.
- Anaerobic microbial populations shifted into the overlying cap (confirmed by microbial colonization studies).

8.2. Microbial Colonization

- Microorganisms indigenous to sediments colonized an overlying sand-based cap in spatially distinct communities.
- Anaerobic microbial populations migrated from sediment into the cap.
    - Microbes capable of iron reduction, sulfate reduction, and methanogenesis were present in the overlying cap and originated from the native sediment.

    - Microorganisms performing anaerobic respiratory process also remained active in the underlying the sediment.
- The spatial distributions of microbial populations associated with terminal electron accepting processes (e.g., iron-reducing bacteria, sulfate-reducing prokaryotes, methanogens) were consistent with porewater geochemical concentrations.
- Microorganisms capable of contaminant biotransformation (*Anaeromyxobacter* spp., *Geobacter* spp., and *Shewanella* spp.) inhabited the emplaced cap.
- Bacterial numbers were be greatest in the aerobic portion of the cap and within the sediment; Archaeal numbers were greatest within the anaerobic sediment
    - Regions of the cap that possessed the greatest bacterial numbers also had the greatest bacterial richness and diversity.
    - The greatest abundance of methanogenic organisms occurred in the underlying, anaerobic sediment.
- Microbial colonization of a cap by bacteria capable of contaminant biotransformation may provided *in situ* capping with an intrinsic, secondary level of contaminant management to complement physical containment approaches.

8.3. Flow Direction and Redox Conditions

- Advective flow direction strongly contributed to redox conditions and biogeochemical processes within a sand-based sediment cap overlying Satilla River sediment.

- Under static flow conditions, anaerobic redox environments developed within the bulk of the overlying cap.
    - Oxygen was limited to the top few centimeters of the cap.
    - Reduced geochemical species migrated from the underlying sediment into the overlying cap.
- When upflow conditions were present, anaerobic redox environments required less time to develop within the overlying cap compared to static conditions.
- When oxic, overlying water flowed vertically downward through the cap, the entire thickness of the cap become oxic.
    - After cap emplacement, the cap was initially subject to anaerobic conditions, but oxic conditions developed with time within the cap under steady-state downward flow.
    - Dissolved oxygen concentrations approached zero below the sediment-cap interface.
    - The sediment-cap interface initially become anaerobic, then returned to aerobic conditions.

- Relocation of tube-building benthic macrofauna from the underlying sediment to the cap-water interface was restricted.

8.4. Natural Attenuation Processes within Capped Sediments

- Microbial activity decreased with time within a capped sediment due to electron donor limitations arising from prevention of deposition of labile organic matter.

    - Contaminant biotransformations decreased within capped sediments.
    - Reductions in natural bioattenuation processes occurred within capped sediments.
    - Methanogenic activity decreased with time.
- Chlorinated ethenes (e.g. PCE, TCE) present in groundwater seepage may travel through sediment to discharge into overlying caps.
    - Sorption of chlorinated ethenes onto organic matter initially retarded contaminant breakthrough into the cap.
    - Recalcitrant parent contaminants (e.g., PCE, TCE) eventually was present in sediment effluent due to reduced microbial activity.
- Addition of fermentable substrates as electron donor stimulated the microbial activity of indigenous organisms within sediments.
    - Dechlorination activity by native dechlorinating organisms increased during biostimulation to achieve complete dechlorination of PCE to ethene, since proper organisms are present (e.g., *Dehalococcoides* strains).
    - Chloride concentrations increased corresponding to increases in dechlorination activity.
    - Methane and hydrogen production increased within Anacostia sediment following biostimulation with fermentable substrates.
- Stimulation of contaminant biotransformations induced biologically-enhanced desorption, leading to a short-term release of chloroethenes.
- Solute transport was influenced by physical non-equilibrium conditions, arising from biogenic gas production and immobile porewater.

- Increased flow rates associated with capping can contribute to the loss of contaminant bioattenuation.
- Microbial iron reduction decreases with time within capped sediments.
- The fraction of recalcitrant organic matter within the sediment column appeared to increase with time, evidenced by reductions in microbial activity.

8.5. Development of a Bioreactive Cap

- In the presence of sediment effluent and dissolved-phase PCE in batch culture, a PCE-to-ethene mixed consortium achieved complete dechlorination to ethene.
- To sustain the dechlorinating activity of a mixed PCE-to-ethene dechlorinating consortium within a bioreactive cap, sediment effluent required amendment with fermentable substrates under advective flow conditions.
    - Biostimulation with electron donor was required to achieve complete dechlorination of chlorinated ethenes eluting from a sediment bed.
    - Sediment porewater eluting into an overlying cap lacked suitable electron donors for microbial utilization.
- Contaminant mass flux into a bioreactive appeared to limit the success of a bioreactive cap.

8.6. Summary

In summary, this work demonstrates that a sand-based *in situ* cap placed over contaminated sediment can become anaerobic under static and upflow conditions, with redox stratification generally conserved. Microorganisms indigenous to the sediment are

capable of colonizing the overlying cap and contribute to the biogeochemical stratification. When downward flow of oxic surface water occurs through a cap, such as tidally-induced recharge, oxic conditions can develop throughout the cap. At sites with contaminated groundwater seeps, it is expected that capping will lead to a reduction in bioattenuation processes within the sediment, stemming from the elimination of labile organic matter deposition to sedimentary microorganisms. Thus, parent contaminants subject to minimal biotransformations within the sediment are likely to enter a reducing cap. A bioreactive cap, with active microorganisms capable of reductive biotransformations placed within the capping material, may require amendments of electron donor to the sediment effluent to achieve success under flow conditions.

CHAPTER 9.
ENGINEERING SIGNIFICANCE

This work provides information useful for practitioners considering emplacing an *in situ* sediment cap as a remedial solution for contaminated sediments. The introduction of an engineered environment at the sediment-water interface can perturb the surrounding natural environment in multiple ways which should be considered during remedial design. At contaminated sediment sites with static or upflow conditions, a sand-based cap will be largely anaerobic with stratified redox zones shifting from the sediment into the overlying cap. At sites subject to downflow of oxygenated surface waters, oxic redox conditions will develop throughout the thickness of the cap. Microorganisms indigenous to the sediment are expected to shift into the cap under upflow and static conditions and contribute to biogeochemical stratification. A sand-based sediment cap naturally colonized by microorganisms capable of contaminant biotransformation may provide a secondary level of treatment to complement physical isolation. Biogenic gas production by methanogenic populations, demonstrated to be present within a cap but more abundant in the underlying sediment, may create cap instability and facilitate gas-phase transport of volatile contaminants. Research indicates a marked decline in microbial activity in capped sediment with time, however, due to electron donor limitations. Reductions of contaminant bioattenuation mechanisms within capped sediment are therefore expected, leading to the discharge of parent contaminants into caps at locations subject to groundwater seepage. The development of a bioreactive cap for placement at the sediment-water interface will likely require electron donor amendments to sustain microbial activity and contaminant biotransformation.

CHAPTER 10.
FUTURE RESEARCH RECOMMENDATIONS

Recommendations for future research directions are presented here regarding biogeochemical and contaminant biotransformation processes following *in situ* capping. These recommendations identify opportunities to build upon conclusions drawn from completed studies, and also identify research areas that were not able to be addressed in this thesis. Recommendations for future research are in the areas of (1) biogeochemical conditions in caps subject to mixing, (2) biogeochemical processes within marine sediments subject to seasonal temperature fluctuations, (3) microbial populations associated with metal reduction along a redox gradient, (4) fate of contaminants within a sand-based cap, (5) redox conditions within physicochemical-based active caps, and (6) continued bioreactive capping development.

10.1. Biogeochemistry of Caps Subject to Mixing Processes

Oxygen penetration into sediment caps may be influenced by bioturbation activities and by cross-flow and hyporheic flow paths at the cap-water interface in high-energy environments. Bioturbation can effectively mix cap porewaters with overlying water and introduce solutes from surface water (e.g., dissolved oxygen) deeper into the cap. An example of how tubular burrows can impact the sediment-water interface and dissolved oxygen depth profiles was provided in Figure 2.4. Bioturbation can also disrupt redox gradients and microbial populations along those gradients. Koretsky et al. (*172*) attributed a lack of segregation among microbial populations, despite observed geochemical gradients, to the effects of bioturbation by macrofauna. Characterizing the

effect of bioturbating organisms on biogeochemical processes would provide environmentally-relevant information at sites with significant benthic activity. Bioturbation was not observed in completed studies presented in this work, however. The flow of oxic water across the top of the cap may also increase oxygen penetration depth. Although caps are generally not deployed in high-energy settings, transient instances of cross-flow (e.g., storms, boating activity) may induce hyporheic flow paths at the cap-water interface. Similar to bioturbation, this is a mechanism to overcome diffusion-limited conditions and provide oxic surface water deeper into the cap. Increased microbial activity has been correlated to hyporheic flow paths (*283*), potentially leading to the disruption of biogeochemical gradients. Determining the effects of bioturbation and cross-flow on oxygen penetration and redox gradients should improve predictions of contaminant transport within caps at various environmental settings.

10.2. Biogeochemical Processes in Marine Sediments

Biogeochemical studies documented within this thesis have largely focused on freshwater sediments from the Anacostia River, with less extensive work presented on the biogeochemical processes within marine sediments from the Satilla River. Sulfate-reducing conditions are expected to be more prevalent in microbially-active marine sediments compared to freshwater systems because of the input of oceanic saltwater. The profiles of freshwater caps presented here were dominated by reduced iron, with minimal levels of sulfide present. This trend may be reversed in marine sediments, however, and could have implications for microbial speciation, contaminant transformations, and metal

mobility within the cap and underlying sediment. Many contaminated sediment sites are located in coastal estuarine settings, and knowledge of contaminant transport processes within a cap placed in marine environments is required for remedial design and active capping development. It is also possible that seasonal fluctuations in temperatures could effect sediment and cap biogeochemistry. Increased microbial activity in warmer seasons can impact porewater redox profiles and contaminant transport (*170*). Investigations are also suggested to examine how the lack of microbial activity in colder seasons impacts cap biogeochemistry and contaminant transport. This knowledge could be used to predict if/when greater contaminant fluxes through the cap occur, which could in turn be incorporated into remedial cap design.

10.3. Metal-Reducing Populations along Redox Gradients

Opportunities exist to gain insight on how microbes sense, adapt, and respond to perturbations to their surrounding environment, such as the placement of an *in situ* cap. For example, interesting spatial patterns were observed for dissimilatory metal- and iron-reducing bacterial populations in Chapter 4, specifically among *Anaeromyxobacter*, *Geobacteracea*, and *Shewanellae*. *Geobacter* spp. consistently were the most abundant metal-reducer among the three populations quantified. Reasons for this remain unclear, but possibilities include the ability of *Geobacter* spp. to use more diverse carbon and energy sources, and fundamental differences in iron metabolism compared to its competitors (*55*). Another possibility is that *Anaeromyxobacter* spp. are characterized by gliding motility whereas *Geobacter* spp. possess flagellar motility, thereby allowing *Geobacter* organisms to rapidly move, colonize, and populate the new cap environment.

However, the populations of *Anaeromyxobacter* spp. and *Shewanella* spp. were relatively high in the top cap layer, where oxygen was present. Confirmation that *Anaeromyxobacter* and *Shewanella* were indeed participating in aerobic metabolism could help explain how members of these genera were able to flourish in these regions. 16S rRNA clone libraries could also be used to identify the strains present at different locations of the redox gradient. Understanding fundamental reasons behind the population dynamics of metal-reducing bacteria could allow for selected stimulation of genera of interest, especially in regards to contaminant biotransformations.

10.4. Fate of Contaminants within a Cap

Research opportunities are available to couple biogeochemical measurements presented in this work with contaminant fate and transport within an *in situ* cap. Characterizations of redox zones and processes within a sand-based cap have been performed here with speculation on contaminant movement within those redox zones. It is recommended that the fate of contaminants within redox-stratified caps be examined and confirmed. Research addressing metal mobility following sediment capping is especially needed. Metals are one of the most prevalent sediment contaminants and need to be considered during remedial design at many sites. Metal mobility is strongly dependent on redox conditions, however, and simultaneous monitoring of metals and redox zones via electrochemical techniques may provide interesting data that can be used to predict metal fate, and ultimately exposure to aquatic organisms. Monitoring redox zone stratification and organic contaminant transformations (e.g., PCBs) would also provide practical data for remedial design, but could also expand knowledge regarding redox requirements for anaerobic biotransformations. For example, geochemical

speciation and redox data observed with voltammetric microelectrodes could be overlaid with measures of reductive dechlorination activity by dehalorespiring microorganisms. This may improve our understanding of the conditions under which these organisms most effectively perform contaminant biotransformations.

10.5. Biogeochemistry of Active Caps

Recent interests in the field of sediment remediation have focused on the feasibility and development of active capping technology, which incorporates sorptive or reactive constituents into the capping material to sequester or destroy contaminants (a review is provided in Chapter 2, subsection 4.3.2.). Although sediment caps composed solely of sand are still being employed, the utilization of active caps is expected to become more common following successful pilot- and field-scale demonstrations (*158*). A lack of peer-reviewed literature is available regarding commercially available active capping materials, however. Active capping materials, such as reactive mats and clay-based products, may impact biogeochemical and contaminant attenuation processes differently than sand caps. The synthetic materials create a chemical and biological barrier within the cap, possibly preventing geochemical and microbial shifting observed in sand caps. Also, the physicochemical properties of some active cap constituents (e.g., activated carbon, Fe^0) can create distinct geochemical environments. Understanding the biogeochemical conditions within active caps can help ensure treatment success, especially for active caps dependent upon chemical transformations.

10.6. Continued Bioreactive Cap Development

Research described within this thesis indicates that a biologically-active cap capable of contaminant biotransformations is feasible, however certain engineering challenges will need to be met prior to scale-up. One key requirement for success appears to be the delivery of electron donor to the microbes in the bioreactive cap. Prior research is available regarding electron donor selection and delivery methods for groundwater remediation, but the addition of carbon and energy sources to sediments has not previously been addressed. At sites subject to groundwater seepage, passive-release technologies for electron donor delivery may be a promising approach, allowing advective flow to carry substrates into the microbially-active capping material. Under diffusive conditions the application of passive-release materials could also be effective, but measures to prevent uncontrolled microbial growth and biofouling may need to be implemented. The emplacement of microbial species into an overlying cap (i.e., bioaugmentation) can also provide technical challenges. The optimal method would allow precise microbial culture emplacement while maintaining cell viability. This may be especially difficult if anaerobic microbial populations are being utilized. Geochemical indicators of microbial activity, coupled with the use of molecular biological tools, could verify microbial activity immediately following placement and could also be utilized during long-term monitoring. Identifying such indicators and tools, and how to properly sample for them, is another research challenge that can be pursued. Finally, additional testing of bioreactive cap efficacy under environmentally-relevant conditions is suggested. Larger-scale laboratory studies should be designed to further identify

limitations on microbial activity, with successful demonstrations possibly followed by pilot-scale testing in environmental settings.

APPENDIX A

Appendix A contains additional experimental information for obtaining porewater geochemical profiles with voltammetric microelectrodes. This information pertains directly to Chapters 3 and 5, and indirectly to Chapter 4. Included are procedural details and screen-captured images for determining analyte concentrations from electrochemical output of the electrodes.

Data presented in Chapters 3, 4, and 5 included porewater geochemical profiles obtained with gold amalgam voltammetric microelectrodes. This section provides a brief overview and description of how analyte concentrations were derived from electrochemical measurements.

Voltammetric electrochemical techniques increase the potential difference between a working electrode and a reference electrode. For the studies described in this dissertation, the working electrode was a gold wire encased within glass housing and was plated with mercury at the tip. The reference electrode consisted of silver chloride (Ag/AgCl/KCl(3M)) wire. The range of potentials analyzed (electrode window or analytical window) is specific to each reference-working electrode couple. The analytical window for the electrodes utilized in these studies was -0.1 V to -1.75 V, with a scan rate of 200 $mV \cdot s^{-1}$. As the working electrode was gradually inserted into sediment/cap, dissolved analytes present in the porewaters diffused into the mercury tip of the electrode. As the potential difference between the working and reference electrodes increased, rections occured between the mercury of the electrode and dissolved analytes. The current produced from the reactions on the electrode tip was measured using a platinum counter (auxiliary) electrode. The total current measured is the sum of a faradaic current and a charging current. The faradaic current is the result of diffusion of analytes and redox processes, while the charging current results from the existence of a compact layer at the surface of the electrode (*359*). The charging current decrease with time and can be minimized by small electrode surfaces. Species concentrations can be theoretically calculated from measured current with the Ilkovic equation.

To obtain porewater profiles of environmental samples (e.g., sediment columns, capped sediment columns), the reference and counter electrodes were suspended in the overlying water of columns while the working Au/Hg electrode was gradually inserted through the overlying water and into sediment/cap porewaters at discrete intervals via a computer-operated micromanipulator. All electrodes were connected to a computer-operated DLK-100A potentiostat. Voltammetric scans were performed from -0.1 V to -1.75 V. Linear sweep voltammetry (LSV) was employed to measure dissolved oxygen. Cathodic square wave voltammetry was utilized to measure all other species. Dissolved analytes measured by the Au/Hg voltammetric microelectrodes are listed with their respective potential and voltammetric technique in Table A.1.

Table A.1. Dissolved porewater species monitored by Au/Hg microelectrodes.

Analyte	Approximate Potenial (V)	Technique
$O_{2(aq)}$	-0.3	Linear Sweep Voltammetry (LSV)
$H_2O_{2(aq)}$	-1.3	LSV
Mn^{2+}	-1.6	Cathodic Square Wave Voltammetry (CSWV)
Fe^{2+}	-1.4	CSWV
Organic-$Fe^{III}_{(aq)}$	-0.3 (broad)	CSWV
$Fe_xS_{y(aq)}$	-1.1	CSWV
H_2S, HS^-, S^{2-}, S^0, S_x^{2-} (ΣH_2S)	-0.6	CSWV; Anodic square wave voltammetry
$S_2O_3^-$	-0.15	CSWV

Three to ten voltammetric scans were performed at each depth depending on the species observed. For instance, at locations where both dissolved oxygen and Mn^{2+} were present, a set of LSV scans and a set of CSWV scans were performed to measure each species. A preconditioning potential of -0.1 V for 10 s was performed between measurements to clean the surface of the microelectrodes. When organic-$Fe^{III}_{(aq),}$ ΣH_2S, and $Fe_xS_{y(aq)}$ complexes were present, however, a cleaning step at -0.9 V for 10 seconds was added to remove species adsorbed at the electrode surface between scans (*224*). Peaks were assigned for each scan according to their potential, and every scan was examined to track shifting of peaks to more positive potentials. Standard deviations for each analyte at a specific depth represent analytical error in the measurement of the analytes, derived from replicate scans at a constant depth and at the same loction (i.e., one insertion of the electrode into the porewaters).

Current (amps) produced from each reaction at the electrode tip was analyzed in terms of peak heights, obtained through the Matlab®-based Voltint program (*261*). For the determination of dissolved oxygen using LSV, peak height was calculated as the difference between the currents produced from the reaction with O_2 and H_2O_2 (Figure A.1A). For species measured by CSWV, peak heights were obtained from the baseline to the top of the current peak (Figure A.1B-C). Concentrations were derived from peak heights according to oxygen and manganese calibrations performed in simulated freshwater (0.1 M NaCl in nanopure water) or simulated saltwater (0.5 M NaCl in nanpure water). Oxygen concentrations in standards were assumed to be at saturation and were corrected for temperature and salinity of the standard solution. Manganese calibrations were performed under anaerobic conditions following sparging of standard

solutions with nitrogen. Manganese calibration concentrations ranged from 10 to 400 μM, with Mn^{2+} added from a stock solution of 0.1 M $MnCl_2$ in 0.01 M HCl with a micro-pippette. Concentrations of other species (Fe^{2+}, ΣH_2S) were determined via the pilot-ion method, based upon established ratios of electrode response between manganese and other analytes (*222*). The concentration of Fe^{2+} was determed by adjusting the manganese calibration slope by a factor of 0.6; the concentration of ΣH_2S was determined by adjusting the manganese calibration slope by a factor of 12.3. For example, if an ΣH_2S peak height of 50 nA was observed, and the Mn^{2+} calibration slope was calculated to be 0.12 $nA \cdot \mu M^{-1}$, then the resulting ΣH_2S concentration would be 50 nA/(12.3·0.12 $nA \cdot \mu M^{-1}$) = 33 μM. For the organic-$Fe^{III}_{(aq)}$ and $Fe_xS_{y(aq)}$ complexes, uncharacterized electrode responses and molecular stoichiometries prevented quantitation. These complexes were therefore reported in current intensity (nA), as calculated directly in the Voltint program.

Porewater profiles were constructed using average species concentrations at each depth. The y-axis was assigned to column depth, with y=0 defined as the solids-water interface (e.g., cap-water interface, sediment-water interface, sand-water interface). A lower x-axis provided quantifyable species, while an upper x-axis provided the non-quantifyable organic-$Fe^{III}_{(aq)}$ and $Fe_xS_{y(aq)}$ complexes.

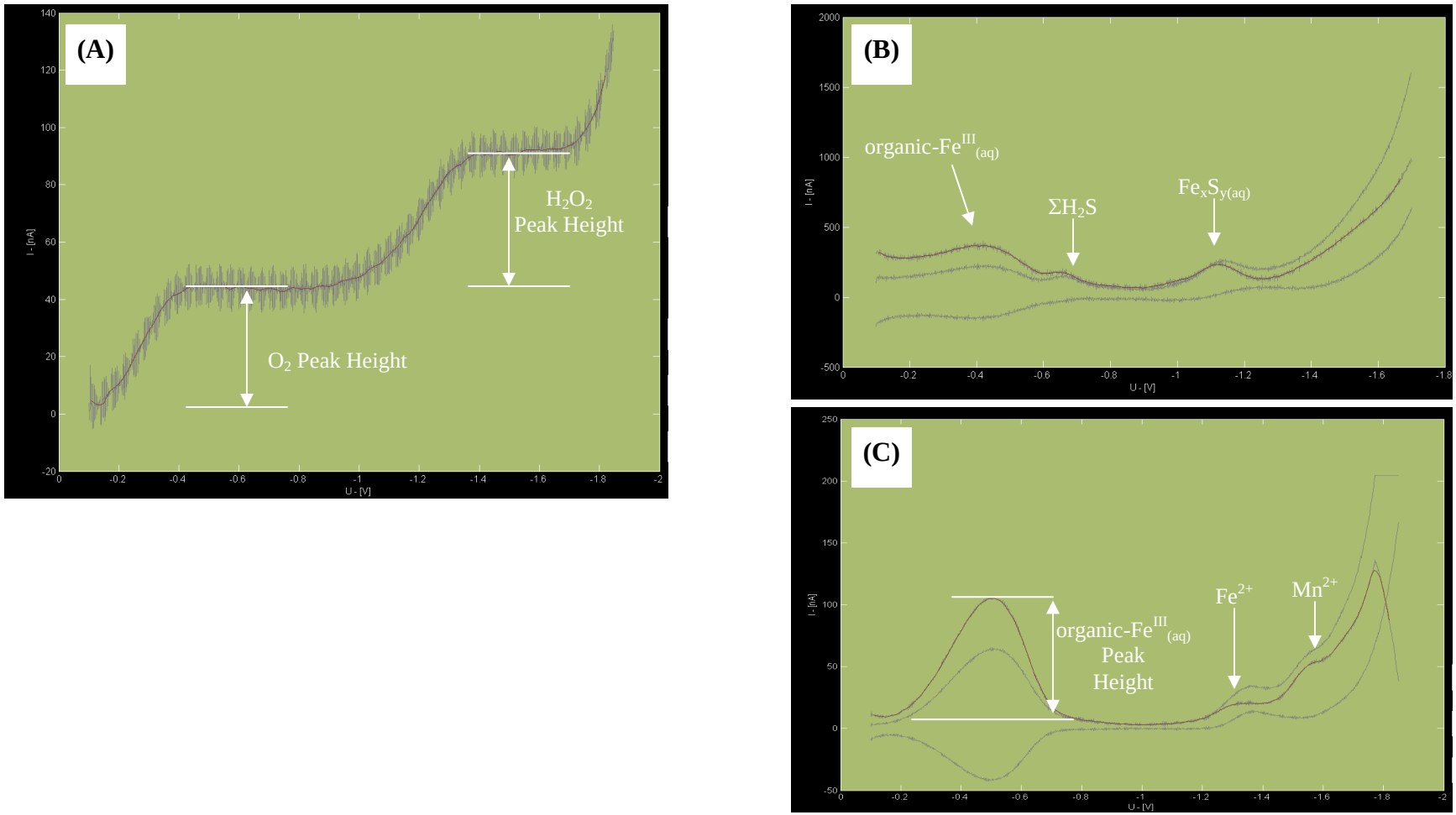

Figures A.1A-C. Screen-capture images of voltammagrams obtained from the capped Anacostia River sediment column. Figure A is a linear sweep voltammetric scan obtained at a depth of 32.8 mm, incubated for 13 weeks under static flow. Figure B is a cathodic square wave voltammetric scan obtained 6 weeks after the initation of upflow at a depth of -27 mm. Figure C is a cathodic square wave voltammetric scan obtained at a depth of -87.8 mm, incubated 13 weeks under static flow.

APPENDIX B

Appendix B contains supplementary information for Chapter 3, entitled “Spatial and Temporal Evolution of Biogeochemical Processes Following In Situ Capping”. Included is a schematic and photograph of the capped sediment column, photographs of the control columns, all porewater geochemical profiles obtained from the capped sediment column under both static and upflow conditions, and all porewater profiles obtained for the uncapped sediment control and the sediment-free sand control. Representative porewater profiles were utilized in Chapter 3 for the capped sediment column and the control columns.

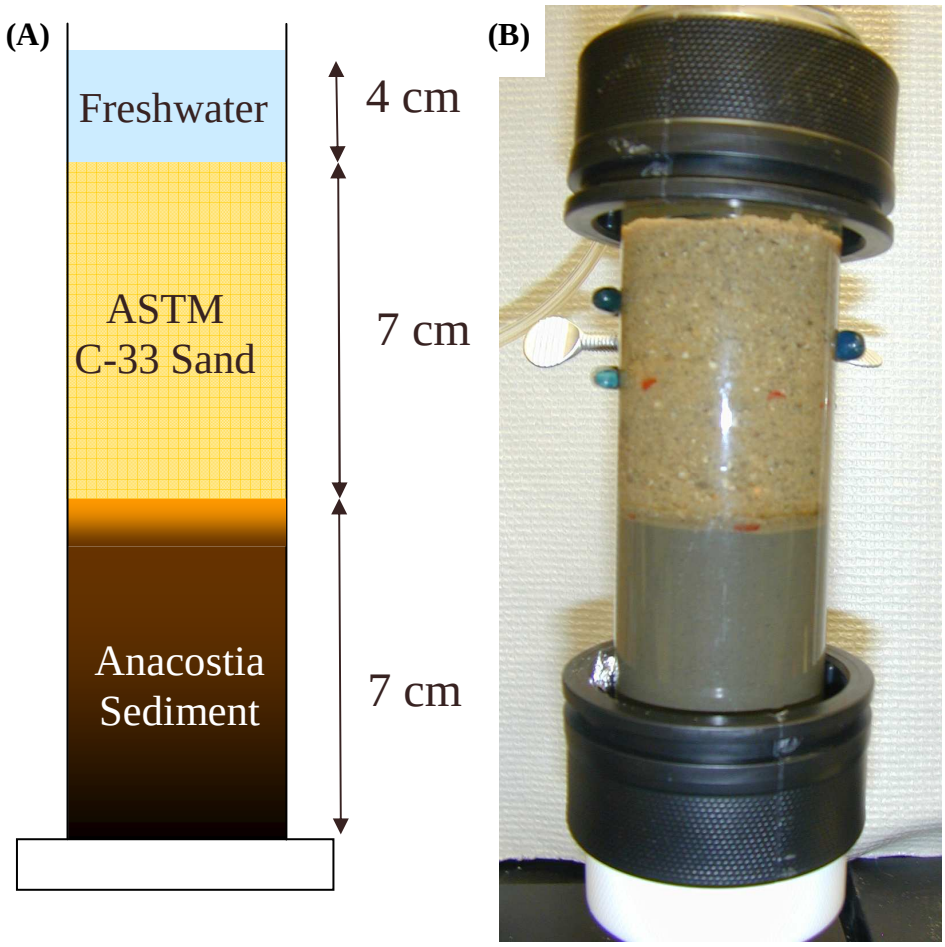

Figures B.1A-B. (A) Schematic of capped Anacostia River sediment column. (B) Photograph of capped Anacostia River sediment column.

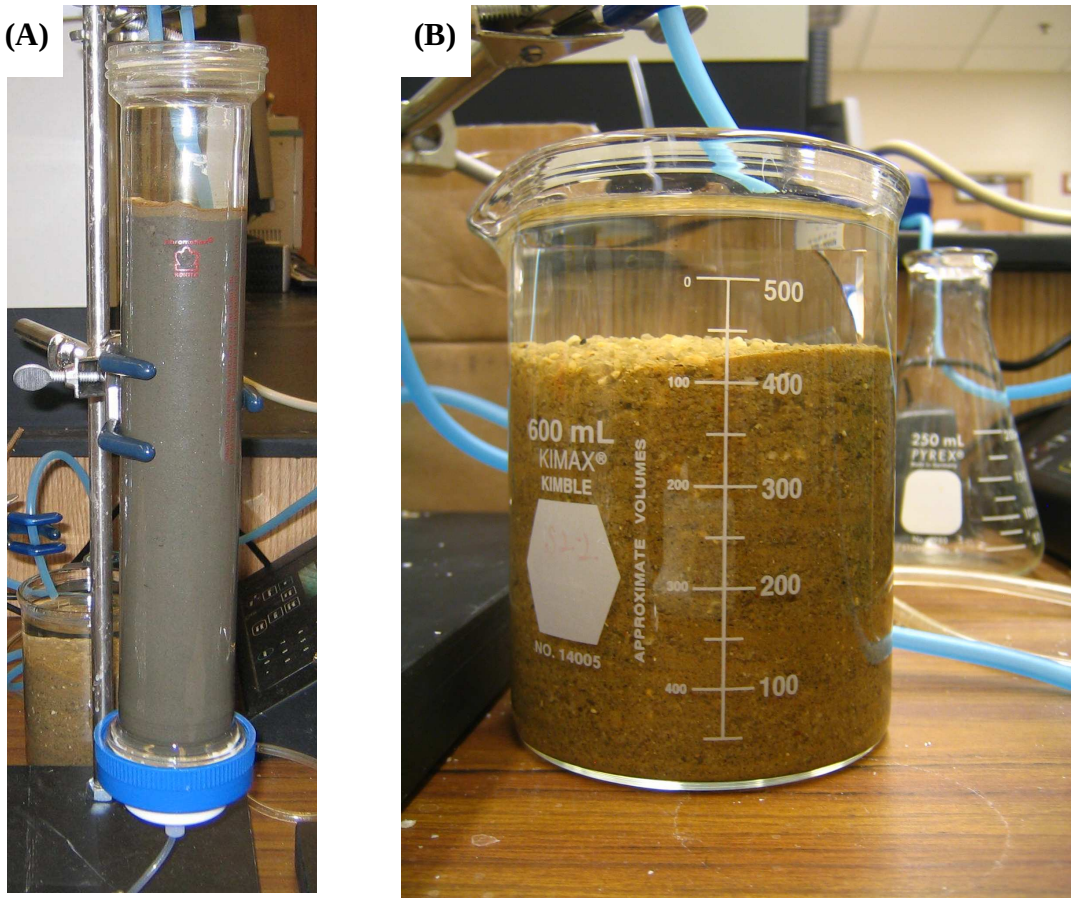

Figures B.2A-B. (A) Photograph of uncapped Anacostia River sediment control column. (B) Photograph of sediment-free sand control column.

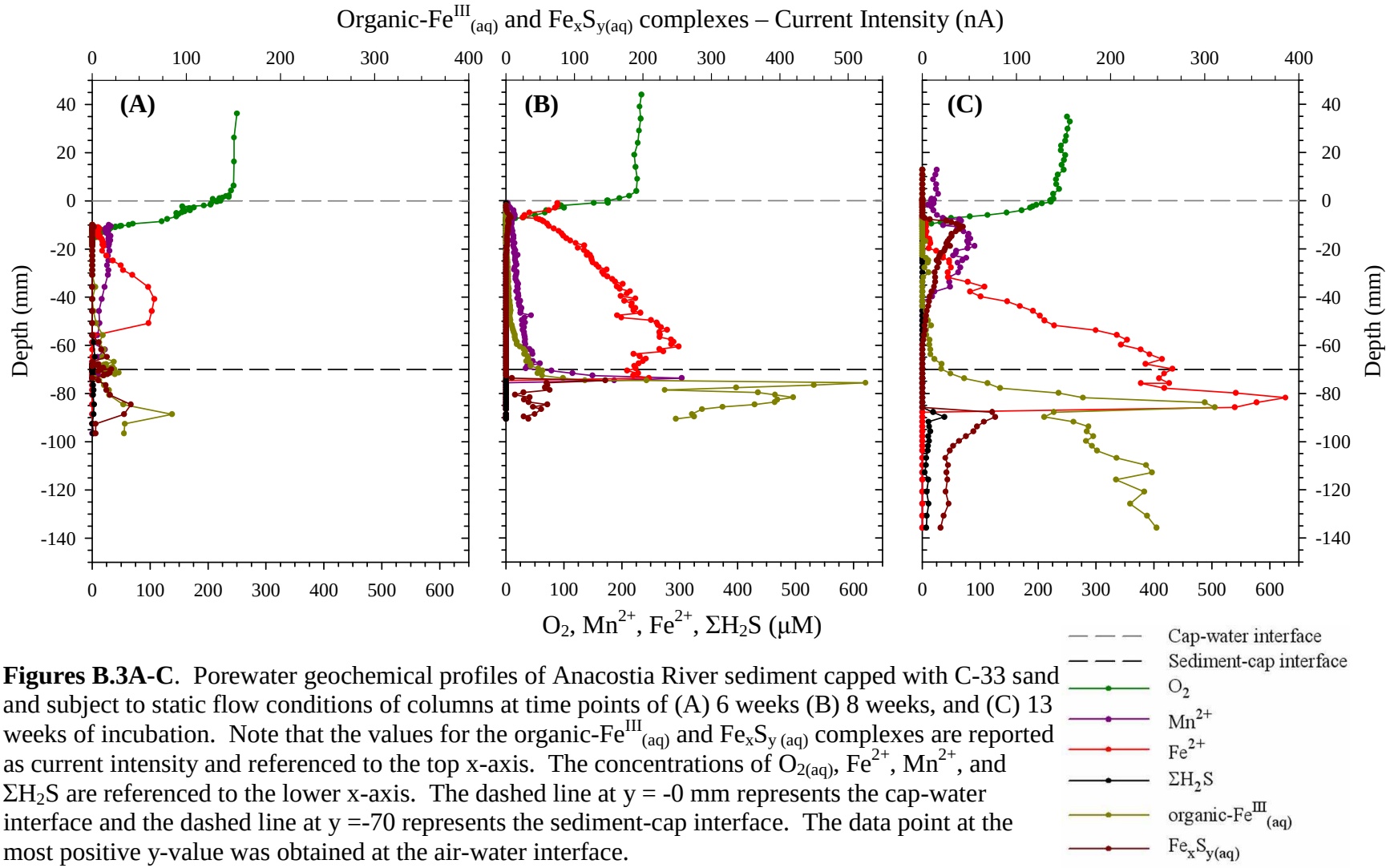

Figures B.3A-C. Porewater geochemical profiles of Anacostia River sediment capped with C-33 sand and subject to static flow conditions of columns at time points of (A) 6 weeks (B) 8 weeks, and (C) 13 weeks of incubation. Note that the values for the organic-$Fe^{III}_{(aq)}$ and $Fe_xS_{y\,(aq)}$ complexes are reported as current intensity and referenced to the top x-axis. The concentrations of $O_{2(aq)}$, Fe^{2+}, Mn^{2+}, and ΣH_2S are referenced to the lower x-axis. The dashed line at y = -0 mm represents the cap-water interface and the dashed line at y =-70 represents the sediment-cap interface. The data point at the most positive y-value was obtained at the air-water interface.

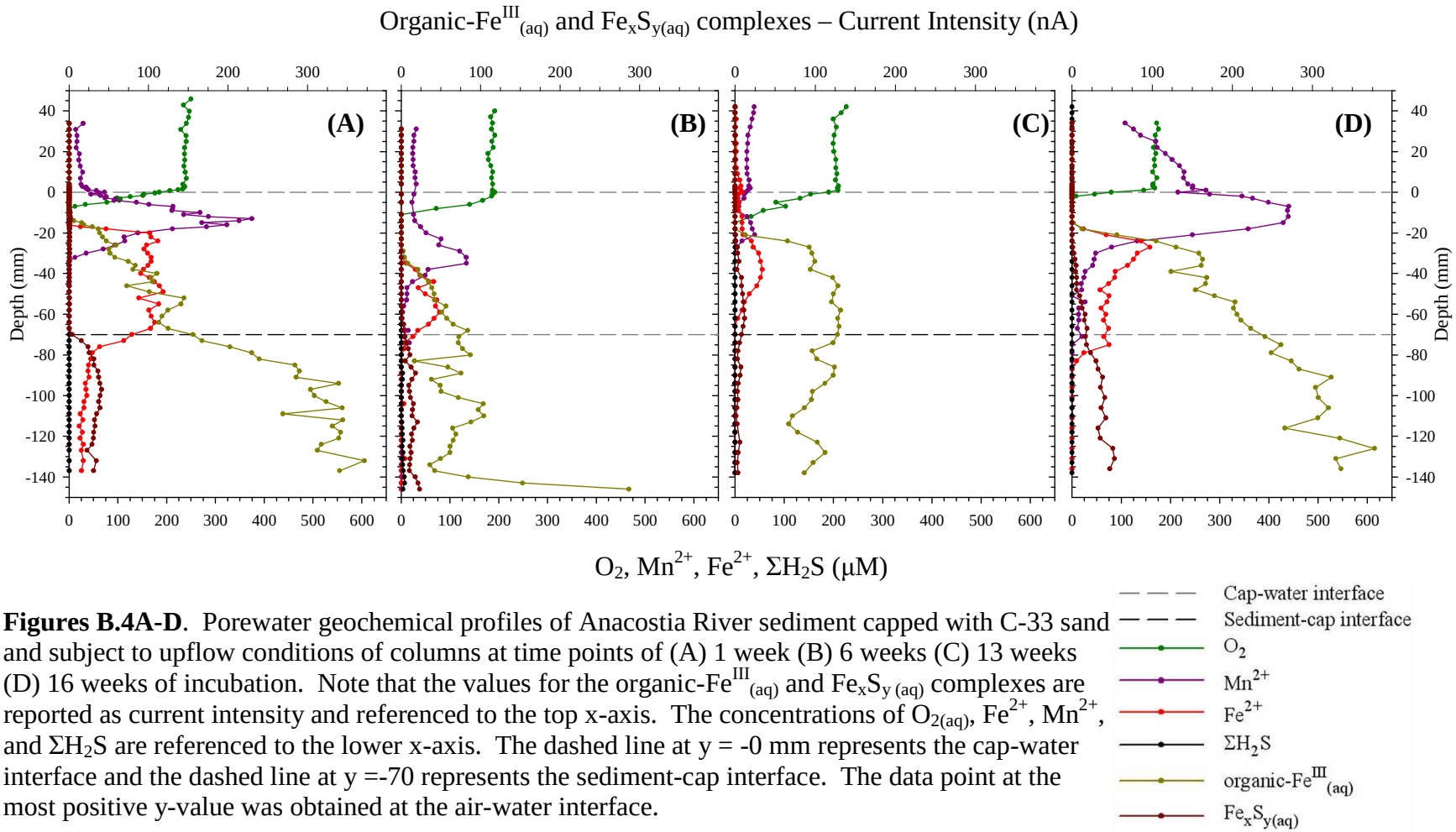

Figures B.4A-D. Porewater geochemical profiles of Anacostia River sediment capped with C-33 sand and subject to upflow conditions of columns at time points of (A) 1 week (B) 6 weeks (C) 13 weeks (D) 16 weeks of incubation. Note that the values for the organic-$Fe^{III}_{(aq)}$ and $Fe_xS_{y\,(aq)}$ complexes are reported as current intensity and referenced to the top x-axis. The concentrations of $O_{2(aq)}$, Fe^{2+}, Mn^{2+}, and ΣH_2S are referenced to the lower x-axis. The dashed line at y = -0 mm represents the cap-water interface and the dashed line at y =-70 represents the sediment-cap interface. The data point at the most positive y-value was obtained at the air-water interface.

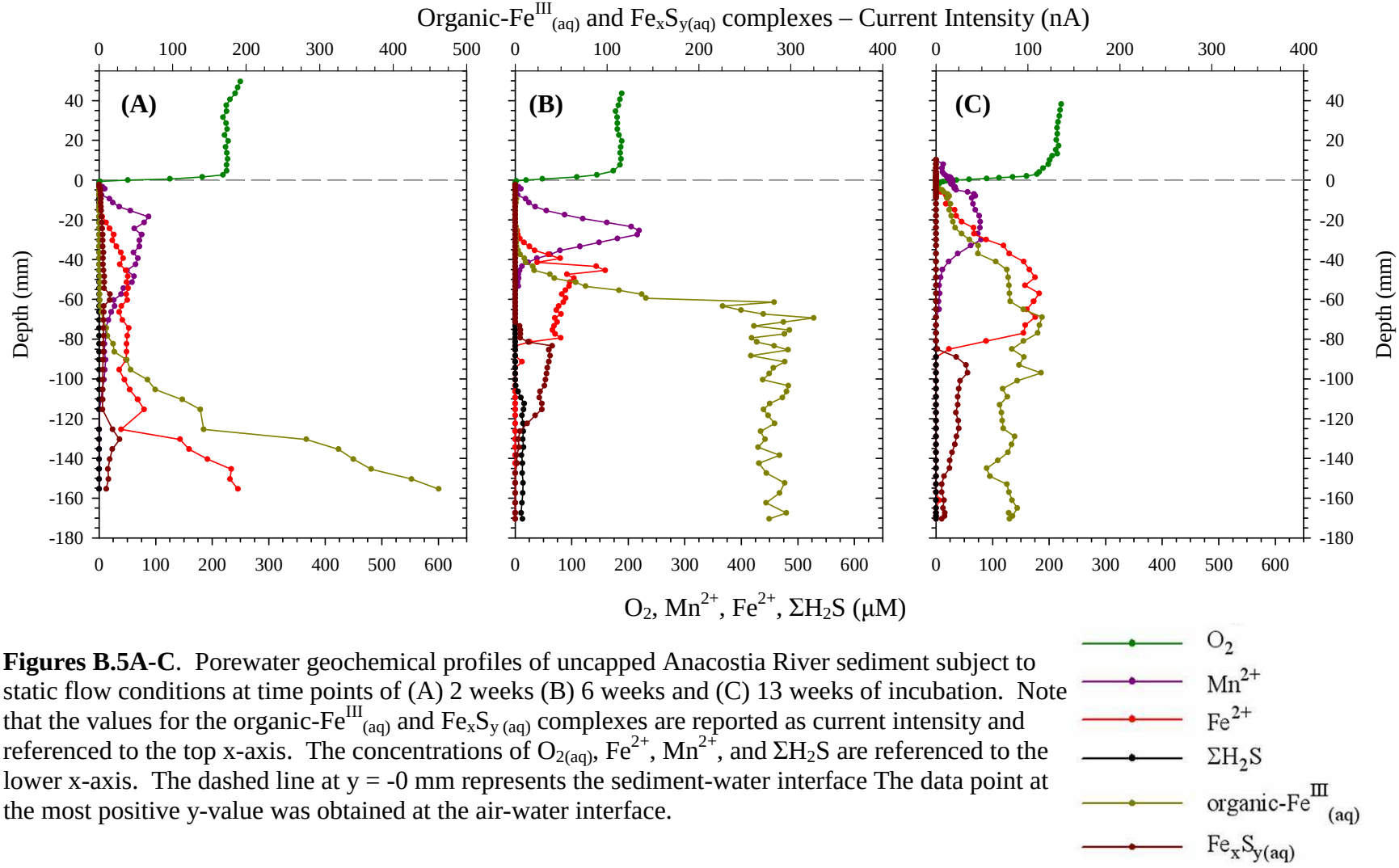

Figures B.5A-C. Porewater geochemical profiles of uncapped Anacostia River sediment subject to static flow conditions at time points of (A) 2 weeks (B) 6 weeks and (C) 13 weeks of incubation. Note that the values for the organic-$Fe^{III}_{(aq)}$ and $Fe_xS_{y\,(aq)}$ complexes are reported as current intensity and referenced to the top x-axis. The concentrations of $O_{2(aq)}$, Fe^{2+}, Mn^{2+}, and ΣH_2S are referenced to the lower x-axis. The dashed line at y = -0 mm represents the sediment-water interface The data point at the most positive y-value was obtained at the air-water interface.

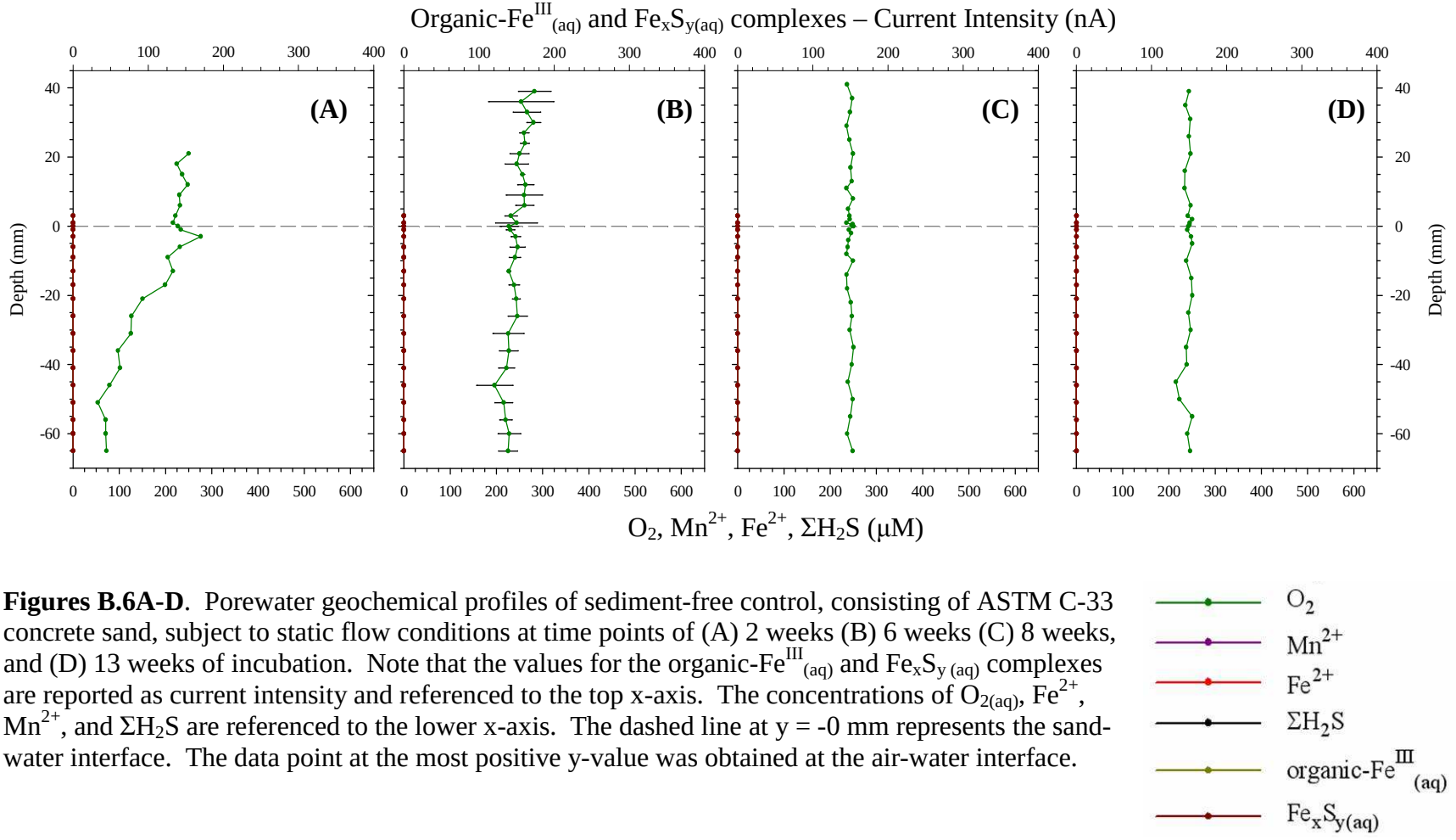

Figures B.6A-D. Porewater geochemical profiles of sediment-free control, consisting of ASTM C-33 concrete sand, subject to static flow conditions at time points of (A) 2 weeks (B) 6 weeks (C) 8 weeks, and (D) 13 weeks of incubation. Note that the values for the organic-Fe$^{III}_{(aq)}$ and Fe$_x$S$_{y\,(aq)}$ complexes are reported as current intensity and referenced to the top x-axis. The concentrations of $O_{2(aq)}$, Fe^{2+}, Mn^{2+}, and ΣH_2S are referenced to the lower x-axis. The dashed line at y = -0 mm represents the sand-water interface. The data point at the most positive y-value was obtained at the air-water interface.

APPENDIX C

Appendix C contains supplementary information for Chapter 5, entitled “The Effect of Advective Flow Directon on Redox Environments Within *In Situ* Sediment Caps”. Included are photographs of the capped Satilla River sediment columns.

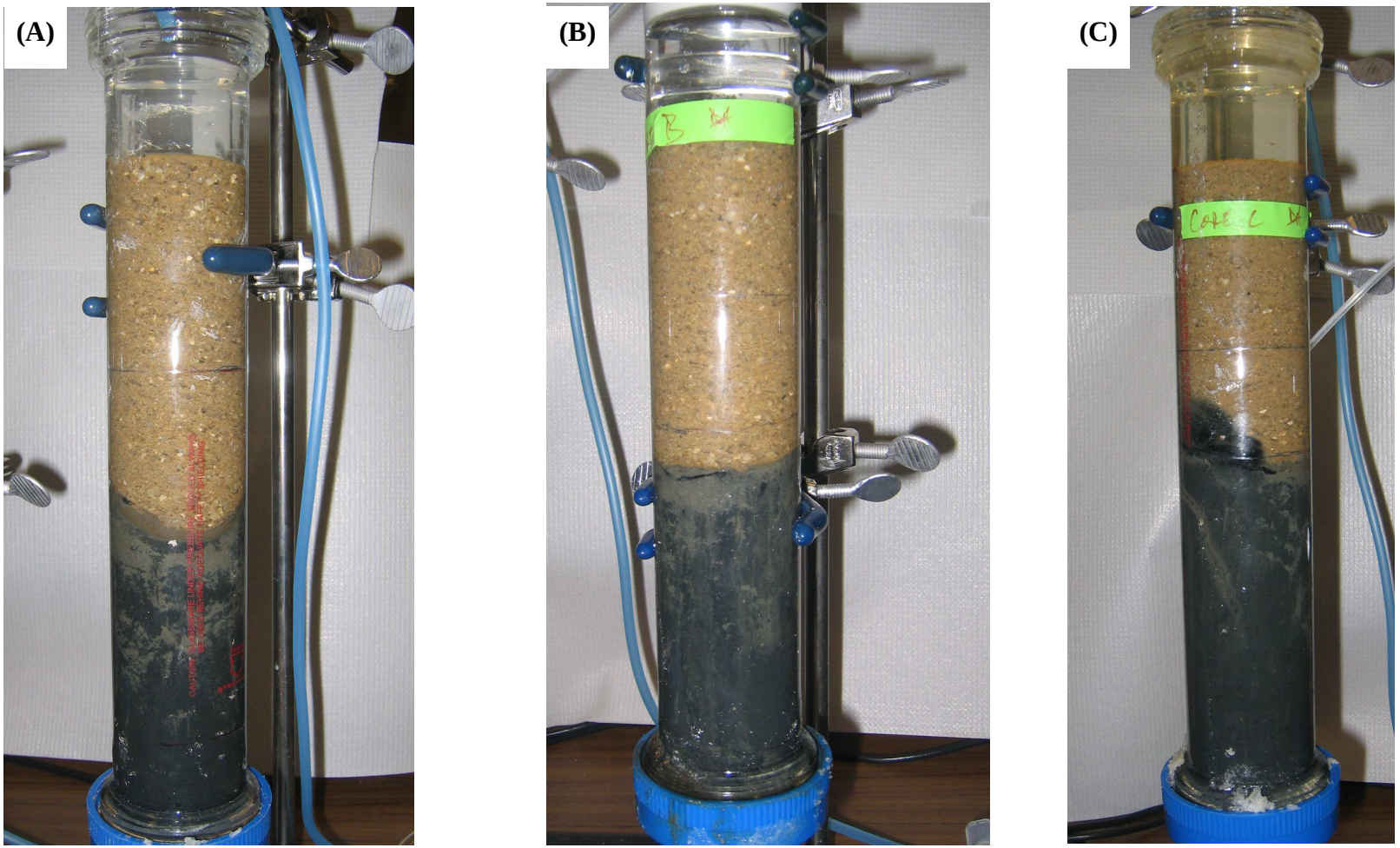

Figures C.1A-C. Photographs of capped Satilla River sediment columns subject to (A) static flow, (B) upflow, and (C) downward flow.

LITERATURE CITED

(1) USEPA. Contaminated Sediment Management Strategy, Office of Water, 1998, EPA-823-R-98-001.

(2) Rice, K. C. Trace-element concentrations in streambed sediment across the conterminous United States. *Environmental Science & Technology.* 1999, 33, (15), 2499-2504.

(3) Lopes, T. J.; Furlong, E. T. Occurrence and potential adverse effects of semivolatile organic compounds in streambed sediment, United States, 1992-1995. *Environmental Toxicology and Chemistry.* 2001, 20, (4), 727-737.

(4) Van Metre, P. C.; Mahler, B. J. Trends in hydrophobic organic contaminants in urban and reference lake sediments across the United States, 1970-2001. *Environmental Science & Technology.* 2005, 39, (15), 5567-5574.

(5) Baumann, P. C.; Smith, W.D.; Parland, W.K.. Tumor frequencies and contaminant concentrations in brown bullheads from an industrialized river and a recreational lake. *Transactions of the American Fisheries Society.* 1987, 116, 79-80.

(6) USEPA. Fact sheet: 2005/2006 National Listing of Fish Advisories, Office of Water, 2007, EPA-823-F-07-003.

(7) Kremer, F., Nakles, D.V., Biksey, T. Monitored natural attenuation forum: Monitored natural recovery of contaminated sediments. *Remediation.* 2006, 17, (1), 139-147.

(8) SERDP and ESTCP Expert Panel Workshop on Research and Development Needs for the In Situ Management of Contaminated Sediments, Final Report October 2004.

(9) Ramsburg, C. A.; Pennell, K. D. Experimental and economic assessment of two surfactant formulations for source zone remediation at a former dry cleaning facility. *Ground Water Monitoring and Remediation.* 2001, 21, (4), 68-82.

(10) Serdp/estcp expert panel workshop on research and development needs for cleanup of chlorinated solvent sites, final report. 2001.

(11) USEPA. Contaminated Sediments in Superfund, updated September 18, 2007. Accessed October, 2007. http://www.epa.gov/superfund/health/conmedia/sediment/index.htm

(12) Baudo, R., Muntau, H. Lesser known in-place pollutants and diffuse source problems. In *Sediments: Chemistry and Toxicity of In-Place Pollutants*; Baudo, R., Giesy, JP, Muntau, H, Ed. Lewis Publishers: Ann Arbor, 1990.

(13) Luthy, R. G.; Aiken, G. R.; Brusseau, M. L.; Cunningham, S. D.; Gschwend, P. M.; Pignatello, J. J.; Reinhard, M.; Traina, S. J.; Weber, W. J.; Westall, J. C. Sequestration of hydrophobic organic contaminants by geosorbents. *Environmental Science & Technology.* 1997, 31, (12), 3341-3347.

(14) Tessier, A., Carignan, R., Belzile, N. Reactions of trace elements near the sediment-water inteface in lakes. In *Transport and Transformation of Contaminants Near the Sediment-Water Interface*; DePinto, J. V., Lick, W., Paul, J.F., Ed. Lewis Publishers: Boca Raton, FL, 1994.

(15) USEPA. Cleaning up the Nation's Waste Sites: Markets and Technology Trends, Office of Solid Waste and Emergency Response, 2004, EPA-542-R-04-015.

(16) Naval Facilities Engineering Command. Contaminated Sediments at Navy Facilities: Policy, Guidance, and Characterization, 2002, Technical Data Sheet TDS-2091-ENV.

(17) Eisenreich, S. J.; Capel, P. D.; Robbins, J. A.; Bourbonniere, R. Accumulation and diagenesis of chlorinated hydrocarbons in lacustrine sediments. *Environmental Science & Technology.* 1989, 23, (9), 1116-1126.

(18) Van Metre, P. C.; Wilson, J. T.; Callender, E.; Fuller, C. C. Similar rates of decrease of persistent, hydrophobic and particle-reactive contaminants in riverine systems. *Environmental Science & Technology.* 1998, 32, (21), 3312-3317.

(19) Harvey, J. W., Wagner, B.J. Quantifying hydrologic interactions between streams and their subsurface hyporheic zones. In *Streams and Ground Waters*; Jones, J. B., Mulholland, Patrick J., Ed. Academic Press: San Diego, 2000.

(20) Tomassoni, G., A federal statutory/regulatory/policy perspective on remedial decision-making with respect to ground-water/surface-water interaction. In *Ground-Water/Surface-Water Interactions Workshop*, USEPA, Office of Solid Waste and Emergency Response.

(21) Samanta, S. K. EPA evaluation of the likelihood of DNAPL presence at NPL sites, national results. 1993.

(22) Conant, B.; Cherry, J. A.; Gillham, R. W. A PCE groundwater plume discharging to a river: Influence of the streambed and near-river zone on contaminant distributions. *Journal of Contaminant Hydrology.* 2004, 73, (1-4), 249-279.

(23) Lendvay, J. M.; Dean, S. M.; Adriaens, P. Temporal and spatial trends in biogeochemical conditions at a groundwater-surface water interface: Implications for natural bioattenuation. *Environmental Science & Technology.* 1998, 32, (22), 3472-3478.

(24) Lendvay, J. M.; Sauck, W. A.; McCormick, M. L.; Barcelona, M. J.; Kampbell, D. H.; Wilson, J. T.; Adriaens, P. Geophysical characterization, redox zonation, and

contaminant distribution at a groundwater surface water interface. *Water Resources Research.* 1998, 34, (12), 3545-3559.

(25) Lorah, M. M.; Olsen, L. D. Natural attenuation of chlorinated volatile organic compounds in a freshwater tidal wetland: Field evidence of anaerobic biodegradation. *Water Resources Research.* 1999, 35, (12), 3811-3827.

(26) Lorah, M. M.; Voytek, M. A. Degradation of 1,1,2,2-tetrachloroethane and accumulation of vinyl chloride in wetland sediment microcosms and in situ porewater: Biogeochemical controls and associations with microbial communities. *Journal of Contaminant Hydrology.* 2004, 70, (1-2), 117-145.

(27) Chapman, S. W.; Parker, B. L.; Cherry, J. A.; Aravena, R.; Hunkeler, D. Groundwater-surface water interaction and its role on tce groundwater plume attenuation. *Journal of Contaminant Hydrology.* 2007, 91, (3-4), 203-232.

(28) Ruder, A. M. Potential health effects of occupational chlorinated solvent exposure. *Living in a Chemical World: Framing the Future in Light of the Past.* 2006, 1076, 207-227.

(29) Reible, D. D., Valsaraj, K.T., and Thibodeaux, L.J. Chemodynamic models for transport of contaminants from sediment beds. In *The Handbook of Environmental Chemistry*; Hutzinger, O., Ed. Springer-Verlag: Berlin, 1991.

(30) Eggleton, J.; Thomas, K. V. A review of factors affecting the release and bioavailability of contaminants during sediment disturbance events. *Environment International.* 2004, 30, (7), 973-980.

(31) Liu, C. H.; Jay, J. A.; Ika, R.; Shine, J. P.; Ford, T. E. Capping efficiency for metal-contaminated marine sediment under conditions of submarine groundwater discharge. *Environmental Science & Technology.* 2001, 35, (11), 2334-2340.

(32) Cornett, R. J.; Risto, B. A.; Lee, D. R. Measuring groundwater transport through lake-sediments by advection and diffusion. *Water Resources Research.* 1989, 25, (8), 1815-1823.

(33) Work, P. A.; Moore, P. R.; Reible, D. D. Bioturbation, advection, and diffusion of a conserved tracer in a laboratory flume. *Water Resources Research.* 2002, 38, (6), -.

(34) Findlay, S. Importance of surface-subsurface exchange in stream ecosystems - the hyporheic zone. *Limnology and Oceanography.* 1995, 40, (1), 159-164.

(35) Triska, F. J.; Duff, J. H.; Avanzino, R. J. The role of water exchange between a stream channel and its hyporheic zone in nitrogen cycling at the terrestrial aquatic interface. *Hydrobiologia.* 1993, 251, (1-3), 167-184.

(36) Findlay, S.; Strayer, D.; Goumbala, C.; Gould, K. Metabolism of streamwater dissolved organic-carbon in the shallow hyporheic zone. *Limnology and Oceanography.* 1993, 38, (7), 1493-1499.

(37) Harvey, J. W.; Fuller, C. C. Effect of enhanced manganese oxidation in the hyporheic zone on basin-scale geochemical mass balance. *Water Resources Research.* 1998, 34, (4), 623-636.

(38) Schneider, A. R.; Porter, E. T.; Baker, J. E. Polychlorinated biphenyl release from resuspended Hudson River sediment. *Environmental Science & Technology.* 2007, 41, (4), 1097-1103.

(39) Valsaraj, K. T.; Sojitra, I. Transport of hydrophobic organic compounds by colloids through porous media .3. Diffusion from sediment porewater to overlying water in laboratory microcosms. *Colloids and Surfaces A-Physicochemical and Engineering Aspects.* 1997, 121, (2-3), 125-133.

(40) Sojitra, I.; Valsaraj, K. T.; Reible, D. D.; Thibodeaux, L. J. Transport of hydrophobic organics by colloids through porous-media .1. Experimental results. *Colloids and Surfaces A-Physicochemical and Engineering Aspects.* 1995, 94, (2-3), 197-211.

(41) Matsui, G. Y.; Ringelberg, D. B.; Lovell, C. R. Sulfate-reducing bacteria in tubes constructed by the marine infaunal polychaete *Diopatra cuprea*. *Applied and Environmental Microbiology.* 2004, 70, (12), 7053-7065.

(42) Alongi, D. M. Microbes, meiofauna, and bacterial productivity on tubes constructed by the polychaete *Capitella capitata*. *Marine Ecology-Progress Series.* 1985, 23, (2), 207-208.

(43) Huttel, M. Influence of the lugworm *Arenicola marina* on porewater nutrient profiles of sand flat sediments. *Marine Ecology-Progress Series.* 1990, 62, (3), 241-248.

(44) Kristensen, E.; Jensen, M. H.; Aller, R. C. Direct measurement of dissolved inorganic nitrogen exchange and denitrification in individual polychaete (*Nereis virens*) burrows. *Journal of Marine Research.* 1991, 49, (2), 355-377.

(45) Van Rees, K. C. J.; Reddy, K. R.; Rao, P. S. C. Influence of benthic organisms on solute transport in lake sediments. *Hydrobiologia.* 1996, 317, (1), 31-40.

(46) Reible, D. D.; Popov, V.; Valsaraj, K. T.; Thibodeaux, L. J.; Lin, F.; Dikshit, M.; Todaro, M. A.; Fleeger, J. W. Contaminant fluxes from sediment due to tubificid oligochaete bioturbation. *Water Research.* 1996, 30, (3), 704-714.

(47) Forster, S.; Graf, G. Impact of irrigation on oxygen flux into the sediment - intermittent pumping by *Callianassa subterranea* and piston-pumping by *Lanice conchilega*. *Marine Biology.* 1995, 123, (2), 335-346.

(48) Kristensen, E. Benthic fauna and biogeochemical processes in marine sediments: Microbial activities and fluxes. In *Nitrogen Cycling in Coastal Marine Sediments*; Blackburn, T. H., Sorensen, J.Ed. John Wiley & Sons: Chichester, UK, 1988.

(49) Kristensen, E.; Jensen, M. H.; Andersen, T. K. The impact of polychaete (nereis-virens sars) burrows on nitrification and nitrate reduction in estuarine sediments. *Journal of Experimental Marine Biology and Ecology.* 1985, 85, (1), 75-91.

(50) Steward, C. C.; Nold, S. C.; Ringelberg, D. B.; White, D. C.; Lovell, C. R. Microbial biomass and community structures in the burrows of bromophenol producing and non-producing marine worms and surrounding sediments. *Marine Ecology-Progress Series.* 1996, 133, (1-3), 149-165.

(51) Allen, H. E. Partitioning of toxic metals in natural water-sediment systems. In *Transport and Transformation of Contaminants Near the Sediment-Water Interface*; DePinto, J. V., Lick, W., Paul, J.F., Ed. Lewis Publishers: Boca Raton, 1994.

(52) Gadd, G. M. Microbial influence on metal mobility and application for bioremediation. *Geoderma.* 2004, 122, (2-4), 109-119.

(53) Sung, Y.; Fletcher, K. F.; Ritalaliti, K. M.; Apkarian, R. P.; Ramos-Hernandez, N.; Sanford, R. A.; Mesbah, N. M.; Löffler, F. E. *Geobacter lovleyi* sp. nov strain SZ, a novel metal-reducing and tetrachloroethene-dechlorinating bacterium. *Applied and Environmental Microbiology.* 2006, 72, (4), 2775-2782.

(54) Wu, Q.; Sanford, R. A.; Löffler, F. E. Uranium(VI) reduction by *Anaeromyxobacter dehalogenans* strain 2CP-C. *Applied and Environmental Microbiology.* 2006, 72, (5), 3608-3614.

(55) Lovley, D. R.; Holmes, D. E.; Nevin, K. P. Dissimilatory Fe(III) and Mn(IV) reduction. *Advances in Microbial Physiology, Vol. 49.* 2004, 49, 219-286.

(56) Carlton, R. G., Klug, M.J. Spatial and temporal variations in microbial processes in aquatic sediments: Implications for the nutrient status of lakes. In *Sediments: Chemistry and Toxicity of In-Place Pollutants*; Baudo, R., Giesy, JP, Muntau, H., Ed. Lewis Publishers, Inc: Chelsea, MI, 1990.

(57) Kile, D. E.; Chiou, C. T.; Zhou, H. D.; Li, H.; Xu, O. Y. Partition of nonpolar organic pollutants from water to soil and sediment organic matters. *Environmental Science & Technology.* 1995, 29, (5), 1401-1406.

(58) Lopez-Sanchez, J. F.; Rubio, R.; Samitier, C.; Rauret, G. Trace metal partitioning in marine sediments and sludges deposited off the coast of Barcelona, Spain. *Water Research.* 1996, 30, (1), 153-159.

(59) Calmano, W.; Hong, J.; Forstner, U. Binding and mobilization of heavy-metals in contaminated sediments affected by pH and redox potential. *Water Science and Technology.* 1993, 28, (8-9), 223-235.

(60) Fan, W. H.; Wang, W. X.; Chen, J. S.; Li, X. D.; Yen, Y. F. Cu, Ni, and Pb speciation in surface sediments from a contaminated bay of northern China. *Marine Pollution Bulletin.* 2002, 44, (8), 820-826.

(61) Shulkin, V. M.; Bogdanova, N. N. The Zn, Cu, Cd and Pb release into aerated sea water from unpolluted and polluted sediments. *Okeanologiya.* 1998, 38, (5), 685-693.

(62) Li, X. D.; Shen, Z. G.; Wai, O. W. H.; Li, Y. S. Chemical partitioning of heavy metal contaminants in sediments of the Pearl River estuary. *Chemical Speciation and Bioavailability.* 2000, 12, (1), 17-25.

(63) Dong, D. M.; Nelson, Y. M.; Lion, L. W.; Shuler, M. L.; Ghiorse, W. C. Adsorption of Pb and Cd onto metal oxides and organic material in natural surface coatings as determined by selective extractions: New evidence for the importance of Mn and Fe oxides. *Water Research.* 2000, 34, (2), 427-436.

(64) Morse, J. W.; Luther, G. W. Chemical influences on trace metal-sulfide interactions in anoxic sediments. *Geochimica Et Cosmochimica Acta.* 1999, 63, (19-20), 3373-3378.

(65) Forstner, U.; Ahlf, W.; Calmano, W. Studies on the transfer of heavy-metals between sedimentary phases with a multi-chamber device - combined effects of salinity and redox variation. *Marine Chemistry.* 1989, 28, (1-3), 145-158.

(66) Zhuang, Y. Y.; Allen, H. E.; Fu, G. M. Effect of aeration of sediment on cadmium-binding. *Environmental Toxicology and Chemistry.* 1994, 13, (5), 717-724.

(67) Hursthouse, A. S. The relevance of speciation in the remediation of soils and sediments contaminated by metallic elements - an overview and examples from central scotland, uk. *Journal of Environmental Monitoring.* 2001, 3, (1), 49-60.

(68) Chen, W.; Kan, A. T.; Fu, G.; Vignona, L. C.; Tomson, M. B. Adsorption-desorption behaviors of hydrophobic organic compounds in sediments of lake charles, louisiana, USA. *Environmental Toxicology and Chemistry.* 1999, 18, (8), 1610-1616.

(69) Woodhead, R. J.; Law, R. J.; Matthiessen, P. Polycyclic aromatic hydrocarbons in surface sediments around England and Wales, and their possible biological significance. *Marine Pollution Bulletin.* 1999, 38, (9), 773-790.

(70) Langston, W. J.; Pope, N. D. Determinants of tbt adsorption and desorption in estuarine sediments. *Marine Pollution Bulletin.* 1995, 31, (1-3), 32-43.

(71) Conaway, C. H.; Squire, S.; Mason, R. P.; Flegal, A. R. Mercury speciation in the San Francisco bay estuary. *Marine Chemistry.* 2003, 80, (2-3), 199-225.

(72) Schwarzenbach, R. P., Gschwend, P.M., and Imboden, D.M. Sorption I: General introduction and sorption processes involving organic matter. In *Environmental Organic Chemistry*; Schwarzenbach, R. P., Gschwend, P.M., and Imboden, D.M., Ed. John Wiley & Sons: Hoboken, NJ, 2003.

(73) Zimmerman, J. R.; Ghosh, U.; Millward, R. N.; Bridges, T. S.; Luthy, R. G. Addition of carbon sorbents to reduce PCB and PAH bioavailability in marine sediments: Physicochemical tests. *Environmental Science & Technology.* 2004, 38, (20), 5458-5464.

(74) McLeod, P. B.; Van Den Heuvel-Greve, M. J.; Allen-King, R. M.; Luoma, S. N.; Luthy, R. G. Effects of particulate carbonaceous matter on the bioavailability of benzo[a]pyrene and 2,2 ',5,5 '-tetrachlorobiphenyl to the clam, *Macoma balthica*. *Environmental Science & Technology.* 2004, 38, (17), 4549-4556.

(75) Tang, J. X.; Petersen, E. J.; Huang, Q. G.; Weber, W. J. Development of engineered natural organic sorbents for environmental applications: 3. Reducing pah mobility and bioavailability in contaminated soil and sediment systems. *Environmental Science & Technology.* 2007, 41, (8), 2901-2907.

(76) Cornelissen, G., Haftka, J., Parsons, J, Gustafsson, Ö. Sorption to black carbon of organic compounds with varying polarity and planarity. *Environmental Science & Technology.* 2005, 39, 3688-3694.

(77) Weber, W. J. J., Pennell, K.D., Dekker, T.J., Abriola, L.M. Sorption and retardation of organic contaminants in subsurface systems: Effects on transport and fate. In *Advances in Groundwater Pollution Control and Rememdiation*; Aral, M. M., Ed. Kluwer Academic Publishers: Boston, MA, 1996.

(78) Pignatello, J. J., Xing, B.S. Mechanisms of slow sorption of organic chemicals to natural particles. *Environmental Science & Technology.* 1996, 30, 1-11.

(79) Brusseau, M. L.; Rao, P. S. C. The influence of sorbate-organic matter interactions on sorption nonequilibrium. *Chemosphere.* 1989, 18, (9-10), 1691-1706.

(80) Piatt, J. J., Brusseau, M.L. Rate-limited sorption of hydrophobic organic compounds by soils with well-characterized organic matter. *Environmental Science & Technology.* 1998, 32, 1604-1608.

(81) Brusseau, M. L.; Jessup, R. E.; Rao, P. S. C. Nonequilibrium sorption of organic-chemicals - elucidation of rate-limiting processes. *Environmental Science & Technology.* 1991, 25, (1), 134-142.

(82) McGroddy S.E., F. J. W., Gschwend P.M. Comparison of the in situ and desorption sediment-water partitioning of polycyclic aromatic hydrocarbons and polychlorinated biphenyls *Environmental Science & Technology.* 1996, (30), 172-177.

(83) Schneider, A. R., Porter, E.T., Baker, J.E. Polychlorinated biphenyl release from resuspended Hudson River sediment. *Environmental Science & Technology.* 2007, 41, 1097-1103.

(84) You, J., Landrum, P.F., Lydy, M.J. Comparison of chemical approaches for assessing bioavailability of sediment-associated contaminants. *Environmental Science & Technology.* 2006, 40, 6348-6353.

(85) Connaughton, D. F., Stedinger, J.R., Lion, L.W., Shuler, M.L. Description of time-varying desorption-kinetics - release of naphthalene from contaminated soils. *Environmental Science & Technology.* 1993, 12, (2397-2403).

(86) Landrum, P. F., Robinson,S.D., Gossiaux, D.C., Jing, Y., Lydy M.J., Mitra, S., Ten Hulscher, T.E.M. Predicting bioavailability of sediment-associated organic contaminants for *Diporeia* spp. and oligochaetes. *Environmental Science & Technology.* 2007, 41.

(87) Shor, L. M.; Kosson, D. S.; Rockne, K. J.; Young, L. Y.; Taghon, G. L. Combined effects of contaminant desorption and toxicity on risk from PAH contaminated sediments. *Risk Analysis.* 2004, 24, (5), 1109-1120.

(88) Wood, L. W.; O'Keefe, P.; Bush, B. Similarity analysis of PAH and PCB bioaccumulation patterns in sediment-exposed *Chironomus tentans* larvae. *Environmental Toxicology and Chemistry.* 1997, 16, (2), 283-292.

(89) Kraaij, R.; Seinen, W.; Tolls, J. Direct evidence of sequestration in sediments affecting the bioavailability of hydrophobic organic chemicals to benthic deposit-feeders. *Environmental Science & Technology.* 2002, 36, (16), 3525-3529.

(90) Ghosh, U.; Luthy, R. G.; Talley, J. W.; Tucker, S.; Furey, J. S. Kinetics and thermodynamics of PAH desorption processes from sediment particles. *Abstracts of Papers of the American Chemical Society.* 2000, 220, U325.

(91) Ghosh, U.; Talley, J. W.; Luthy, R. G. Particle-scale investigation of PAH desorption kinetics and thermodynamics from sediment. *Environmental Science & Technology.* 2001, 35, (17), 3468-3475.

(92) Kan, A. T.; Fu, G. M.; Tomson, M. B. Adsorption-desorption hysteresis in organic pollutant and soil sediment interaction. *Environmental Science & Technology.* 1994, 28, (5), 859-867.

(93) Huang, W. L.; Weber, W. J. A distributed reactivity model for sorption by soils and sediments. 10. Relationships between desorption, hysteresis, and the chemical characteristics of organic domains. *Environmental Science & Technology.* 1997, 31, (9), 2562-2569.

(94) Braida, W. J.; Pignatello, J. J.; Lu, Y. F.; Ravikovitch, P. I.; Neimark, A. V.; Xing, B. S. Sorption hysteresis of benzene in charcoal particles. *Environmental Science & Technology.* 2003, 37, (2), 409-417.

(95) Elsner, M.; Schwarzenbach, R. P.; Haderlein, S. B. Reactivity of Fe(II)-bearing minerals toward reductive transformation of organic contaminants. *Environmental Science & Technology.* 2004, 38, (3), 799-807.

(96) Zwank, L.; Elsner, M.; Aeberhard, A.; Schwarzenbach, R. P.; Haderlein, S. B. Carbon isotope fractionation in the reductive dehalogenation of carbon tetrachloride at

iron (hydr)oxide and iron sulfide minerals. *Environmental Science & Technology.* 2005, 39, (15), 5634-5641.

(97) Williams, A. G. B.; Scherer, M. M. Spectroscopic evidence for Fe(II)-Fe(III) electron transfer at the iron oxide-water interface. *Environmental Science & Technology.* 2004, 38, (18), 4782-4790.

(98) Kriegman-King, M. R.; Reinhard, M. Transformation of carbon-tetrachloride by pyrite in aqueous-solution. *Environmental Science & Technology.* 1994, 28, (4), 692-700.

(99) Butler, E. C.; Hayes, K. F. Effects of solution composition and pH on the reductive dechlorination of hexachloroethane by iron sulfide. *Environmental Science & Technology.* 1998, 32, (9), 1276-1284.

(100) Heijman, C. G., Grieder, E., Holliger, C., Schwarzenbach, R.P. Reduction of nitroaromatic compounds coupled to microbial iron reduction in laboratory aquifer columns *Environmental Science & Technology.* 1995, 29, 775-783.

(101) Arnold, W. A.; Roberts, A. L. Pathways of chlorinated ethylene and chlorinated acetylene reaction with Zn(0). *Environmental Science & Technology.* 1998, 32, (19), 3017-3025.

(102) Arnold, W. A., Roberts, L.A. Pathways and kinetics of chlorinated ethylene and chlorinated acetylene reaction with Fe(0) particles *Environmental Science & Technology.* 2000, 34, (9), 1794-1805.

(103) Benoit JM, G. C., Heyes A, Mason RP, Miller CL. Geochemical and biological controls over methylmercury production and degradation in aquatic ecosystems. In *Biogeochemistry of Environmentally Important Trace Elements*; Yong Cai, O. C. B., Ed. Oxford University Press: Washington, D.C., 2003.

(104) Schallenberg, M.; Kalff, J. The ecology of sediment bacteria in lakes and comparisons with other aquatic ecosystems. *Ecology.* 1993, 74, (3), 919-934.

(105) Cole, J. J.; Findlay, S.; Pace, M. L. Bacterial production in fresh and saltwater ecosystems - a cross-system overview. *Marine Ecology-Progress Series.* 1988, 43, (1-2), 1-10.

(106) Hedin, L. O. Factors controlling sediment community respiration in woodland stream ecosystems. *Oikos.* 1990, 57, (1), 94-105.

(107) Wilms, R.; Sass, H.; Kopke, B.; Koster, H.; Cypionka, H.; Engelen, B. Specific bacterial, archaeal, and eukaryotic communities in tidal-flat sediments along a vertical profile of several meters. *Applied and Environmental Microbiology.* 2006, 72, (4), 2756-2764.

(108) Van Cappellen, P.; Gaillard, J.-F. Biogeochemical dynamics in aquatic sediments. In *Reactive Transport in Porous Media*; Lichtner, P. C.; Steefel, C. I.; Oelkers, E. H., Eds.; Mineralogical Society of America: Washington, DC, 1996.

(109) Atlas, R. M., Unterman, R. Bioremediation. In *Industrial Microbiology and Biotechnology*; 2 ed.; Atlas, R. M., Unterman, R., Ed. American Society for Microbiology (ASM) Press: Washington, D.C., 1999.

(110) Samanta, S. K.; Singh, O. V.; Jain, R. K. Polycyclic aromatic hydrocarbons: Environmental pollution and bioremediation. *Trends in Biotechnology.* 2002, 20, (6), 243-248.

(111) Bedard, D. L.; Wagner, R. E.; Brennan, M. J.; Haberl, M. L.; Brown, J. F. Extensive degradation of aroclors and environmentally transformed polychlorinated-biphenyls by *Alcaligenes eutrophus* H850. *Applied and Environmental Microbiology.* 1987, 53, (5), 1094-1102.

(112) Maltseva, O. V.; Tsoi, T. V.; Quensen, J. F.; Fukuda, M.; Tiedje, J. M. Degradation of anaerobic reductive dechlorination products of Aroclor 1242 by four aerobic bacteria. *Biodegradation.* 1999, 10, (5), 363-371.

(113) Bedard, D. L., Quensen, J.F. Microbial reductive dechlorination of polychlorinated biphenyls. In *Microbial Transformation and Degradation of Toxic Organic Chemicals*; Young, L. Y., Cerniglia, C.E., Ed. Wiley-Liss: New York, 1995.

(114) Bedard, D. L., Ritalahti, K.M, and F.E. Löffler. The *Dehalococcoides* population in sediment-free mixed cultures metabolically dechlorinates the commercial polychlorinated biphenyl mixture Aroclor 1260. *Applied and Environmental Microbiology.* 2007, 73, 2513-2521.

(115) He, J. Z.; Ritalahti, K. M.; Yang, K. L.; Koenigsberg, S. S.; Löffler, F. E. Detoxification of vinyl chloride to ethene coupled to growth of an anaerobic bacterium. *Nature.* 2003, 424, (6944), 62-65.

(116) Maymo-Gatell, X.; Chien, Y. T.; Gossett, J. M.; Zinder, S. H. Isolation of a bacterium that reductively dechlorinates tetrachloroethene to ethene. *Science.* 1997, 276, (5318), 1568-1571.

(117) Sung, Y.; Ritalahti, K. M.; Apkarian, R. P.; Löffler, F. E. Quantitative PCR confirms purity of strain GT, a novel trichloroethene-to-ethene-respiring *Dehalococcoides* isolate. *Applied and Environmental Microbiology.* 2006, 72, (3), 1980-1987.

(118) Cupples, A. M.; Spormann, A. M.; McCarty, P. L. Growth of a *Dehalococcoides*-like microorganism on vinyl chloride and *cis*-dichloroethene as electron acceptors as determined by competitive PCR. *Applied and Environmental Microbiology.* 2003, 69, (2), 953-959.

(119) Duhamel, M.; Mo, K.; Edwards, E. A. Characterization of a highly enriched *Dehalococcoides*-containing culture that grows on vinyl chloride and trichloroethene. *Applied and Environmental Microbiology.* 2004, 70, (9), 5538-5545.

(120) Yang, Y. R.; McCarty, P. L. Competition for hydrogen within a chlorinated solvent dehalogenating anaerobic mixed culture. *Environmental Science & Technology.* 1998, 32, (22), 3591-3597.

(121) Smatlak, C. R.; Gossett, J. M.; Zinder, S. H. Comparative kinetics of hydrogen utilization for reductive dechlorination of tetrachloroethene and methanogenesis in an anaerobic enrichment culture. *Environmental Science & Technology.* 1996, 30, (9), 2850-2858.

(122) Carr, C. S.; Hughes, J. B. Enrichment of high rate PCE dechlorination and comparative study of lactate, methanol, and hydrogen as electron dopers to sustain activity. *Environmental Science & Technology.* 1998, 32, (12), 1817-1824.

(123) Fennell, D. E.; Gossett, J. M.; Zinder, S. H. Comparison of butyric kid, ethanol, lactic acid, and propionic acid as hydrogen donors for the reductive dechlorination of tetrachloroethene. *Environmental Science & Technology.* 1997, 31, (3), 918-926.

(124) Adrian, L.; Szewzyk, U.; Wecke, J.; Gorisch, H. Bacterial dehalorespiration with chlorinated benzenes. *Nature.* 2000, 408, (6812), 580-583.

(125) Bunge, M.; Adrian, L.; Kraus, A.; Opel, M.; Lorenz, W. G.; Andreesen, J. R.; Gorisch, H.; Lechner, U. Reductive dehalogenation of chlorinated dioxins by an anaerobic bacterium. *Nature.* 2003, 421, (6921), 357-360.

(126) Adrian, L., Hansen, S.K., Fung, J.M., Gorisch, H., Zinder, S.H. Growth of dehalococcoides strains with chlorophenols as electron acceptors *Environmental Science & Technology.* 2007, 41, 2318-2323.

(127) He, J. Z.; Robrock, K. R.; Alvarez-Cohen, L. Microbial reductive debromination of polybrominated diphenyl ethers (PBDEs). *Environmental Science & Technology.* 2006, 40, (14), 4429-4434.

(128) Cole, J. R., Fathepure, B.Z., and Tiedje, J.M. Tetrachloroethene and 3-chlorobenzoate dechlorination activities are co-induced in *Desulfomonile tiedjei* DCB-1. *Biodegradation.* 1995, 6, (2), 167-172.

(129) Holliger, C.; Hahn, D.; Harmsen, H.; Ludwig, W.; Schumacher, W.; Tindall, B.; Vazquez, F.; Weiss, N.; Zehnder, A. J. B. Dehalobacter restrictus gen. nov. and sp. nov., a strictly anaerobic bacterium that reductively dechlorinates tetra- and trichloroethene in an anaerobic respiration. *Archives of Microbiology.* 1998, 169, (4), 313-321.

(130) Krumholz, L. R.; Sharp, R.; Fishbain, S. S. A freshwater anaerobe coupling acetate oxidation to tetrachloroethylene dehalogenation. *Applied and Environmental Microbiology.* 1996, 62, (11), 4108-4113.

(131) Daprato, R. C. Population dynamics of tetrachloroethene dechlorinating consortia for surfactant and bioaugmentation remediation applications. Rice University, Houston, TX, 2006.

(132) Dolan, M. E.; Mccarthy, P. L. Methanotrophic chloroethene transformation capacities and 1,1-dichloroethene transformation product toxicity. *Environmental Science & Technology.* 1995, 29, (11), 2741-2747.

(133) Fox, B. G.; Borneman, J. G.; Wackett, L. P.; Lipscomb, J. D. Haloalkene oxidation by the soluble methane monooxygenase from methylosinus-trichosporium OB3B - mechanistic and environmental implications. *Biochemistry.* 1990, 29, (27), 6419-6427.

(134) Magar, V. S.; Brenner, R. C.; Johnson, G. W.; Quensen, J. F. Long-term recovery of pcb-contaminated sediments at the Lake Hartwell superfund site: PCB dechlorination. 2. Rates and extent. *Environmental Science & Technology.* 2005, 39, (10), 3548-3554.

(135) Pakdeesusuk, U.; Lee, C. M.; Coates, J. T.; Freedman, D. L. Assessment of natural attenuation via in situ reductive dechlorination of polychlorinated biphenys in sediments of the Twelve Mile Creek arm of Lake Hartwell, SC. *Environmental Science & Technology.* 2005, 39, (4), 945-952.

(136) USEPA. Contaminated Sediment Remediation Guidance for Hazardous Waste Sites, Office of Solid Waste and Emergency Response, 2005, EPA-540-R05-012.

(137) Van den Berg, G. A.; Meijers, G. G. A.; Van der Heijdt, L. M.; Zwolsman, J. J. G. Dredging-related mobilisation of trace metals: A case study in the netherlands. *Water Research.* 2001, 35, (8), 1979-1986.

(138) Maddock, J. E. L.; Carvalho, M. F.; Santelli, R. E.; Machado, W. Contaminant metal behaviour during re-suspension of sulphidic estuarine sediments. *Water Air and Soil Pollution.* 2007, 181, (1-4), 193-200.

(139) Ravikrishna, R.; Valsaraj, K. T.; Thibodeaux, L. J.; Price, C. B.; Brannon, J. M.; Yost, S. Volatilization of contaminants from suspended sediment in a water column during dredging. *Journal of the Air & Waste Management Association.* 2002, 52, (10), 1214-1229.

(140) Je, C.; Kim, K. Web-based application for estimating water quality impacts due to environmental dredging. *Environmental Geology.* 2004, 46, (2), 217-225.

(141) Nayar, S.; Goh, B. P. L.; Chou, L. M. Environmental impact of heavy metals from dredged and resuspended sediments on phytoplankton and bacteria assessed in in situ mesocosms. *Ecotoxicology and Environmental Safety.* 2004, 59, (3), 349-369.

(142) Reible, D.; Hayes, D.; Lue-Hing, C.; Patterson, J.; Bhowmik, N.; Johnson, M.; Teal, J. Comparison of the long-term risks of removal and in situ management of contaminated sediments in the Fox River. *Soil & Sediment Contamination.* 2003, 12, (3), 325-344.

(143) Palermo, M.; Maynord, S.; Miller, J.; Reible, D. Guidance for in situ subaqueous capping of contaminanted sediments, 1998, Great Lakes National Program Office, USEPA, EPA 905-B96-004.

(144) Hazardous Substance Research Center - South and Southwest. Summary of contaminated sediment capping projects, Accessed October, 2007. http://www.hsrc-ssw.org/capsummary.pdf.

(145) Palermo, M. Design considerations for in-situ capping of contaminated sediments. *Water Science and Technology.* 1998, 37, (6-7), 315-321.

(146) Mohan, R. K.; Brown, M. P.; Barnes, C. R. Design criteria and theoretical basis for capping contaminated marine sediments. *Applied Ocean Research.* 2000, 22, (2), 85-93.

(147) Zeman, A. J. Subaqueous capping of very soft contaminated sediments. *Canadian Geotechnical Journal.* 1994, 31, (4), 570-577.

(148) Moo-Young, H.; Myers, T.; Tardy, B.; Ledbetter, R.; Vanadit-Ellis, W.; Kim, T. H. Centrifuge simulation of the consolidation characteristics of capped marine sediment beds. *Engineering Geology.* 2003, 70, (3-4), 249-258.

(149) Moo-Young, H.; Myers, T.; Tardy, B.; Ledbetter, R.; Vanadit-Ellis, W.; Sellasie, K. Determination of the environmental impact of consolidation induced convective transport through capped sediment. *Journal of Hazardous Materials.* 2001, 85, (1-2), 53-72.

(150) Alshawabkeh, A. N.; Rahbar, N.; Sheahan, T. A model for contaminant mass flux in capped sediment under consolidation. *Journal of Contaminant Hydrology.* 2005, 78, (3), 147-165.

(151) Thoma, G. J.; Reible, D. D.; Valsaraj, K. T.; Thibodeaux, L. J. Efficiency of capping contaminated sediments in-situ .2. Mathematics of diffusion adsorption in the capping layer. *Environmental Science & Technology.* 1993, 27, (12), 2412-2419.

(152) SERDP and ESTCP Expert Panel Workshop on Research and Development Needs for the In Situ Management of Contaminated Sediments, Final Report, 2004.

(153) Kaplan, D. I.; Knox, A. S. Enhanced contaminant desorption induced by phosphate mineral additions to sediment. *Environmental Science & Technology.* 2004, 38, (11), 3153-3160.

(154) Jacobs, P. H.; Forstner, U. Concept of subaqueous capping of contaminated sediments with active barrier systems (ABS) using natural and modified zeolites. *Water Research.* 1999, 33, (9), 2083-2087.

(155) Tarabara, V. V.; Wiesner, M. R. Physical and transport properties of bentonite-cement composites: A new material for in situ capping of contaminated underwater sediments. *Environmental Engineering Science.* 2005, 22, (5), 578-590.

(156) Murphy, P.; Marquette, A.; Reible, D.; Lowry, G. V. Predicting the performance of activated carbon-, coke-, and soil-amended thin layer sediment caps. *Journal of Environmental Engineering-Asce.* 2006, 132, (7), 787-794.

(157) Lowry, G. V., Johnson, K.M. In situ containment and treatment of pcb-contaminated sediments using Fe(0)- and coke-amended "active" sediment caps. In *EPRI technical report #1005508: Current practices in in-situ contaminated sediment capping*; EPRI: Cincinnati, OH, 2003.

(158) Reible, D. D., Lampert, D., Constant, D.W., Mutch, R.D., Zhu, Y. Active capping demonstration in the Anacostia River, Washington, DC. *Remediation.* 2007, 17, (1), 39-53.

(159) Lendvay, J. M.; Löffler, F. E.; Dollhopf, M.; Aiello, M. R.; Daniels, G.; Fathepure, B. Z.; Gebhard, M.; Heine, R.; Helton, R.; Shi, J.; Krajmalnik-Brown, R.; Major, C. L.; Barcelona, M. J.; Petrovskis, E.; Hickey, R.; Tiedje, J. M.; Adriaens, P. Bioreactive barriers: A comparison of bioaugmentation and biostimulation for chlorinated solvent remediation. *Environmental Science & Technology.* 2003, 37, (7), 1422-1431.

(160) Ellis, D. E.; Lutz, E. J.; Odom, J. M.; Buchanan, R. J.; Bartlett, C. L.; Lee, M. D.; Harkness, M. R.; Deweerd, K. A. Bioaugmentation for accelerated in situ anaerobic bioremediation. *Environmental Science & Technology.* 2000, 34, (11), 2254-2260.

(161) Song, D. L.; Conrad, M. E.; Sorenson, K. S.; Alvarez-Cohen, L. Stable carbon isotope fractionation during enhanced in situ bioremediation of trichloroethene. *Environmental Science & Technology.* 2002, 36, (10), 2262-2268.

(162) Major, D. W.; McMaster, M. L.; Cox, E. E.; Edwards, E. A.; Dworatzek, S. M.; Hendrickson, E. R.; Starr, M. G.; Payne, J. A.; Buonamici, L. W. Field demonstration of successful bioaugmentation to achieve dechlorination of tetrachloroethene to ethene. *Environmental Science & Technology.* 2002, 36, (23), 5106-5116.

(163) Rodriguez, E.; McGuinness, K. A.; Ophori, D. U. A field evaluation of enhanced reductive dechlorination of chlorinated solvents in groundwater, New York metropolitan area. *Environmental Geology.* 2004, 45, (5), 623-632.

(164) Da Silva, M. L. B.; Daprato, R. C.; Gomez, D. E.; Hughes, J. B.; Ward, C. H.; Alvarez, P. J. J. Comparison of bioaugmentation and biostimulation for the enhancement of dense nonaqueous phase liquid source zone bioremediation. *Water Environment Research.* 2006, 78, (13), 2456-2465.

(165) Dybas, M. J.; Hyndman, D. W.; Heine, R.; Tiedje, J.; Linning, K.; Wiggert, D.; Voice, T.; Zhao, X.; Dybas, L.; Criddle, C. S. Development, operation, and long-term performance of a full-scale biocurtain utilizing bioaugmentation. *Environmental Science & Technology.* 2002, 36, (16), 3635-3644.

(166) Jorgensen, B. B.; Revsbech, N. P. Diffusive boundary-layers and the oxygen-uptake of sediments and detritus. *Limnology and Oceanography.* 1985, 30, (1), 111-122.

(167) Nakamura, Y., Satoh, H., Okabe, S., Watanabe, Y. Photosynthesis in sediments determined at high spatial resolution by the use of microelectrodes. *Water Research.* 2004, 38, 2440-2448.

(168) Zehnder, A. J. B.; Stumm, W. Geochemistry and biogeochemistry of anaerobic habitats. In *Biology of Anaerobic Microorganisms*; Zehnder, A. J. B., Ed. Wiley: New York, 1988.

(169) Stumm, W., Morgan, J.J. *Aquatic Chemistry*; 3 ed.; John Wiley & Sons: New York, 1996.

(170) Koretsky, C. M.; Haas, J. R.; Ndenga, N. T.; Miller, D. Seasonal variations in vertical redox stratification and potential influence on trace metal speciation in minerotrophic peat sediments. *Water Air and Soil Pollution.* 2006, 173, (1-4), 373-403.

(171) Koretsky, C. M.; Haas, J. R.; Miller, D.; Ndenga, N. T. Seasonal variations in pore water and sediment geochemistry of littoral lake sediments (Asylum Lake, MI, USA). *Geochemical Transactions.* 2006, 7, -.

(172) Koretsky, C. M.; Van Cappellen, P.; DiChristina, T. J.; Kostka, J. E.; Lowe, K. L.; Moore, C. M.; Roychoudhury, A. N.; Viollier, E. Salt marsh pore water geochemistry does not correlate with microbial community structure. *Estuarine Coastal and Shelf Science.* 2005, 62, (1-2), 233-251.

(173) Sell, K. S.; Morse, J. W. Dissolved Fe^{2+} and ΣH_2S behavior in sediments seasonally overlain by hypoxic-to-anoxic waters as determined by CSV microelectrodes. *Aquatic Geochemistry.* 2006, 12, (2), 179-198.

(174) Böttcher, M. E.; Thamdrup, B. Anaerobic sulfide oxidation and stable isotope fractionation associated with bacterial sulfur disproportionation in the presence of MnO_2. *Geochimica Et Cosmochimica Acta.* 2001, 65, (10), 1573-1581.

(175) Postma, D. Concentration of mn and separation from Fe in sediments. 1. Kinetics and stoichiometry of the reaction between binessite and dissolved Fe(II) at 10 degrees C. *Geochimica Et Cosmochimica Acta.* 1985, 49, (4), 1023-1033.

(176) Myers, C. R.; Nealson, K. H. Bacterial manganese reduction and growth with manganese oxide as the sole electron-acceptor. *Science.* 1988, 240, (4857), 1319-1321.

(177) Thamdrup, B. Bacterial manganese and iron reduction in aquatic sediments. *Advances in Microbial Ecology, Vol 16.* 2000, 16, 41-84.

(178) Hem, J. D. Rates of manganese oxidation in aqueous systems. *Geochimica Et Cosmochimica Acta.* 1981, 45, (8), 1369-1374.

(179) Diem, D.; Stumm, W. Is dissolved Mn^{2+} being oxidized by O_2 in absence of Mn-bacteria or surface catalysts. *Geochimica Et Cosmochimica Acta.* 1984, 48, (7), 1571-1573.

(180) Canfield, D. E. The geochemistry of river particulates from the continental USA: Major elements. *Geochimica Et Cosmochimica Acta.* 1997, 61, (16), 3349-3365.

(181) Kostka, J. E.; Luther, G. W. Partitioning and speciation of solid-phase iron in salt-marsh sediments. *Geochimica Et Cosmochimica Acta.* 1994, 58, (7), 1701-1710.

(182) Reguera, G.; McCarthy, K. D.; Mehta, T.; Nicoll, J. S.; Tuominen, M. T.; Lovley, D. R. Extracellular electron transfer via microbial nanowires. *Nature.* 2005, 435, (7045), 1098-1101.

(183) Taillefert, M., Beckler, J.S., Carey, E., Burns, J.L., Fennessey, C.M., DiChristina, T.D. *Shewanella putrefaciens* produces an Fe(III)-solubilizing organic ligand during anaerobic respiration on insoluble Fe(III) oxides. *Journal of Inorganic Biochemistry*, in press.

(184) Lovley, D. R.; Coates, J. D.; Blunt-Harris, E. L.; Phillips, E. J. P.; Woodward, J. C. Humic substances as electron acceptors for microbial respiration. *Nature.* 1996, 382, (6590), 445-448.

(185) Nevin, K. P.; Lovley, D. R. Mechanisms for accessing insoluble Fe(III) oxide during dissimilatory Fe(III) reduction by *Geothrix fermentans*. *Applied and Environmental Microbiology.* 2002, 68, (5), 2294-2299.

(186) Kostka, J. E.; Haefele, E.; Viehweger, R.; Stucki, J. W. Respiration and dissolution of iron(III) containing clay minerals by bacteria. *Environmental Science & Technology.* 1999, 33, (18), 3127-3133.

(187) Taillefert, M.; Bono, A. B.; Luther, G. W. Reactivity of freshly formed Fe(III) in synthetic solutions and (pore)waters: Voltammetric evidence of an aging process. *Environmental Science & Technology.* 2000, 34, (11), 2169-2177.

(188) Weber, K. A.; Achenbach, L. A.; Coates, J. D. Microorganisms pumping iron: Anaerobic microbial iron oxidation and reduction. *Nature Reviews Microbiology.* 2006, 4, (10), 752-764.

(189) Yao, W. S.; Millero, F. J. Oxidation of hydrogen sulfide by hydrous Fe(III) oxides in seawater. *Marine Chemistry.* 1996, 52, (1), 1-16.

(190) Peiffer, S.; Afonso, M. D.; Wehrll, B.; Gachter, R. Kinetics and mechanism of the reaction of H_2S with lepidocrocite. *Environmental Science & Technology.* 1992, 26, (12), 2408-2413.

(191) Davison, W.; Seed, G. The kinetics of the oxidation of ferrous iron in synthetic and natural-waters. *Geochimica Et Cosmochimica Acta.* 1983, 47, (1), 67-79.

(192) Weber, K. A.; Urrutia, M. M.; Churchill, P. F.; Kukkadapu, R. K.; Roden, E. E. Anaerobic redox cycling of iron by freshwater sediment microorganisms. *Environmental Microbiology.* 2006, 8, (1), 100-113.

(193) Holmer, M.; Storkholm, P. Sulphate reduction and sulphur cycling in lake sediments: A review. *Freshwater Biology.* 2001, 46, (4), 431-451.

(194) Hoehler, T. M.; Alperin, M. J.; Albert, D. B.; Martens, C. S. Field and laboratory studies of methane oxidation in an anoxic marine sediment - evidence for a methanogen-sulfate reducer consortium. *Global Biogeochemical Cycles.* 1994, 8, (4), 451-463.

(195) Boetius, A.; Ravenschlag, K.; Schubert, C. J.; Rickert, D.; Widdel, F.; Gieseke, A.; Amann, R.; Jorgensen, B. B.; Witte, U.; Pfannkuche, O. A marine microbial consortium apparently mediating anaerobic oxidation of methane. *Nature.* 2000, 407, (6804), 623-626.

(196) Wagner, M.; Loy, A.; Klein, M.; Lee, N.; Ramsing, N. B.; Stahl, D. A.; Friedrich, M. W. Functional marker genes for identification of sulfate-reducing prokaryotes. *Environmental Microbiology.* 2005, 397, 469-489.

(197) Widdel, F. Microbiology and ecology of sulfate- and sulfur-reducing bacteria. In *Biology of Anaerobic Microorganisms*; Zehnder, A. J. B., Ed. John Wiley & Sons: New York, 1988.

(198) Bak, F.; Pfennig, N. Chemolithotrophic growth of *Desulfovibrio sulfodismutans* sp. nov. by disproportionation of inorganic sulfur-compounds. *Archives of Microbiology.* 1987, 147, (2), 184-189.

(199) Theberge, S. M.; Luther, G. W. Determination of the electrochemical properties of a soluble aqueous FeS species present in sulfidic solutions. *Aquatic Geochemistry.* 1997, 3, (3), 191-211.

(200) Rickard, D., Schoonen, M.A.A., Luther, G.W. Chemistry of iron sulfides in sedimentary environments. In *Geochemical Transformations of Sedimentary Sulfur*; Vairavamurthy, V., Schoonen, M.A.A., Eds. American Chemical Society: Washington, D.C., 1995.

(201) Van Cappellen, P.; Wang, Y. F. Cycling of iron and manganese in surface sediments: A general theory for the coupled transport and reaction of carbon, oxygen, nitrogen, sulfur, iron, and manganese. *American Journal of Science.* 1996, 296, (3), 197-243.

(202) Thamdrup, B., Finster, K., Hansen, J.W., and Bak, F. Bacterial disproportionation of elemental sulfur coupled to chemical reduction of iron or manganese. *Applied and Environmental Microbiology.* 1993, 59, (1), 101-108.

(203) Jörgensen, B. B.; Bak, F. Pathways and microbiology of thiosulfate transformations and sulfate reduction in a marine sediment (Kattegat, Denmark). *Applied and Environmental Microbiology.* 1991, 57, (3), 847-856.

(204) Bonnissel-Gissinger, P.; Alnot, M.; Ehrhardt, J. J.; Behra, P. Surface oxidation of pyrite as a function of pH. *Environmental Science & Technology.* 1998, 32, (19), 2839-2845.

(205) Madigan, M. T., Martinko. J.M. *Brock Biology of Microorganisms*; 11 ed.; Pearson Prentice Hall: Upper Saddle River, NJ, 2006.

(206) Vogels, G. D., Keltjens, J.T., van der Drift, C. Biochemistry of methane production. In *Biology of Anaerobic Microorganisms*; Zehnder, A. J. B., Ed. John Wiley & Sons: New York, 1988.

(207) Friedrich, M. W. Methyl-coenzyme m reductase genes: Unique functional markers for methanogenic and anaerobic methane-oxidizing archaea. *Environmental Microbiology.* 2005, 397, 428-442.

(208) Hallam, S. J.; Girguis, P. R.; Preston, C. M.; Richardson, P. M.; DeLong, E. F. Identification of methyl-coenzyme m reductase A (*mcrA*) genes associated with methane-oxidizing archaea. *Applied and Environmental Microbiology.* 2003, 69, (9), 5483-5491.

(209) Hallam, S. J.; Putnam, N.; Preston, C. M.; Detter, J. C.; Rokhsar, D.; Richardson, P. M.; DeLong, E. F. Reverse methanogenesis: Testing the hypothesis with environmental genomics. *Science.* 2004, 305, (5689), 1457-1462.

(210) Viollier, E.; Rabouille, C.; Apitz, S. E.; Breuer, E.; Chaillou, G.; Dedieu, K.; Furukawa, Y.; Grenz, C.; Hall, P.; Janssen, F.; Morford, J. L.; Poggiale, J. C.; Roberts, S.; Shimmield, T.; Taillefert, M.; Tengberg, A.; Wenzhofer, F.; Witte, U. Benthic biogeochemistry: State of the art technologies and guidelines for the future of in situ survey. *Journal of Experimental Marine Biology and Ecology.* 2003, 285, 5-31.

(211) Taillefert, M.; Luther, G. W.; Nuzzio, D. B. The application of electrochemical tools for in situ measurements in aquatic systems. *Electroanalysis.* 2000, 12, (6), 401-412.

(212) Taillefert, M.; Rozan, T. F. Electrochemical methods for the environmental analysis of trace elements biogeochemistry. In *Environmental Electrochemistry: Analysis of Trace Element Biogeochemistry*; Taillefert, M.; Rozan, T. F., Eds.; Oxford University Press: Washington, D.C., 2002.

(213) Reimers, C. E. Applications of microelectrodes to problems in chemical oceanography. *Chemical Reviews.* 2007, 107, (2), 590-600.

(214) Revsbech, N. P.; Nielsen, L. P.; Ramsing, N. B. A novel microsensor for determination of apparent diffusivity in sediments. *Limnology and Oceanography.* 1998, 43, (5), 986-992.

(215) Larsen, L. H.; Kjaer, T.; Revsbech, N. P. A microscale NO_3^- biosensor for environmental applications. *Analytical Chemistry.* 1997, 69, (17), 3527-3531.

(216) Kuhl, M.; Steuckart, C.; Eickert, G.; Jeroschewski, P. A H_2S microsensor for profiling biofilms and sediments: Application in an acidic lake sediment. *Aquatic Microbial Ecology.* 1998, 15, (2), 201-209.

(217) Damgaard, L. A.; Revsbech, N. P. A microscale biosensor for methane containing methanotrophic bacteria and an internal oxygen reservoir. *Analytical Chemistry.* 1997, 69, (13), 2262-2267.

(218) Cai, W. J.; Reimers, C. E. The development of pH and pCO_2 microelectrodes for studying the carbonate chemistry of pore waters near the sediment-water interface. *Limnology and Oceanography.* 1993, 38, (8), 1762-1773.

(219) Revsbech, N. P.; Jorgensen, B. B.; Blackburn, T. H.; Cohen, Y. Microelectrode studies of the photosynthesis and O_2, H_2S, and pH profiles of a microbial mat. *Limnology and Oceanography.* 1983, 28, (6), 1062-1074.

(220) Zhao, P. S.; Cai, W. J. An improved potentiometric pCO_2 microelectrode. *Analytical Chemistry.* 1997, 69, (24), 5052-5058.

(221) Muller, B.; Buis, K.; Stierli, R.; Wehrli, B. High spatial resolution measurements in lake sediments with PVC based liquid membrane ion-selective electrodes. *Limnology and Oceanography.* 1998, 43, (7), 1728-1733.

(222) Brendel, P. J.; Luther, G. W. Development of a gold amalgam voltammetric microelectrode for the determination of dissolved Fe, Mn, O_2, and S(-II) in porewaters of marine and fresh-water sediments. *Environmental Science & Technology.* 1995, 29, (3), 751-761.

(223) Lewis, B. L.; Glazer, B. T.; Montbriand, P. J.; Luther, G. W.; Nuzzio, D. B.; Deering, T.; Ma, S.; Theberge, S. Short-term and interannual variability of redox-sensitive chemical parameters in hypoxic/anoxic bottom waters of the Chesapeake Bay. *Marine Chemistry.* 2007, 105, (3-4), 296-308.

(224) Taillefert, M.; Neuhuber, S.; Bristow, G. The effect of tidal forcing on biogeochemical processes in intertidal salt marsh sediments. *Geochemical Transactions.* 2007, 8, -.

(225) Komada, T.; Reimers, C. E.; Luther, G. W.; Burdige, D. J. Factors affecting dissolved organic matter dynamics in mixed-redox to anoxic coastal sediments. *Geochimica Et Cosmochimica Acta.* 2004, 68, (20), 4099-4111.

(226) Luther, G. W.; Rozan, T. F.; Taillefert, M.; Nuzzio, D. B.; Di Meo, C.; Shank, T. M.; Lutz, R. A.; Cary, S. C. Chemical speciation drives hydrothermal vent ecology. *Nature.* 2001, 410, (6830), 813-816.

(227) Ma, S. F.; Noble, A.; Butcher, D.; Trouwborst, R. E.; Luther, G. W. Removal of H_2S via an iron catalytic cycle and iron sulfide precipitation in the water column of dead end tributaries. *Estuarine Coastal and Shelf Science.* 2006, 70, (3), 461-472.

(228) SERDP and ESTCP Expert Panel Workshop on Reserch and Development Needs for the Environmental Remediation Application of Molecular Biological Tools, Final Report. 2005.

(229) Heid, C. A.; Stevens, J.; Livak, K. J.; Williams, P. M. Real time quantitative PCR. *Genome Research.* 1996, 6, (10), 986-994.

(230) Harms, G.; Layton, A. C.; Dionisi, H. M.; Gregory, I. R.; Garrett, V. M.; Hawkins, S. A.; Robinson, K. G.; Sayler, G. S. Real-time PCR quantification of nitrifying bacteria in a municipal wastewater treatment plant. *Environmental Science & Technology.* 2003, 37, (2), 343-351.

(231) Ritalahti, K. M.; Amos, B. K.; Sung, Y.; Wu, Q. Z.; Koenigsberg, S. S.; Löffler, F. E. Quantitative PCR targeting 16S rRNA and reductive dehalogenase genes simultaneously monitors multiple *Dehalococcoides* strains. *Applied and Environmental Microbiology.* 2006, 72, (4), 2765-2774.

(232) Michalsen, M. M.; Peacock, A. D.; Spain, A. M.; Smithgal, A. N.; White, D. C.; Sanchez-Rosario, Y.; Krumholz, L. R.; Istok, J. D. Changes in microbial community composition and geochemistry during uranium and technetium bioimmobilization. *Applied and Environmental Microbiology.* 2007, 73, (18), 5885-5896.

(233) Schippers, A.; Neretin, L. N. Quantification of microbial communities in near-surface and deeply buried marine sediments on the Peru continental margin using real-time PCR. *Environmental Microbiology.* 2006, 8, (7), 1251-1260.

(234) Anderson, R. T.; Vrionis, H. A.; Ortiz-Bernad, I.; Resch, C. T.; Long, P. E.; Dayvault, R.; Karp, K.; Marutzky, S.; Metzler, D. R.; Peacock, A.; White, D. C.; Lowe, M.; Lovley, D. R. Stimulating the in situ activity of *Geobacter* species to remove uranium from the groundwater of a uranium-contaminated aquifer. *Applied and Environmental Microbiology.* 2003, 69, (10), 5884-5891.

(235) North, N. N.; Dollhopf, S. L.; Petrie, L.; Istok, J. D.; Balkwill, D. L.; Kostka, J. E. Change in bacterial community structure during in situ biostimulation of subsurface sediment cocontaminated with uranium and nitrate. *Applied and Environmental Microbiology.* 2004, 70, (8), 4911-4920.

(236) Cummings, D. E.; Snoeyenbos-West, O. L.; Newby, D. T.; Niggemyer, A. M.; Lovley, D. R.; Achenbach, L. A.; Rosenzweig, R. F. Diversity of geobacteraceae species inhabiting metal-polluted freshwater lake sediments ascertained by 16S rDNA analyses. *Microbial Ecology.* 2003, 46, (2), 257-269.

(237) Smits, T. H. M.; Devenoges, C.; Szynalski, K.; Maillard, J.; Holliger, C. Development of a real-time PCR method for quantification of the three genera *Dehalobacter*, *Dehalococcoides*, and *Desulfitobacterium* in microbial communities. *Journal of Microbiological Methods.* 2004, 57, (3), 369-378.

(238) Wilms, R.; Sass, H.; Kopke, B.; Cypionka, H.; Engelen, B. Methane and sulfate profiles within the subsurface of a tidal flat are reflected by the distribution of sulfate-reducing bacteria and methanogenic archaea. *FEMS Microbiology Ecology.* 2007, 59, (3), 611-621.

(239) Dunbar, J.; Ticknor, L. O.; Kuske, C. R. Phylogenetic specificity and reproducibility and new method for analysis of terminal restriction fragment profiles of 16S rRNA genes from bacterial communities. *Applied and Environmental Microbiology.* 2001, 67, (1), 190-197.

(240) Marsh, T. L. Terminal restriction fragment length polymorphism (T-RFLP): An emerging method for characterizing diversity among homologous populations of amplification products. *Current Opinion in Microbiology.* 1999, 2, (3), 323-327.

(241) Kitts, C. Terminal restriction fragment patterns: A tool for comparing microbial communities and assessing community dynamics. *Current Issues of Interest in Microbiology* 2001, 2, (1), 17-25.

(242) Thies, J. E. Soil microbial community analysis using terminal restriction fragment length polymorphisms. *Soil Science Society of America Journal.* 2007, 71, (2), 579-591.

(243) Noll, M.; Matthies, D.; Frenzel, P.; Derakshani, M.; Liesack, W. Succession of bacterial community structure and diversity in a paddy soil oxygen gradient. *Environmental Microbiology.* 2005, 7, (3), 382-395.

(244) Urakawa, H.; Yoshida, T.; Nishimura, M.; Ohwada, K. Characterization of depth-related population variation in microbial communities of a coastal marine sediment using 16S rDNA-based approaches and quinone profiling. *Environmental Microbiology.* 2000, 2, (5), 542-554.

(245) Lin, X. J.; Scranton, M. I.; Varela, R.; Chistoserdov, A.; Taylor, G. T. Compositional responses of bacterial communities to redox gradients and grazing in the anoxic cariaco basin. *Aquatic Microbial Ecology.* 2007, 47, (1), 57-72.

(246) Pett-Ridge, J.; Firestone, M. K. Redox fluctuation structures microbial communities in a wet tropical soil. *Applied and Environmental Microbiology.* 2005, 71, (11), 6998-7007.

(247) Schwarz, J. I. K.; Eckert, W.; Conrad, R. Community structure of archaea and bacteria in a profundal lake sediment Lake Kinneret (Israel). *Systematic and Applied Microbiology.* 2007, 30, (3), 239-254.

(248) Rahm, B. G.; Chauhan, S.; Holmes, V. F.; Macbeth, T. W.; Sorenson, K. S. J.; Alvarez-Cohen, L. Molecular characterization of microbial populations at two sites with differing reductive dechlorination abilities. *Biodegradation.* 2006, 17, (6), 523-534.

(249) Kemnitz, D.; Kolb, S.; Conrad, R. Phenotypic characterization of rice cluster III archaea without prior isolation by applying quantitative polymerase chain reaction to an enrichment culture. *Environmental Microbiology.* 2005, 7, (4), 553-565.

(250) Braker, G.; Ayala-del-Rio, H. L.; Devol, A. H.; Fesefeldt, A.; Tiedje, J. M. Community structure of denitrifiers, bacteria, and archaea along redox gradients in pacific northwest marine sediments by terminal restriction fragment length polymorphism analysis of amplified nitrite reductase (*nirS*) and 16S rRNA genes. *Applied and Environmental Microbiology.* 2001, 67, (4), 1893-1901.

(251) Dong, H. L.; Zhang, G. X.; Jiang, H. C.; Yu, B. S.; Chapman, L. R.; Lucas, C. R.; Fields, M. W. Microbial diversity in sediments of saline Qinghai Lake, China: Linking geochemical controls to microbial ecology. *Microbial Ecology.* 2006, 51, (1), 65-82.

(252) Tankere, S. P. C.; Bourne, D. G.; Muller, F. L. L.; Torsvik, V. Microenvironments and microbial community structure in sediments. *Environmental Microbiology.* 2002, 4, (2), 97-105.

(253) Ludemann, H.; Arth, I.; Liesack, W. Spatial changes in the bacterial community structure along a vertical oxygen gradient in flooded paddy soil cores. *Applied and Environmental Microbiology.* 2000, 66, (2), 754-762.

(254) Severmann, S.; Mills, R. A.; Palmer, M. R.; Telling, J. P.; Cragg, B.; Parkes, R. J. The role of prokaryotes in subsurface weathering of hydrothermal sediments: A combined geochemical and microbiological investigation. *Geochimica Et Cosmochimica Acta.* 2006, 70, (7), 1677-1694.

(255) Taillefert, M. M., B.J.; Gaillard, J.-F.; Lienemann, C.-P.; Perret, D.; Stahl, D.A. Evidence for a dynamic cycle between Mn and Co in the water column of a stratified lake. *Environmental Science & Technology.* 2002, 36, 468-476.

(256) Lowe, K. L. D., T.J.; Roychoudhury, A. N.; Van Cappellen, P. . Microbiological and geochemical characterization of microbial Fe(III) reduction in salt marsh sediments. *Geomicrobiology Journal.* 2000, 17, 163-178.

(257) USEPA. The Incidence and Severity of Sediment Contamination in Surface Waters of the United States, National Sediment Quality Survey: Second edition. Office of Solid Waste and Emergency Response, 2004.

(258) Drzyzga, O.; EL Mamouni, R.; Agathos, S. N.; Gottschal, J. C. Dehalogenation of chlorinated ethenes and immobilization of nickel in anaerobic sediment columns under sulfidogenic conditions. *Environmental Science & Technology.* 2002, 36, (12), 2630-2635.

(259) Azcue, J. M.; Zeman, A. J.; Mudroch, A.; Rosa, F.; Patterson, T. Assessment of sediment and porewater after one year of subaqueous capping of contaminated sediments in Hamilton Harbour, Canada. *Water Science and Technology.* 1998, 37, (6-7), 323-329.

(260) Himmelheber, D. W., Pennell, Kurt D., Hughes, Joseph B. Natural attenuation processes during in situ capping. *Environmental Science & Technology.* 2007, 41, (15), 5306-5313.

(261) Bristow, G., Taillefert, M. Voltint: A matlab-based program for semi-automated processing of geochemical data acquired by voltammetry. *Computers & Geosciences,* in press.

(262) Rickard, D. Kinetics of FeS precipitation. 1. Competing reaction-mechanisms. *Geochimica Et Cosmochimica Acta.* 1995, 59, (21), 4367-4379.

(263) Postma, D.; Jakobsen, R. Redox zonation: Equilibrium constraints on the Fe(III)/SO_4^- reduction interface. *Geochimica Et Cosmochimica Acta.* 1996, 60, (17), 3169-3175.

(264) Kirk, M. F.; Holm, T. R.; Park, J.; Jin, Q. S.; Sanford, R. A.; Fouke, B. W.; Bethke, C. M. Bacterial sulfate reduction limits natural arsenic contamination in groundwater. *Geology.* 2004, 32, (11), 953-956.

(265) Lovley, D. R.; Klug, M. J. Model for the distribution of sulfate reduction and methanogenesis in fresh-water sediments. *Geochimica Et Cosmochimica Acta.* 1986, 50, (1), 11-18.

(266) Ingvorsen, K.; Zehnder, A. J. B.; Jorgensen, B. B. Kinetics of sulfate and acetate uptake by *Desulfobacter postgatei*. *Applied and Environmental Microbiology.* 1984, 47, (2), 403-408.

(267) Ingvorsen, K.; Jorgensen, B. B. Kinetics of sulfate uptake by fresh-water and marine species of *Desulfovibrio*. *Archives of Microbiology.* 1984, 139, (1), 61-66.

(268) Lovley, D. R.; Klug, M. J. Sulfate reducers can out-compete methanogens at fresh-water sulfate concentrations. *Applied and Environmental Microbiology.* 1983, 45, (1), 187-192.

(269) Burdige, D. J.; Nealson, K. H. Chemical and microbiological studies of sulfide-mediated manganese reduction. *Geomicrobiology Journal.* 1986, 4, (4), 361-387.

(270) Canfield, D. E., Thamdrup, B., and Hansen, J.W. The anaerobic degradation of organic-matter in danish coastal sediments - iron reduction, manganese reduction, and sulfate reduction. *Geochimica Et Cosmochimica Acta.* 1993, 57, (16), 3867-3883.

(271) van der Zee C, S. C., Rancourt DG, de Lange GJ, van Raaphorst W. A Mossbauer spectroscopic study of the iron redox transition in eastern Mediterranean sediments. *Geochimica Et Cosmochimica Acta.* 2005, 69, (2), 441-453.

(272) Roden, E. E.; Tuttle, J. H. Sulfide release from estuarine sediments underlying anoxic bottom water. *Limnology and Oceanography.* 1992, 37, (4), 725-738.

(273) Silver, W. L.; Lugo, A. E.; Keller, M. Soil oxygen availability and biogeochemistry along rainfall and topographic gradients in upland wet tropical forest soils. *Biogeochemistry.* 1999, 44, (3), 301-328.

(274) Gerhardt, S.; Brune, A.; Schink, B. Dynamics of redox changes of iron caused by light-dark variations in littoral sediment of a freshwater lake. *Biogeochemistry.* 2005, 74, (3), 323-339.

(275) Rozan, T. F.; Taillefert, M.; Trouwborst, R. E.; Glazer, B. T.; Ma, S. F.; Herszage, J.; Valdes, L. M.; Price, K. S.; Luther, G. W. Iron-sulfur-phosphorus cycling in the sediments of a shallow coastal bay: Implications for sediment nutrient release and benthic macroalgal blooms. *Limnology and Oceanography.* 2002, 47, (5), 1346-1354.

(276) Gambrell, R. P.; Wiesepape, J. B.; Patrick, W. H.; Duff, M. C. The effects of pH, redox, and salinity on metal release from a contaminated sediment. *Water Air and Soil Pollution.* 1991, 57-8, 359-367.

(277) Fredrickson, J. K.; Zachara, J. M.; Kennedy, D. W.; Kukkadapu, R. K.; McKinley, J. P.; Heald, S. M.; Liu, C. X.; Plymale, A. E. Reduction of TcO_4^- by sediment-associated biogenic Fe(II). *Geochimica Et Cosmochimica Acta.* 2004, 68, (15), 3171-3187.

(278) Istok, J. D.; Senko, J. M.; Krumholz, L. R.; Watson, D.; Bogle, M. A.; Peacock, A.; Chang, Y. J.; White, D. C. In situ bioreduction of technetium and uranium in a nitrate-contaminated aquifer. *Environmental Science & Technology.* 2004, 38, (2), 468-475.

(279) Anderson, R. T.; Rooney-Varga, J. N.; Gaw, C. V.; Lovley, D. R. Anaerobic benzene oxidation in the Fe(III) reduction zone of petroleum contaminated aquifers. *Environmental Science & Technology.* 1998, 32, (9), 1222-1229.

(280) Tuccillo, M. E.; Cozzarelli, I. M.; Herman, J. S. Iron reduction in the sediments of a hydrocarbon-contaminated aquifer. *Applied Geochemistry.* 1999, 14, (5), 655-667.

(281) Zachara, J. M.; Kukkadapu, R. K.; Gassman, P. L.; Dohnalkova, A.; Fredrickson, J. K.; Anderson, T. Biogeochemical transformation of Fe minerals in a petroleum-contaminated aquifer. *Geochimica Et Cosmochimica Acta.* 2004, 68, (8), 1791-1805.

(282) Hyun, S.; Jafvert, C. T.; Lee, L. S.; Rao, P. S. C. Laboratory studies to characterize the efficacy of sand capping a coal tar-contaminated sediment. *Chemosphere.* 2006, 63, (10), 1621-1631.

(283) Findlay, S.; Sobczak, W. K. Microbial communities in hyporheic sediments. In *Streams and Ground Waters*; Jones, J. B.; Mulholland, P. J., Eds.; Academic Press: Sand Diego, CA, 2000.

(284) Bradley, P. M.; Landmeyer, J. E.; Chapelle, F. H. Widespread potential for microbial MTBE degradation in surface-water sediments. *Environmental Science & Technology.* 2001, 35, (4), 658-662.

(285) Phelps, C. D.; Young, L. Y. Anaerobic biodegradation of BTEX and gasoline in various aquatic sediments. *Biodegradation.* 1999, 10, (1), 15-25.

(286) Magar, V. S.; Johnson, G. W.; Brenner, R. C.; Quensen, J. F.; Foote, E. A.; Durell, G.; Ickes, J. A.; Peven-McCarthy, C. Long-term recovery of PCB-contaminated sediments at the Lake Hartwell superfund site: PCB dechlorination. 1. End-member characterization. *Environmental Science & Technology.* 2005, 39, (10), 3538-3547.

(287) Sanford, R. A.; Cole, J. R.; Tiedje, J. M. Characterization and description of *Anaeromyxobacter dehalogenans* gen. nov., sp nov., an aryl-halorespiring facultative anaerobic myxobacterium. *Applied and Environmental Microbiology.* 2002, 68, (2), 893-900.

(288) Treude, N.; Rosencrantz, D.; Liesack, W.; Schnell, S. Strain FAC12, a dissimilatory iron-reducing member of the *Anaeromyxobacter* subgroup of *Myxococcales*. *FEMS Microbiology Ecology.* 2003, 44, (2), 261-269.

(289) Petrie, L.; North, N. N.; Dollhopf, S. L.; Balkwill, D. L.; Kostka, J. E. Enumeration and characterization of iron(III)-reducing microbial communities from acidic subsurface sediments contaminated with uranium(VI). *Applied and Environmental Microbiology.* 2003, 69, (12), 7467-7479.

(290) Caccavo, F.; Lonergan, D. J.; Lovley, D. R.; Davis, M.; Stolz, J. F.; Mcinerney, M. J. *Geobacter sulfurreducens* sp. nov., a hydrogen-oxidizing and acetate-oxidizing dissimilatory metal-reducing microorganism. *Applied and Environmental Microbiology.* 1994, 60, (10), 3752-3759.

(291) Lovley, D. R.; Phillips, E. J. P. Novel mode of microbial energy-metabolism - organic-carbon oxidation coupled to dissimilatory reduction of iron or manganese. *Applied and Environmental Microbiology.* 1988, 54, (6), 1472-1480.

(292) Coates, J. D.; Bhupathiraju, V. K.; Achenbach, L. A.; McInerney, M. J.; Lovley, D. R. *Geobacter hydrogenophilus, Geobacter chapellei* and *Geobacter grbiciae*, three new, strictly anaerobic, dissimilatory Fe(III)-reducers. *International Journal of Systematic and Evolutionary Microbiology.* 2001, 51, 581-588.

(293) Stults, J. R.; Snoeyenbos-West, O.; Methe, B.; Lovley, D. R.; Chandler, D. P. Application of the 5 ' fluorogenic exonuclease assay (Taqman) for quantitative ribosomal DNA and rRNA analysis in sediments. *Applied and Environmental Microbiology.* 2001, 67, (6), 2781-2789.

(294) Lovley, D. R.; Baedecker, M. J.; Lonergan, D. J.; Cozzarelli, I. M.; Phillips, E. J. P.; Siegel, D. I. Oxidation of aromatic contaminants coupled to microbial iron reduction. *Nature.* 1989, 339, (6222), 297-300.

(295) Liu, C. X.; Gorby, Y. A.; Zachara, J. M.; Fredrickson, J. K.; Brown, C. F. Reduction kinetics of Fe(III), Co(III), U(VI) Cr(VI) and Tc(VII) in cultures of

dissimilatory metal-reducing bacteria. *Biotechnology and Bioengineering.* 2002, 80, (6), 637-649.

(296) Coates, J. D.; Councell, T.; Ellis, D. J.; Lovley, D. R. Carbohydrate oxidation coupled to Fe(III) reduction, a novel form of anaerobic metabolism. *Anaerobe.* 1998, 4, (6), 277-282.

(297) Karkhoffschweizer, R. R.; Huber, D. P. W.; Voordouw, G. Conservation of the genes for dissimilatory sulfite reductase from *desulfovibrio vulgaris* and *Archaeoglobus fulgidus* allows their detection by PCR. *Applied and Environmental Microbiology.* 1995, 61, (1), 290-296.

(298) Todorova, S. G., Costello, A.M. Design of *Shewanella*-specific 16S rRNA primers and application to analysis of *Shewanella* in a minerotrophic wetland. *Environmental Microbiology.* 2006, 8, (3), 426-432.

(299) Da Silva, M. L. B.; Alvarez, P. J. J. Enhanced anaerobic biodegradation of benzene-toluene-ethylbenzene-xylene-ethanol mixtures in bioaugmented aquifer columns. *Applied and Environmental Microbiology.* 2004, 70, (8), 4720-4726.

(300) Hales, B. A.; Edwards, C.; Ritchie, D. A.; Hall, G.; Pickup, R. W.; Saunders, J. R. Isolation and identification of methanogen-specific DNA from blanket bog feat by PCR amplification and sequence analysis. *Applied and Environmental Microbiology.* 1996, 62, (2), 668-675.

(301) Suzuki, M. T.; Taylor, L. T.; DeLong, E. F. Quantitative analysis of small-subunit rRNA genes in mixed microbial populations via 5 '-nuclease assays. *Applied and Environmental Microbiology.* 2000, 66, (11), 4605-4614.

(302) He, J. Z.; Ritalahti, K. M.; Aiello, M. R.; Löffler, F. E. Complete detoxification of vinyl chloride by an anaerobic enrichment culture and identification of the reductively dechlorinating population as a *Dehalococcoides* species. *Applied and Environmental Microbiology.* 2003, 69, (2), 996-1003.

(303) Kent, A. D.; Smith, D. J.; Benson, B. J.; Triplett, E. W. Web-based phylogenetic assignment tool for analysis of terminal restriction fragment length polymorphism profiles of microbial communities. *Applied and Environmental Microbiology.* 2003, 69, (11), 6768-6776.

(304) Terbraak, C. J. F.; Verdonschot, P. F. M. Canonical correspondence-analysis and related multivariate methods in aquatic ecology. *Aquatic Sciences.* 1995, 57, (3), 255-289.

(305) Liu, W. T.; Marsh, T. L.; Cheng, H.; Forney, L. J. Characterization of microbial diversity by determining terminal restriction fragment length polymorphisms of genes encoding 16S rRNA. *Applied and Environmental Microbiology.* 1997, 63, (11), 4516-4522.

(306) Blackwood, C. B., Hudleston, D., Zak, D.R., Buyer, J.S. Interpreting ecological diversity indices applied to terminal restriction fragment length polymorphism data: Insights from simulated microbial communities. *Applied and Environmental Microbiology.* 2007, 73, (16), 5276-5283.

(307) Smith, B.; Wilson, J. B. A consumer's guide to evenness indices. *Oikos.* 1996, 76, (1), 70-82.

(308) Lin, W. C.; Coppi, M. V.; Lovley, D. R. *Geobacter sulfurreducens* can grow with oxygen as a terminal electron acceptor. *Applied and Environmental Microbiology.* 2004, 70, (4), 2525-2528.

(309) Stein, L. Y.; La Duc, M. T.; Grundl, T. J.; Nealson, K. H. Bacterial and archaeal populations associated with freshwater ferromanganous micronodules and sediments. *Environmental Microbiology.* 2001, 3, (1), 10-18.

(310) Snoeyenbos-West, O. L.; Nevin, K. P.; Anderson, R. T.; Lovley, D. R. Enrichment of *Geobacter* species in response to stimulation of Fe(III) reduction in sandy aquifer sediments. *Microbial Ecology.* 2000, 39, (2), 153-167.

(311) Lin, B.; Braster, M.; Roling, W. F. M.; van Breukelen, B. M. Iron-reducing microorganisms in a landfill leachate-polluted aquifer: Complementing culture-independent information with enrichments and isolations. *Geomicrobiology Journal.* 2007, 24, (3-4), 283-294.

(312) Marschall, C.; Frenzel, P.; Cypionka, H. Influence of oxygen on sulfate reduction and growth of sulfate-reducing bacteria. *Archives of Microbiology.* 1993, 159, (2), 168-173.

(313) Abdollahi, H.; Wimpenny, J. W. T. Effects of oxygen on the growth of *Desulfovibrio desulfuricans*. *Journal of General Microbiology.* 1990, 136, 1025-1030.

(314) Fareleira, P.; Santos, B. S.; Antonio, C.; Moradas-Ferreira, P.; LeGall, J.; Xavier, A. V.; Santos, H. Response of a strict anaerobe to oxygen: Survival strategies in *Desulfovibrio gigas*. *Microbiology-Sgm.* 2003, 149, 1513-1522.

(315) Mogensen, G. L.; Kjeldsen, K. U.; Ingvorsen, K. *Desulfovibrio aerotolerans* sp nov., an oxygen tolerant sulphatereducing bacterium isolated from activated sludge. *Anaerobe.* 2005, 11, (6), 339-349.

(316) Löffler, F. E.; Edwards, E. A. Harnessing microbial activities for environmental cleanup. *Current Opinion in Biotechnology.* 2006, 17, (3), 274-284.

(317) Fennell, D. E.; Nijenhuis, I.; Wilson, S. F.; Zinder, S. H.; Haggblom, M. M. *Dehalococcoides ethenogenes* strain 195 reductively dechlorinates diverse chlorinated aromatic pollutants. *Environmental Science & Technology.* 2004, 38, (7), 2075-2081.

(318) Hartenbach, A.; Hofstetter, T. B.; Berg, M.; Bolotin, J.; Schwarzenbach, R. P. Using nitrogen isotope fractionation to assess abiotic reduction of nitroaromatic compounds. *Environmental Science & Technology.* 2006, 40, (24), 7710-7716.

(319) Fendinger, N. J.; Adams, D. D.; Glotfelty, D. E. The role of gas ebullition in the transport of organic contaminants from sediments. *Science of the Total Environment.* 1992, 112, (2-3), 189-201.

(320) Packman, A. I., and Bencala, K.E. Modeling surface-subsurface hydrological interactions. In *Streams and Ground Waters*; Jones, J. B., Mulholland, Patrick J., Ed. Academic Press: San Diego, 2000.

(321) Saunders, T. J.; McClain, M. E.; Llerena, C. A. The biogeochemistry of dissolved nitrogen, phosphorus, and organic carbon along terrestrial-aquatic flowpaths of a montane headwater catchment in the peruvian amazon. *Hydrological Processes.* 2006, 20, (12), 2549-2562.

(322) Alber, M., Alexander, C., Blanton, J., Chalmers, A., and Gates, K. *The Satilla River Estuarine System: The Current State of Knowledge*; The Georgia Sea Grant College Program and The South Carolina Sea Grant Consortium: 2003.

(323) Schilling, E. B.; Lockaby, B. G. Relationships between productivity and nutrient circulation within two contrasting southeastern US floodplain forests. *Wetlands.* 2006, 26, (1), 181-192.

(324) Weber, W. J.; Tang, J. X.; Huang, Q. G. Development of engineered natural organic sorbents for environmental applications. 1. Materials, approaches, and characterizations. *Environmental Science & Technology.* 2006, 40, (5), 1650-1656.

(325) Revised draft site characterization report for comparative validation of innovating "active capping" Technologies, Anacostia River, Washington, DC. Horne Engineering 2003, Submitted to Hazardous Substance Research Center - South and Southwest.

(326) Dries, J.; Bastiaens, L.; Springael, D.; Agathos, S. N.; Diels, L. Competition for sorption and degradation of chlorinated ethenes in batch zero-valent iron systems. *Environmental Science & Technology.* 2004, 38, (10), 2879-2884.

(327) Daprato, R. C.; Löffler, F. E.; Hughes, J. B. Comparative analysis of three tetrachloroethene to ethene halorespiring consortia suggests functional redundancy. *Environmental Science & Technology.* 2006, 41, (7), 2261-2269.

(328) Lee, W.; Batchelor, B. Abiotic reductive dechlorination of chlorinated ethylenes by iron-bearing soil minerals. 1. Pyrite and magnetite. *Environmental Science & Technology.* 2002, 36, (23), 5147-5154.

(329) Lee, W.; Batchelor, B. Abiotic, reductive dechlorination of chlorinated ethylenes by iron-bearing soil minerals. 2. Green rust. *Environmental Science & Technology.* 2002, 36, (24), 5348-5354.

(330) Magnuson, J. K.; Romine, M. F.; Burris, D. R.; Kingsley, M. T. Trichloroethene reductive dehalogenase from *Dehalococcoides ethenogenes*: Sequence of tcea and substrate range characterization. *Applied and Environmental Microbiology.* 2000, 66, (12), 5141-5147.

(331) Muller, J. A.; Rosner, B. M.; von Abendroth, G.; Meshulam-Simon, G.; McCarty, P. L.; Spormann, A. M. Molecular identification of the catabolic vinyl chloride reductase from *Dehalococcoides* sp. strain VS and its environmental distribution. *Applied and Environmental Microbiology.* 2004, 70, (8), 4880-4888.

(332) Krajmalnik-Brown, R.; Holscher, T.; Thomson, I. N.; Saunders, F. M.; Ritalahti, K. M.; Löffler, F. E. Genetic identification of a putative vinyl chloride reductase in *Dehalococcoides* sp. strain BAV1. *Applied and Environmental Microbiology.* 2004, 70, (10), 6347-6351.

(333) Kube, M.; Beck, A.; Zinder, S. H.; Kuhl, H.; Reinhardt, R.; Adrian, L. Genome sequence of the chlorinated compound respiring bacterium *Dehalococcoides* species strain cbdb1. *Nature Biotechnology.* 2005, 23, (10), 1269-1273.

(334) Seshadri, R.; Adrian, L.; Fouts, D. E.; Eisen, J. A.; Phillippy, A. M.; Methe, B. A.; Ward, N. L.; Nelson, W. C.; Deboy, R. T.; Khouri, H. M.; Kolonay, J. F.; Dodson, R. J.; Daugherty, S. C.; Brinkac, L. M.; Sullivan, S. A.; Madupu, R.; Nelson, K. T.; Kang, K. H.; Impraim, M.; Tran, K.; Robinson, J. M.; Forberger, H. A.; Fraser, C. M.; Zinder, S. H.; Heidelberg, J. F. Genome sequence of the PCE-dechlorinating bacterium *Dehalococcoides ethenogenes*. *Science.* 2005, 307, (5706), 105-108.

(335) Löffler, F. E.; Tiedje, J. M.; Sanford, R. A. Fraction of electrons consumed in electron acceptor reduction and hydrogen thresholds as indicators of halorespiratory physiology. *Applied and Environmental Microbiology.* 1999, 65, (9), 4049-4056.

(336) Viollier, E.; Inglett, P. W.; Hunter, K.; Roychoudhury, A. N.; Van Cappellen, P. The ferrozine method revisited: Fe(II)/Fe(III) determination in natural waters. *Applied Geochemistry.* 2000, 15, (6), 785-790.

(337) Bradley, P. M.; Chapelle, F. H. Anaerobic mineralization of vinyl chloride in Fe(III)-reducing, aquifer sediments. *Environmental Science & Technology.* 1996, 30, (6), 2084-2086.

(338) Koene-Cottaar, F. H. M.; Schraa, G. Anaerobic reduction of ethene to ethane in an enrichment culture. *FEMS Microbiology Ecology.* 1998, 25, (3), 251-256.

(339) Oremland, R. S.; Taylor, B. F. Inhibition of methanogenesis in marine sediments by acetylene and ethylene - validity of acetylene-reduction assay for anaerobic microcosms. *Applied Microbiology.* 1975, 30, (4), 707-709.

(340) He, J. Z.; Sung, Y.; Dollhopf, M. E.; Fathepure, B. Z.; Tiedje, J. M.; Löffler, F. E. Acetate versus hydrogen as direct electron donors to stimulate the microbial reductive

dechlorination process at chloroethene-contaminated sites. *Environmental Science & Technology.* 2002, 36, (18), 3945-3952.

(341) Hoelen, T. P.; Reinhard, M. Complete biological dehalogenation of chlorinated ethylenes in sulfate containing groundwater. *Biodegradation.* 2004, 15, (6), 395-403.

(342) Prytula, M. T.; Pavlostathis, S. G. Effect of contaminant and organic matter bioavailability on the microbial dehalogenation of sediment-bound chlorobenzenes. *Water Research.* 1996, 30, (11), 2669-2680.

(343) USEPA. Soil Screening Guidance: Technical Background Document, 1996, EPA-540-R-95-128.

(344) Holmes, V. F.; He, J. Z.; Lee, P. K. H.; Alvarez-Cohen, L. Discrimination of multiple *Dehalococcoides* strains in a trichloroethene enrichment by quantification of their reductive dehalogenase genes. *Applied and Environmental Microbiology.* 2006, 72, (9), 5877-5883.

(345) He, J.; Sung, Y.; Krajmalnik-Brown, R.; Ritalahti, K. M.; Löffler, F. E. Isolation and characterization of *Dehalococcoides* sp. strain FL2, a trichloroethene (tce)- and 1,2-dichloroethene-respiring anaerobe. *Environmental Microbiology.* 2005, 7, (9), 1442-1450.

(346) Yan, T.; LaPara, T. M.; Novak, P. J. The reductive dechlorination of 2,3,4,5-tetrachlorobiphenyl in three different sediment cultures: Evidence for the involvement of phylogenetically similar *Dehalococcoides*-like bacterial populations. *Fems Microbiology Ecology.* 2006, 55, (2), 248-261.

(347) Fagervold, S. K.; Watts, J. E. M.; May, H. D.; Sowers, K. R. Sequential reductive dechlorination of meta-chlorinated polychlorinated biphenyl congeners in sediment microcosms by two different *Chloroflexi* phylotypes (vol 71, pg 8085, 2005). *Applied and Environmental Microbiology.* 2006, 72, (2), 1717-1717.

(348) Gossett, J. M. Measurement of henrys law constants for C1 and C2 chlorinated hydrocarbons. *Environmental Science & Technology.* 1987, 21, (2), 202-208.

(349) Percival, J. B.; Lindsay, P. J. Measurement of physical properties of sediments. In *Physico-Chemical Analysis of Aquatic Sediments*; Mudroch, A.; Azcue, J. M.; Mudroch, P.Eds.; Lewis Publishers: Boca Raton, FL, 1996.

(350) Schlotelburg, C.; von Wintzingerode, C.; Hauck, R.; von Wintzingerode, F.; Hegemann, W.; Gobel, U. B. Microbial structure of an anaerobic bioreactor population that continuously dechlorinates 1,2-dichloropropane. *FEMS Microbiology Ecology.* 2002, 39, (3), 229-237.

(351) Löffler, F. E.; Sun, Q.; Li, J. R.; Tiedje, J. M. 16S rRNA gene-based detection of tetrachloroethene-dechlorinating *Desulfuromonas* and *Dehalococcoides* species. *Applied and Environmental Microbiology.* 2000, 66, (4), 1369-1374.

(352) El Fantroussi, S.; Mahillon, J.; Naveau, H.; Agathos, S. N. Introduction of anaerobic dechlorinating bacteria into soil slurry microcosms and nested-PCR monitoring. *Applied and Environmental Microbiology.* 1997, 63, (2), 806-811.

(353) Johnson, D. R.; Lee, P. K. H.; Holmes, V. F.; Alvarez-Cohen, L. An internal reference technique for accurately quantifying specific mRNAs by real-time PCR with a application to the *tceA* reductive dehalogenase gene. *Applied and Environmental Microbiology.* 2005, 71, (7), 3866-3871.

(354) Adrian, L.; Szewzyk, U.; Gorisch, H. Bacterial growth based on reductive dechlorination of trichlorobenzenes. *Biodegradation.* 2000, 11, (1), 73-81.

(355) McDonough, K. M.; Murphy, P.; Olsta, J.; Zhu, Y. W.; Reible, D.; Lowry, G. V. Development and placement of a sorbent-amended thin layer sediment cap in the Anacostia River. *Soil & Sediment Contamination.* 2007, 16, (3), 313-322.

(356) Reible, D., personal communication, 2005.

(357) Scow, K. M.; Hicks, K. A. Natural attenuation and enhanced bioremediation of organic contaminants in groundwater. *Current Opinion in Biotechnology.* 2005, 16, (3), 246-253.

(358) Haas, J. E.; Trego, D. A. A field application of hydrogen-releasing compound (HRC ™) for the enhanced bioremediation of methyl tertiary butyl ether (MTBE). *Soil & Sediment Contamination.* 2001, 10, (5), 555-575.

(359) Buffle J.; Tercier-Waeber, M.-L. In situ oltammetry: Concepts and practice for trace analysis and speciation. In *In Situ Monitoring of Aquatic Systems: Chemical Analysis and Speciation*; Buffle, J., Horvai, G., Eds. John Wiley & Sons 2000.

VITA

David (Dave) Whims Himmelheber was born to Tim and Terry Himmelheber in Baltimore, MD on March 4, 1980. Dave was born one minute before his twin brother Jack, who together joined older sister Anne Marie and older brother Chris to complete the family. Dave resided with his family in Abingdon, MD for 18 years and graduated from Bel Air High School in 1998. Dave majored in Chemistry at Salisbury University, Salisbury, MD while earning scholarships from Emmorton Recreation Council and Salisbury University. In the summer of 2001, Dave was selected for a Research Experience for Undergraduates (REU) program at the Johns Hopkins University. During his REU, Dave was introduced to environmental engineering and subsurface remediation research and decided to continue studying in the field. Following graduation from Salisbury with a Bachelor of Science degree in 2002, Dave immediately began pursuit of a Ph.D. in Environmental Engineering at Georgia Tech as a Presidential Fellow. Dave studied under Drs. Joe Hughes and Kurt Pennell and earned a Master of Science degree from the School of Civil and Environmental Engineering in December 2003. In recognition of his research efforts, Dave was awarded 2nd place in a student research contest sponsored by an environmental consulting company in 2007. Dave has served the Association of Environmental Engineers and Scientists (AEES) as a senator, vice president, and president. Dave has also participated in multiple intramural sports and was a member of the Georgia Tech Roller Hockey Club.

While in Tybee Island, GA in April 2006, Dave proposed to Denise Langley, whom he had met in class at Salisbury. Dave and Denise were married in Pennsville, NJ in May 2007 after five years together. Dave and Denise have enjoyed Atlanta, and spent time exploring the north Georgia Mountains, completing a marathon, tailgating and attending many Georgia Tech football games, and generally enjoying the culture of the South. After earning his Ph.D., Dave and Denise plan to reside in Maryland and look forward to living closer to family, but will miss the weather.